Effect of Cellular Aging on Fibroblastic Phenotype & Regulation by Hyaluronan

Russell Michael Lloyd Simpson BSc (Hons)

Thesis presented for the degree of Philosophiae Doctor

2010

Institute of Nephrology School of Medicine Cardiff University Heath Park Cardiff CF14 4XN



UMI Number: U518535

All rights reserved

INFORMATION TO ALL USERS

The quality of this reproduction is dependent upon the quality of the copy submitted.

In the unlikely event that the author did not send a complete manuscript and there are missing pages, these will be noted. Also, if material had to be removed, a note will indicate the deletion.



UMI U518535

Published by ProQuest LLC 2013. Copyright in the Dissertation held by the Author.

Microform Edition © ProQuest LLC.

All rights reserved. This work is protected against unauthorized copying under Title 17, United States Code.



ProQuest LLC 789 East Eisenhower Parkway P.O. Box 1346 Ann Arbor, MI 48106-1346 This thesis is dedicated to my mother and father.

Thank you both for everything, I'm proud to be your son x

Acknowledgement

First and foremost I would like to thank my supervisors, Professor Aled Phillips and Dr. Robert Steadman. I am sure Robert will not miss the echoing sound of flip-flops ascending toward his office on no less than a daily basis. He has always provided invaluable supervision and I am indebted to him for his patience, support and friendship. Inevitably all does not go to plan and it is very easy to lose focus, however, I could always rely on Aled to steer me clear and set me back on track, as though my life may have depended on it! He has been a constant inspiration and I feel fortunate for receiving his vision and guidance over the past three years....Simply dandy!

The success of this project has largely been as a result of the collaboration with the Wound Biology Group in Cardiff University's Dental School. I would sincerely like to thank Professor David Thomas and Professor Phillip Stephens for their support and guidance. My gratitude also extends to Professor Alan Wells from the Department of Pathology, University of Pittsburgh, for his invaluable assistance. Furthermore, my appreciation goes to Mr. Marc Isaacs, Dr. Anthony Hayes, and Dr. Jim Ralphs from Cardiff University School of Biosciences, for their help in generation of confocal images.

From day one I have relied on the experience and supervision of those in the laboratory to grasp the technical aspects of this project. I was fortunate enough to have been surrounded by fantastic scientists. Five individuals in particular have been crucial to the success of my project; Dr. John Martin, Dr. Robert Jenkins, Dr Jason Webber, Dr. Daryn Michael and the Queen of them all, Dr Soma Meran. Thank you for your support and friendship. I would also like to give my thanks to Dr. Donald Fraser and Dr. Timothy Bowen for all their welcomed advice. Thank you also to Dr. Ruth Mackenzie, Cheryl Ward, Kim Abberley and Professor John Williams for their invaluable assistance during the last three years. Huge thanks also go to all my friends and colleagues at the Institute of Nephrology, it has been an absolute pleasure to work here and I feel very privileged to have met you all. A special thanks goes to Rachel Neville who has made my time in the Institute that extra special.

I would like to take this opportunity to thank Professor J Schwok, Dr. S Wilson, Dr A Robinson, Dr J Ducie and Dr. C Wellaway from the Circle Group Laboratory, Weymouth, H.Q. Our in depth conversations on fibroblasting and quantum dynamics of Wray and Nephew theorem proved invaluable during the last three years. Cheers guys!

Mostly, I would like to thank my family. Thank you to my father and beautiful mother for supporting me not just these past three years but for the last nine years that I have frequented at Cardiff University. Without your unconditional love (and cash) it would not have been possible. I am truly indebted to you both for believing in me and allowing me to reach my goals. I would finally like to thank Patrick. He has always been a role model to whom I look up to and I feel privileged to have a man of his calibre for my big brother, I only regret that his fate as No.2 son is now sealed. All my love, LB.

Thesis Summary

The presence of α -smooth muscle actin (α -SMA) containing myofibroblasts are responsible for closure of wounds and formation of the collagen-rich scar. The current study demonstrated a failure of TGF- β_1 -mediated fibroblast-myofibroblast differentiation associated with *in-vitro* aging. This was associated with age-dependent attenuation of hyaluronan (HA) synthase (HAS) 2 dependent HA induction and its assembly into a pericellular coat.

Removal of the HA coat by hyaluronidase (Hyal) digestion led to abrogation of dependent induction of α -SMA in young cells. Whilst this illustrated the importance of the HA coat during phenotypic activation, its restoration in aged cells as a result of HAS2 over-expression, did not lead to the acquisition of a myofibroblast phenotype. The HA pericellular coat was necessary but not sufficient to correct for the age-dependent defect in phenotypic conversion.

In addition to HAS2 there was loss of EGF receptor (EGF-R) in aged cells and both were required for normal fibroblast functionality. The data demonstrated that the HA receptor, CD44, co-localises with EGF-R following activation by TGF- β_1 . This interaction was HA-dependent as disruption of the HA coat abrogates the association and inhibits downstream ERK1/2 signalling, required for phenotypic conversion. In aged fibroblasts the association was lost with resultant suppression of ERK1/2 activation. Forced over-expression of EGF-R and HAS2 in aged cells restored TGF- β_1 -mediated HA-CD44/EGF-R association and α -SMA induction.

Collectively, the data demonstrated that HA can serve as a signal integrator by facilitating TGF- β_1 -mediated CD44-EGF-R-ERK interactions and ultimately regulate fibroblast phenotype. I propose a model to explain this novel mechanism and the functional consequence of age-dependent dysregulation. This mechanism may have direct implications for modifying the wound healing response, particularly for developing therapeutic strategies to improve healing in the elderly.

Publications and presentations arising from the thesis

Publications

Simpson R. M. L., Meran S., Thomas D.W., Stephens P., Bowen T., Steadman R., and Phillips A. O., Age related changes in pericellular hyaluronan organisation leads to impaired dermal fibroblast to myofibroblast differentiation. American Journal of Pathology, 2009;

Simpson R. M. L., Meran S., Thomas D.W., Stephens P., Bowen T., Steadman R., and Phillips A. O., Aging Fibroblasts resist phenotypic maturation due to impaired Hyaluronan-dependent CD44/EGF receptor signalling. American Journal of Pathology, 2010;

Presentations

Simpson R. M. L., Meran S., Thomas D.W., Stephens P., Bowen T., Steadman R., and Phillips A. O., Fibroblasts resist $TGF\beta_1$ driven myofibroblastic differentiation during in-vitro aging. Cardiff Institute of Tissue Engineering and Repair, Abergavenny, 2007 (Oral).

Simpson R. M. L., Meran S., Thomas D.W., Stephens P., Bowen T., Steadman R., and Phillips A. O., Fibroblasts resist TGFβ₁ driven myofibroblastic differentiation during in-vitro aging. European Renal Cell Study Group, Wales 2008 (Oral).

Simpson R. M. L., Meran S., Thomas D.W., Stephens P., Bowen T., Steadman R., and Phillips A. O., Age related changes in pericellular hyaluronan organisation leads to impaired dermal fibroblast to myofibroblast differentiation. Cardiff University Interdisciplinary Research Group (Metabolism, regeneration and Repair), Cardiff 2008 (Oral). 1st Prize awarded.

Simpson R. M. L., Meran S., Thomas D.W., Stephens P., Bowen T., Steadman R., and Phillips A. O., Age related changes in pericellular hyaluronan organisation leads to impaired dermal fibroblast to myofibroblast differentiation. Cardiff Institute of Tissue Engineering and Repair, Abergavenny, 2008 (Oral).

Simpson R. M. L., Meran S., Thomas D.W., Stephens P., Bowen T., Steadman R., and Phillips A. O., Age related changes in pericellular hyaluronan organisation leads to impaired dermal fibroblast to myofibroblast differentiation. British Society for Matrix Biology, Cardiff 2008 (Poster).

Simpson R. M. L., Meran S., Thomas D.W., Stephens P., Bowen T., Steadman R., and Phillips A. O., Age related changes in pericellular hyaluronan organisation leads to impaired dermal fibroblast to myofibroblast differentiation. European Renal Cell Study Group, Greece, 2009 (Oral).

Simpson R. M. L., Meran S., Thomas D.W., Stephens P., Bowen T., Steadman R., and Phillips A. O., Aging fibroblasts resist phenotypic maturation because of impaired hyaluronan-dependent CD44/EGF-R signalling. International Society for Hyaluronan Sciences 8th International Conference, Kyoto, Japan, 2010 (Poster).

Contents

Chapter 1: General Introduction and Project Overview	
1.1 Aging and Wound Healing2	,
1.2 Phases of Wound Healing 3	,
1.2.1 Alterations in Hemostasis and Inflammation	
1.2.2 Alterations in Proliferation	
1.2.3 Alterations in matrix deposition	,
1.2.4 Alterations in Remodelling Phase	;
1.3 Replicative Senescence 8	;
1.4 The Fibroblast)
1.4.1 Fibroblast Origin	
1.4.2 Role of Fibroblast in Wound Healing	
1.4.3 Myofibroblastic Differentiation	į
1.4.4 Fibroblast Heterogeneity	,
1.5 Transforming Growth Factor beta 17	,
1.5.1 TGF- β in Wound Healing	,
1.5.2 TGF-β Signalling)
1.5.2.1 Smad Related TGF-β1 Signalling)
1.5.2.2 Non-Smad Related TGF-β1 Signalling	
1.5.3 TGF-β1 signalling and aging22)
1.6 Extracellular Matrix23	}
1.7 Hyaluronan (HA)24	ļ
1.7.1 Structure and Biology of HA	ļ
1.7.2 Synthesis and Catabolism	ć

1.7.3 HA Binding Proteins and Receptors	29
1.7.3.1 TSG-6	29
1.7.3.2 CD44	30
1.7.4 HA Pericellular Coats	31
1.7.5 HA and Wound Healing	33
1.7.6 HA and Aging	36
Project Aims	39
Chapter 2 : Materials and Methods	40
2.1 Materials	41
2.2 Patient Samples	41
2.3 Tissue Culture	42
2.3.1 Isolation of Fibroblasts	42
2.3.2 Fibroblast Culture	43
2.3.3 Calculation of population doubling levels	43
2.3.4. Fibroblast Sub-culture	44
2.3.5. Fibroblast Cryo-preservation and Retrieval	45
2.4 Histochemistry	45
2.4.1 Immuno-Fluorescence	45
2.4.2 FITC-Phalloidin Staining	46
2.5 Analysis of Cell Proliferation	46
2.6 Reverse Transcription (RT)	48
2.7 Quantitative PCR (Q-PCR)	49
2.8 Generation of HAS2 and EGF-R Over-expressing Clone	51

2.9 Transient Transfection 53
2.10 Small Interfering RNA Transfection54
2.11 Visualisation of pericellular HA by particle exclusion assay
2.12 Analysis of ³ H-Radiolabeled HA56
2.13 Determination of HA concentration 57
2.14 Western Blot Analysis57
2.15 Immunoprecipitation 59
2.16 Statistical Analysis 60
Chapter 3: Characterisation of Fibroblast Phenotype and HA Regulation with in-
vitro Aging61
3.1 Introduction
3.2 Results
3.2.1 Characterisation of phenotypic conversion in young and aged fibroblasts
3.2.2 Analysis of HA generation and molecular weight profile in young and aged
fibroblasts67
3.2.3 The expression of hyaluronan synthase enzymes in young and aged fibroblasts 68
3.2.4 Accumulation of hyaluronan-dependent pericellular coats in young and aged
fibroblasts69
3.2.5 The expression of TSG-6 in young and aged fibroblasts
Chapter 3 Figures
3.3 Discussion

Chapter 4 : Differential Effects of Aging on TGF-β1 Signalling and Organisation	
of Pericellular Hyaluronan89	9
4.1 Introduction 90	0
4.2 Results	4
4.2.1 The Effect of ALK-5 inhibition on phenotypic activation	4
4.2.2 The expression of endogenous TGF-β1 in young and aged fibroblasts	4
4.2.3 The effect of Smad2 and Smad3 knock-down in TGF-β1 mediated responses in	
young fibroblasts	5
4.2.4 The effect of in-vitro aging on Smad 2 and Smad 3 signalling	5
4.2.5 The effect of inhibition of HA synthesis on fibroblast phenotypic conversion 9	6
4.2.6 The relationship between HAS2 and fibroblast phenotype	7
4.2.7 The role of TSG-6 in myofibroblastic differentiation	8
4.2.8 The effect of HAS2 restoration and TGF stimulation on phenotype in aged	
fibroblasts9	8
4.2.9 The effect of IL-1β on phenotype of young and aged fibroblasts9	9
4.2.10 The relationship between hyaluronan-dependent pericellular coat assembly and	
myofibroblastic differentiation	0
4.2.11 The effects of Smad siRNA on hyaluronan-dependent pericellular coat	
accumulation	0
4.2.12 The effect of HA coat removal on Smad signalling	1
Chapter 4 Figures 10	2
4.3 Discussion	1

Chapter 5: The Role of Hyaluronan-Dependent CD44/EGF Receptor Signalling 129
5.1 Introduction
5.2 Results
5.2.1 The role of the EGF-R in TGF-β1-mediated myofibroblastic differentiation 134
5.2.2 Effect of aging on EGF-R expression. 134
5.2.3 The effect of EGF-R restoration on TGF-β1-mediated myofibroblastic
differentiation in aged fibroblasts
5.2.4 The role of EGF in TGF-β1-mediated myofibroblastic differentiation
5.2.5 The relationship between the EGF-R and HAS2
5.2.6 TGF-β1 activates ERK through EGF-R signalling
5.2.7 The differential requirement of EGF and HA signalling in TGF-β1 mediated
activation of ERK and Smad2
5.2.8 The expression of CD44 in young and aged fibroblasts and its role in
myofibroblastic differentiation through ERK signalling
5.2.9 The interaction of CD44 and the EGF-R in phenotypic activation of young and
aged fibroblasts
5.2.10 Involvement of calcium calmodulin-dependent kinase II
5.2.11 Effect of disrupting the cytoskeleton on pericellular HA organisation
Chapter 5 Figures
5.3 Discussion
Chapter 6 : General Discussion
References
Annendix 1. Ruffers and Reagents

Glossary of Abbreviations

α-SMA Alpha-smooth muscle actin

Anti-GBM Anti-glomerular basement membrane

AP-1 Activator Protein-1

BMP-7 Bone Morphogenic Protein-7

BNS Basic Nucleofector Solution

BSA Bovine Serum Albumin

CaMKII Calcium calmodulin-dependent kinase II

CD44 Cluster of differentiation-44

cDNA Complementary DNA

CKI Cyclin Dependant Kinase Inhibitors

CM Conditioned Medium

cRNA Complementary RNA

C_T Threshold cycle

CTGF Connective Tissue Growth Factor

DMSO Dimethyl Sulphoxide

DMEM Dulbecco's Modified Eagles Medium

DNA Deoxyribose Nucleic Acid

dNTP's Deoxynucleoside triphosphate

DPM Disintegrations Per Minute

ECM Extracellular Matrix

ED-A Extra Domain-A

EDTA Ethylenediaminetetraacetic acid

EGF Epidermal Growth Factor

EGF-R Epidermal Growth Factor

ELISA Enzyme linked immuno-sorbent assay

EMT Epithelial Mesenchymal Transition

ERK Extracellular Regulated Kinase

f-Actin Filamentous Actin

FCS Fetal Calf Serum

FGF-2 Fibroblast Growth Factor -2 (basic)

FITC Fluorescein Isothiocyanate

F-SCM Fibroblast Serum Containing Medium

GAG Glycosaminoglycans

GFP Green Fluorescent Protein

GTP Guanosine Triphosphate

HA Hyaluronan

HABP Hyaluronan Binding Protein

HAS Hyaluronan Synthase

HCl Hydrogen Chloride

HGF Hepatocyte Growth Factor

HMW High Molecular Weight

Hyal Hyaluronidase

 $I\alpha I$ inter- α inhibitor

ICAM Intracellular Adhesion Molecule-1

Il-1 Interleukin-1

ION Institute of Nephrology

KCl Potassium Chloride

KGF Keratinocyte Growth Factor

LAP Latent Associated Protein

LB Lysogeny broth

LMW Low Molecular Weight

MAP Kinase Mitogen Activated Protein Kinase

MCS Multiple Cloning Site

MCP-1 Monocyte Chemotactic Protein-1

MgCl₂ Magnesium Chloride

MMP Matrix Metalloproteinase's

MMW Middle Molecular Weight

4MU 4-Methyl Umbelliferone

NaCl Sodium Chloride

NaOH Sodium Hydroxide

ORF Open Reading Frame

PAI-1 plasminogen activation inhibitor-1

PBS Phosphate Buffered Saline

PDGF Platelet Derived Growth Factor

PI Propidium Iodide

PI3K phosphatidylinositol 3-kinase

PKA Protein Kinase A

PLC Phospholipase C

Q-PCR Quantitative Polymerase Chain Reaction

RHAMM Receptor Hyaluronan Mediated Motility

RNA Ribonucleic Acid

RPM Revolutions Per Minute

R-Smads Receptor Regulated Smads

RT-PCR Reverse Transcription – Polymerase Chain Reaction

SDS Sodium Dodecyl Sulphate

SDS-PAGE SDS - Polyacrylamide Gel Electrophoresis

SiRNA Small Interfering RNA

SP-1 Stimulatory Protien-1

TBS Tris Buffered Saline

TGF Transforming Growth Factor

TIMP Tissue Inhibitor of Metalloproteinase's

TNF-α Tumour Necrosis Factor-α

TSG-6 Tumour Necrosis Factor Stimulating Gene-6

UDP Uridine Diphosphate

VEGF Vascular Endothelial Growth Factor

Chapter 1 General Introduction and Project Overview

1.1 Aging and Wound Healing

Alterations in response to injury in the aged occur in virtually every system of the body from the musculoskeletal system to the central nervous system. The analysis of impaired skin wound healing provides a powerful and accessible route to address the link between cellular changes (proliferation, differentiation, senescence - all amenable to *in-vitro* dissection) and alterations at the whole tissue level *in-vivo*. In addition to these practical scientific considerations impaired wound healing in the skin represents an important health issue with corresponding morbidity and mortality [1].

Put simply, wound healing is impaired with advancing age. The morbidity associated with age-related impaired wound healing presents a major clinical and economic problem [2]. The financial burden for treatment of age related acute and chronic wounds has been estimated to be in excess of £1 billion per year [3]. In the U.S trauma is the fifth leading reason for death of people over the age of 65 [4]. Unless improved wound care strategies are developed, the projected relative and absolute increases in the elderly population will further exacerbate this problem. Despite the obvious clinical impact however, the basic cellular and molecular mechanisms underlying impaired human wound healing are largely unknown.

Impaired wound healing in the aged is due partly to comorbidities common among the elderly, but evidence also suggests that inherent differences in cellular structure and function may impair tissue repair and regeneration as well [5]. Progress in understanding the role that growth factors play in wound healing and the ability to synthesise adequate quantities of these factors for clinical use has led to clinical trials evaluating their use in wound healing. The results of these studies however have been disappointing.

The aim of this thesis is to try further the understanding of the mechanisms involved in wound healing but critically, how these processes falter with age. Continuing progress in understanding the complex interaction between the aging cell and the wound healing process is essential in order to explore and develop focussed therapeutic strategies to improve healing in the elderly.

1.2 Phases of Wound Healing

The response to injury is a primitive but essential, innate host immune response which comprises a closely orchestrated cascade of biochemical events that lead to tissue reorganisation and restoration of its integrity and function. The molecular interactions that underlie wound healing involve the collaborative efforts of many different tissues, cell lineages, signalling molecules and matrix proteins. The literature has been comprehensively reviewed by Martin [6] and Singer and Clark [7]. Although the wound healing process is a continuum it is classically separated into four sequential, yet overlapping, phases which are defined as hemostasis, inflammation, proliferation, and remodelling.

During hemostasis a fibrin clot is formed at the site of endothelium injury and platelets aggregate. Platelets adhere to the injured endothelium and release chemokines, thereby attracting the cellular components of the inflammatory phase [8, 9]. The inflammatory phase of wound healing is characterised by the presence of neutrophils, macrophages, and lymphocytes [9]. The inflammatory cells then serve to release pro-inflammatory cytokines and growth factors, ingest foreign materials, increase vascular permeability, and promote fibroblast activity [10]. The proliferative phase begins several days after the initial injury. In this phase, capillary growth and granulation tissue formation occur. Cellular proliferation and abundant collagen synthesis by fibroblasts lead to reepithelialization and construction of a preliminary dermis. The final phase of wound healing resolution is a long process of tissue remodelling and increasing wound strength. During this phase, type I collagen synthesis and turnover continues and fibroblasts differentiate into myofibroblasts, allowing further wound contraction. An acellular vascular scar is the final result of the wound healing process. However this fibrous scar does not contain the same proportion of strength and functionality of uninjured tissue.

All four phases of healing (hemostasis, inflammation, proliferation and remodelling) exhibit characteristic age-related changes (Table 1). Impaired/delayed healing in the elderly is associated with decreased levels of growth factors, diminished cell proliferation and migration, an excessive inflammatory response and matrix degradation, suggesting that the process of in-vivo aging is a dynamic, complex process in which the balance of synthesis and degradation are disrupted [3].

Hemostasis	Proliferation
Enhanced platelet aggregation	Delayed re-epithelialisation
Increased release of alpha-	Delayed angiogenesis
granules	
	Delayed collagen deposition
Inflammation	Resolution
Decreased vascular aggregation	Reduced collagen turnover and
	remodelling
Increased secretion of	Delayed wound strength
inflammatory mediators	
Delayed infiltration of	Decreased wound strength
macrophages and lymphocytes	
Decreased secretion of growth	Charles Carlotte
factors	

Table 1. Summary of age-related changes in wound healing phases. [2].

1.2.1 Alterations in Hemostasis and Inflammation

Specific age-related changes in the coagulation and immune systems which influence healing processes include alterations in cell adhesion, migration, and functional responses. Exposure of collagen promotes platelet adherence following endothelial damage. Enhanced platelet release [11], adherence [12], and their secretion of alpha-

granules, which contain transforming growth factor β (TGF- β), TGF- α , and platelet-derived growth factor (PDGF) [11] have been shown to increase with advanced age.

Nitric oxide is an important vasoactive mediator and its secretion has been shown to decrease in aged endothelial cells [13], leading to reduced capillary permeability at the injury site. Evidence for the alteration of the inflammatory response in aged individuals has also been demonstrated. Cohen et al have reported increased numbers of wound inflammatory cells in aged mice, when compared to young mice, particularly with regards to neutrophil infiltration during the early stages of wound healing [14]. Conversely, whilst neutrophil numbers increase with age their ability to undergo respiratory burst activity and phagocytose bacteria is impaired [15]. Age related changes in macrophages appear to be critical in defective wound healing. Whilst matrix adherence of peritoneal macrophages may be delayed [16], animal studies demonstrate that influx is amplified in aged subjects [17]. Wounded young mice subjected with rabbit anti-macrophage serum exhibited impaired healing compared to untreated aged mice [14] and moreover, accelerated wound healing following application of young peritoneal macrophages was demonstrated in cutaneous wounds of aged mice [18]. Studies demonstrate that macrophage function in terms of phagocytic ability [17], maturation [16, 19] and growth factor release [20], is also defective with age.

1.2.2 Alterations in Proliferation

Angiogenesis, collagen synthesis and re-epithelialization display an age-related delay in aged animals [20]. The proliferative response of fibroblasts, endothelial cells and keratinocytes is impaired in aged animals [21]. With increasing age, there is a decrease in the number and size [22] and proliferative response [21, 23] of fibroblasts. Aged fibroblasts have also been shown to exhibit a diminished response to growth factors and diminished replicative capacity [22, 24]. These changes result in an age-related delay in wound closure in animal models as well as in human wounds [25, 26]. Whole wound studies have shown decreased rates of epithelialisation and contraction in older animals [27, 28] and humans [29].

The process of angiogenesis is altered with age although the literature is inconsistent in method. The more popular standpoint associates aging with reduced angiogenesis [20]. The process of angiogenesis is mediated by release of substances such as Fibroblast Growth Factor -2 (FGF-2), vascular endothelial growth factor (VEGF) and PDGF secreted by platelets and macrophages and it is thought that an age-related decline in secretion of these mediators may be responsible for delayed angiogenesis and subsequent impaired wound healing in aged subjects [13, 24]. Data has demonstrated that wound capillary ingrowth is reduced with age [30, 31] and that restoration of such growth factors specifically reversed impaired microvessel growth in aged mice [31]. Some authors, however, have reported an increased angiogenic response with age [16]. Whilst Ashcroft et al report delayed angiogenesis, they ultimately demonstrate an amplified response in aged mice when compared with young mice [3]. In line with this notion one study showed that thrombospondins, proteins with antiangiogenic abilities, were abundant in matrix produced by newborn cells but virtually undetectable in the matrix of adult cells [32]. By their own admission, Ashcroft et al recognise that conflicting data may reflect differences in animal model used, the differences in validation of 'aged' animals and differences in the time course of angiogenesis used [3]. It would seem, however, that further enquiry is needed to fully realise the specific role of angiogenesis in age-related impaired wound healing.

Despite there being no difference in the overall content of collagen in a young or aged mature wound, its synthesis is certainly delayed with aging [20] and this delay (with type 1 collagen production in particular) can have a negative effect on deposition of connective tissue [21]. Degradation of the ECM is necessary for deposition of a new collagen scaffold, a process mediated by the matrix metalloproteinases (MMPs). The activities of MMPs are kept in check by tissue inhibitors of metalloproteinases (TIMPs). Studies have revealed that induction of MMPs and suppression of TIMPs, have been attributed to age-related delayed wound healing [33, 34]. In addition, a loss of responsiveness of *in vitro* and *in vivo* aged human fibroblasts to a variety of cytokines and hormones including insulin, epidermal growth factor (EGF), keratinocyte growth factor (KGF) and PDGF has been reported [3, 19].

Studies have reported reduced EGF responsiveness due to preferential loss of EGF receptors in aging fibroblasts [35]. Furthermore, a marked delay in expression levels of EGF and its receptor were observed in aged mouse cells, compared to young expression [36]. With age, cells lose responsiveness to PDGF and require increased PDGF concentrations to restore proliferative capacity of younger phenotype and moreover, in humans, secretion of TGF-β is attenuated with increasing age [19, 37]. Dysregulated expression of cytokines at the wound site together with reduced levels of fibroblast and inflammatory cell-associated TGF-β and PDGF have been observed in aged mice [38]. The keratinocyte expression of cytokines and their receptors were found to alter dramatically in an aging mouse model of acute wound healing [36].

1.2.3 Alterations in matrix deposition

In the aging human dermis the fibroblast takes on a quiescent state, with poorly developed endoplasmic reticulum [39]. Pienta and Coffey [40] have demonstrated that when comparing 20 year old fibroblasts with 66 year old fibroblasts, the aged phenotype was characterised with a global decline in all aspects of human fibroblast motility. It has also been reported that aging cells are less responsive to chemotactic cues from matrix constituents such as fibronectin [41]. Although the observation was only made in females it was reported that serum from aged individuals (but not young individuals) had an inhibitory effect on the migration of lung fibroblasts [42].

Shevitz et al [43] documented that deposition of fibronectin, one of the main components of the provisional matrix, is advanced in late passage fibroblasts. Aged fibroblasts exhibit impaired migration, actin cytoskeletal organisation and integrin function, [23, 44]. *In-vitro* wounding experiments demonstrated that, with increasing donor age patients, the ability of human skin fibroblasts to re-establish a confluent monolayer is decreased [44].

1.2.4 Alterations in Remodelling Phase

Late passage human diploid fibroblasts demonstrate an increased contractile phenotype on a collagen gel and filamentous actin (f-actin) content. Gibson et al postulate that increased f-actin in aged cells facilitates increased contractile strength through interactions with the fibronectin integrin receptor [45].

Tissue remodelling inevitably results in formation of a scar with reduced mechanical strength from that of normal skin. Animal models have described variable results with respect to the effect of age on wound breaking strength [3]. Studies have shown that older animals gain wound strength at a slower rate [46]. A significant delay in wound closure by old rats was documented during the early phases of repair, after which closure rates were equivalent and in-vitro studies showed that despite differences in contraction by skin fibroblasts there are no changes in apoptotic or myofibroblast cells [3]. A 20% to 60% delay in healing rates has been reported in aged animals when compared to their young counterparts [47]. Intriguingly, despite non-healing wounds being more prevalent in aged skin, there is now a consensus that rather than being defective, healing in elderly patients not suffering from concomitant diseases is simply delayed and the final result is qualitatively similar to that of the young. In fact, Ashcroft et al [16, 38] demonstrated that acute wounds heal with an enhanced quality of scarring in aged individuals. Associated with this was an increased level of elastin and fibrillin expression (particularly in females) leading to regeneration of the dermal architecture and enhanced macroscopic and microscopic scar quality. The phenomenon of enhanced scar quality with age may reflect upregulated type III collagen [48] and reduced levels of TGF-β [3], properties which distinguish the regenerative ability of foetal over adult wound healing.

1.3 Replicative Senescence

It is universally accepted that human aging has, at least in part, a cellular origin. The principle changes that occur in the resident cell populations within the dermis have been suggested to result from the accumulation there of senescent cells with an altered cellular phenotype and a decreased ability to divide in response to damage or cell loss

[49]. While a number of these changes may relate to environmental factors such as photodamage [50], the inverse relationship between donor age and replicative lifespan suggests that the histochemically observed accumulation of senescent cells within the dermis represents a component of organismal aging [51, 52].

The phenomenon 'replicative senescence' is the term used to describe cells that have lost the ability to divide yet remain metabolically active [53]. It is well established that in replicative senescence, with the exception of 'immortal' embryonic germ and tumour cells [54], all human cells exhibit a limited number of population doublings before they enter a non-dividing state, which is characterised by irreversible growth arrest of cell proliferation within the G1 phase [49], even if stimulated with mitogens [55]. This limited replicative potential is also associated with increased cell size and distinct flat morphology, senescence associated β-galactosidase activity, a wide change in gene expression [49, 54-56] and synthesis of growth factors, cytokines and ECM components [57]. It has been reported that such changes in gene expression may occur much earlier in the replicative lifespan[56].

Cellular senescence can be brought about by a number of factors, including oxidative stress [49, 54, 58] radiation [58] and may be induced experimentally by repeated subdivision in culture, a model developed by Hayflick in the 1960s and for this reason replicative senescence is sometimes referred to as Hayflick's Limit [53]. Gradual telomere erosion with successive cell division is thought to be the primary intrinsic trigger of replicative senescence in many somatic cell populations [57, 59] and may have the potential to contribute to organismal aging [57, 60]. However, *in-vivo* cellular senescence which seems to increase with age may result from stresses that the cells sustain through their lifetime and not because they are replicatively exhausted and the term stress-induced premature senescence rather than true replicative senescence could account for impairment of fibroblast function in non-healing wounds [54]. Accordingly, in one study, telomere length in fibroblasts did not correlate with donor age, as fibroblasts from centenarians still undergo many population doublings *in-vitro* [61] and telomere independent senescence has been described [49]. Senescence may be an underlying cause of aging that evolved to prevent the uncontrolled growth of cells,

known as cancers and accordingly senescence plays an important role as a tumour-suppressor mechanism [62-64].

It was proposed early on that replicative senescence in culture mimics organismal aging, particularly aspects of aging, such as delayed wound healing, declining immune response, and thinning of the skin [59]. The general assumption that the aging process is mirrored by cellular senescence *in vit*ro is based on lower replicative capacity of human fibroblasts from patients with accelerated aging syndromes [65], patients with age related diseases such as diabetes mellitus, and donors of higher chronological age [54]. However, these inverse relations have not been reported unequivocally [54, 66], particularly when health status and biopsy conditions were controlled [55]. The relationship between cellular senescence and aging *in vivo* is still not clear but given the duration of aging in humans, cell culture studies are a promising approach to the study of human aging.

1.4 The Fibroblast

This thesis is principally concerned with the activities of the fibroblast. Fibroblasts within the dermis play a pivotal role in controlling wound healing responses; both age-and site-specific variations in fibroblast phenotype have been related to the observed wound healing phenotype [49]. Within each wound healing phase, fibroblasts execute critical tasks dependent upon the fibroblast capacity to migrate to the wound bed and proliferate. The fibroblasts capacity to migrate and proliferate basally and in response to growth factors has been shown to be decreased markedly as fibroblasts near senescence both *in vivo* and *in vitro* [35, 67]. This is likely to be a major causative reason for the delay and decrease in wound healing in aged individuals, a phenomenon which is the main tenet of this thesis.

Fibroblasts are the most abundant cell-type in physiological connective tissue [68] and their prime function relates to the disposition of the extracellular matrix (ECM) and its remodelling during normal and pathological processes, such as wound healing [69]. Like other cells from the connective tissue, fibroblasts are derived from the embryonic

mesoderm and thus express the intermediate filament protein, vimentin. Fibroblasts are mesenchymal cells and are generally considered to have a uniform morphology and are bipolar and spindle-shaped [68] and their actin cytoskeleton is organised into a cortical network mostly concentrated just beneath the plasma membrane and they display immature focal adhesions

1.4.1 Fibroblast Origin

Depending on the type of tissue to be remodelled, myofibroblast precursor cells are recruited from different sources; among these locally residing fibroblasts seem to be the most common [70]. Other mesenchymal cells that serve as fibroblastic progenitors are pericytes and smooth muscle cells (SMCs) from the vasculature; they seem to play an important role during vessel repair and have been suggested to contribute to fibrosis in scleroderma [71]. In addition, bone marrow derived cells or fibrocytes have been suggested to represent an alternative source for fibroblastic cells during skin wound healing and in liver, lung, and kidney fibrosis and represent an important source of fibroblasts during healing of extensive burn wounds where it might be difficult for fibroblasts to migrate from the edges of the injury [72]. This large spectrum of precursors further underlines the crucial function of the fibroblast in maintaining tissue homeostasis.

1.4.2 Role of Fibroblast in Wound Healing

After tissue injury, cytokines locally released from inflammatory and resident cells [6] induce fibroblastic migration into the provisional matrix formed by the fibrin clot, whereupon the fibroblasts proliferate and restore ECM components [68] to initiate and perpetuate the wound healing processes. Gradually, fibroblastic cells replace the provisional fibrin matrix with a loose matrix called granulation tissue, composed of new blood vessels, fibroblasts, inflammatory cells, endothelial cells, myofibroblasts, and the components of a new, provisional ECM which supports further ingrowth of cells and are essential for the repair process. Crucial interactions between the ECM and fibroblasts help regulate further ECM synthesis and its subsequent remodelling.

Fibroblasts produce the matrix components fibronectin, hyaluronan (HA) and later collagen and proteoglycans.

Once within the wound site, fibroblasts proliferate and differentiate into an activated phenotype called myofibroblasts. These differentiated fibroblasts are the main cell type involved in deposition and remodelling of ECM and ultimately they undergo contraction [73], decreasing the size of the wound and bringing the wound edges into closer proximity. The formation of granulation tissue in an open wound allows for reepithelialization and construction of a preliminary dermis. Whilst the age-related changes in proliferative and migrative capacity have been well documented [35], less is known regarding alterations in phenotypic transformations that accompany aged fibroblasts. This thesis attempts to clarify these changes.

In normal conditions, fibroblastic cells exhibit few or no actin-associated cell-cell and cell-matrix contacts and little ECM production [74]. Within the ECM, fibroblasts are under resting mechanical tension, thus ensuring that the connective tissue maintains its shape. Fibroblasts are also stress shielded by the ECM preventing development of stress fibres [70, 75] On a cellular level, mechanical strain on the ECM is transmitted through integrins to intracellular focal adhesion complexes and the actin cytoskeleton, to alter cell signalling [76]. This process, termed mechanotransduction, integrates mechanical cues and growth factor-induced intracellular signals to modulate cell functions important for wound healing. Fibroblasts in intact tissue are generally stress-shielded by the crosslinked ECM and do not develop contractile features and cell-matrix adhesions. In the continuously remodelled ECM of injured tissue this protective structure is lost. Numbers of fibroblasts increase within the wound and continuous synthesis of ECM components [77] enhances matrix rigidity by applying small transitional forces to the newly formed granulation tissue [78].

In response to mechanical challenge following injury fibroblasts become activated and acquire a migratory phenotype termed the proto-myofibroblast that contain initially only β - and γ -cytoplasmic actins [68, 70].

1.4.3 Myofibroblastic Differentiation

With increasing stress in the ECM resulting from their autocrine remodelling activity, proto-myofibroblasts further develop into differentiated myofibroblasts (see figure 1.1). Their actin skeleton reorganises to form large bundles that run in parallel and terminate at the cell periphery and they display an increase in the thickness and number of stress fibres [79]. In addition to pre-existing β - and γ -cytoplasmic actins they are characterised by expression of α -smooth muscle actin (α -SMA) [72], a mechanosensitive protein [70] normally found in smooth muscle cells. Hence, myofibroblasts have structural properties between those of a fibroblast and a smooth muscle cell [80].

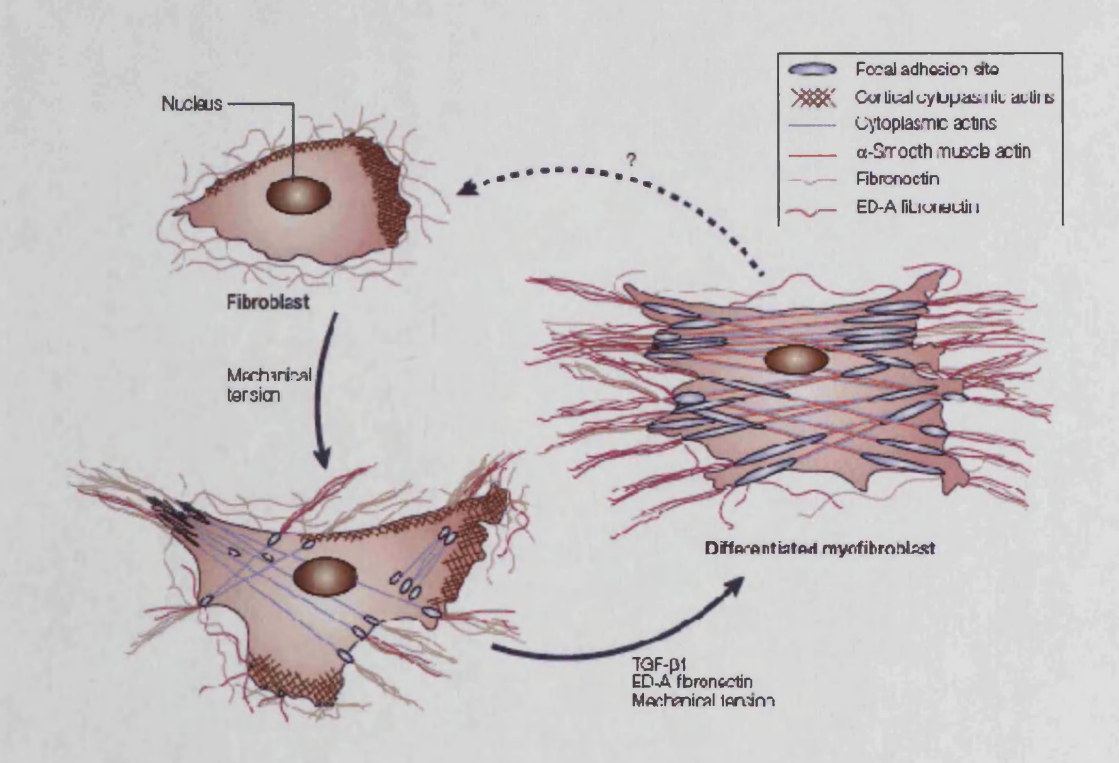


Figure 1.1: Two step process of myofibroblastic differentiation *in-vivo*. Following an increase in mechanical tension fibroblasts become activated and acquire a migratory phenotype termed the protomyofibroblast. Proto-myofibroblast are characterised by the presence of stress fibres containing filamentous actins and synthesis of ED-A fibronectin. In the presence of prolonged mechanical tension, ED-A fibronectin and TGF- β 1 further differentiation occurs to a contractile phenotype, termed a differentiated myofibroblast, characterised by the expression of α -SMA. Taken from [74].

Morphologically, myofibroblasts have characteristic flattened, irregular shapes and well-developed cell matrix interactions and intracellular gap junctions [81]. They can also be recognized by the ability to express other smooth muscle cell contractile proteins such as desmin, calponin and smooth muscle myosin [74, 82]. Nevertheless, incorporation of α -SMA into stress fibres remains the most reliable marker of the myofibroblastic phenotype [72].

Expression of α -SMA in stress fibres confers to the differentiated myofibroblast at least a two-fold stronger contractile activity compared with α -SMA negative fibroblasts in culture [70]. The cellular mechanisms responsible for the α -SMA mediated increase in contraction are largely unknown. What is certain is that generation of α -SMA-positive differentiated myofibroblasts is dependent on the production by inflammatory cells of biologically active transforming growth factor- β , the most accepted stimulator of myofibroblastic differentiation [72]. TGF- β neutralizing monoclonal antibody strongly reduces α -SMA induction in dermal fibroblasts [83]. The action of TGF- β is dependent also on the local presence of the cellular fibronectin splice variant ED-A [72]. ED-A fibronectin is expressed in the initial stages of wound healing and along with collagen I is positively regulated by TGF- β [84]. In the absence of TGF- β and/or the ED-A fibronectin, fibroblasts can differentiate into the proto-myofibroblast but not to the myofibroblast phenotype [74, 85].

Myofibroblasts are involved in the remodelling and deposition of new ECM and ultimately granulation tissue contraction and wound closure [68, 70, 72, 86]. They are also responsible for subsequent wound contracture and formation of a collagen rich scar [86]. They produce the matrix proteins fibronectin, and later collagen types I and III, elastin, glycosaminoglycans and proteoglycans [79, 87]. Myofibroblasts also secrete various enzymes such as MMPs and tissue inhibitor of the ECM [88], which are capable of altering the composition of the ECM. In addition, myofibroblasts can function as immune cells and play a significant role in modulating wound repair through the release of chemokines, growth factors, and cytokines such as monocyte chemotactic protein-1 (MCP-1), interleukin-1 (IL)-1, IL-6, IL-8, hepatocyte growth factor (HGF), TGF-β and EGF, reviewed in [89].

Although both fibroblasts and myofibroblasts contribute to normal wound repair the latter are present for a finite period and when contraction stops and the wound is fully epithelialized few if any α-SMA-containing myofibroblasts are found in the scar [90]. It is still unclear whether, during healing, all myofibroblasts undergo apoptosis [68] and hence represent terminally differentiated cells [86] or if some revert back becoming fibroblasts suggesting that these fibrotic cells in fact represent alternate phenotypes [91]. It should be noted that whilst massive apoptosis has been demonstrated *in-vivo* reversal of the myofibroblast has not [68]. Whilst the signals leading to mass suicide are still unclear, at the end of tissue repair, the reconstructed ECM once again takes over the mechanical burden and this stress release appears to be a powerful promoter of cell death and myofibroblast removal [68, 70].

1.4.4 Fibroblast Heterogeneity

Fibroblastic cells represent a heterogeneous group of cells that show functional subpopulations during normal conditions in-vivo [92]. Fibroblasts differ between organs and also within tissues and show intrinsic differences with respect to size, morphology, proliferation rates and collagen turnover [93]. Fibroblasts derived from non-glabrous versus glabrous skin (e.g. palms and soles) demonstrate differential proliferative capacity and myofibroblastic differentiation [84]. It has been suggested that some pathological conditions could be due to the recruitment of fibroblast subtypes, leading to the predominance of a particular population or alternatively to the modulation of phenotypic features of fibroblasts. For example, distinct fibroblast subpopulations in the human reproductive tract contribute differently to the development of inflammation by their secretion of soluble mediators [93]. Wall et al demonstrated that, compared to healthy skin normal fibroblasts, chronic wound fibroblasts aberrantly express genes that regulate the ECM and cytoskeleton, show a decreased ability to repopulate wounds and an impaired ability to produce the correct stromal address code required to drive an acute-phase inflammatory response [94]. In the same study, chronic wound fibroblasts, from different patients, demonstrated very different proliferative capacities. By the authors' own admission this was an indication of the heterogeneous wound environments that the cells were derived from, despite the wounds demonstrating clinical parallels.

In most cases, repair involves a healing process that is imperfect, producing a fibrotic scar rather than flawless regeneration of the original tissue architecture. In contrast to the scarring observed in adult dermal wounds, wound healing in the oral mucosa is clinically distinguishable by an increased ability to migrate and repopulate a wound with no discernable scar formation [95]. The oral mucosal healing process includes the same basic steps as cutaneous wounds, however, the unique outcome in the mucosa suggests that an altered series of events occurs in response to injury [96]. Several studies have demonstrated that the differences in these two tissues in healing potential may be a direct result of distinct phenotypic differences between respective fibroblast populations [95]. As with wounds in the oral mucosa, human foetus cutaneous wounds heal rapidly and perfectly with no scar formation [69, 97]. Foetal fibroblasts are the major effector cells responsible for this phenomenon [98]. However, it is unclear as to whether myofibroblasts play a role during foetal wound healing. Some authors report that there is no apparent conversion from fibroblast to myofibroblast in embryonic healing [6], whilst others maintain that fibroblasts do indeed differentiate into myofibroblasts, but that this response is altogether more rapid and short lived [99].

The fibroblast lineage is thus not a homogeneous population of cells but rather one that is typified by an enormous degree of phenotypic plasticity. A delineation of the role of each fibroblast subpopulation may provide insight into the development of treatments for pathological conditions such as age-related chronic wounds. The question this thesis attempts to answer is whether fibroblast phenotypic plasticity extends to cellular aging? Numerous studies have investigated embryonic and oral tissue repair in a search for molecular differences that could explain the near "perfect" manner in which they heal when compared to their adult dermal counterparts. It has been demonstrated that site-specific differences in TGF-β production may contribute to their superior healing.

1.5 Transforming Growth Factor beta

Previous work has demonstrated the importance of TGF- β 1 in controlling wound healing and mediating the "scarring" phenotype of adult dermal wounds. Furthermore, alterations in the migratory and signal transduction responsiveness to TGF- β 1 have been postulated to explain the age-related defects in human wound healing [100]. Many factors influence repair and one factor that has been intimately linked to wound healing and scar formation is TGF- β . TGF- β is an extracellular protein ubiquitously produced by all cells [101]. Major sources of TGF- β include activated macrophages, lymphocytes, bone, kidneys, fibroblasts, smooth muscle cells and due to the influence of mechanical tension, myofibroblasts themselves [78, 101].

The TGF- β family of proteins consists of several structurally related but functionally distinct isoforms. In mammals, three isoforms, TGF- β 1, - β 2 and - β 3, have been identified [78, 102]. These isoforms are known to play distinct roles in cell growth, differentiation and ECM formation [78] migration and angiogenesis [101]. All of these processes are important in tissue development and wound healing [102]. They are encoded by different genes but share the same receptors and intracellular signalling pathways [103, 104].

TGF- β 1 is synthesised as an inactive precursor. Following translation the inactive propeptide is secreted as a large latent complex, covalently bound with latency associated peptide (LAP) and is stored in this inactive form in the matrix. Activation of TGF- β 1 occurs by proteolytic cleavage of the LAP from the latent molecule, allowing the bio-active TGF- β 1 to interact with specific receptors at the cell surface [105].

1.5.1 TGF- β in Wound Healing

A central event in tissue repair is the release of cytokines in response to injury. A wealth of evidence points to TGF- β as a key cytokine that initiates and terminates tissue repair. Upon cutaneous injury, TGF- β is rapidly induced [106]. Expression of TGF- β receptors are also elevated [106]. Immediately after injury, degranulating platelets release TGF- β 1 that is chemotactic for the inflammatory cells neutrophils and macrophages and

mitogenic for collagen-producing fibroblasts [102], which in turn release more TGF-β1 [106]. TGF-β1 is also known to promote fibroblast proliferation [107]. In addition, production and activation occur during the wound healing process through autocrine and paracrine feedback loops [102]. In injured tissue, TGF-β1 continues to be produced and activated during all phases of wound healing and in response to several stimuli including plasmin, thrombospondin and reactive oxygen species [102]. TGF-β1 is known to induce the formation of granulation tissue and has been shown to stimulate fibroblast collagen synthesis *in vitro* [108].

TGF- β 1 inhibits the expression of MMPs, proteases that regulate ECM degradation [78]. TGF- β 1 also enhances the expression of protease inhibitors, including plasminogen activation inhibitor-1 (PAI-1) and TIMPs and also increases the expression of the ECM components collagen, laminin, and fibronectin [78]. Hence TGF- β 1 not only enhances collagen and ECM production, it also inhibits their degradation. Also, focal adhesions are known to mature in response to TGF- β 1, resulting in increased cellmatrix adhesions and ECM deposition [109]. This control of the ECM has implicated TGF- β 1 as an important factor in fibrotic tissue formation, and scar formation, suggesting a central role for TGF- β 1 in wound healing. [68, 70, 102]. Significant to this body of work, TGF- β 1 is also the main promoter of fibroblast-myofibroblast transdifferentation, associated with enhanced α -SMA expression [72, 110-112].

Dysregulation of TGF- β 1 action has been implicated in a variety of pathological processes including cancer [113], autoimmune disease and inflammatory disorders [114]. Mice over-expressing or lacking specific TGF- β family members or their receptors demonstrate profound effects in the development or homeostasis of many organs [115, 116]. Dysregulated TGF- β receptor (TGF- β R) signalling has been shown to play a role in chronic fibrotic disease such as scleroderma [106]. Alterations in the ratio between TGF- β RI and TGF- β RII may contribute to sustained fibrosis [117].

TGF- β 1 is responsible for accumulation of myofibroblasts and ECM deposition [118-120], making the prolonged release of TGF- β 1 a candidate for fibrotic disorders [121]. TGF- β 1 itself is insufficient to result in persistent fibrotic responses *in vivo* or *in vitro*,

and synergy between other extracellular ligands such as connective tissue growth factor (CTGF) was shown in a mouse fibrotic model [122]. Increased levels of TGF-β1 have been reported in a variety of diseases associated with renal fibrosis including glomerulonephritis [123] and diabetic nephropathy [124]. Furthermore, the over expression of TGF-β1 has been shown to induce chronic kidney disease [125]. TGF-β1 null mice showed a decreased rate of granulation tissue formation and increased rate of epithelialisation compared to wild-type controls suggesting that TGF-β1 may act to increase inflammation and delay wound closure [126]. That said the administration of TGF-β1 greatly enhances the repair of injured tissues in several studies. When applied topically, healing is improved in a variety of wound models, including incisional and excisional wounds, punch wounds and ulcers [101].

1.5.2 TGF-β Signalling

TGF- β 1 is known to be involved in a wide range of cellular processes, and for TGF- β signalling to occur TGF- β must bind to one of its receptors. There are three types of TGF- β R termed type I, type II, and type III. These are located on the cell membrane of virtually all cells [127]. The type III receptor (TGF- β RIII), also known as Betaglycan, is a membrane anchored proteoglycan that has no signalling structure but acts to present TGF- β to other receptors. The type I and type II receptors are trans-membrane serine-threonine kinases that interact with one another and appear to be directly involved with TGF- β signalling [128]. For signalling to occur binding of active TGF- β 1 to the TGF receptor type II serine/threonine kinase receptor (TGF- β RII), leads to the phosphorylation and recruitment of TGF- β type I receptors (TGF- β RII) into a heteromeric receptor complex. The serine/threonine kinase activity of the activated complex propagates signals inside the cell leading to transcription of various genes. This occurs principally through activation of the Smad signalling pathway although TGF- β signalling can also occur via a number of Smad independent pathways.

1.5.2.1 Smad Related TGF-\(\beta\)1 Signalling

The serine/threonine kinase activity of the activated complex propagates signals inside the cell through phosphorylation of receptor-activated (R)-Smads, a family of transcriptional factors which can be subdivided into two branches: those which are activated by TGF-β and activin (Smad2 and Smad 3) and those which are activated by bone morphogenetic protein 7 (BMP-7) signalling (Smad1, Smad5 and Smad8) [129, 130].

Once phosphorylated, Smads associate as heterodimeric complexes with Smad4, enter the nucleus, and bind to specific DNA sequences where they initiate target gene transactivation, either alone or in association with other transcriptional partners [131]. The inhibitory Smads, Smad6 and Smad7, have the ability to form stable associations with TGF- β RI and to interfere with both phosphorylation of Smads and heteroligomerization with Smad4 [78].

As earlier mentioned, TGF- β 1 is the main mediator of myofibroblastic differentiation, characterised by the up-regulation of α -SMA. The major pathway through which TGF β 1 regulates expression of α -SMA in fibroblastic cells is via Smad signalling [112, 132]. Transcription of α -SMA in lung myofibroblasts and in myofibroblast-like activated hepatic cells was reportedly predominantly mediated by the binding of Smad3 to the Smad-binding element 1 upstream of the α -SMA core promoter sequence [132, 133]. In contrast, another study demonstrated that overexpression of Smad2 but not Smad3 induces myofibroblastic differentiation in lung fibroblasts [112]. This discrepancy may be due to different roles of Smad2 and Smad3 depending on the level of myofibroblast differentiation [134]. Interestingly Ashcroft showed that Smad3 null mice present enhanced cutaneous epithelialisation and wound healing [135], whereas overexpression or exogenous application of Smad3 was found to accelerate myofibroblast differentiation and subsequent wound healing in rabbit dermal fibroblasts [136]. Targeted deletion of Smad2 or Smad3 genes in mice and in embryonic fibroblasts revealed distinct non-redundant roles for each of these transcription factors [137].

Whereas Smad2 null mice die in early gestation from defects in gastrulation and mesoderm formation, mice with homozygous deletions in the Smad3 gene are viable but display impaired immune function and defective neutrophil chemotaxis [138]. These observations suggest that there are fundamental differences in the processes mediated by Smad 2 and Smad3 *in-vivo*. Currently, it is debatable as to which of the R-Smads is the most important in terms of myofibroblastic differentiation; this thesis will attempt to clarify Smad signalling in dermal fibroblasts.

TGF- β 1-induced α -SMA expression during myofibroblastic differentiation has been shown to proceed in a Smad-independent manner under certain circumstances [68, 139]

1.5.2.2 Non-Smad Related TGF-β1 Signalling

Smad proteins are critical to many of the actions of TGF- β 1. Alternatively, TGF- β 1 can regulate fibroblast gene expression independent from Smad signalling [129, 140]. In one study Smad-independent TGF- β 1 mediated induction of myofibroblastic differentiation was shown to be regulated via activation of phosphatidylinositol 3-kinase (PI3K) and the downstream effector p21-activated kinase-2 [141] and regulated through the TGF- β 1 control element [142]. The mitogen-activated protein kinase /extracellular-signal-regulated kinases (MAPK/ERK) pathway is required for fibroblast spreading and actin stress fibre formation in fibroblasts [139]. Chen et al showed that syndecan 4 is required in fibroblasts to integrate TGF- β /ERK signals to induce α -SMA expression [139].

Non-Smad signalling proteins have several general mechanisms by which they contribute to physiological responses to TGF-\$\beta\$1. Non-Smad signalling proteins can directly modify Smad activity either positively or negatively [106]. TGF-\$\beta\$1 activation of the PI3K pathway has been shown to phosphorylate Smad3 and enhance its transcriptional activation of the collagen I gene in mesangial cells [129]. In contrast, the absence of Smad3 confers radioprotection in primary dermal fibroblasts through enhanced MAPK-ERK signalling [143]. Such 'lateral signalling' by Smad and non-Smad interactions helps to explain the diverse array of responses, sometimes conflicting

(i.e. apoptosis or differentiation), that can result from binding of TGF- β 1 to a single receptor complex.

Secondly, Smads can directly interact and modulate the activity of non-Smad proteins which transmit signals to other pathways. ERK-MAPK has been shown to directly affect Smad3 phosphorylation and vice versa [140]. TGF- β receptors can directly interact with or phosphorylate non-Smad-proteins, thus initiating parallel signalling that cooperates with the Smad pathway [129].

ERK, p38 MAPK (p38) and c-Jun N-terminal kinases (JNKs) have all been implicated in TGF-β1 signalling [129]. Chondrocyte differentiation involves Smads and non-Smad effectors such as Protein Kinase A (PKA), p38 and ERK [129, 144]. One study demonstrated that antagonising either MAPK/ERK or TGF/ALK-5 suppressed matrix contraction by dermal fibroblasts, suggesting that integrating TGF-β and ERK signals is essential for contraction [139].

Overall, these studies point to the potential complexity of the interplay among Smad and non-Smad signalling interactions in the control of wound healing processes.

1.5.3 TGF-\$1 Signalling and aging

Wound healing is critically affected by age and growth factors such as TGF-β1. The combined effect of these factors on fibroblast migration proliferation and differentiation, essential components of wound healing, are poorly understood. Mogford et al have demonstrated that alterations in the migratory and signal transduction responsiveness to TGF-β1 may explain the age-related defects in human wound healing [100]. They demonstrate that age-dependent differences in TGF-β1 responsiveness are, in part, supported by a depressed expression of TGF-β receptors and activation of downstream effectors. This might explain why application of TGF-β1 has failed to, [145] or only partially [146], reversed the healing deficit associated with wounds in aged animals because of intrinsic cellular deficits. Failure of TGF-β1 to stimulate an

increase in age-related wound healing correlates with a failure of growth factors to produce favourable clinical trials [147].

1.6 Extracellular Matrix

One emerging theme in aging research is that a number of changes may not have their origins in age-related cellular changes but rather in the cellular microenvironment, including the local structural architectures. Each can influence the other in a manner where cause and effect are difficult to separate. Thus, an understanding of age-related changes in the structural microenvironment of the skin is an important factor in any discussion in aging and wound healing.

It is beginning to be appreciated that the materials that lie between cells, the matrix components, have major instructive roles for cellular activities. This extracellular matrix (ECM) is the principle component of connective tissue but its functions extend from its role as a scaffold to include tissue homeostasis and it is implicated in cell migration, growth, differentiation, wound healing and a variety of disease states. ECM components are synthesised by a variety of mesenchymal and parenchymal cells. Its extracellular distribution can be in the form of cell-associated pericellular matrices and structures that surround the periphery of the cells. Synthesis and remodelling of the ECM is necessary for scar tissue formation, however, excessive synthesis and remodelling of the ECM can lead to progressive fibrosis, characteristic of numerous fibrotic disorders. The components of the ECM, although appearing amorphous by light microscopy, form a structure of glycosaminoglycans (GAGs), proteoglycans, highly organised glycoproteins, peptide growth factors and structural proteins such as collagen and to a lesser extent, elastin.

In terms of morphology, aged skin is characterised by reduced dermal thickness, reduced number of cells, and a disorganised microcirculation [3]. The thickness of the epidermis, which functions as a barrier to water, remains the same with age but is associated with flattening of the dermal-epidermal junction, giving the appearance of atrophy [148]. GAG and collagen levels not only fall but the physical properties of

collagen itself changes with age [3]. Elastin levels appear to remain constant but as with collagen it is functionally different with age, leading to decreased elasticity of the skin [149]. Such changes may lead to modified cellular responses resulting from altered matrix binding of growth factors, impaired cellular migration/proliferation in response to changes in matrix structure, quantity and/or adhesion molecule expression and altered signalling between matrix and cells leading to downstream changes in gene expression [3]. Changes in the composition of the ECM and matrix receptors occur under physiological and pathological conditions such as the menstrual cycle, the development of diabetes, tumour progression and, significantly, the aging process and wound healing [150]. During wound healing, particularly the early stages, the ECM is rich in HA [151] where it functions as an organiser of the ECM; as a scaffold about which other macromolecules of the ECM orient themselves.

1.7 Hyaluronan (HA)

1.7.1 Structure and Biology of HA

HA is a high-molecular-weight, anionic linear polymer [151] composed of repeating alternating units of glucuronic acid and N-acetylglucosamine, all connected by β-linkages (See Figure 1.2), that can reach a molecular mass of several million Daltons [152]. HA is unusual among the GAG family because it is not sulphated or covalently linked to a core protein throughout its length [152, 153]. HA is, hence, the only non-proteoglycan GAG. Furthermore, unlike other macromolecules, which are synthesised in the Golgi apparatus, HA is synthesised at the inner leaflet of the plasma membrane which allows for extrusion of HA chains of unconstrained size [154].

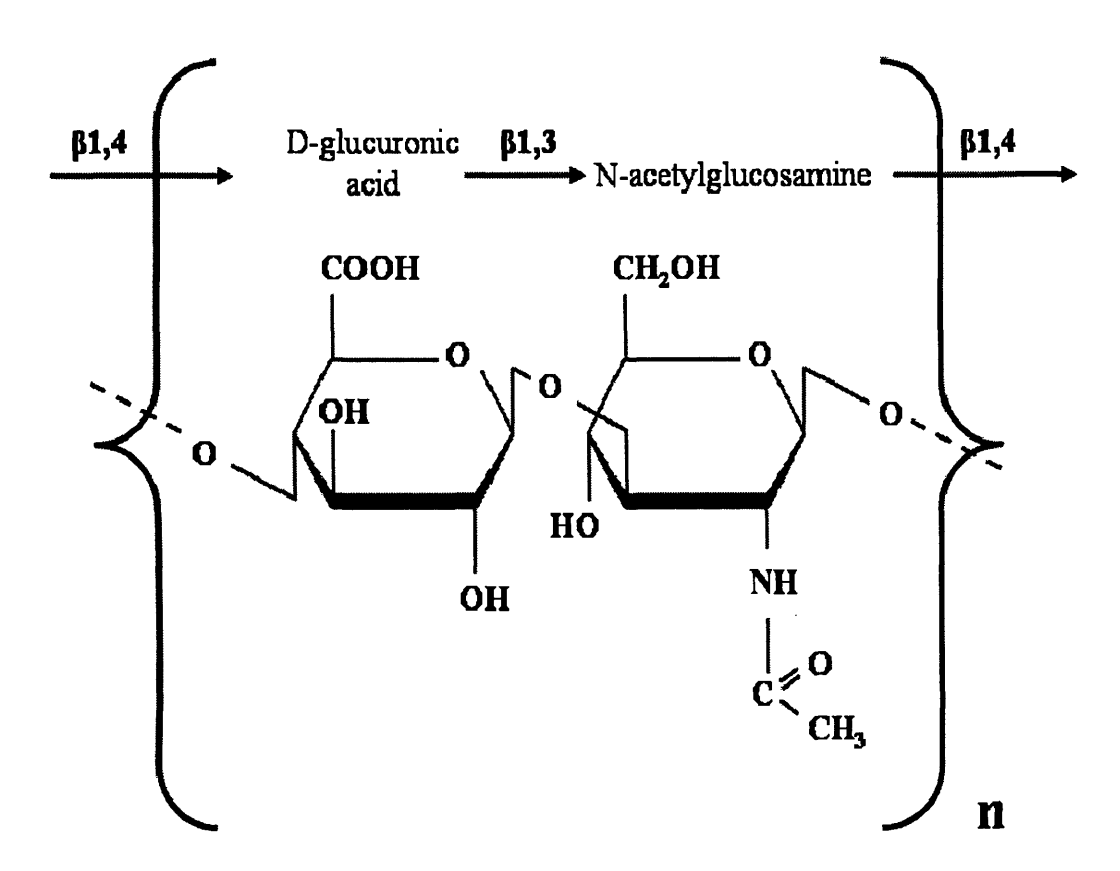


Figure 1.2: The chemical structure of hyaluronan.

HA is present throughout the body, identified in virtually every vertebrate tissue. The total amount of HA in an adult human has been estimated to be 20 g, the highest concentrations occurring in the vitreous of the eye, (where it was first found), soft connective tissues (synovial fluid of articular joints and the intercellular space of the epidermis) and in the umbilical cord as Wharton jelly [152, 153]. More than 50% of total body HA is present in the skin, of which the majority is found in the dermis as opposed to epidermis [155].

Physicochemical studies indicate that the polymer can take on a vast number of shapes and configurations, dependent on polymer size, pH, salt concentration and associated cations. HA also occurs in a number of physiologic states, circulating freely, tissue-associated by way of electrostatic interactions but easily dissociated and in equilibrium with the HA in the rest of the body [151].

Despite the simplicity of its composition, without branch points or apparent variations in sugar composition, HA has a great number of diverse functions which fall into three

overlapping categories: Firstly, HA greatly influences the hydration and physical properties of tissues. The molecular domain of HA encompasses a large volume of water that expands extracellular space, hydrates tissues and, in high concentrations, as found in the ECM of the dermis is responsible for skin moisture [151, 156, 157]. Due to its moisturising effect it has also widely been used as an ingredient in skin care products and has been used as a space-filling complex in cosmetic surgery [158]. Secondly, HA acts as an organizer of the ECM; it is not only the central scaffold about which other macromolecules of the ECM orient themselves [151], it also interacts with other ECM macromolecules (including the proteoglycans aggrecan and versican), which are essential to the structure and assembly of several tissues [157]. Finally, HA interacts with cell surface receptors, notably CD44, and thereby influences cell behaviour [158]. The ability of HA to form a pericellular coat, a unique environment in which many cell types reside, illustrates the interrelation of these three functions. Formation of pericellular coats depends on the large hydrodynamic domain occupied by HA, its interaction with extracellular proteoglycans, and its interaction with the cell surface [157] (see HA Pericellular Coats below). Furthermore, HA promotes cell motility, regulates cell-cell and cell-matrix adhesion, promotes proliferation and influences differentiation [159-162]. It participates in such fundamental processes as embryological development and morphogenesis [163], wound healing [164], repair and regeneration and inflammation [165]. HA levels increase in response to severe stress and in tumour progression and invasion [166]. The tight regulation required for HA deposition in association with these multiple and diverse processes depends on net levels of synthesis and degradation.

1.7.2 Synthesis and Catabolism

In vertebrates, the HA cytoplasmic product is produced on the inner face of the plasma membrane of fibroblasts and directly extruded through the plasma membrane into the extracellular space permitting unconstrained polymer growth. This is unlike other extracellular polysaccharides that are synthesised in the Golgi [152]. Synthesis occurs by hyaluronan synthase (HAS) sequentially adding sugars to the reducing terminus [152]. HAS are glycosyl transferases that occur in vertebrates, bacteria, and algal

viruses [167]. There are three synthase genes in the mammalian genome, coding for HAS1, 2, and 3 [153]. They have distinct expression patterns controlled, in part, by various growth factors and cytokines [168]. Expression of the HAS genes also appear to be tissue specific [168], each producing a different size polymer [169]. HA is very metabolically active, with a $t_{1/2}$ of 3 to 5 minutes in the circulation, less than 1 day in skin and even in an inert a tissue as cartilage, the HA turns over with a $t_{1/2}$ of 1 to 3 weeks [151]. The turnover of HA in mammalian tissue is astonishing. There are 15 g of hyaluronan in the 70-kg individual, of which 5 g are cycled daily through this pathway [153]. This rapid turnover is due in part to lymphatic removal of HA from the tissues and subsequent degradation in lymph nodes and liver [170]. It is proposed that scavenger receptors expressed on liver endothelial cells are responsible for part of this degradative process [171]. The principle enzymes involved in turnover of HA are the hyaluronidases (Hyals), endoglycolytic enzymes with a specificity in most cases for the β -1,4-glycosidic bond that break down the HA polymer into smaller fragments. Six homologous Hyals genes have been found in the human genome. Recent work has been focused on elucidating the function of these Hyal proteins. The two primary mammalian Hyals, Hyal-1 and Hyal-2 are involved predominately in HA catabolism in somatic tissues and have different activities and degrade HA to either oligosaccharides or larger fragments [172].

Degradation begins when extracellular high mass HA polymers of the ECM are tethered to the cell surface through the combined action of CD44 and Hyal-2 [167]. This metabolic cascade begins in lipid raft invaginations at the cell membrane surface. Hyal-2 interacts with CD44 and with a Na⁺-H⁺ exchanger termed NHE1 that creates an acidic microenvironment for the acid-active Hyal enzyme [173]. Endolytic cleavage by the Hyal occurs in a series of discreet steps generating HA chains of decreasing sizes. The enzyme makes the initial cleavage generating 20 kDa sized products of approx 100 saccharides [174]. The Hyal-2-generated HA fragments are internalised, delivered to endosomes and ultimately to lysosomes, where Hyal-1 degrades the 20kDa fragments to small disaccharides [153]. Despite their exceedingly simple primary structure, HA fragments have extraordinary wide-ranging and often opposing biological functions. The biological functions of the oligomers at each quantum step differ widely. The very

large HA polymers are among the largest of matrix molecules and depending on tissue source and physiological conditions can reach sizes of 10⁵ kDa. [175]. They are space filling, hydrating, anti-angiogenic, [176] anti-inflammatory and immunosuppressive [177, 178] extracellular polymers [151, 153, 165, 167, 179]. This derives in part from the ability of the space-filling polymers to prevent ligand access to cell surface receptors. The foetal circulation and amniotic fluid contain high concentrations of HA. This may account for some of the immunosuppression in the developing foetus [153]. High molecular HA can also have an array of regulatory and structural functions. Additional functions include ovulation, embryogenesis, protection of epithelial layer integrity wound healing and regeneration [167].

20-kDa intermediate polymers are highly angiogenic, inflammatory immunostimulatory [153]. They stimulate endothelial recognition of injury [180], induce inflammatory gene expression in dendritic cells [181] attracting inflammatory cells, and also induce expression of inflammatory cytokines in such cells [165]. HA degradation products are reported to contribute to scar formation [182]. Foetal wounds heal without scar formation and wound fluid HA is high molecular weight [183]. When Hyal is added to generate fragments, there is increased scar formation [182]. Collectively, these data support the concept that while high molecular mass HA promotes cell quiescence and tissue integrity, HA breakdown products act as endogenous "danger signals" and alert the body that injury may have occurred, initiating an inflammatory response [184]. Hence whilst turnover of HA is high in mammals, the presence of abnormally high levels of oligosaccharide fragments signal tissue damage or invasion, which can elicit defence mechanisms, cellular differentiation and tissue morphogenesis (e.g. angiogenesis).

Degradation into yet smaller oligomers induces expression of heat shock proteins which are anti-apoptotic [185]. So fragments of HA in the course of catabolism generates products with size-specific and widely differing biological activities; fragments that are involved in essential processes. Wound healing serves as a fine example of the precise regulation required of HA catabolism (see HA and Wound Healing below).

1.7.3 HA Binding Proteins and Receptors

The wide range of biological actions of HA is postulated to derive in part from its interaction with a wide number of hyaladherins, a term coined by Toole [186] to describe a heterogeneous group of proteins with the ability to bind HA. The hyaladherins associate with HA through electrostatic or covalent bonds [187]. Growth factors, collagen and a myriad of other proteins have been identified, are widely distributed in the body and have diverse functions [151]. Most of the known HA binding proteins and receptors couple to HA through a 100 amino acid globular binding domain called the "link module". The link module region is comprised of an immunoglobulin domain and two adjacent link modules. The immunoglobulin domains are most likely responsible for the link protein-proteoglycan interaction, whereas the link modules mediate binding to HA [188, 189].

Extracellular hyaladherins are a group of HA-binding proteoglycans that include aggrecan, neurocan, and brevican, constituting a gene family collectively termed 'hyalectins' [158]. These proteoglycans are components of the ECM and each proteoglycan has a characteristic distribution, with versican present in different soft tissues, aggrecan prominent in cartilage, and neurocan and brevican prominent in the central nervous system.

1.7.3.1 TSG-6

Tumor necrosis factor–stimulated gene 6 (TSG-6) is an extracellular hyaladherin closely related to the hyaluronan receptor CD44, the expression of which is tightly regulated [190]. There is little or no constitutive expression of TSG-6 in adult tissues, but the protein is synthesised by fibroblasts, chondrocytes, monocytes and vascular endothelial and smooth muscle cells in response to stimulation with pro-inflammatory mediators or certain growth factors [190, 191], where it has been shown to have anti-inflammatory and protective functions in arthritis and asthma [191]. TSG-6 has been implicated in the stabilization of ECM structure, particularly by supporting the formation of cross-linked HA networks [192]. TSG-6 catalyses the transfer of inter-α inhibitor (IαI) heavy chains to HA forming a stable, covalently linked complex which has an important role in

formation of the pericellular matrix [193, 194] and is detected in several inflammatory disease states and in the context of inflammation-like processes, such as ovulation, by influencing the expansion of the HA-rich cumulus ECM in the preovulatory follicle [195].

1.7.3.2 CD44

Cellular hyaladherins that are responsible for attaching HA to the cell surface constitute the HA receptors. HA binds to cells via three main classes of cell surface receptors: Cluster of Differentiation 44 (CD44), receptor for HA-mediated motility (RHAMM) and Intracellular adhesion molecule-1 (ICAM-1) [151, 196]. CD44 is the most prominent among these and is, therefore, considered the principle receptor for HA [151]. It is a multifunctional single-pass transmembrane glycoprotein that is encoded by a single gene that consists of 19 exons [197] consisting of four functional domains [158]. It is very widely distributed in the body being found on virtually all cells except red blood cells [151]. The appearance of HA in the dermis and epidermis parallels the histolocalization of CD44 [151]. Alternate slicing and variations in CD44 polypeptide sequence, glycosylation and oligomerization generates different isoforms and confers specific functions to the CD44 protein and its affinity for HA binding [197].

The precise biological role of CD44 *in-vivo* in various tissues remains to be determined but has been shown to be critical in maintenance of local HA homeostasis. HA-CD44 interactions participate in a wide variety of cellular functions, including cell-cell aggregation, retention of pericellular matrix, matrix cell and cell-matrix signalling, receptor mediated internalization/degradation of HA, cell migration and proliferation [151, 198]. For this reason HA-CD44-mediated interactions are critical in wound healing. For example, CD44 plays an important part in regulating leukocytes extravasation into inflammatory sites [199] and mediates phagocytosis [200]. CD44 plays an important role in resolution of inflammation and regulation of fibroblast function. CD44^{null} animals exhibited enhanced and prolonged infiltration followed by reduced myofibroblast infiltration. The healing defect in CD44-/- mice was associated

with impaired fibroblast function and markedly diminished collagen deposition in the scar [198].

Furthermore, CD44 is important in maintaining the integrity of the actin cytoskeleton [201]. The cytoplasmic tail of CD44 can interact with the actin cytoskeleton, through interaction with a number of membrane-associated cytoskeletal proteins, such as ankyrin [202, 203] and cortactin [204] which are expressed in a variety of biological systems. Such interactions cause, cytoskeleton activation and result in several important HA-mediated functions such as cell adhesion, proliferation and migration and appear to have important roles in activation of a number of signalling pathways, particularly in tumour progression [173, 205-208]. CD44 can also function as a co-receptor, physically co-localising with receptors such as TGF-β type I and type II receptors and resulting in the modulation of intracellular transduction pathways involved in TGF-β signalling [161, 203, 209, 210].

The ability of HA to associate with itself, with its receptor CD44, with proteins, or with other GAGs [211] speaks to the versatility of this molecule, qualities which are particularly advantageous for the assembly of HA-dependent pericellular coats.

1.7.4 HA Pericellular Coats

When retained at the cell surface, HA can generate a voluminous pericellular matrix or "coat". The HA-dependent coat has multiple important roles, from serving structural and mechanochemical functions, to the regulation of cell division and motility. Prominent HA coats are observed during embryogenesis, tissue remodelling, wound healing and tumour invasion [194, 212-214]. The particle exclusion assay is the most widely used technique to visualise the HA-dependent pericellular coat [215]. In this assay, a suspension of particles, usually fixed erythrocytes, is allowed to settle and a clear zone surrounding the cell is made apparent by virtue of the exclusion of the red blood cells by negatively charged pericellular HA present. Treatment of cells with HA-specific Hyal removes the pericellular coat, indicating that matrix integrity is HA-dependent [216]. HA can be tethered to the cell surface by the HAS synthases or cell

surface receptors such as CD44 (See Figure 1.3). HA crosslinking occurs with several proteoglycan molecules, which are highly negatively charged and repel each other, causing HA to extend out from the cell surface in a bottle brush-like configuration [213]. The aggregating proteoglycans interact with HA via the link module in the N-terminal globular G1 domain [213]. In chondrocytes, aggrecan is the predominant proteoglycan in the pericellular matrix, while in fibroblasts and smooth muscle cells, versican is the major HA binding proteoglycan [217, 218]. The expression of individual pericellular coats in culture has been shown to mimic the extracellular volume of cells *in-vivo* [219].

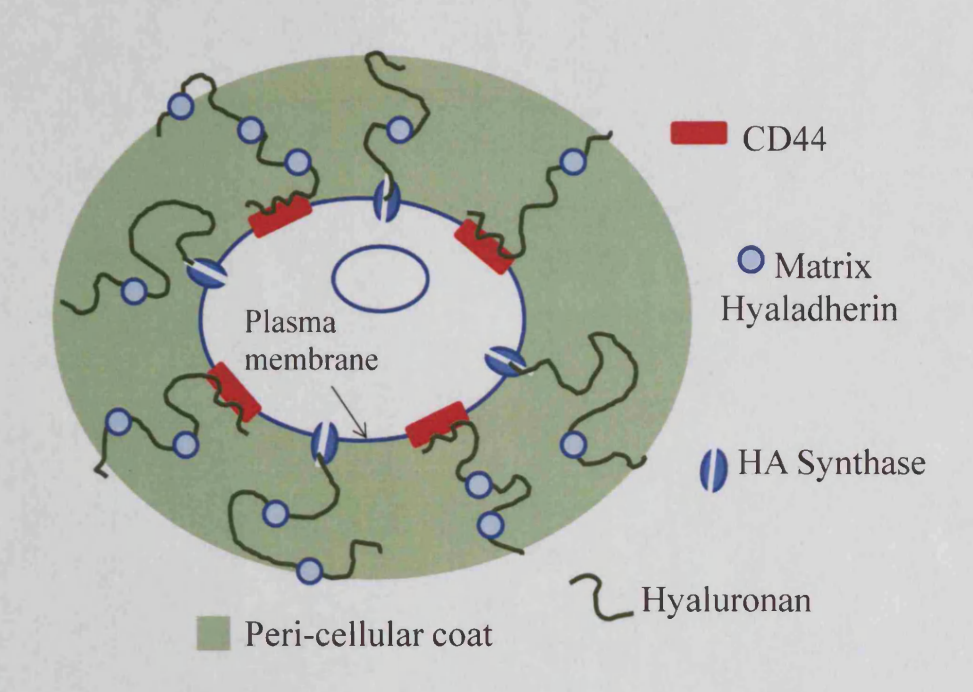


Figure 1.3 Representation of HA-dependent pericellular coat. Adapted from [219].

The HA coat is thought to regulate the assembly of the ECM by serving as a scaffold or through interactions of pericellular constituents with other matrix proteins. For example, fibronectin and collagen were found in the pericellular matrix of fibroblasts. The HA-versican pericellular coat has been shown to play a role in maintenance of proliferative and migratory phenotypes in various cells following growth factor treatment or injury [218]. HA coats promote proliferation by enabling cell detachment and rounding during mitosis and facilitate migration by separating cellular and fibrous barriers. The

pericellular HA coat has been shown to inhibit cell-cell contact essential for subsequent cellular differentiation [175].

Other HA-binding molecules such as TSG-6 can also be retained within the coat [193-195, 214], creating higher order levels of structural HA that regulate important biological processes [213]. Studies from this laboratory have demonstrated that TSG-6-mediated formation of heavy chain-HA complexes is critical in the formation of a pericellular HA coat in proximal tubular epithelial cells [194].

In addition to pericellular coats, HA can form cable like structures in association with HA binding proteins which promote monocyte binding independent of TSG-6 [193]. HA cables are distinct from HA coats most notably in their differential regulation by HAS; over-expression of HAS2 was shown to promote HA coat assembly but inhibit cable formation [194], over-expression of HAS1 led to increased cable formation [213] and over-expression of HAS3 was associated with induction of both HA pericellular structures in proximal tubular epithelial cells [193]. This is a fine example of how different HAS isoforms can regulate opposing cellular responses.

1.7.5 HA and Wound Healing

HA has an important biological role in skin wound healing, by virtue of its presence in high concentrations in skin [179]. Tissue injury and repair is characterised by synthesis and degradation of extracellular matrix components. One of the earliest components of the newly formed temporary matrix is HA [220]. Many of the biological processes mediated by HA are also central in the wound healing process. The wound tissue in the early inflammatory phase of wound repair is rich in HA, probably as a result of increased synthesis [221]. Changes in HA expression that occur in injured tissues can have profound effects upon the migration and activation of inflammatory cells, including monocytes and macrophages [222]. Therefore, injury induced changes in HA are likely to be critical for regulating the influx of inflammatory cells that occur immediately after wounding of the skin. Upregulation of HAS gene expression has been found in tissue injury [179], consistent with the observation that HA accumulation

occurs following injury. HAS2 mRNAs are increased following rat lung injury by irradiation [179]. Epidermal trauma in adult mice is associated with increased epidermal HA [223]. Higher expression of HAS have been demonstrated in autoimmune [224] and mechanical renal injury [225].

HA has two multiple roles in inflammation. Whether HA is bound to cells or to extracellular matrix components, its hydrophilic nature creates an environment permissive for migration of cells and early on in the response to tissue injury the HArich environment supports the influx of fibroblasts and endothelial cells into the provisional wound matrix and subsequent formation and organisation of granulation tissue [156]. Fibroblasts isolated from granulation tissue synthesise increased HA levels compared to fibroblasts isolated from normal skin, suggesting they are an important source of HA generation during early tissue repair [226]. HA degradation products can stimulate inflammatory cells to produce chemokines and cytokines that recruit inflammatory cells to the site of injury to modulate and resolve tissue injury. HA fragments are responsible for induction of proinflammatory cytokines such as Tumour Necrosis Factor- α (TNF- α), IL-1 β and IL-8 [156]. Cell proliferation is also an essential part of tissue repair and increased HA is essential for fibroblast detachment from the matrix and mitosis [156].

Moderation of the inflammatory response is required to stabilise the granulation tissues matrix and in a somewhat contradictory role to its inflammatory stimulation functions HA can also serve to offer protection to cells and extracellular matrix molecules against free-radical and proteolytic damage mediated through a free-radical scavenging and protein exclusion property [227]. This property is believed to confer HA a healing promoting ability in chronic wounds such as venous leg ulcers where damage is a result of prolonged inflammation by free radical [228]. TSG-6 expression is induced following generation of the inflammatory cytokine TNF- α in fibroblasts and inflammatory cells. TSG-6 is thought to bind with HA and serves as a potent negative feedback loop to moderate inflammation and stabilise granulation tissue in the latter part of the inflammatory process [229].

HA is also critical in the regulation of angiogenesis. Low molecular weight HA promotes whereas high molecular HA inhibits angiogenesis [156]. HA and its fragments may play crucial roles in the skin wound-healing process, by modulating the expression of fibroblast genes involved in remodelling and repair of ECM. Through its ability to enhance type III collagen synthesis and TGF-β3 expression in dermal fibroblasts, high molecular weight HA promotes the creation of a foetal-like cell environment, which is known to favour scarless healing, whereas low molecular weight HA might favour a fibrotic phenotype through stimulation of type I collagen [230].

Although the exact mechanisms through which HA and enzymatically derived fragments, affect the ECM metabolism during wound repair remain unclear, much has been elucidated: The earliest phases following injury is characterised by induction of high molecular weight HA, synthesised by platelets [231], which binds fibringen, one of the first reactions in clot formation [232]. A combination of increased synthesis and impaired clearance by hyal-2 inhibitors maintains accumulation of large HA polymers. Its anti-angiogenic and immunosuppressive properties opens up tissue spaces, facilitating access of neutrophils to the wound site for removal of dead tissue debris and bacteria. During the inflammatory phase inhibitors would then have to be removed for the lager HA molecule to be fragmented by Hyal-2. Smaller HA fragments induce inflammatory cytokines leading to infiltration by monocytes and lymphocytes. Following inflammation, further HA fragmentation leads to angiogenesis [233] and subsequent proliferation of fibroblasts and synthesis of collagen for reparative processes [234]. Inhibition of Hyal-1 activity must be invoked temporarily at this stage of wound healing in order for intermediate sized HA fragments to accumulate. Whilst HA breakdown products are integral for the cascade events essential to normal wound healing mechanisms, their subsequent removal in tissues is paramount for resolution of injury as demonstrated following experimental lung injury [235]. It is clear that the relative proportion of HA molecular sizes exerts a fine regulation of matrix state, from the early inflammatory steps to the final tissue recovery.

Many reports have verified the effects of exogenous hyaluronan in producing beneficial wound healing outcome. In animal experiments, topically applied hyaluronan has been

shown to accelerate skin wound healing in rats [227] and hamsters [236]. Corneal epithelial wound healing is also reported to be stimulated by exogenously applied hyaluronan [237]. An increased and prolonged presence of HA has been reported to be associated with the scarless quality of foetal tissue repair [230]. In contrast, its accumulation is reduced in adult tissues where wound healing is characterised by scarring [179].

HA has been reported to inhibit scar formation in healing adult wounds when applied topically and to reduce the packing density of collagen bundles [69] and, therefore, lead to reduced scarring [164]. These suggestions are in agreement with the work of Laurent et al. [238] who showed that applied HA resulted in scarless healing of tympanic membranes and with Balasz and Denlinger [239] who hypothesized that a HA-rich environment inhibits the matrix cells responsible for fibrous scars. In chronic wounds, such as venous leg ulcers, HA application has been shown to promote healing [156].

ECM HA is prominent in development and in the early phases of wound healing, especially in the foetus where the repair process is scar free [240]. In contrast its accumulation is reduced in adult tissues where wound healing is characterised by scarring [241]. These observations have led to the suggestion that HA may lead to reduced scarring [156] and reduce fibrosis. Conversely, work by Jenkins et al and Meran et al in this laboratory propose that increased HA associated with fibroblasts may promote differentiation into myofibroblasts and, therefore, facilitate the formation of scar tissue and promote the fibrotic response. They demonstrated that inhibition of HA synthesis in dermal fibroblasts significantly attenuated the capacity for cells to differentiate and proliferate in response to TGF- β 1. These studies indicate HA plays a pivotal role in regulating TGF- β 1 driven cellular differentiation in that it facilitates fibroblast-myofibroblast transition [242, 243].

1.7.6 HA and Aging

The majority of papers that evaluate HA regulation as a function of age are confined to those differences exhibited between foetal and adult fibroblasts, whilst a limited number of studies centre on differences exhibited by cellular aging. Some of these are now reviewed.

Ellis et al demonstrated that foetal fibroblasts assemble large HA pericellular coats and show no alterations in HA synthesis with age. In complete contrast, their adult counterparts failed to package HA into a coat, associated with an age-related decline in HA synthesis [244]. Chen et al indicated that foetal dermal fibroblasts display an elevated level of migratory activity compared to adult cells and that this may result from inherent differences in the production of HA, specifically that foetal cells synthesis higher levels of HA *in-vitro* compared to adult cells [245]. Ellis et al expand on these observations and demonstrate that, in addition to differential migratory capacity and HA generation, foetal and adult fibroblasts differ in their response to TGF-β1. In foetal fibroblasts both cell migration and HA synthesis were inhibited by TGF-β1, whereas adult fibroblasts were unaffected by TGFβ1 [69].

Matuoka et al demonstrated differential GAG production associated with aged human diploid fibroblasts *in-vivo* and *in-vitro* [246]. They specifically demonstrated in one study that cultured normal human fibroblasts during *in vitro* aging exhibited increased proportions of heparan sulfate GAG associated with marked depletion of HA, through a decrease in HA synthase activity [247]. They suggested that the change in HA synthesis was responsible, at least to some extent, for the observed growth reduction, during aging, of normal human fibroblasts.

Vigetti et al established an *in-vitro* model consisting of sequential passages of human aortic smooth muscle cells and in contrast showed that cell migration and HA synthesis significantly increases in aged cells, when compared to young cells, as does HAS2 and HAS3 and the HA receptor CD44 [248]. Associated with this was an age-related increase in CD44 signalling mediated ERK1/2 phosphorylation. Addition of HA oligosaccharides or an anit-CD44 blocking antibody inhibited ERK1/2 activation and cellular migration. In contrast, age-related reduction in the deposition of the ECM and in particular HA levels have been reported in humans [249].

HA contributes to the viscoelastic properties of the vocal fold lamina propria in elderly humans. Butler et al reported decreased HA levels in the vocal fold propria in elderly humans [250]. In a rat model decreased density of extracellular HA was shown to be associated with an age-dependent attenuation of expression of genes coding HAS. The authors propose that accumulation of dysfunctional senescent cells may contribute to the observed mRNA changes associated with aging.

In evaluating alterations in GAG biosynthesis during *in-vitro* aging by dermal fibroblasts Isnard et al demonstrated biphasic modifications in HA levels; from passage 5 to passage 13, incorporation of HA was decreased, only then to increase through passages 17-27 [251].

Meyer et al [252] tested the hypothesis that decreasing levels of HA deposition might underlie the changes associated with the aging process. They concluded that neither the concentration nor polymer size of HA changes as a function of age, however, enhanced association with tissues occurs, through HA-binding proteins and alterations in the histolocalization of HA, with a shift of HA towards the lower dermal layers.

Despite the extensive previous research on HA, there have been few studies that have assessed the impact of HA in regulating fibroblast-myofibroblast differentiation in the context of aging.

Project Aims

Fibroblastic differentiation into myofibroblasts is a key event during normal wound repair and previously this laboratory has demonstrated that TGF-β1-driven phenotypic activation is associated with accumulation of HA and its assembly into a pericellular coat. The overall purpose of this work is to understand the effects of *in-vitro* aging on dermal fibroblast differentiation in the adult. Specifically, this thesis will determine the regulatory role that HA may play in fibroblastic behaviour and the phenotypic changes associated with aging.

My specific objectives were:

- 1) To characterise phenotypic alterations of dermal fibroblasts associated with *in vitro* aging under basal and TGF-β1 stimulated conditions.
- 2) To characterise age-related changes in HA homeostasis and determine what role this has on wound healing outcomes.
- 3) To compare TGF-β1 signalling in young and aged dermal fibroblasts and determine the regulatory role HA plays
- 4) To determine the functional significance of the alterations in HA associated with the myofibroblast phenotype. How does this change with age?
- 5) To perform interventional experiments to control cellular HA levels to specifically direct cellular wound healing responses. Is it possible to influence the fibroblast response by altering their synthesis of HA?

Crucially an understanding of how HA levels are controlled within cells and whether this alters with aging, together with understanding how this impacts on cellular responses and wound healing outcomes, is important in the future targeting of HA therapy/manipulation for dysfunctional wounds in the aged.

Chapter 2 Materials and Methods

2.1 Materials

All general and tissue culture reagents were purchased from Sigma-Aldridge (Poole, Dorset, UK), Fisher Scientific (Leicestershire, UK) and GIBCO/BRL Life Technology (Paisley, UK) unless otherwise stated. PCR and QPCR reagents and primers were purchased from Invitrogen Life Technologies (Paisley, UK) and Applied Biosystems (Cheshire, UK). Radioisotopes were purchased from Amersham Pharmacia Biotech (Little Chalfont, Bucks, UK). Other reagents used were: recombinant TGF-β, EGF, goat anti-human EGF antibody from R&D Systems (Oxford, UK), Mouse monoclonal anti-CD44 blocking antibody from Ancell (Bayport, MN); MAP Kinase (MEK) inhibitor PD98059, p38 kinase inhibitor SB203580 and KN-92/93 were from Calbiochem (Nottingham, UK). The EGF-R inhibitor AG1478 was from Invitrogen, the ALK5 inhibitor SB431542, Cytochalasin B, bovine testicular hyaluronidase (H3884) IL-1β and 4-methylumbelliferone (4MU) were from Sigma (Poole, UK).

2.2 Patient Samples

All experiments were performed with dermal fibroblasts obtained by biopsy from consenting adults undergoing routine minor surgery. The biopsies were obtained from normal uninjured skin of patients and were attained with the support of Professor D. Thomas, Wound Biology Group, Dental School and ethical approval for the samples was obtained from the South-East Wales Local Research Ethics Committee (Ref No: 02/4836). Clinical details of patients involved are provided in Table 2.1

Table 2.1 Patient Details.

Patient number	Sex	Date of birth	Age biopsy obtained	Site of skin biopsy	Relevant medical History
Patient I	F	06.06.1946	56	Arm	Smoker; low haemoglobin; mild hypertension
Patient II	М	18.06.1925	77	Arm	Non-smoker; hypertension;
Patient III	M	06.06.1955	48	Arm	Smoker; nil significant
Patient IV	F	17.03.1914	89	Arm	Non-smoker; moderate atherosclerosis

2.3 Tissue Culture

2.3.1 Isolation of Fibroblasts

Fibroblast isolation was performed by the Wound Biology Group according to their previously established techniques [86]. Tissue biopsies were transported immediately to the laboratory in sterile phosphate buffered saline (PBS) in a sterile universal container (Greiner Bio-one, Gloucester, UK) for isolation of cells. Cultures were established by a single-cell suspension technique following enzymatic degradation of the specimens. Specimens were washed thoroughly in PBS under aseptic conditions in a class II biological safety cabinet. The tissues were trimmed of all excess fat and washed in a 53 mm diameter bacteriological grade petri dish (Fahrenheit Laboratory Supplies, Milton Keynes, UK). Specimens were then immersed in 70% (w/v) ethanol for 30 – 45 seconds to surface sterilize them. The tissue was then transferred to another petri dish, washed again in PBS and then dissected with a scalpel into 2 mm² portions. The pieces of tissue were then added to a universal containing Fibroblast-Containing Serum Medium (F-SCM) [Dulbecco's Modified Eagles Medium (DMEM) and F-12 medium supplemented with L-glutamine (2mM), non-essential amino acids (1x), antibiotics (100 U/ml penicillin G; 100 µg/ml streptomycin sulphate), anti-mycotics (0.25 µg/ml amphotericin B) and 10% (v/v) foetal calf serum (FCS) (Biologic Industries Ltd., Cumbernauld, UK)] and Dispase (2 mg/ml; Boehringer Mannheim, Lewes, UK) which had been filter sterilised and incubated overnight at 4°C. The tissues were then brought to room temperature, and the epidermal and the dermal layers of the skin were carefully separated using a pair of fine-toothed forceps. The dermal tissue was then transferred to a 1 mg/ml solution of bacterial Clostridium histolyticum A collagenase (Boehringer Mannheim) made up in F-SCM which had been previously filter sterilized. The tissue was then minced and incubated at 37°C overnight.

Subsequently, the cell suspension was pipetted through a 21-gauge needle to fragment any remaining tissue and centrifuged in a conical based tube at 1,500 revolutions per minute (RPM) for five minutes. The supernatant was carefully removed and the pellet washed twice with PBS. The pellet was then re-suspended in 2 ml of F-SCM and plated in 12.5 cm² tissue culture flasks.

2.3.2 Fibroblast Culture

The cells from 12.5 cm^2 tissue culture flasks were transferred to 75 cm^2 flasks once they attained confluence, and cultured in Dulbecco's modified Eagles medium supplemented with L-glutamine (2mM), 100 units/ml penicillin and $100 \mu \text{g/ml}$ streptomycin and 10% foetal calf serum (FCS) (Biologic Industries Ltd., Cumbernauld, UK). The cultures were maintained at 37% in a humidified incubator in an atmosphere of 5% CO₂ and fresh growth medium was added to the cells every 3 to 4 days. At 90% confluence, fibroblasts were trypsinized and 1.5×10^5 cells were re-seeded into T75's each time and either utilised for experiments, cultured further to senescence or cryo-preserved as described below.

2.3.3 Calculation of population doubling levels

At each passage, the total number of viable cells was determined by direct counting using a haemocytometer. Population doublings (PDs) were calculated using the following formula as previously described [253]:

$$PD = \frac{\log_{10} \text{ (total cells harvested at passage)} - \log_{10} \text{ (total cells reseeded)}}{\log_{10}(2)}$$

Cumulative population doubling levels were calculated by adding the derived increase to the previous PD level (PDL) and fibroblast populations were cultured and cryopreserved at various passages until senescence. Senescence was determined when the population doubling/week was <0.5 [254]. Previously, work by Dr Stuart Enoch in the dental school has extensively characterized the growth kinetics and entry into replicative senescence using dermal fibroblasts taken from the four patients [254]. From this work, typical population doubling data based on the replicative lifespan for each patient was calculated (Table 2.2).

	Patient					
	I	II	III	IV		
Passage		Number of Population Doublings				
	(PDs)					
Early pass	6.76	6.65	7.5	6.64		
Mid-pass	22.7	26.03	33.74	35.93		
Senescent	45.63	49.61	63.09	70.05		

Table 2.2 Population doubling Data. Number of population doublings undergone by dermal fibroblasts for each patient throughout their replicative lifespan [254].

Senescence varied for each patient, occurring over the range PDL 46-70. For the purpose of this project it was decided that the PDs at which cells reached midpassage would be selected for 'aged' cells. Based on the data, in the experiments, 10-15 PDL and 23-36 PDL are used and referred to as young and aged dermal fibroblasts, respectively. Prior to experimentation all cells were growth-arrested in serum-free medium for 48 hours to allow cell-cycle synchronisation. All experiments, unless otherwise stated, were performed in serum-free medium to avoid any influence of serum factors. Furthermore all experiments were performed on equivalent cell numbers.

2.3.4. Fibroblast Sub-culture

Confluent fibroblasts were sub-cultured by treatment with Trypsin/ ethylenediamineetetraacetic acid (EDTA) diluted 1:1 with PBS. The trypsin was evenly distributed over the base of the flask and incubated at 37°C for 1-3 minutes, after which the cells became detached from the base of the flask and appeared rounded when examined under light microscope. The resulting cell suspension was treated with an equal volume of FCS to neutralise the protease activity. The total volume was then transferred to a centrifuge tube and the suspension centrifuged at 1500 RPM for 7

BSA in HBSS and then incubated with the appropriate secondary antibody (DAKO, Cambridgeshire, UK) (Table 2.4), diluted in 0.1 % (wt/vol) BSA in HBSS, for 1 h at room temperature. The cells were washed extensively with 0.1 % (wt/vol) BSA in HBSS, mounted in Vectashield fluorescent mountant (Vecta Laboratories, Peterborough, UK) and examined under UV-light on a Leica Dialux 20 fluorescent microscope (Leica Microsystems (UK) Ltd, Milton Keynes, UK).

2.4.2 FITC-Phalloidin Staining

Following stimulation, cells were fixed in 4 % (wt/vol) paraformaldehyde for 15 min at room temperature. Cell were left to air dry, and permeabilised in 0.1 % (vol/vol) Tween-20 in PBS for 5 min at room temperature. Non-specific binding sites on the cells were blocked with 5 % (wt/vol) BSA in PBS for 20 min at room temperature. The cells were washed thoroughly in 0.1 % (wt/vol) BSA in PBS. Cells were incubated with the phalloidin (Table 2.5), diluted in 0.1 % (wt/vol) BSA in PBS, for 1 h at room temperature whilst avoiding light. The cells were washed repeatedly in 0.1 % (wt/vol) BSA in PBS and then mounted in Vectashield fluorescent mountant and examined under UV-light on a Leica Dialux 20 fluorescent microscope.

2.5 Analysis of Cell Proliferation

Fibroblast proliferation was assessed by the incorporation of D-[3H]-Thymidine into DNA. Cells were grown in 35mm dishes and assessed at sub-confluence ($\sim 50\%$ confluence). Metabolic labelling was performed by incubation with 1 μ Ci/ml D-[3H]-Thymidine for 24 hours. The medium was then discarded and the cells washed repeatedly with PBS containing 1mM Thymidine prior to fixing with 500 μ l of 5% trichloracetic acid containing 1mM Thymidine at 4°C for 1 hour. The cell layer was extracted by incubation with 1ml of 0.1M NaOH at 20°C for 24 hours and neutralised with 0.1M HCl. Radioactivity was determined by β -counting on a Packard Tri-Carb 1900 liquid scintillation analyser and the results represented as disintegrations per minute (dpm).

Table 2.3: Primary Antibodies for Immuno-Fluorescence

Antibody	Cat. no	Host	Type	Dilution
Anti-Human Vimentin (Dako)	M0725	Mouse	Monoclonal	1:50
			IgG_1	
Anti-Human Cytokeratin (Dako)	M0717	Mouse	Monoclonal	1:50
			IgG_1	
Anti-Human α-SM Actin (Sigma)	A5691	Mouse	Monoclonal	1:30
			IgG _{2a}	
Anti-Human CD44 (Calbiochem)	A020	Rat	Monoclonal	1:200
			IgG _{2b}	
Anti-Human EGF-R (Santa Cruz	1005:sc-	Rabbit	Polyclonal	1:50
Biotechnology)	03		IgG	

Table 2.4: Secondary Antibody for Immuno-fluorescence

Antibody	Cat. no	Host	Туре	Dilution
Fluorescein Isothiocyanate (FITC)-	F0261	Rabbit	Polyclonal	1:40
Conjugated Anti-Mouse IgG (Dako)				
Fluorescein Isothiocyanate (FITC)-	F0205	Swine	Polyclonal	1:40
Conjugated Anti-Rabbit IgG (Dako)				
Alexa Fluor® 555 Anti-rat IgG	A21434	goat	Polyclonal	1:10,000
(H+L) (Invitrogen)				

Table 2.5: Phalloidin FITC-Conjugate

Reagent	Cat. no	Biological	Dilution
		Source	
Phalloidin FITC-Conjugate (Fluka,	77415	Amanita	1:50
Sigma-Aldrich)		phalloides	

2.6 Reverse Transcription (RT)

Dermal fibroblasts were grown to confluence in 35mm dishes and washed with PBS prior to lysis with 200µl Tri-reagent and RNA purification according to the manufacturer's protocol. Briefly, 200 µl of chloroform was added to the sample and agitated by inversion until completely emulsified. The sample was incubated at 4°C for 3 min to allow the phases to separate then centrifuged at 130,000 RPM for 20 min at 4°C. The colourless aqueous layer was pipette and mixed with an equal volume of isopropanol. The mixture was incubated at 4°C for 24 hours then the precipitate was pelleted by centrifugation at 130,000 RPM at 4°C for 20 min. The supernatant was removed and the pellet was washed repeatedly in 0.5 ml ice-cold 70 % (vol/vol) ethanol by briefly vortexing then centrifuging at 130,000 RPM for 20 min at 4°C. The RNA pellet was air dried at room temperature then dissolved in 10 µl of H₂O. One µl of the RNA sample was diluted in 99 µl of H₂O and the absorbance was measured at 260 nm and 280 nm using a Beckman UV-DU64 spectrophotometer (Beckman Instruments Ltd, High Wycombe, UK). The ratio of 260:280 gave an indication of protein contamination (>1.6 was considered to indicate sufficiently pure RNA). The concentration of RNA was calculated from the absorbance at 260 nm:

Abs₂₆₀ x dilution factor (100) x RNA coefficient (40) = RNA in μ g/ml

The RT was performed using the random primer method. The RT was carried out in a final volume of 20 μl per reaction, containing 1 μg of RNA sample, 2 μl of 10x RT random primers, 2 μl of 10x RT buffer, 0.8 μl of 25 mM dNTPs (deoxynucleotide triphosphate) (mixed nucleotides: dATP, dCTP, dGTP and dTTP), 1 μl of MultiscribeTM reverse transcriptase, and 1 μl of RNase inhibitor. All reagents used were supplied as a high-capacity cDNA reverse transcriptase kit (Applied Biosystems). The RT was performed using an Applied Biosystems "Gene Amp PCR System 9700" thermocycler. As a negative control RT was performed with sterile H₂O replacing the RNA sample. The solution was incubated at 25 °C for 10 min to allow the random hexamer primers to anneal to the RNA. The primers were then extended using the reverse transcriptase in the presence of the four dNTPs by heating the solution to 37 °C for 2 h, thus generating cDNA. The cDNA is then heated to 85 °C for 5 s, thus separating the hybridised

complexes consisting of the RNA template and the newly synthesised cDNA and deactivating the reverse transcriptase. The resulting single stranded complementary DNA (cDNA) was stored at -20 °C.

2.7 Quantitative PCR (Q-PCR)

Q-PCR was carried out in a final volume of 20 µl per reaction, containing 1 µl of cDNA, 10 µl of TaqMan Fast Universal Master Mix (20X) (Applied Biosystems), 8 µl of H₂O, and 1 µl of a TaqMan gene expression assay primer and probe mix (Applied Biosystems) (Table 2.2). A negative control (-PCR) was prepared with H₂O substituted for the cDNA. PCR was simultaneously done for ribosomal RNA (primer and probe commercially designed and purchased from Applied Biosciences) as a standard reference gene.

Quantitative PCR was performed using the 7900HT Fast Real-Time PCR System from Applied Biosciences using Taqman Universal PCR Master Mix (Applied Biosystems) following the manufacturer's instructions. The Taqman gene expression assays used are shown in Table 2.6.

The comparative CT method was used for relative quantification of gene expression. The CT (Threshold cycle where amplification is in the linear range of the amplification curve) for the standard reference gene (ribosomal RNA) was subtracted from the target gene CT to obtain the delta CT (dCT). The mean dCT for similar samples were then calculated. The expression of the target gene in experimental samples relative to expression in control samples was then calculated using the formula:

$$2^{-(dCT(1)-dCT(2))}$$

where: dCT(1) is the mean dCT calculated for the experimental samples and dCT(2) is the mean dCT calculated for the control samples.

Table 2.6: TaqMan Gene Expression Assays (Applied Biosystems)

Primer	Catalogue Number
α-SMA	Hs_00426835_g1
HAS 1	Hs_00155410_m1
HAS 2	Hs_00193435_m1
HAS 3	Hs_00193436_m1
SMAD 2	Hs_00183425_m1
SMAD 3	Hs_00232222_m1
TGF-β1	Hs_00171257_m1
TSG6	Hs_00200180_m1
EGF	Hs_01099999_m1
EGF-R	Hs_01076073_m1

Note: Applied Biosystems do not supply sequences of their Q-PCR primers.

2.8 Generation of HAS2 and EGF-R Over-expressing Clone

A HAS2 and EGF-R expression vector was constructed by cloning the appropriate coding region into the multiple cloning site (MCS) of the pCR3.1 vector (Invitrogen; figure 2.2). HAS2 open reading frame (ORF) was a gift from Dr. Andrew Spicer (Texas A&M University, College Station, TX). EGF-R ORF was a gift from Prof. Alan Wells (University of Pittsburgh, Pennsylvania). Standard PCR was amplified to generate the ORF using *Pfx50* DNA polymerase (Invitrogen) to increase the fidelity of the PCR product. The primers used in the reaction, include sites for the restriction enzymes KpnI and NotI (for HAS2) and Xba1 & HindIII (for EGF-R). The ORF was inserted into the vector (pCR3.1) using a standard ligation reaction with Promega T4 DNA *Ligase*. Amplification of the cloned vector was performed *via* bacterial transformation (JM109 competent Escheria coli, Promega). The integrity and orientation of the HAS2 ORF was confirmed by restriction enzyme digestion (see Figure 2.1).

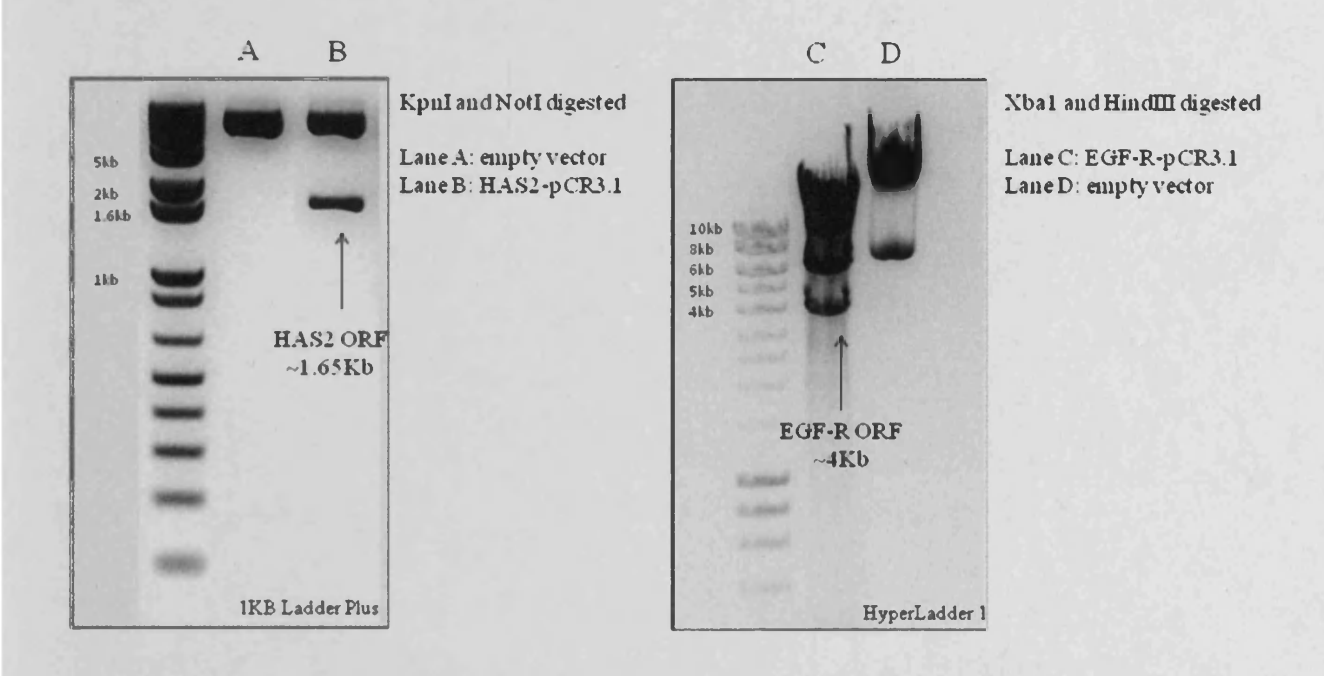


Figure 2.1 Confirmation of HAS2 and EGF-R cloning into pCR3.1 vector. Purified DNA that was extracted from transformed Escherichia coli and subjected to restriction-enzyme double-digestion and was then resolved using 2% (wt/vol) agarose gel electrophoresis. Lane A and D show the empty vector that was treated similarly with the restriction enzymes. Land B and C shows a sample that was cloned successfully with HAS2 open reading frame (~1.65Kb) and EGF-R open reading frame (~4Kb), respectively.

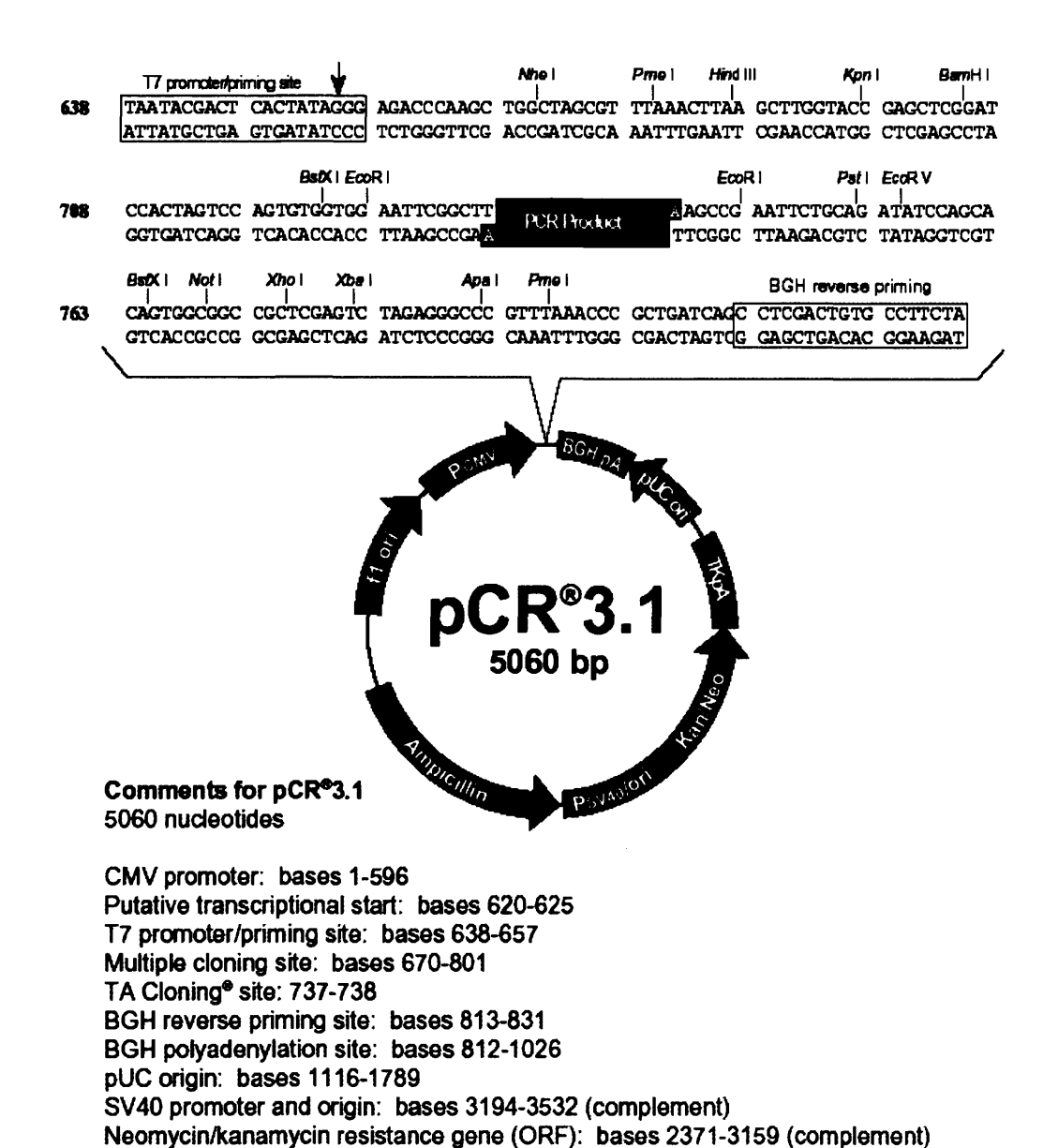


Figure 2.2 Restriction map and multiple cloning site of the pCR3.1 vector.

Thymidine kinase polyadenylation site: bases 1926-2196 (complement) Ampicillin resistance gene (ORF): bases 3611-4471 (complement)

f1 origin: bases 4602-5058

2.9 Transient Transfection

Transient transfection was performed with the aid of Nucleofector technology (Amaxa Biosystems) in accordance with the manufacturer's protocol for transfection of primary mammalian fibroblasts. Fibroblasts were grown to 70% confluence in T75 flasks. The medium was then removed and the cells harvested by trypsinisation (solution containing 0.05% trypsin and 0.53 mM EDTA. Once the cells detached, the resulting cell suspension was treated with an equal volume of FCS to neutralise the protease activity. Cell counting was performed using a haemocytometer and cell numbers adjusted to a final concentration of 0.5 x 10⁶ cells/ml. The cells were then centrifuged (100xg for 10mins) and the resulting pellet resuspended in Basic Nucleofector solution (BNS) (Amaxa Biosciences). The cells were transfected either with HAS2-pCR3.1 and/or EGF-R-pCR3.1 or pCR3.1 alone (control-transfection). The utilised concentrations were 100µl of BNS to 1µg of DNA. The solution was then transferred to an amaxa certified cuvette and placed in the nucleofector. Nucleofection was carried out for 5 seconds according to the pre-specified program designed for mammalian fibroblasts and the cells were subsequently transferred to either 35mm dishes or 8 well permanox chamber slides containing pre-warmed medium supplemented with 10% FCS. pCR3.1 alone (empty vector) or pmaxGFP (Green Fluorescent Protein, provided by Amaxa Biosciences) vector was used as a control (control transfections). Co-transfection with pmaxGFP was also performed in parallel, and expression was determined by fluorescence microscopy after 48 hours to access efficiency (see figure 2.3). Transfection efficiency was calculated according to the formula:

Transfection efficiency = [Number of GFP-transfected cells (assessed by fluorescent microscopy) / Number of total cells (assessed by light microscopy)] x 100

Two negative controls were performed: 1) 0.5×10^6 cells in $100 \mu l$ of BNS containing $1 \mu g$ DNA but without application of the program and 2) 0.5×10^6 cells in $100 \mu l$ of BNS without DNA but with application of the program. The cells were incubated in medium supplemented with 10% FCS for 24 hours followed by a 24 hour incubation in serum-free medium prior to experimentation. GFP positivity in pmaxGFP-HAS2 co-

transfected or pmaxGFP-mock cotransfected cells was also used to visualise individual cells for HA coat analysis.

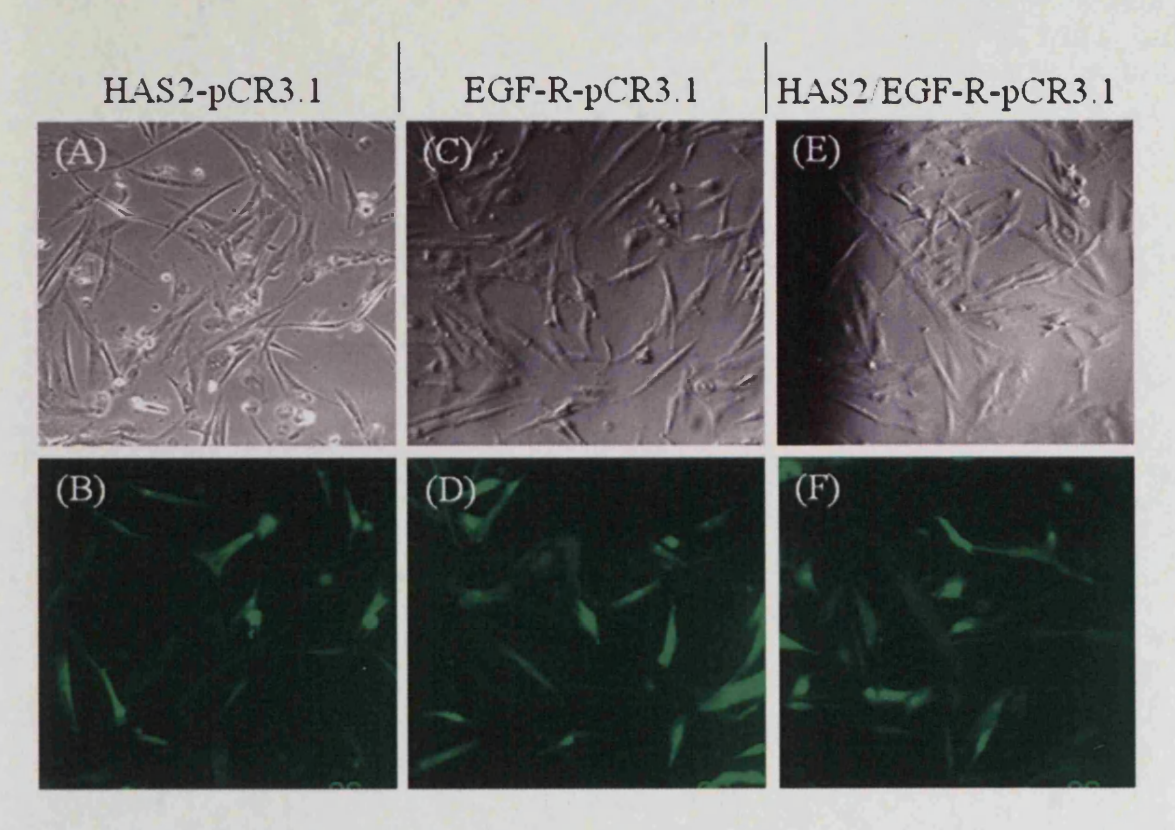


Figure 2.3 Transfection with pmaxGFP vector. Cells were transiently co-transfected with pmaxGFP DNA as described in section 2.9 and incubated in the presence of serum for 24 hours. The medium was then replaced with serum-free medium and the incubations continued for a further 24 hours. The cells were imaged using light (A,C and E) and fluorescent microscopy (B, D and F) at 48 hours post-transfection to assesses transfection efficiency. Panels A, C and E illustrate overall number of cells present in the culture and panels B, D and F are images of the same cells, illustrating the percentage which have co-transfected with pmaxGFP and either HAS2-pCR3.1 (B), EGF-R-pCR3.1 (D) or HAS2-pCR3.1 and EGF-R-pCR3.1 (F). Transfection efficiency was found to be 41.5%, 44.1 % and 37.8% respectively.

2.10 Small Interfering RNA Transfection

Transient transfection of dermal fibroblasts was performed with specific siRNA nucleotides (Ambion) targeting either Smad2 (115717) Smad3 (107875) HAS2 (16704) TSG-6 (139706) or CD44 (114068). Transfection was performed using Lipofectamine 2000 transfection reagent (Invitrogen) in accordance with the manufacturer's protocol. Briefly, cells were grown to 50% confluence in antibiotic free medium in either 12 well culture plates or 8 well permanox chamber slides. 2µl of transfection agent was diluted

in 98μl Opti- MEM reduced growth medium (Gibco) and left to incubate at room temperature for 5 minutes. The specific siRNA oligonucleotides were diluted in Opti-MEM reduced growth medium to give a final concentration of 20μM in a total volume of 100μl. The transfection agent mix and siRNA mix were then combined and incubated at room temperature for a further 10 minutes. The newly formed transfection complexes (200μl) were then added to cells and incubated at 37°C with 5% CO2 for 24 hours in medium supplemented with 10% FCS followed by a 24 hour incubation in serum-free medium prior to experimentation. As a control, cells were transfected with negative control siRNA (a scrambled sequence that bears no homology to the human genome).

2.11 Visualisation of pericellular HA by particle exclusion assay

The exclusion of horse erythrocytes was used to visualise the HA pericellular coat. Formalized horse erythrocytes were washed in PBS and centrifuged at 1,000xg for 7 min at 4°C. The pellet was resuspended in serum-free medium at an approximate density 1x10⁸ erythrocytes/ml. One millilitre of this suspension was added to each 35mm dish containing sub-confluent cells and swirled gently for even distribution. The dishes were incubated at 37°C for 15 min to allow the erythrocytes to settle around the cells. Control cells were incubated with 200µg/ml bovine testicular hyaluronidase in serum-free medium for 30 min prior to the addition of formalized horse erythrocytes. On settling, the erythrocytes are excluded from zones around the cells with HA pericellular coats. This is viewed under the microscope as an area of erythrocyte exclusion. Zones of exclusion were visualised on a Zeiss Axiovert 135 inverted microscope. Due to the elongated shape of the cells, the exclusion zone at some areas of the cell was not visible. Therefore, the width of the exclusion zone was calculated at the widest point of the cell (usually the nucleus).

2.12 Analysis of ³H-Radiolabeled HA

Cells were grown to full confluence in T75 flasks and growth-arrested for 48 h in serum-free medium. The medium was then replaced with either serum-free medium alone or serum-free medium containing 10ng/ml TGF-β1 and the incubations continued for 72 hours. Metabolic labelling was then performed by incubation with 20μCi/ml D-[³H]-glucosamine hydrochloride for 24 hours. The culture medium was then removed and the cells washed with PBS. The wash and medium were combined to form the conditioned medium extract. This was then treated with an equal volume of 200µg/ml Pronase in 100mM Tris-HCL, pH 8.0, 0.05% sodium azide for 24 hours. Samples were passed over DEAE-Sephacel ion exchange columns equilibrated with 8M urea in 20mM BisTris buffer, pH6, containing 0.2% Triton X100. This removed any low molecular weight peptides and unincorporated radiolabel. HA was eluted in 8M urea buffer containing 0.3M NaCl. Each sample was split into two, and the HA was precipitated with 3 volumes of 1% potassium acetate in 95% ethanol in the presence of 50µg/ml of each HA, heparin and chondroitin sulphate as co-precipitants. The first half of each sample was resuspended in 500µl of 4M guanidine buffer and analysed on a Sephacryl S-500 column equilibrated with 4M guanidine buffer. To confirm that the chromatography profile generated was the result of radiolabeled HA, the second half of each sample was digested at 37°C overnight with 1 unit of Streptomyces hyalurolyticus hyaluronidase (ICN pharmaceuticals Ltd.) in 200µl of 20mM sodium acetate, pH6, containing 0.05% sodium azide and 0.15M sodium chloride. The sample was then mixed with an equal volume of 4M guanidine buffer and analysed on the same Sephacryl S-500 column equilibrated with 4M guanidine buffer. To produce the chromatography profile the 3H activity for each half of the sample was normalised, corrected for dilution, and then the Hyal-resistant counts were subtracted. The column was calibrated with [3H]-glucosamine hydrochloride, M_r 215; [35S]-chondroitin sulphate glycosaminoglycans, M_r 25x10³; decorin, M_r 10x10⁴; and [³⁵S]versican, M_r 1.3x10⁶. The radioactivity was determined by β-counting on a Packard Tri-Carb 1900 liquid scintillation analyser and the results represented as disintegrations per minute (dpm).

2.13 Determination of HA concentration

Cells were grown to confluence in 35mm dishes and the HA concentration in the cell culture supernatant was determined using a commercially available enzyme-linked HA binding protein assay (HA "Chugai" quantitative test kit; Congenix, Petersborough, UK). The assay used microwells coated with a highly specific HA binding protein (HABP) from bovine cartilage to capture HA and an enzyme-conjugated version of HABP to detect and measure HA in the samples. Briefly, diluted samples and HA reference solutions were incubated in HABP-coated microwells allowing binding of the HA in the samples to the immobilised HABP. The wells were then washed and HABP conjugated with HRP was added to the wells forming complexes with bound HA. Following a second washing step, a chromogenic substrate (TMB/H₂O₂) was added to develop a coloured reaction. Stopping solution was added to the wells, and the intensity of the resulting colour measured in optical density units using a spectrophotometer at 450nm. HA concentrations were calculated by comparing the absorbance of the sample against a reference curve prepared from the reagent blank and five HA reference solutions (50, 100, 200, 500 and 800 ng/ml) included in the kit. The assay is sensitive to 10 ng/ml, with no cross-reactivity with other glycosaminoglycan compounds.

2.14 Western Blot Analysis

Western Blot analysis to assess changes in protein expression was performed according to previously established techniques in our laboratory [210]. Briefly, cells were grown to confluence in 35 mm dishes and rinsed with cold PBS. Cells were then lysed using 1% protease inhibitor, 1% phenymethylsulphonyl flouride and 1% sodium orthanadate in RIPA lysis buffer (Santa Cruz biotechnology inc, Germany). The samples were scraped, collected and centrifuged at 2500 g for 10 minutes. The supernatant was collected, protein concentrations were determined by Bradford assay and the samples were stored at -70°C until use. Equal amounts of protein were mixed with equal volumes of reducing SDS sample buffer and boiled for 5 minutes at 95°C before loading onto 10% SDS PAGE gels. Electrophoresis was carried out under reducing conditions at 150 volts for 1 hour and the separated proteins were then transferred at 150 volts over 90 minutes to a nitrocellulose membrane (GE Healthcare, Buckinghamshire, UK). The

membrane was blocked with Tris-buffered saline (TBS) containing 5% non-fat powdered milk for 1 hour and incubated with the appropriate primary antibody at 4°C overnight (See Table 2.7 for antibody dilutions). The blots were subsequently washed with TBS containing 1% Tween prior to incubation with the appropriate HRP-conjugated secondary antibody for 1 hour at room temperature (See Table 2.8 for antibody dilutions). Proteins were visualized using enhanced chemiluminescence (GE Healthcare) according to the manufacturer's instructions.

Table 2.7: Primary Antibodies and Dilutions used in Western Blot Analysis

Antibody	Cat. no	Host	Type	Dilution
Anti-Human GAPDH (Abcam plc, Cambridge, UK)	ab9485	Rabbit	Polyclonal	1:7500
Anti-Human Phospho-Smad2 Ser245/250/255	#3104	Rabbit	Polyclonal	1:1000
(Cell Signaling Technology) Anti-Human Phospho-Smad3	#9520	Rabbit	Monoclonal	1:1000
(Ser423/425) (C25A9) (Cell Signaling Technology)			IgG_1	
Anti-Human Phospho-p44/42-MAPK (ERK1 and ERK2) (Cell Signaling)	#9106	Mouse	Monoclonal	1:1000
Anti-Human EGF-R (Santa Cruz Biotechnolgy)	1005:sc-03	Rabbit	Polyclonal IgG	1:200
Anti-Human p-EGFR (Santa Cruz Biotechnolgy)	sc-12351-R	Rabbit	polyclonal IgG	1:500

Table 2.8: Secondary Antibodies and Dilutions used in Western Blot Analysis

Antibody	Cat. no	Host	Туре	Dilution
HRP-Conjugated Anti-Mouse IgG (Santa Cruz Biotechnology Inc)	sc-2005	Goat	Polyclonal	1:5000
HRP-Conjugated Anti-Rabbit IgG (Santa Cruz Biotechnology Inc)	sc-2004	Goat	Polyclonal	1:10000

2.15 Immunoprecipitation

Cells were grown washed and lysed as for Western analysis above. Cell protein samples (200µg) were pre-cleared with 25µl packed protein A cross-linked 4% beaded agarose (Sigma) at 4°C over-night. The beads were removed by centrifugation (13.000 rpm, 10 min) and the supernatant collected. Samples were subjected to immunoprecipitation using rat anti-CD44 antibody (A020 Calbiochem) (2µg/ml) and incubated at 4°C with constant mixing over-night. The immune complex was captured by the addition of packed agarose protein A beads (50µl) over-night at 4°C. Beads were washed with RIPA buffer (50mM Tris, 150mM NaCl, 0.5% sodium deoxycholate, 10mM MgCl2, 0.1% SDS, 1% Triton X-100); 30µl of sample buffer was then added prior to boiling for 10mins. Separation of the beads was achieved by centrifugation (13,000xg for 10mins) and the supernatant removed. Samples were subjected to SDS PAGE and subsequently transferred to nitrocellulous membranes and processed as described for Western blot analysis using rabbit anti-EGF-R antibody (Santa Cruz Biotechnolgy) as the primary antibody. The blots were subsequently washed in Trisbuffered saline-Tween and incubated with the appropriate HRP-conjugated secondary antibody (Sigma) in TBS-Tween. Proteins were visualised using enhanced chemiluminescence (Amersham) according to the manufacturer's instructions. Specificity of immunoprecipitation was confirmed by negative control reactions performed with IgG control.

2.16 Statistical Analysis

All experiments were performed at least in triplicate for individual patient donors. All values are provided as means \pm standard error. An unpaired Student's *t*-test was used to assess differences between young and aged cell populations. A paired Student's *t*-test was used for comparisons of treatments within the same cell population, i.e young or aged cells. For multiple variables one-way analysis of variance was used for global comparison followed by Tukey's honestly significant difference method for pairwise comparison. Probability values of P < 0.05 were considered to indicate a significant difference.

Chapter 3 Characterisation of Fibroblast Phenotype and HA Regulation with *in-vitro* Aging

3.1 Introduction

Wound healing is a complex process involving interaction between resident and migratory cells, the ECM and cytokines/growth factors. In normal wound healing, the regeneration of the epithelial and mesenchymal tissues of the skin is effected by fibroblasts and is co-ordinated via complex cell/cell and cell/matrix interactions [6], which in the adult skin results in healing with scar formation. These responses are, however, altered in chronic/delayed wounds in the aged with prolonged inflammation, a defective wound matrix and a failure of re-epithelialisation. [255].

It has been long established that there is marked alteration in fibroblast function with increasing age. Fibroblast proliferation may also be modulated by age resulting in decreased cell number at the wound site [25]. Aging in an *in-vitro* model of wounding has also demonstrated a delay in the ability of human dermal fibroblasts to re-establish a confluent monolayer with increasing age [44]. Beyond the effects of aging on cellular migration and proliferation, a loss of responsiveness to a variety of cytokines has been reported following *in-vitro* and *in-vivo* aging in human fibroblasts [256, 257].

The accumulation of senescent fibroblasts within tissues has been suggested to play an important role in mediating impaired dermal wound healing in the elderly. As fibroblasts near senescence their responsiveness to extracellular signals diminish [258] and they exhibit a decreased ability to divide in response to damage or cell loss [49, 51]. Such alterations in fibroblastic phenotype are thought to be responsible for the physiological deterioration and limited tissue regeneration observed in aging individuals, however, the cellular mechanisms underlying this phenomenon are not known.

The regulation of cellular phenotype and differentiation, during tissue repair, is an important determinant of wound healing outcomes (including the development of abnormal pathology). When activated, fibroblasts undergo a number of phenotypic transitions and eventually acquire a contractile "myofibroblastic" phenotype, characterised by the expression of α -SMA [259]. These myofibroblasts are responsible

for tissue contraction and wound closure and which ultimately gives rise to the formation of a collagen rich scar.

The cytokine TGF- β 1 is recognised as a mediator of wound healing and its aberrant expression has also been widely implicated in progressive tissue fibrosis [260-262]. It is a constitute of serum alongside a multitude of other growth factors and in addition to its direct effect on ECM turnover, it is known to drive fibroblast–myofibroblast differentiation and is capable of up-regulating α -SMA in fibroblasts both *in-vitro* and *in-vivo* [263, 264]. Deficits in the signal transduction responsiveness to TGF- β 1 have been postulated to explain the age-related defects in wound healing seen in the elderly [265]. Therefore the majority of this thesis has specifically focused on fibroblast behaviour in the presence and absence of this cytokine. Previous studies in this laboratory [159-162, 266] have established the optimal conditions for induction of stable myofibroblastic differentiation in human dermal fibroblasts *in-vitro* and have demonstrated a causal link with HA production.

HA is a ubiquitous carbohydrate component of the ECM found in almost all connective tissues [267]. It influences cellular proliferation and migration [156] following injury and plays an important biological role in wound healing and mediating cellular response to cytokines such as TGF-β1 [268-270]. Although HA production is acutely upregulated following injury of most tissues [267, 271], the function of this in the course of repair has remained elusive [157]. Indeed it has not been clear whether the accumulation of HA is indicative of tissues undergoing re-organisation and repair or whether it contributes directly to wound healing and the scarring process [159, 160, 266].

Previously, work from this laboratory has demonstrated that phenotypic conversion of fibroblasts to myofibroblasts, is associated with major changes in the production and metabolism of HA [266]. Specifically, myofibroblasts were shown to accumulate several-fold more intra and extracellular HA, due to a reduction in their capacity to degrade HA. This disease promoting alteration in cell function was also associated with the development of extensive pericellular HA coats, which have been shown to be associated with cell proliferation and migration [272]. As the formation of the HA

pericellular matrix accompanies myofibroblastic differentiation, it is possible it may be involved in modulating this process. Therefore, the formation of a HA pericellular matrix, during myofibroblastic differentiation, could be a key target for controlling the wound healing response. These observations led to interest in HA as a possible regulator of the wound healing process. The functional significance of the alterations in HA turnover and assembly associated with the myofibroblastic phenotype, however, remain unclear. Despite extensive previous research on HA, there has been limited work focusing on both the role of HA in cellular differentiation and the impact of aging on HA mechanisms and certainly none that has attempted to marry the two. Further insight into how HA can influence behaviour and impact on wound healing processes and how this alters with age remains necessary.

Because of their pivotal role in the control of wound healing, fibroblasts are important therapeutic targets in attempts to improve skin wound healing in elderly patients. Work by Stephens et al have previously demonstrated that site- and disease-specific differences exist in the phenotype of human fibroblasts [49, 273], differences which are not simply related to replicative senescence within the wounds [49]. Fibroblasts have distinct phenotypes depending on the site from which they are isolated. Previously, using a library of patient-matched oral and dermal fibroblasts at low passage number (i.e. "non-aged") Meran et al demonstrated the relationship between generation of HA and site-specific phenotypic variation [242, 243]. TGF-β1 mediated phenotypic differentiation in dermal fibroblasts was associated with an induction of HAS1 and HAS2 expression and Hyal2 up-regulation. In contrast, resistance to TGF-β1 mediated phenotypic differentiation in the non-scarring oral mucosal fibroblast population, was associated with a unique failure of induction of HAS1 expression and a down-regulation of HAS2 expression, while HAS3, Hyal1, Hyal2 and Hyal3 remained unchanged. Combined with no change in the induction of HA-synthetic and degradative enzymes and the lack of HAS1 expression, this suggested that these non-scarring, motile fibroblasts do not respond to factors that normally switch on genes characteristic of the healing phenotype. The aim of this chapter was to identify whether this is also true of "aged" fibroblasts and that as dermal fibroblasts approach senescence, do they exhibit

differences in a) HA metabolism and b) cellular phenotype, associated with TGF- β 1-mediated wound healing.

An *in-vitro* aging model based on cell senescence has previously been described and validated as a model of age related alterations in human aortic smooth muscle cell function [274, 275]. Similarly, alterations in fibroblast function in an *in-vitro* model of aging have demonstrated the validity of this model in terms of *in-vivo* age related alterations in fibroblast motility and mitogenesis. These are associated with age dependent impaired wound healing [276, 277]. The work outlined in this chapter aimed to utilize this *in-vitro* aging model to test the general hypothesis that age-related alterations in human wound healing responses are associated with intrinsic differences in HA generation. Specifically the aim of this chapter was to extend on previous observations [159, 160, 266] and characterise differences in patient matched young and aged dermal fibroblasts in relation to:

- i Morphology
- ii Fibroblast-myofibroblast differentiation
- iii HA generation,
- iv HAS expression
- v HA-dependent pericellular coat formation
- vi TSG-6 expression

The results from this chapter will help establish the effect of cellular aging on fibroblastic phenotype and characterise the relationship with HA homeostasis.

3.2 Results

3.2.1 Characterisation of phenotypic conversion in young and aged fibroblasts

Patient matched young and aged dermal fibroblasts were grown to confluence and serum deprived for 48 hours prior to addition of recombinant TGF- β_1 (10ng/ml) for times up to and including 72 h. To assess the ability of the fibroblasts to undergo differentiation, expression of the myofibroblastic marker α -SMA was assessed by quantitative PCR. As demonstrated previously, using cells at low passage [159], the increase in α -SMA mRNA expression was shown to be time-dependent with maximal induction of α -SMA seen at 72 h for patient matched young (Figure 3.1A) and aged (Figure 3.1B) fibroblasts.

A direct comparison of α -SMA expression between young and aged cells after 72 hours was used to assess their potential for phenotypic activation (Figure 3.1C). Q-PCR revealed that under un-stimulated conditions, young fibroblasts had significantly higher (~5 fold) α -SMA mRNA expression, compared to patient matched aged fibroblasts. Following TGF- β_1 stimulation, both young and aged dermal fibroblasts up-regulated α -SMA expression. Young dermal fibroblasts, however, showed a median 10-fold increase in α -SMA expression compared to a median of only 6-fold increase in aged dermal fibroblasts, in response to the same concentration and duration of TGF- β_1 stimulation. Moreover, a direct comparison between cell populations demonstrated that TGF- β_1 induced α -SMA expression was down-regulated by 8.5-fold in aged fibroblasts when compared to patient matched young fibroblasts.

Microscopic analysis of monolayer cultures of young and aged fibroblasts revealed characteristic changes in their cellular morphology (Figure 3.2). Under basal conditions, young fibroblasts demonstrated an elongated, spindle-like appearance with no evidence of prominent stress fibres (Figure 3.2A), whereas following TGF-β1 stimulation the cells appear larger in size with a polygonal shape and prominent stress fibres (Figure 3.2C). With *in-vitro* aging the cells become wider, larger and irregular in shape under

basal conditions with marginally more stress fibres (Figure 3.2B). Following TGF-β1 stimulation aged cells retain their enlarged morphology but appear more 'dentritic' in appearance. Stress fibres are still visible but less prominent than stimulated young cells (Figure 3.2D).

Both resting and TGF- β_1 -stimulated fibroblasts were negative for expression of the epithelial cell marker cytokeratin (Figure 3.3E-H) and positive for expression of the mesenchymal cell marker vimentin (Figure 3.3A-D) in young and aged fibroblasts. Immunohistochemical analysis of α -SMA was performed to further assess the ability of young and aged fibroblasts to undergo differentiation. In support of Q-PCR data, under basal conditions,, both young and aged fibroblasts were negative for α -SMA (Figure 3.4 E and G). Stimulation of young cells with TGF- β_1 resulted in positive staining of α -SMA (Figure 3.4F), whilst in contrast, aged cells stimulated with TGF- β_1 did not induce the expression of α -SMA (Figure 3.4H).

In addition, FITC-phalloidin staining, a fluorescent probe that binds F-actin, was used to assess the cytoskeletal re-organisation of fibroblasts in response to TGF- β_1 stimulation. Young fibroblasts became larger and polygonal in shape. In addition, they demonstrated prominent cytoskeletal re-organisation with the actin filaments coalescing to form large, thick bundles throughout the cell body (Figure 3.4B). In aged fibroblasts cytoskeletal re-organisation was less prominent following TGF- β_1 stimulation (Figure 3.3D), with less pronounced actin filaments and poorly developed stress fibres not too dissimilar from resting aged cells. Notably in aged cells, individual bundles of actin fibres were more sparse and restricted to the periphery of the cells.

3.2.2 Analysis of HA generation and molecular weight profile in young and aged fibroblasts

Labelling of fibroblasts with [³H]-glucosamine for 24 hours under serum-free conditions demonstrated that aged fibroblasts have reduced baseline synthesis of HA, compared to patient-matched young fibroblasts (Figure 3.5A). Analysis of HA by size exclusion chromatography indicated that there was at least 2.5-fold more HA present in

the conditioned medium of young fibroblasts compared to aged fibroblasts. Furthermore, aged fibroblasts generated around 4-times less HA in the conditioned medium compared to young fibroblasts following TGF-β₁ stimulation (Figure 3.5B). Further analysis on the effect of TGF-\(\beta_1\) on HA synthesis was then assessed using both [³H]-glucosamine labelling and enzyme-linked immuno-sorbent assay. chromatography profiles from the conditioned medium of these cells demonstrated that young fibroblasts up-regulated HA generation in response to TGF- β_1 stimulation (Figure 3.5C), whereas aged fibroblasts were resistant to up-regulation of HA in response to same dose and duration of TGF-\(\beta_1\) stimulation (Figure 3.5D). The majority of HA produced in each of these three compartments consisted of high molecular weight HA polysaccharides of greater than 1.5 x 10⁶ Da in size. These findings were similar in both young and aged cells. These results were further confirmed by measurement of extracellular HA concentration in the conditioned medium using ELISA. In this assay, there was a significant decrease in extracellular HA concentration as fibroblasts were aged in-vitro. Furthermore, although addition of TGF-β₁ led to an increase in HA concentration at every PD, the magnitude of this effect decreased significantly as fibroblasts were aged *in-vitro* (Figure 3.6).

3.2.3 The expression of hyaluronan synthase enzymes in young and aged fibroblasts

Following growth arrest, young and aged dermal fibroblasts were stimulated with TGF- β_1 . HA was quantified by ELISA and in the same cells, HAS2 mRNA quantified by Q-PCR. As previously demonstrated, there was an age dependent decrease in basal HA concentration in the culture supernatant and also a decrease in TGF- β_1 dependent stimulation of HA (Figure 3.7A). In the same cells there was a marked attenuation of TGF- β_1 dependent stimulation of HAS2 mRNA in aged fibroblasts (Figure 3.7B).

Q-PCR was used to assess expression of all three HAS isoforms. HAS1 expression was almost undetectable in both unstimulated young and aged dermal fibroblasts using Q-PCR up to 40 cycles. In young fibroblasts, stimulation with TGF- β_1 led to a significant induction of HAS1 expression whilst levels remained almost undetectable in aged cells (Figure 3.8A). HAS2 was detected in both unstimulated young and aged dermal

fibroblasts but baseline expression was showed not to be statistically significant. The results demonstrated that whilst TGF- β_1 stimulation was associated with a significant up-regulation in HAS2 mRNA expression in young cells, aged cells demonstrated no such induction (Figure 3.8B). A similar pattern was observed for HAS3 expression; young and aged fibroblasts demonstrated comparable levels at baseline but whilst young cells exhibited a significant up-regulation in HAS3 mRNA expression following TGF- β_1 stimulation, aged cells demonstrated no significant change (Figure 3.8C). Figure 3.8D provides the Q-PCR amplification plot for all three HAS genes. Assuming comparable sensitivity throughout all three assays, the approximate C_T values indicate the relative expression level of HAS isoform in the order: HAS2>HAS3>HAS1.

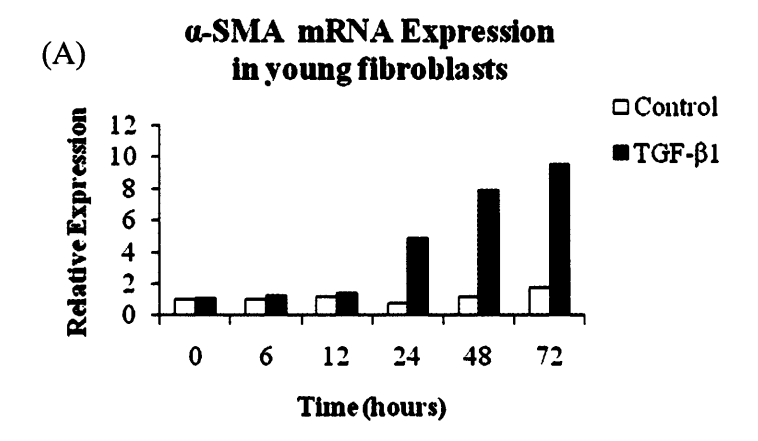
3.2.4 Accumulation of hyaluronan-dependent pericellular coats in young and aged fibroblasts

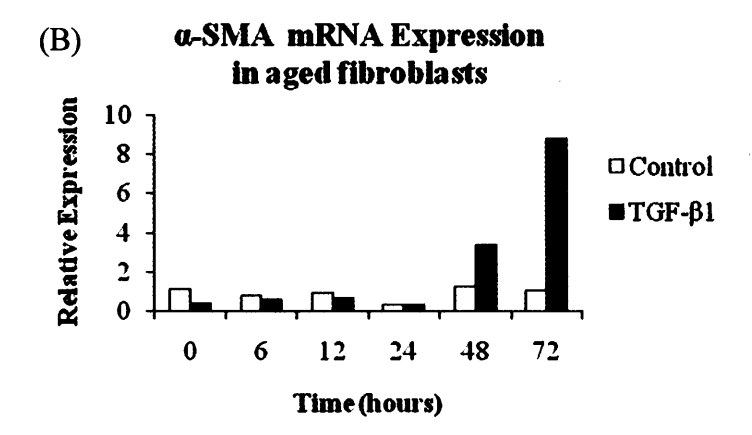
HA accumulation can be assessed using the exclusion of formalized erythrocytes. In this assay erythrocytes are excluded from the cell membrane of the fibroblasts by the large size and negative charge of any pericellular HA present. This is observed under microscopy as a zone of erythrocyte exclusion surrounding the cells. Previously we have demonstrated that fibroblast to myofibroblast phenotypic conversion is associated with the formation of a HA pericellular coat. Consistent with this, unstimulated young or aged fibroblasts did not assemble a significant HA pericellular coat (Figure 3.9A&B). Whilst stimulation of young fibroblasts with TGF- β_1 resulted in the formation of a significant coat (Figure 3.9C), aged fibroblasts failed to assemble a HA pericellular coat following stimulation with TGF- β_1 (Figure 3.9D). Taking measurements of the coat thickness at the widest point of 30 randomly chosen cells of each phenotype and "age" gave a mean thickness for the young fibroblast coat of 2.99 \pm 0.18 μ m at baseline and 7.95 \pm 0.39 μ m following TGF- β_1 stimulation (P < 0.001, paired t-test). For aged fibroblasts the mean coat thickness at baseline was 2.27 \pm 0.16 μ m and following TGF- β_1 stimulation was 2.35 \pm 0.21 μ m (P = 0.78, paired t-test).

3.2.5 The expression of TSG-6 in young and aged fibroblasts

The hyaladherin TSG-6 has been demonstrated to be an important mediator of HA pericellular coat assembly [193, 194, 213]. Following growth arrest, young and aged dermal fibroblasts were stimulated with TGF- β_1 , and TSG-6 mRNA quantified by Q-PCR. In young fibroblasts stimulation by TGF- β_1 resulted in a significant induction of TSG-6 mRNA from basal levels, whilst in contrast, aged fibroblasts demonstrated no significant induction of TSG-6 mRNA. Furthermore, there was an age dependent decrease in TSG-6 expression both at baseline and following TGF- β_1 stimulation (Figure 3.10).

Effect of in-vitro aging on phenotypic activation





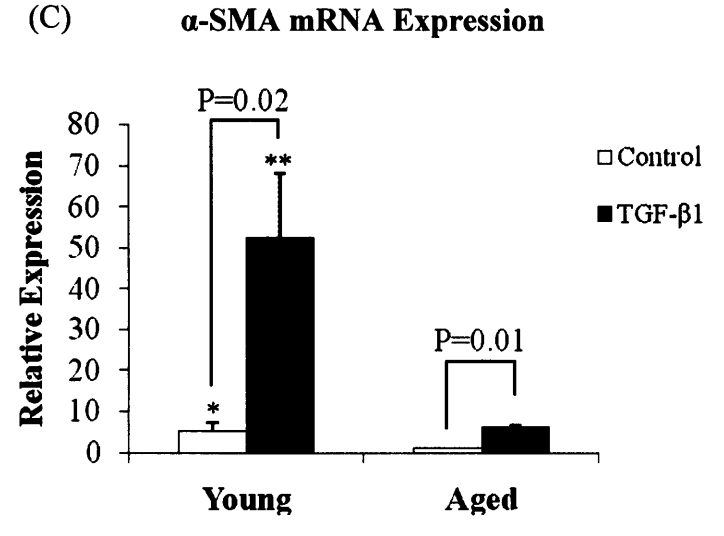


Figure 3.1 Effect of in-vitro aging on α-SMA expression. A-B, confluent monolayers of patient matched young (A) and aged (B) dermal fibroblasts were growth-arrested in serum-free medium for 48 hours, prior to addition of either serum-free medium alone (clear bars) or serum-free medium containing 10ng/ml TGF- $β_1$ (black bars) for the indicated time (hours). C, confluent monolayers of patient matched young and aged dermal fibroblasts were growth-arrested in serum-free medium for 48 hours, prior to addition of either serum-free medium alone (clear bars) or serum-free medium containing 10ng/ml TGF- $β_1$ (black bars) for 72 hours. Total mRNA was extracted and α-SMA expression assessed by RT-QPCR. Ribosomal RNA expression was used as an endogenous control and gene expression was assessed relative to suitable control (Time 0h control for A&B) or (aged-control for C) fibroblasts. The comparative C_T method was used for relative quantification of gene expression and the results are represented as the mean± S.E. of dermal fibroblasts from nine individual experiments with cells isolated from three patient donors. Statistical analysis was performed by the Student's t test: *, p <0.05, **, p<0.01 as compared to aged cells.

Effect of aging on cellular morphology

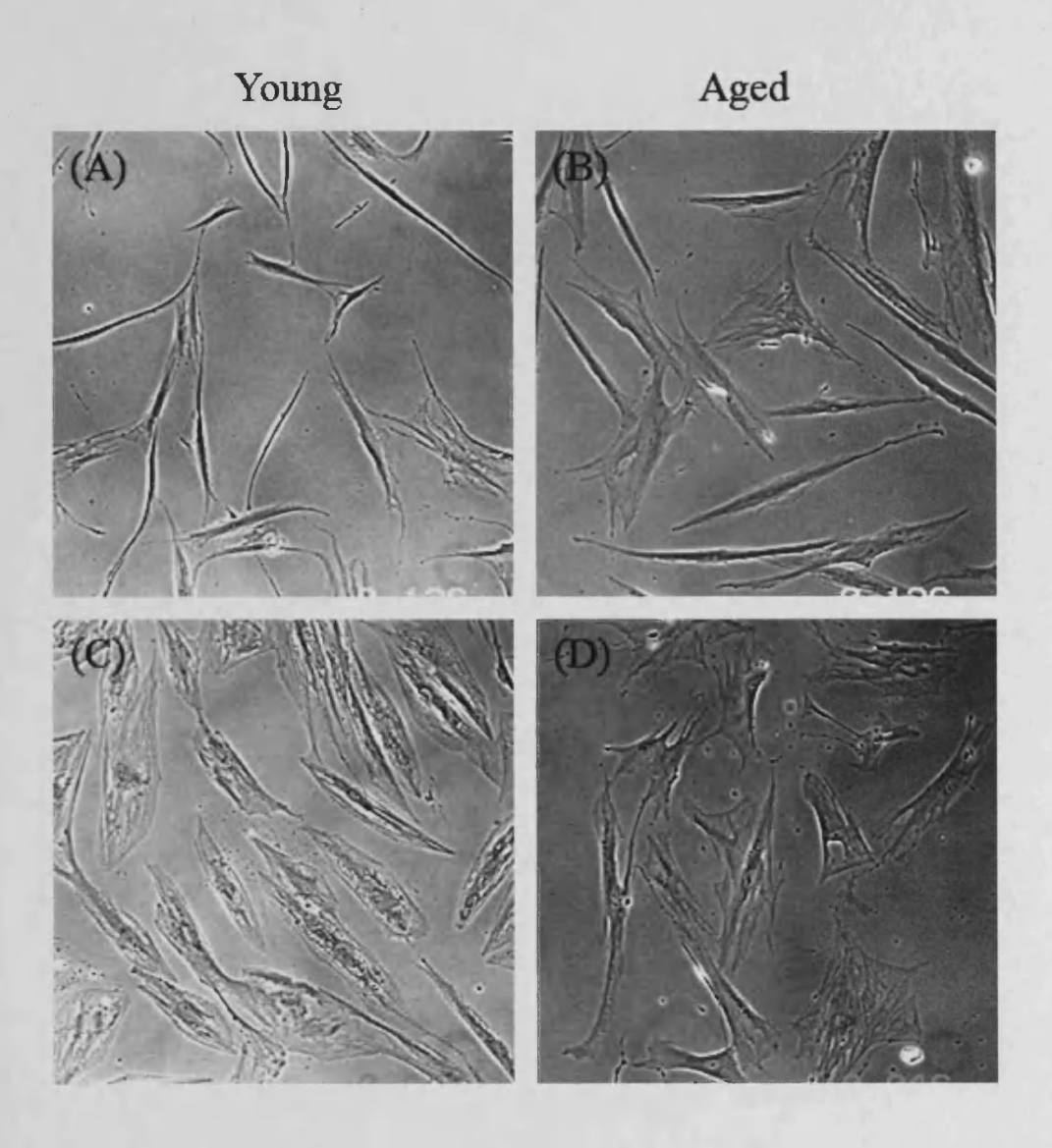


Figure 3.2 Effect of in-vitro aging on cellular morphology. 50% confluent monolayers of patient matched young (A&C) and aged (B&D) dermal fibroblasts were growth-arrested in serum-free medium for 72 h. The medium was then replaced with serum free medium alone (A&B) or containing 10 ng/ml TGFβ₁ (C&D) and the incubations continued for a further 72h. The cells were visualised by phase contrast microscopy on a zeiss Axiovert inverted microscopy. Representative of dermal fibroblasts from four patient donors. Original magnification x 200. Under basal conditions young fibroblasts demonstrate an elongated, spindle-like appearance with little evidence of prominent stress fibres (A), whereas following TGF-β1 stimulation young cells appear larger in size with a polygonal shape and prominent stress fibres (B). With *in-vitro* aging cells become wider, larger and irregular in shape and demonstrate increased stress fibres under basal conditions (C). Following TGF-β₁ stimulation aged cells show little change in appearance form basal conditions (D) and stress fibres are less pronounced than stimulated young cells.

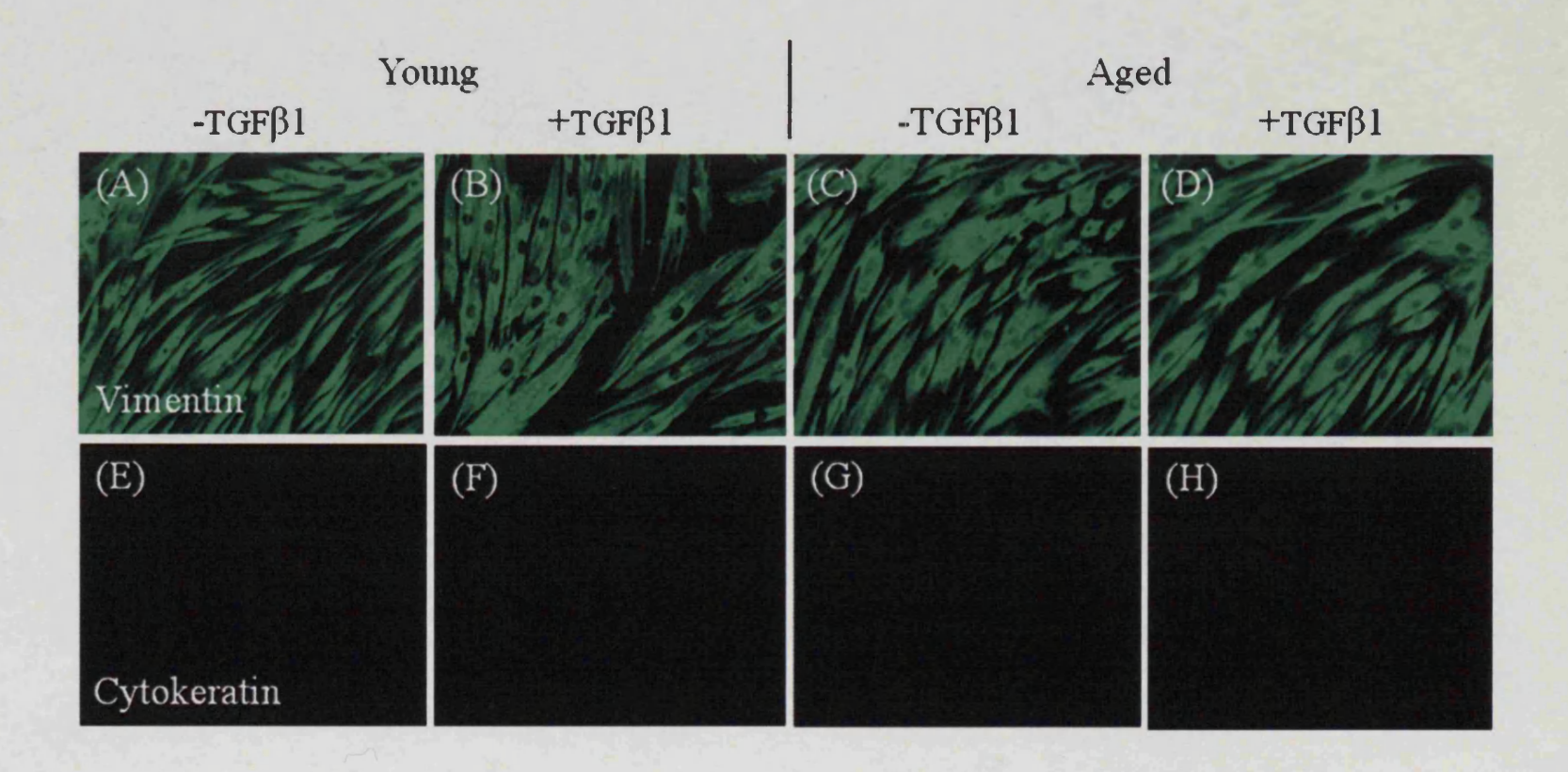


Figure 3.3 Immunohistochemical analysis of vimentin and cytokeratin expression in young and aged fibroblasts. Monolayers of patient matched young (A,B,E,F,) and aged (C,D,G,H) dermal fibroblasts were growth-arrested in serum-free medium for 48 h. The medium was then replaced with either serum-free medium alone (A,E,C,G) or serum-free medium containing 10 ng/ml TGF- β_1 (B,F,D,H) for 72h. The cells were then fixed and antibodies used for the detection of vimentin (A-D), and cytokeratin (E-H) as described under section 2.14. The cells were then mounted in Vectashield fluorescent mountant, and viewed under UV light. All results shown are representative of dermal fibroblasts from three patient donors. Original magnification x 100.

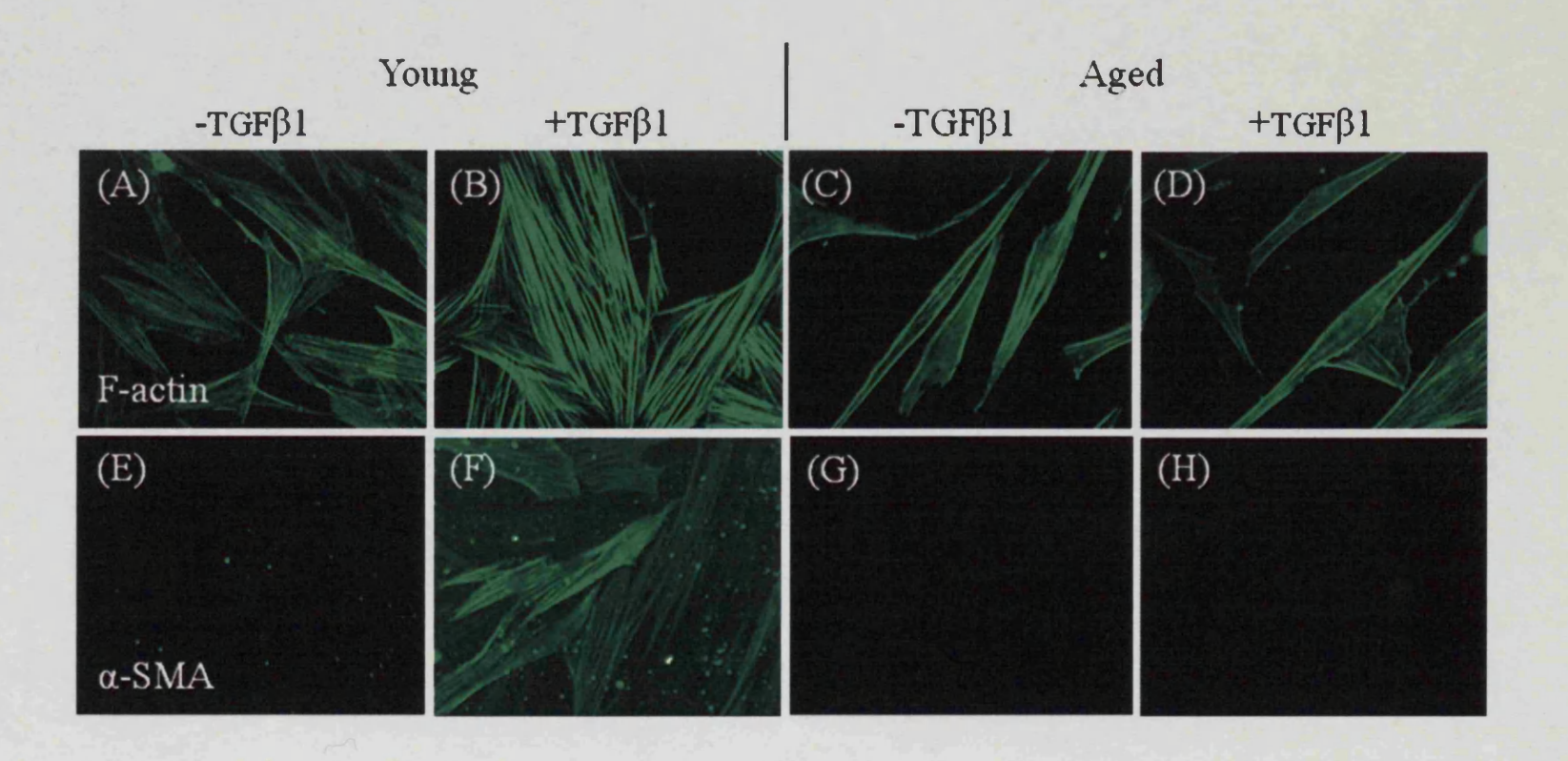


Figure 3.4 Immunohistochemical analysis of F-actin and α-SMA expression in young and aged fibroblasts. Monolayers of patient matched young (A,B,E,F,) and aged (C,D,G,H) dermal fibroblasts were growth-arrested in serum-free medium for 48 h. The medium was then replaced with either serum-free medium alone (A,E,C,G) or serum-free medium containing $10 \text{ng/ml TGF-}\beta_1$ (B,F,D,H) for 72h. The cells were then fixed and filamentous actin was visualised by staining with fluorescein-conjugated phalloidin (A-D) or antibodies for the detection of α-SMA were added as described under section 2.14. The cells were then mounted in Vectashield fluorescent mountant, and viewed under UV light. All results shown are representative of dermal fibroblasts from three patient donors. Original magnification x 100

HA profile of young and aged fibroblasts

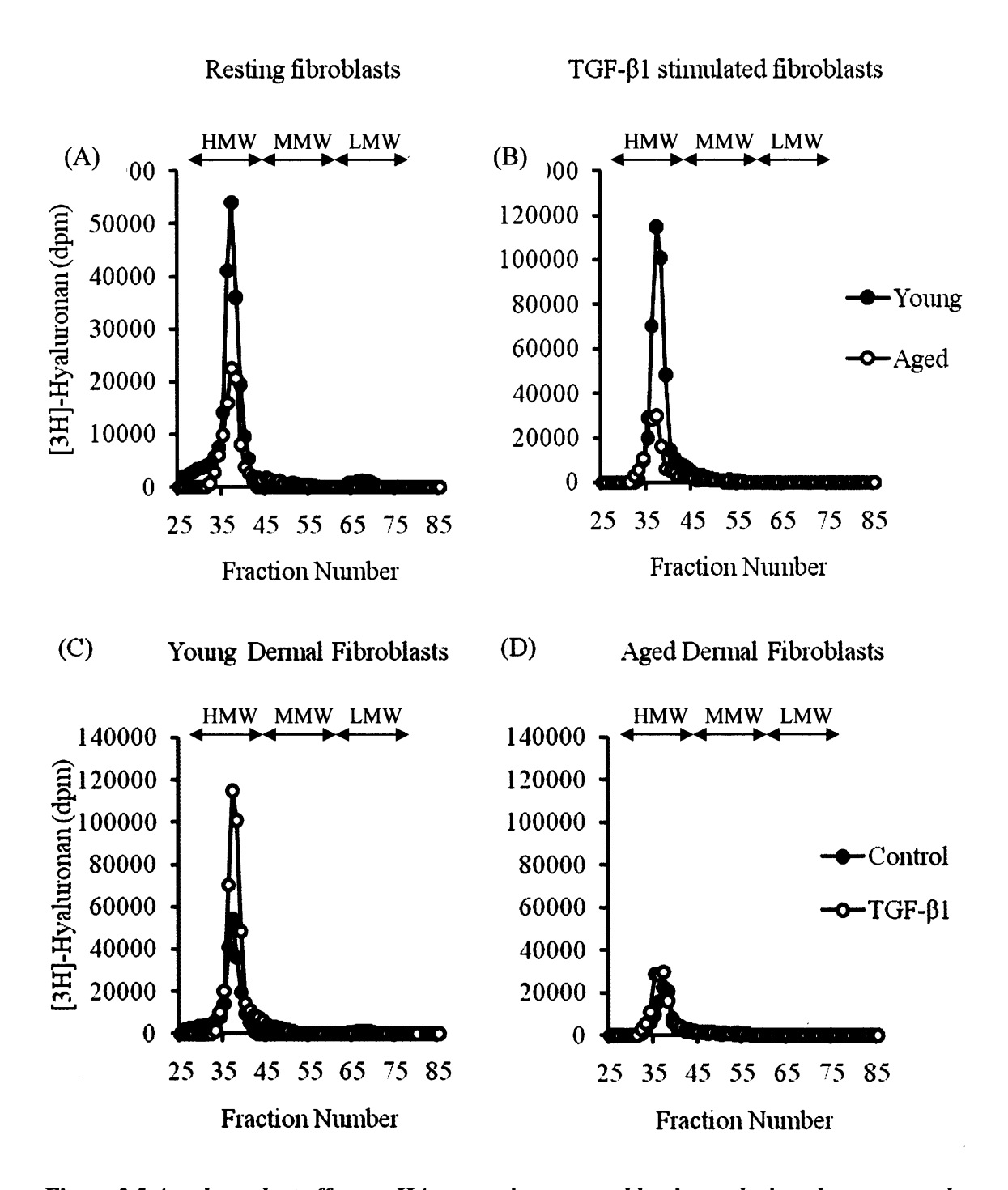


Figure 3.5 Age dependent effect on HA generation assessed by size exclusion chromatography. A,B, confluent monolayers of patient matched young (black circle) and aged (white circle) dermal fibroblasts were growth arrested in serum-free medium for 48 hours. The medium was removed and replaced with either serum-free medium alone (A) or with serum-free medium containing 10ng/ml of TGF- $β_1$ (B) for 72 hours. Cells were subsequently labelled for 24 hours with 20 μCi/ml [3 H]-glucosamine. The radio-labelled HA was isolated from the conditioned medium and subjected to size exclusion chromatography on a Sephacryl S500 column as describe under section 2.12. C,D, confluent monolayers of patient matched young (C), aged (D) dermal fibroblasts were growth arrested in serum-free medium for 48 hours. The medium was removed and cells were metabolically labelled with 20 μCi/ml [3 H]-glucosamine in either serum-free medium alone (black circle) or with serum-free medium containing 10ng/ml of TGF- $β_1$ (white circle) for 72 hours. The radio-labelled HA was isolated from the conditioned medium and subjected to size exclusion chromatography on a Sephacryl S500 column as describe under section 2.12. All results shown are representative of dermal fibroblasts isolated from at least two separate donors. Three arbitrary sizes of HA are indicated, high molecular weight (HMW) >1.5 x 10 6 , medium molecular weight (MMW) 0.4-1.5 x 10 6 and low molecular weight (LMW) < 40 x 10 4 Da.

Age-related changes in HA generation

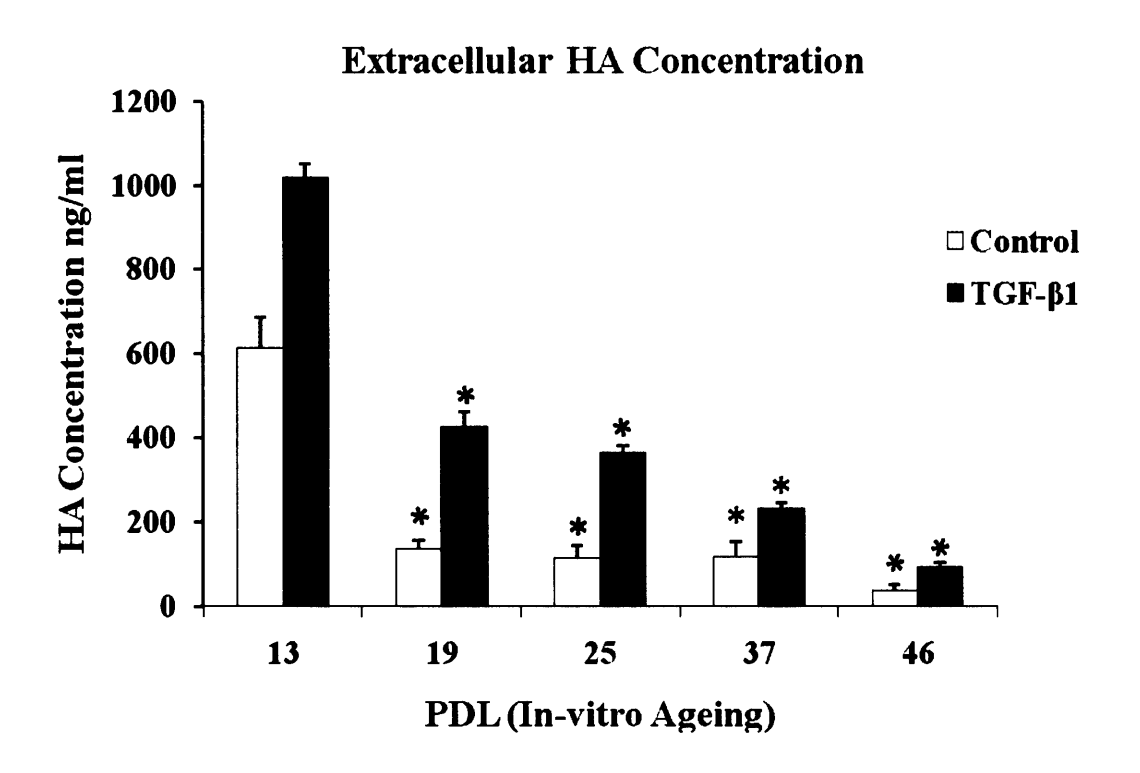
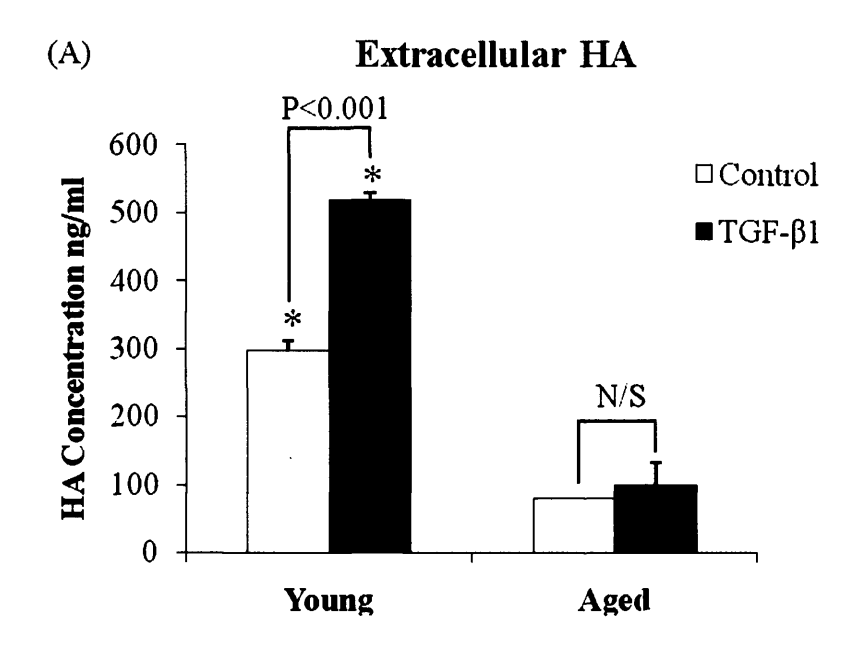


Figure 3.6 Effect of in-vitro aging on extracellular HA generation. At the indicated PDL, confluent monolayers of dermal fibroblasts were growth arrested in serum-free medium for 48 hours. The medium was then replaced with either serum-free medium alone (clear bars) or serum-free medium containing 10ng/ml TGF- β_1 (black bars) for 72 h. HA concentration in the culture medium was quantified by ELISA as describe under section 2.13. The data represent mean \pm S.E. from six separate experiments using cells isolated from one donor. Statistical analysis was performed using ANOVA to show global differences between PDLs for basal (p<0.001) and TGF- β_1 (p<0.001) conditions, followed by Turkey's HSD Post-hoc Test analysis: *, p<0.01 as compared to PDL13.

Age-related changes in HA generation



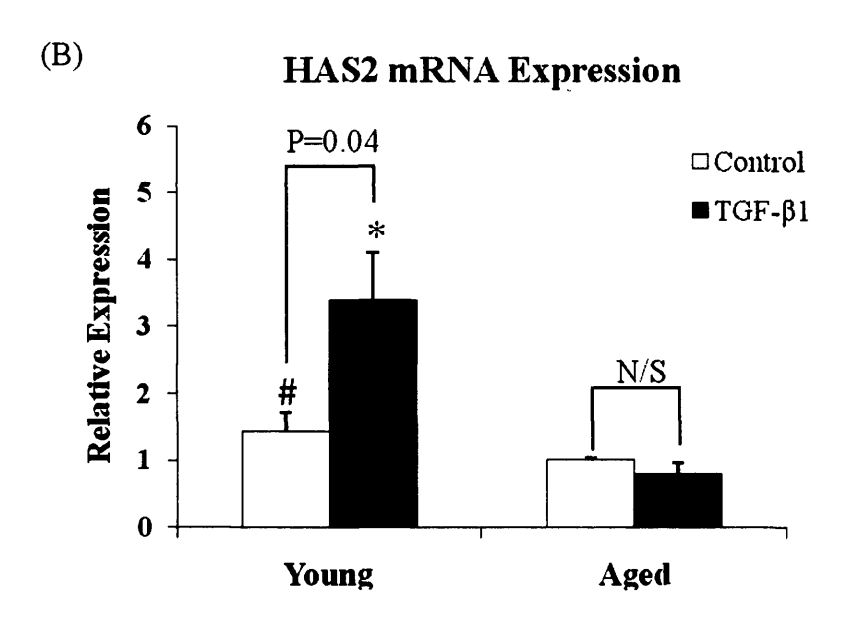
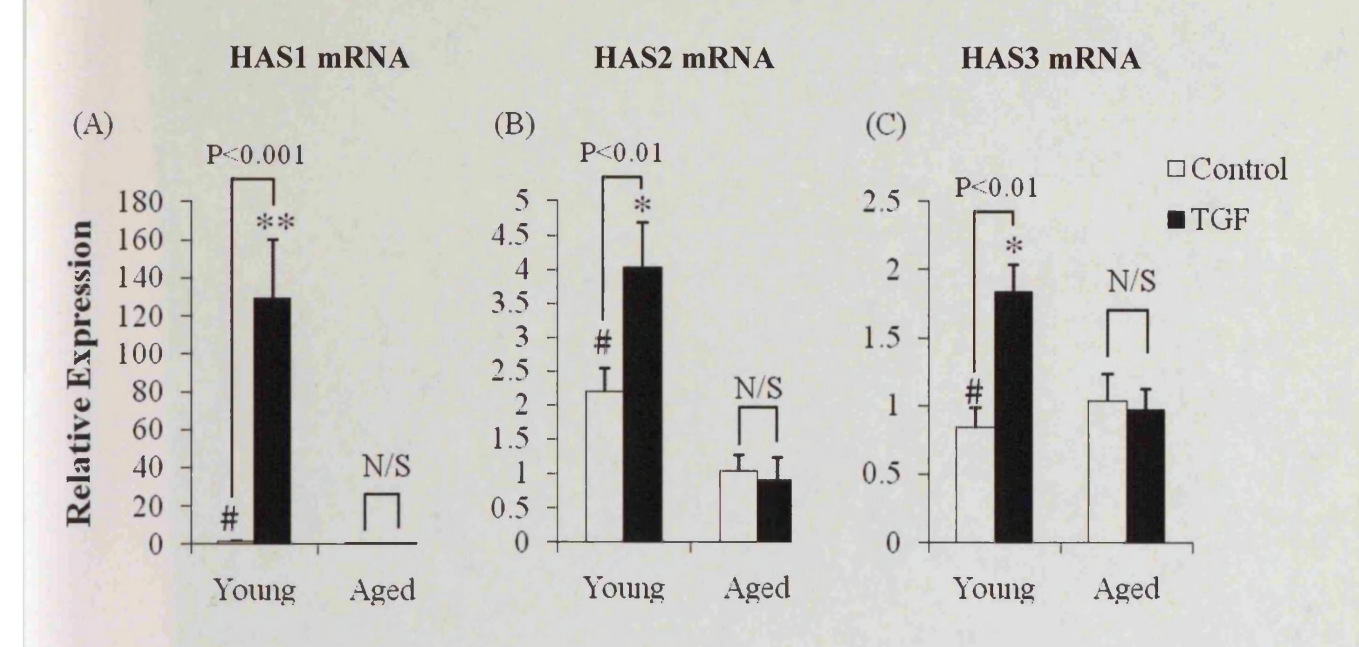
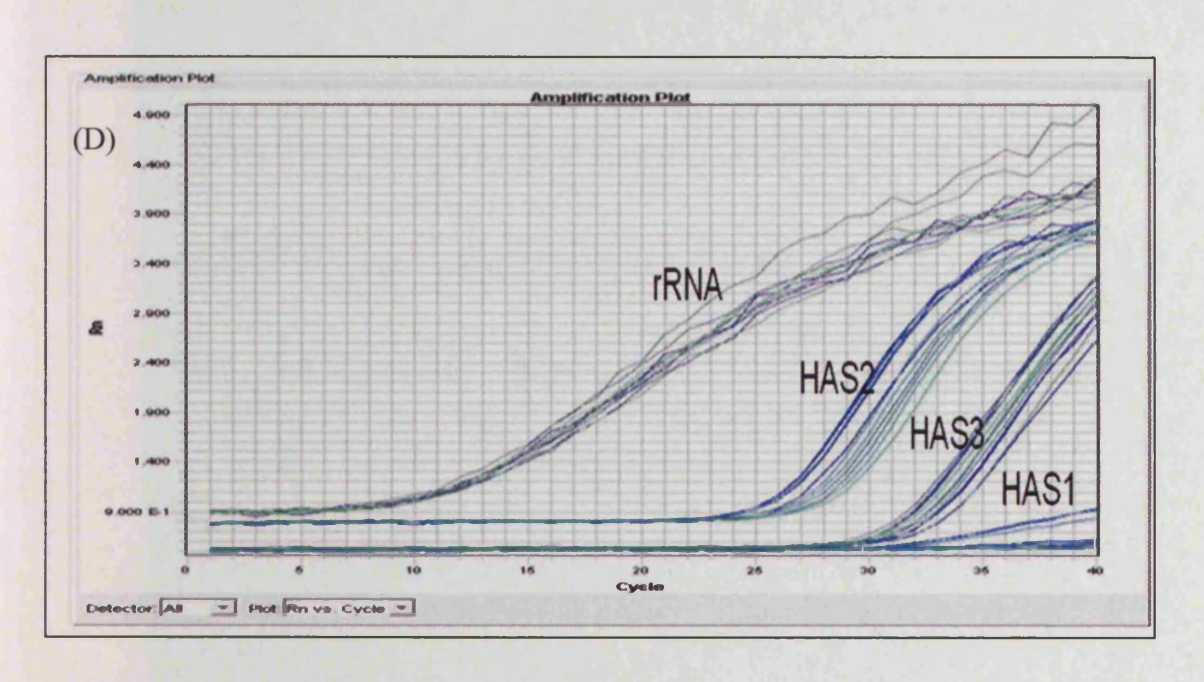


Figure 3.7 HAS2 mRNA expression in young and aged dermal fibroblasts. Confluent monolayers of patient matched young and aged dermal fibroblasts were growth-arrested in serum-free medium for 48 hours. The medium was then replaced with either serum-free medium alone (clear bars) or serum-free medium containing 10 ng/ml TGF- β_1 (black bars) and the incubations were continued for 72 h. HA secreted into the culture medium was quantified by ELISA as describe under section 2.13. Following removal of the culture medium, total mRNA was extracted and cDNA prepared describe under section 2.7. HAS2 expression was assessed by RT-QPCR. Ribosomal RNA expression was used as an endogenous control and gene expression was assessed relative to control aged fibroblasts. The comparative C_T method was used for relative quantification of gene expression. The data are represented as the mean \pm S.E. of six individual experiments using cells from two patient donors. Statistical analysis was performed by Student's t test. *, Not significant, *, p <0.01, as compared to aged cells. N/S (not significant).

Age-related changes in HAS isoform Expression





Hyaluronan-dependent pericellular coats

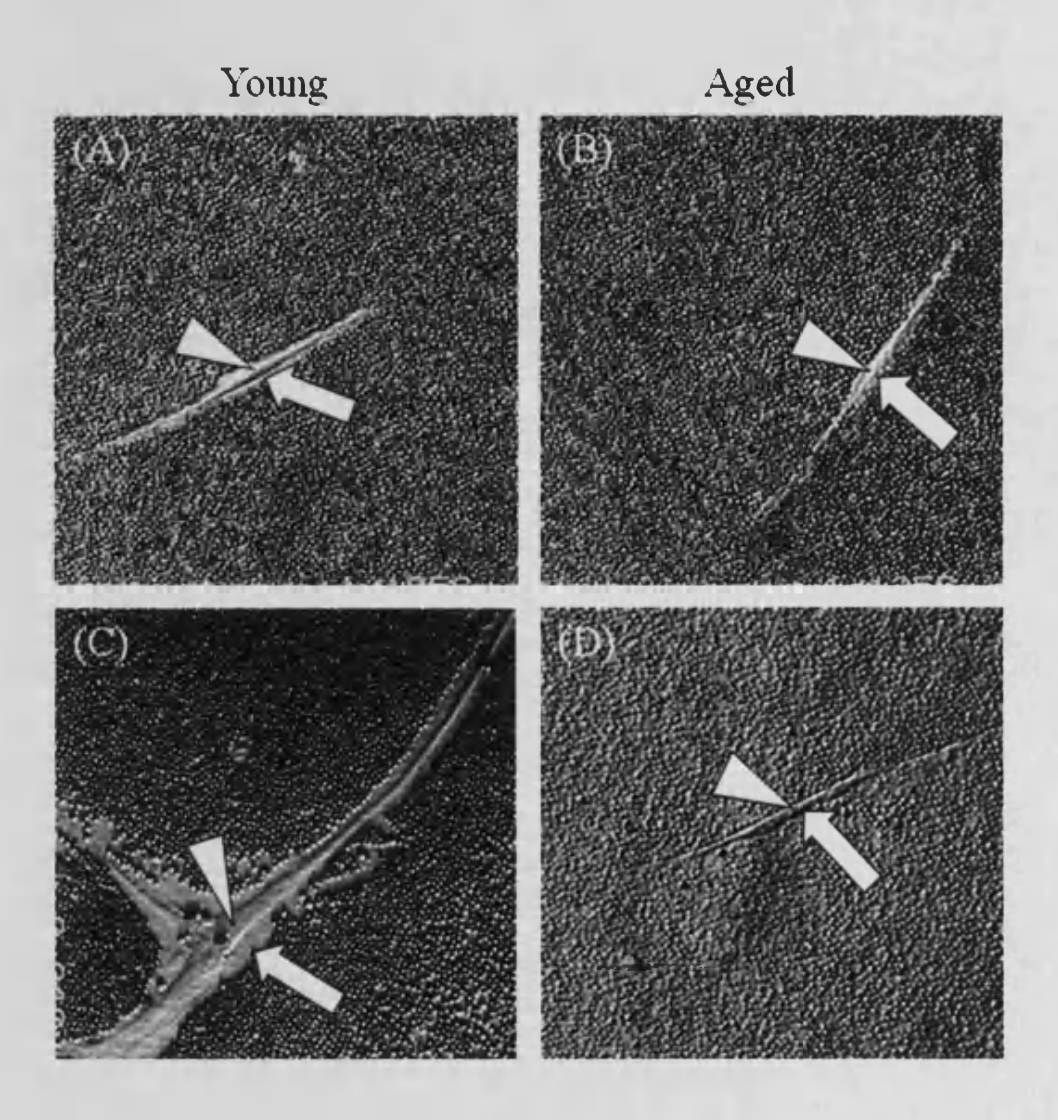


Figure 3.9 Effect of aging on HA pericellular coat assembly. Subconfluent layers of patient matched young (A & C) and aged (B & D) dermal fibroblasts were growth-arrested in serum-free medium for 48 h. The medium was then replaced with either serum-free medium alone (A & B) or with 10 ng/ml TGF- β_1 (C & D) for 72 h. Formalised horse erythrocytes were then added as describe under section 2.11 to visualise the HA pericellular coat. Zones of exclusion were visualised using Zeiss Axiovert 135 inverted microscope. *Arrowheads* indicate the cell body; *Arrows* show the extent of the pericellular matrix. Representative of dermal fibroblasts from three patient donors. Original magnification x 200.

Age-related changes in TSG-6 expression

TSG-6 mRNA Expression

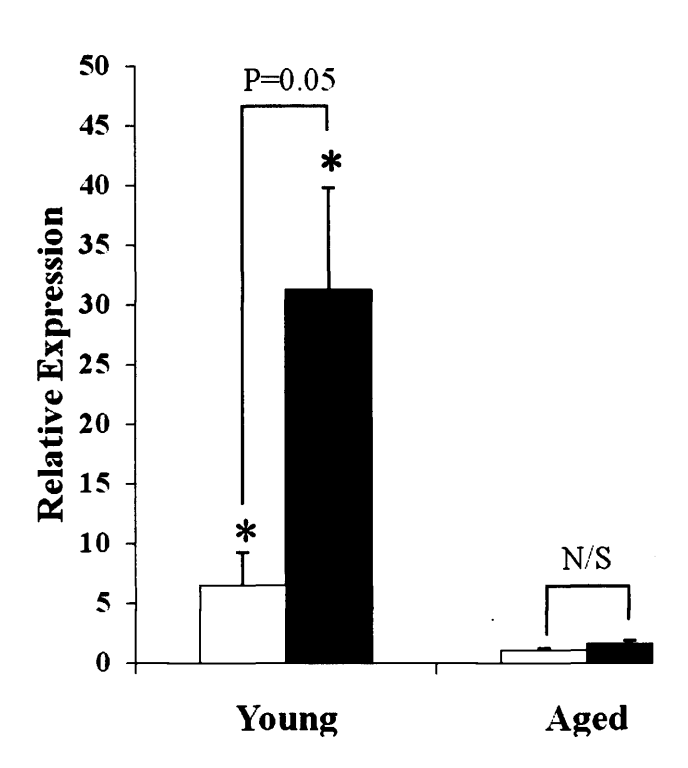


Figure 3.10 Effect of aging on TGF- $β_1$ mediated TSG-6 induction. Confluent monolayers of patient matched young and aged dermal fibroblasts were growth-arrested in serum-free medium for 48 hours. The medium was then replaced with either serum-free medium alone (open bars) or serum-free medium containing 10ng/ml TGF- $β_1$ (black bars) and the incubations were continued for 72 h. mRNA was extracted and cDNA prepared as describe under section 2.7. TSG-6 expression was assessed by RT-QPCR. Ribosomal RNA expression was used as an endogenous control and gene expression was assessed relative to control aged fibroblasts. The comparative C_T method was used for relative quantification of gene expression and the results are represented as the mean± S.E. of dermal fibroblasts from three patient donors. Statistical analysis was performed by the Student's t test: *,p<0.05 as compared to aged cells. N/S, not significant.

3.3 Discussion

Whilst the disruptive effects of aging on the proliferative and migrative capacity of fibroblasts have been well documented [1, 35], the effects of aging on cellular differentiation have not been extensively reviewed. This chapter specifically examines the potential for TGF- β_1 -mediated fibroblast-myofibroblast differentiation associated with *in-vitro* aging and characterises the differences in synthetic enzyme transcription, generation and packaging of HA.

The Results presented in this chapter demonstrate for the first time a failure of dermal fibroblast-myofibroblast differentiation associated with *in-vitro* aging, which may be of relevance to the impaired wound healing associated with aging. In accordance with previous work [159, 160], young dermal fibroblasts readily differentiated into myofibroblasts in response to TGF- β_1 and this was associated with a significant induction in expression and incorporation of α -SMA into their stress fibres. *In-vitro* aged cells demonstrated attenuated α -SMA mRNA expression under both basal and TGF- β_1 stimulated conditions and failed to incorporate α -SMA into their stress fibres, indicating resistance to TGF- β_1 -mediated phenotypic activation. This chapter extends on previous findings and demonstrates in addition to being site specific [159, 160], fibroblastic phenotype is age specific.

Further comparison by young and aged dermal fibroblasts revealed characteristic changes in cellular morphology in addition to the age-dependent changes in phenotypic activation. Under basal conditions young fibroblasts demonstrated an elongated, spindle-like appearance with little evidence of prominent stress fibres. Following TGF- β_1 stimulation, young cells appeared more polygonal in shape, increased in size and demonstrated prominent cytoskeletal re-organisation of filamentous actin stress fibres. Aged cells at rest, appeared larger and more irregular in shape and possessed more stress fibres than their younger counterparts. Furthermore, cytoskeletal re-organisation was less prominent following TGF- β_1 stimulation when compared to young cells and actin fibres appeared more sparse and restricted to the cell periphery.

HA expression is tightly associated with, and is thought to regulate cellular differentiation. In human skin organ cultures, factors like all-trans-retinoic acid, which increase HA synthesis, have been shown to delay differentiation [278]. Likewise, organotypic epidermal cultures show that keratinocyte differentiation is stimulated and inhibited by factors that decrease and increase HA synthesis, respectively [279]. In contrast, enhancing turnover of cell surface HA by Hyaluronidase promotes terminal differentiation of keratinocytes [213] and previously work in the Institute of Nephrology (ION) demonstrated that HA upregulation is associated with TGF- β_1 -driven dermal fibroblast–myofibroblast transition [159, 160, 266]. I subsequently sought to relate age related changes in HA generation to failure of phenotypic activation in the aged phenotype.

The HA profile of young dermal fibroblasts resembled that previously characterised [159, 160]. Under basal conditions, dermal fibroblasts generated large amounts of high molecular weight extracellular HA. Following stimulation by TGF- β_1 , young cells generation of extracellular HA was augmented and cells were characterised by the formation of prominent HA-dependent coats which surrounded the cell. The data presented in this chapter clearly demonstrated a decrease in HA generation both in unstimulated cells and also following addition of TGF- β_1 associated with *in vitro* aging but it should be added that the molecular weight did not vary. Young cells demonstrated at rest, 2.5-fold more HA in the conditioned medium when compared to aged cells and over 4-fold more HA in the conditioned medium following TGF- β_1 stimulation. Further analysis revealed that young and aged cells differentially regulated their HA accumulation by TGF- β_1 . Whilst young fibroblasts demonstrated sizeable gains in HA generation in response to TGF- β_1 , patient matched aged fibroblasts were resistant to HA up-regulation in response to the same dose and duration of TGF- β_1 stimulation. Associated with this was an age-related failure to generate a HA pericellular coat.

These data are consistent with our previous observations suggesting that increased HA generation were causally related to TGF- β_1 mediated fibroblast-myofibroblast conversion [159]. Previously, studies demonstrated a significant difference in HA

generation under basal conditions with cells capable of myofibroblastic change, i.e. young dermal fibroblasts, generating significantly more HA than those resistant to phenotypic change i.e. oral mucosal fibroblasts [159]. Furthermore it was previously demonstrated that the different basal patterns of HA generation were associated with the regulation of differing proliferative responses to TGF-β1 by the two fibroblast populations [160]. Similarly, data presented in this chapter demonstrated that resistance to TGF-β1-mediated phenotypic activation in aged cells is associated with attenuation of HA synthesis.

Upregulation of HASs has been found in the context of tissue injury [179]. Previous work has suggested that specific HA synthase isoform activity plays an essential role in instigating cell differentiation [280]. Recently, direct evidence on the role of HA in epidermal keratinocytes emerged by the finding that HAS2 regulated HA synthesis controls migration rate of keratinocytes in scratch-wounded monolayer cultures [281]. Sugiyama et al [282] found that $TGF-\beta_1$ upregulates HAS1 and HAS2 expression independently in cultured human skin fibroblasts, whilst HAS3 gene expression was downregulated upon $TGF-\beta_1$ -mediated myofibroblastic differentiation and cellular senescence [283]. In addition to HA accumulation, the results from this chapter examined the differential expression of HAS isoforms associated with the aging fibroblast.

Accumulation of extracellular HA in response to TGF- β_1 was consistent with the findings that TGF- β_1 induced the expression of HAS1, HAS2 and HAS3 isoforms in young dermal fibroblasts. Accordingly, the data presented in this chapter demonstrated *in-vitro* aging and resistance to phenotypic conversion was accompanied by a failure of HAS1, HAS2 and HAS3 induction by TGF- β_1 . The observed age-related attenuation in HA generation under resting conditions could not be so easily explained by differences in HAS expression. Baseline expression of HAS1 and HAS3 enzymes did not significantly differ between young and aged cells. Despite not being statistically significant, however, blunted expression of basal HAS2 may play an important role in dictating attenuated HA levels in the aged phenotype. A unique deficiency of the HAS1 isoform was observed in the non-scarring non-differentiating oral fibroblasts. Neither

HAS1 over-expression in oral fibroblasts nor HAS1 down-regulation in dermal fibroblasts influenced TGF- β_1 -mediated phenotypic activation in previous studies [159], suggesting that HAS1 isoform expression is not critical for acquisition of the myofibroblast phenotype. Data from this chapter further support a redundant role of HAS1 in regulating cellular phenotype. Assuming comparable sensitivity of assays for HAS1-3 by QPCR, evaluation of the amplification plot revealed relative expression levels of HAS1 were almost undetectable in quiescent cells, and despite a large 130-fold induction of HAS1 by TGF- β_1 in young fibroblasts, it should be recognised that this is 130-fold induction of negligible levels. Comparison of relative HAS transcription revealed, regardless of age, HAS2 mRNA was more abundant, suggesting it may be important for regulating myofibroblastic differentiation.

Vigetti et al showed that the accumulation of HA during aging is likely to be a result of increased expression of synthetic enzymes, rather than a down-regulation of degrading enzymes [284]. Consistent with this, work from this laboratory demonstrated that no significant differences in Hyal expression was detected between dermal and oral fibroblasts, suggesting that increased HA related to dermal fibroblasts was a result of increased HA generation rather than reduced turnover [285]. In contrast to these studies, Jenkins et al [266] propose that HA accumulation associated with myofibroblastic differentiation in lung fibroblasts was a consequence of a decrease in HA degradation as opposed to an increase in HA synthesis. The authors' specifically showed that cell associated Hyal activity is redistributed and shed from myofibroblasts when they have differentiated, thus reducing their capacity for HA degradation.

A comparison of Hyal expression was not assessed between young and aged dermal fibroblasts in this study and so it cannot be ruled out that *in-vitro* aging may result in upregulation in Hyal activity and increased HA degradation. It is, however, more likely that age-related attenuation in HA generation was attributed solely to reduced HA synthase transcription, based on the notion that augmented Hyal activity in aged cells would have resulted in generation of smaller HA fragments and clearly the molecular weight of HA generated did not decrease with *in-vitro* aging. Therefore, I propose that

age-related attenuation in HA generation was attributed solely to reduced HA synthase transcription.

Recent data suggested that the functional effects of HA depend on the context in which HA is assembled and packaged. This has been aided by a recent report that in proximal tubular epithelial cells HA can be either disease promoting or disease limiting, depending on organisation of HA into coat or cable like structures, respectively [194]. HA-rich matrices are essential for the proliferative and migratory phenotype [212, 213], during embryonic development and organogenesis and are involved in tumour cell invasion [286]. Increased cell-associated HA and increased thickness of the cell coat has also been associated with myofibroblast differentiation [266, 287].

The other striking disparity between young and aged dermal fibroblasts from this chapter was their ability to generate pericellular HA coats. In young cells, phenotypic activation was associated with assembly of pericellular coats, whereas resistance to differentiation in *in-vitro* aged cells was associated with failure of HA coat assembly. The functional consequence of these differences, in terms of potential for phenotypic maturation, will be investigated in the following chapter.

Many studies have demonstrated the importance of HA-binding proteins, termed hyaladherins, in the organisation of HA matrices. One hyaladherin, which has a particular role in the formation of pericellular HA coats, is tumour necrosis factor-α-stimulated gene 6 (TSG-6). It is implicated in the stabilization of ECM structure, particularly by supporting the formation of cross-linked HA networks [288]. Fülöp et al have shown that TSG-6 -/- mice are infertile due to their inability to form a HA-rich extracellular matrix [289]. In addition, work in the ION has shown the importance of TSG-6 in the formation of a pericellular HA in epithelial cells of renal origin [290]. Furthermore, the ability of TSG-6 to modulate the interaction of HA with CD44 has important implications for CD44-mediated cell activity at sites of inflammation [190]. In the current study I have demonstrated an age dependent impairment in HA pericellular coat assembly. Consistent with this, *in-vitro* aged fibroblasts demonstrated a decrease in TSG-6 expression, both in unstimulated cells and in response to TGF-β₁

Data from this chapter presents evidence that *in-vitro* aging is associated with attenuation of numerous TGF- β_1 -dependent responses, including α -SMA induction, HA synthesis, induction of HAS and TSG-6 transcription and assembly of HA-dependent pericellular coats. In fact, all the responses mediated by TGF- β_1 investigated throughout this chapter have displayed impairment with *in-vitro* aging. This strongly suggests that the results observed may be simply a product of an age-dependent global deficit in TGF- β_1 signalling. Several studies have provided a link between dysregulation of TGF- β_1 signalling and disease promotion whether it be through loss of receptor expression [291] [292], increased receptor internalisation [209, 293], or modulation of SMAD and non-SMAD signal transduction pathways [106, 160, 210, 294]. The impact of *in-vitro* aging on TGF- β_1 signalling will be further investigated in the subsequent chapter.

The data presented herein suggest a model of dermal fibroblast aging in which both basal and TGF- β 1-stimulated cell activities decline with increasing PDs. Loss of TGF β 1-mediated responsiveness in aged cells is linked to decreased levels in HA generation and failed acquisition of a HA pericellular coat. The decrease in basal cell activities is likely due to a second, possibly independent cell change that does not involve TGF- β 1 signalling. It remains to be determined whether these two events have a common casual basis at the gene regulation level.

Differential regulation of HAS2 expression by dermal and oral fibroblasts was assumed to be the mechanism responsible for differences in TGF-β₁-directed HA generation [159]. The data from this chapter support a role for HAS2 over HAS1 and HAS3 by virtue of its increased transcription. In addition it serves as the only HAS candidate that could account for differences in basal HA and generation of both high molecular weight and pericellular HA. In light of these results and in light of previous research relating to the HAS2 isoform in cellular differentiation [159, 162], examining the role of this isoform in regulating fibroblast behaviour will be further examined in the next chapter.

The salient findings of this chapter are summarised in figure 3.11. In summary, the data presented demonstrates an age related alteration in fibroblast behaviour which

results in an inability to undergo phenotypic transformation to become a myofibroblast. $TGF-\beta_1$ addition to young cells, induced their differentiation to α -SMA positive myofibroblasts. *In-vitro* aging of dermal fibroblasts confers resistance to $TGF-\beta_1$ -driven fibroblast-myofibroblast conversion and is associated with age-dependent attenuation in HAS transcription, synthesis of HA and its assembly into a pericellular coat. Since it is the myofibroblast that orchestrates the successful formation of granulation tissue and matrix remodelling, this is an important finding that may be central to the delayed healing seen in the elderly. This data adds credence to the hypothesis that the matrix polysaccharide HA is an important component of the regulation of fibroblast phenotype and that its dysregulation may be casually related to failure of a fibroblast to acquire a myofibroblastic phenotype.

The data presented in this chapter demonstrated distinct age-related heterogeneity in HA biosynthesis and packaging by patient matched young and aged cells which may yield important insights into impaired wound healing processes characterised in the elderly

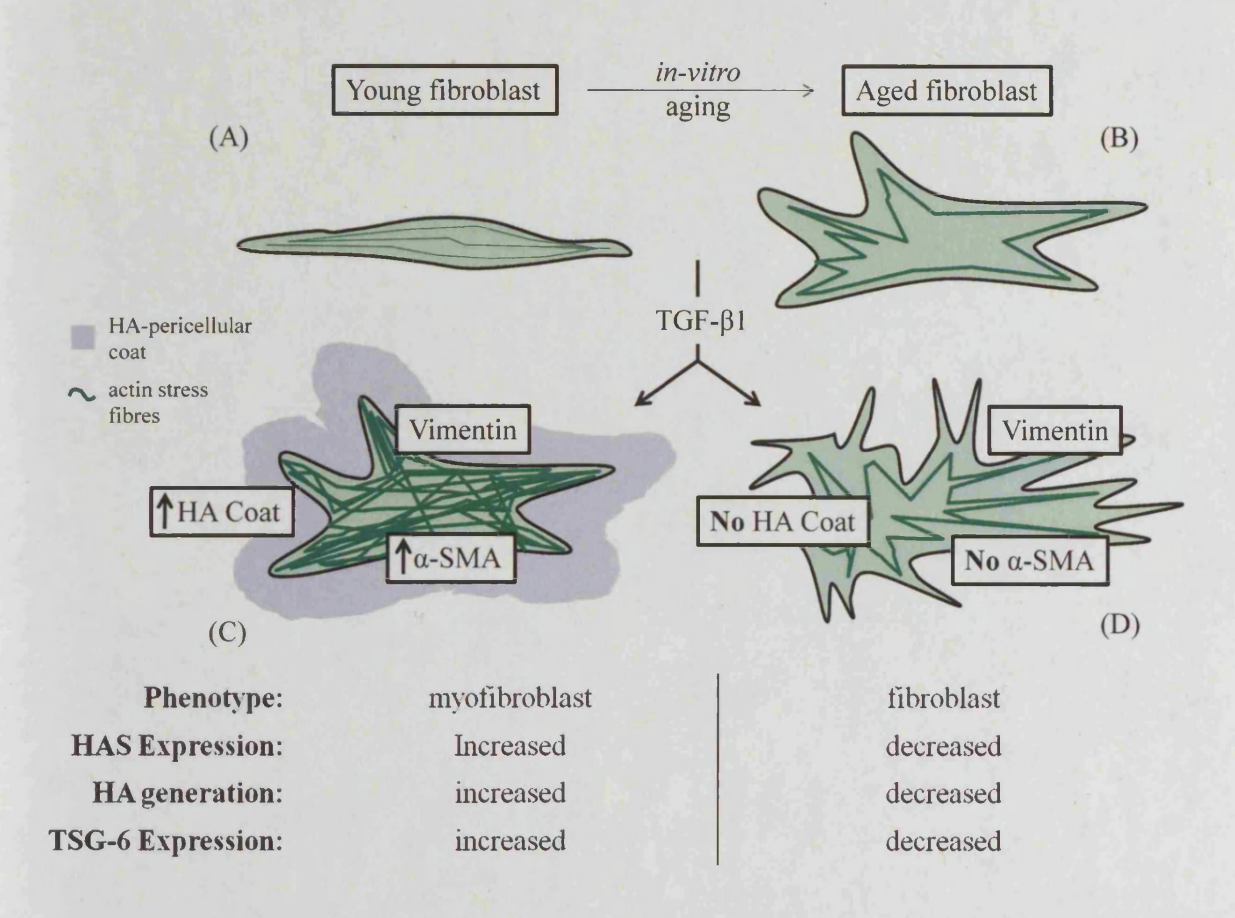


Figure 3.11 Comparison of young and in-vitro aged fibroblast phenotype. A comparison of cell morphology, HA generation and phenotype of patient matched young (A&C) and aged (B&D) dermal fibroblasts at rest (A&B) and following TGF- β 1 stimulation (C&D), based on the analysis compacted from this results chapter. Under basal conditions, vimentin positive young dermal fibroblasts are elongated, spindle-like with no evidence of prominent stress fibres (A). In response to TGF- β 1, fibroblasts readily differentiate into myofibroblastic cells which are lager, polygonal in shape and incorporate prominent stress fibres and α-SMA (C). This is associated with upregulated HAS expression, increased HA synthesis, TSG-6 induction and assembly of a HA pericellular coat. With *in-vitro* aging, vimentin positive fibroblasts become wider, larger and more irregular in shape and exhibit more stress fibres (B). Following TGF- β 1 stimulation the cells appear more dentritic but fail to incorporate α-SMA or assemble prominent stress fibres in contrast to their younger counterparts (D). Resistance to TGF- β 1 mediated myofibroblastic differentiation is associated with attenuated HAS induction, reduced HA synthesis, TSG-6 induction and failure to synthesise a HA pericellular coat.

Chapter 4 Differential Effects of Aging on TGF-β1 Signalling and Organisation of Pericellular Hyaluronan

4.1 Introduction

In the previous chapter failure of TGF-β1-induced cellular differentiation and HA coat formation in aged cells was associated with the inability to induce HAS2. Several studies have confirmed a specific role for HAS2 in both of these processes. Previously it was demonstrated that resistance of oral mucosal fibroblasts to TGF-β1 mediated myofibroblastic change is associated with failure of induction of HAS2 [159]. HA synthesis regulated by HAS2 is an important component in epidermal proliferative and differentiation processes [279]. This is in accordance with previous work demonstrating that HAS2 inactivation in mice embryo is lethal because of failure of cardiac endothelial cells to undergo epithelial to mesenchymal transition [295].

Induction of HAS2 in human vascular smooth muscle cells using the prostacyclin analogue, iloprost markedly increased pericellular formation of HA coats [286]. HA secreted by HAS2 binds to CD44, and functions in pericellular coat formation and hydration in the extracellular space, thus offering an advantageous environment for osteosarcoma cells [296], whilst inhibition of HAS2 activity with HAS2 antisense oligonucleotides has been demonstrated to disable pericellular matrix assembly in human articular chondrocytes [297].

Manipulation of the HAS genes has enabled the over-expression or inhibition of the different HA synthase isoforms, which has provided a preliminary insight into the role of HA synthesis in biological processes. Whilst HA synthesis, induced by HAS1 overexpression led to increased HA cable formation [298], HAS2 overexpression led to the formation of pronounced pericellular coats. This was shown to enhance cell motility, a key early stage in epithelial to mesenchymal transition [194]. HAS2 adenoviral transfection in Madin-Darby canine kidney epithelial cells has been associated with the development of mesenchymal and malignant characteristics [280].

These studies together with the work outlined in the previous chapter lead me to postulate that resistance to phenotypic conversion observed in aged fibroblasts was related to an age-dependent failure in HAS2 induction by TGF-\$1. Furthermore, that the

increase in HA synthase that is driven by the inducible form HAS2, is responsible for pericellular formation of HA coats. For examination of this hypothesis, this chapter utilises siRNA technology and over-expression techniques to characterise the participation of HAS2-driven HA synthesis and its pericellular assembly in regulating fibroblast phenotype.

The results from the previous chapter have demonstrated that young and aged dermal fibroblasts exhibit intrinsic differences in their ability to respond to TGF- β 1, associated with resistance to phenotypic conversion and alterations in HA generation, distribution and HAS isoform expression. Mogford et al [299] demonstrated that aged fibroblasts have an impaired migratory capacity that is a result of decreased TGF β RI levels. The authors propose that such deficits in the migratory and signal transduction responsiveness to TGF- β 1 may partly explain diminished healing capabilities often observed in aged patients. It is therefore interesting to speculate that the diminished response to TGF- β 1 exhibited in my aged cells may be a consequence of either reduced autocrine secretion of, impaired binding of, or dysfunctional receptors for TGF- β 1.

Although it is now appreciated that $TGF-\beta_1$ plays a central role in mediating the response to injury, very little is known of the signalling pathways *in-vivo* that regulate fibroblasts-myofibroblast differentiation. The classical signalling pathway for $TGF-\beta$ involves the Smad family of transcriptional activators [300, 301]. The receptor associated R-Smad, Smad2 and Smad3 are phosphorylated directly by the $TGF-\beta$ type 1 receptor kinase, after which they hetero-oligomerize with Smad4, translocate to the nucleus, and together with their binding partners activate or repress their target genes. *In-vitro* studies have shown that manipulation of Smad2 and Smad3 levels differentially influences cellular responses such as ECM production, chemotaxis, proliferation and stress fibre organisation [302]. Targeted deletion of Smad2 or Smad3 genes in mice and in embryonic fibroblasts, revealed distinct non-redundant roles for each of these transcription factors [303] and $TGF\beta_1$ -Smad-dependent events may be mediated by either or both Smad2 and Smad3. Transcription of α -SMA in lung myofibroblasts-like cells was reported to be predominantly mediated by the binding of Smad3 [133], whereas nuclear translocation of Smad2 was shown to be directly responsible for

myofibroblast differentiation [294]. In this chapter the role of Smad2 and Smad3 in TGF-β1 mediated fibroblasts-myofibroblast differentiation is assessed.

It is interesting to postulate that the differential response to TGF- $\beta1$ in my phenotypically distinct populations of young and aged fibroblasts are due to differences in Smad2 and Smad3 signalling. Therefore in addition, potential age-related alterations in Smad signalling which could account for diminished responsiveness to TGF- $\beta1$ are investigated.

The role of R-Smads have been previously demonstrated in the regulation of TGF- β 1 dependent fibroblast proliferation. Furthermore this effect may be modified by HA [270, 304, 305]. Previous work from this laboratory, using epithelial cells, has demonstrated that HA may modify TGF- β 1 signalling by altering the turnover of TGF- β 1 receptors at the cell surface, resulting in alteration in the pattern of activation and phosphorylation of the signalling intermediates Smad2 and Smad3 [209, 210]. Bourgignon et al demonstrated that in metastatic breast cancer cells, CD44 is physically linked to the TGF- β 1 receptor and that binding of HA to CD44 promotes TGF- β 1 mediated cell migration through augmentation of Smad2/3 signalling [203]. In addition to assessing the role of HA in myofibroblast differentiation this chapter will investigate the relationship between HA and TGF- β 1 signalling.

The aim of this chapter is:

- i To characterise TGF-β1 signalling in young and aged dermal fibroblasts, specifically:
 - the significance of Smad2 and Smad3 in phenotypic activation
 - the significance of age-related alterations in Smad2 and Smad3
- To determine a functional role for HA in myofibroblastic differentiation specifically:
 - the significance of age-related changes in HAS2 expression
 - the significance of age-related changes in HA pericellular coat formation
- iii To examine whether modulating HA levels can influence the aged phenotype
- iv To investigate a relationship between TGF-β1 signalling and pericellular HA organisation

The results from this chapter will help address the hypotheses that age-related resistance to myofibroblastic differentiation results from defective pericellular HA organization and/or defective TGF- $\beta1$ signalling. Furthermore this chapter addresses whether modulation of HA levels alters cellular wound healing responses and the aging phenotype

4.2 Results

4.2.1 The effect of ALK-5 inhibition on phenotypic activation

The importance of TGF-\beta1 signalling for phenotypic activation was investigated using SB431542, an inhibitor of activin receptor-like kinase (ALK)5 (the TGF-β type I receptor). It also inhibits the activin type I receptor ALK4 and the nodal type I receptor ALK7, which are very highly related to ALK5 in their kinase domains. Growth-arrested fibroblasts were incubated for 72 h in serum-free medium alone or containing SB431542 (10 µM) in the absence or presence of TGF-\beta1 (10 ng/ml). Incubation of young fibroblasts with SB431542 resulted in abrogation of TGF-\(\beta\)1 dependent induction of α-SMA mRNA expression compared to control treatments as assessed by Q-PCR (Figure 4.1A) and immunohistochemistry (Figure 4.1D-G). In contrast, incubation with the p38MAPK inhibitor SB203580 had no effect on α-SMA expression (Figure 4.1A). In parallel experiments, the importance of TGF-\beta1 signalling in the induction of HAS2 (Figure 4.1B) and TSG-6 expression (Figure 4.1C) was investigated by Q-PCR analysis. Whilst basal and TGF-\beta1-mediated HAS2 induction was significantly reduced in cells incubated with SB431542, there was no significant variation in levels of TSG-6 expression. The P38MAPK inhibitor SB203580 demonstrated no effect on both HAS2 and TSG-6 expression.

4.2.2 The expression of endogenous TGF-β1 in young and aged fibroblasts

It has been previously demonstrated that autocrine TGF-β1 signalling is necessary for maintenance of myofibroblast phenotype [162]. To determine whether impaired autoinduction of TGF-β1 could account for diminished TGF-β1 responsiveness associated with *in-vitro* aging, generation of TGF-β1 was examined at the level of transcription by Q-PCR in young and aged fibroblasts in the absence and presence of exogenous TGF-β1 (Figure 4.2). Under basal conditions, aged cells demonstrated increased expression of TGF-β1 mRNA but more significantly neither young nor aged cells demonstrated significant variation in autocrine levels. This result suggests

autocrine TGF-β1 signalling is competent in aged fibroblasts and cannot explain the age dependent loss of TGF-β1 dependent phenotypic activation.

4.2.3 The effect of Smad2 and Smad3 knock-down in TGF-β1 mediated responses in young fibroblasts

Given the importance of TGF- β 1 in the phenotypic conversion of fibroblasts, the role of the TGF- β 1 signalling intermediates Smad2 and Smad3 in TGF- β 1 dependent phenotypic activation was examined by gene silencing using siRNA. Suppression of Smad2 expression (Figure 4.3A) and Smad3 expression (Figure 4.4A), following transfection with siRNA was confirmed by Q-PCR.

Inhibition of Smad2 expression was associated with a failure of TGF- β 1 to increase α -SMA in young fibroblasts (Figure 4.3B), confirming previous work suggesting the involvement of this signalling intermediate in fibroblast phenotypic activation [112]. In contrast, successful knockdown of Smad3 using siRNA failed to have an effect on TGF- β 1-mediated phenotypic differentiation (Figure 4.4B). Suppression of Smad2 or Smad3 displayed no significant changes in the expression of HAS2 (Figure 4.3C & 4.4C) or TSG-6 (Figure 4.3D & 4.4D).

4.2.4 The effect of in-vitro aging on Smad 2 and Smad 3 signalling

Given the age dependent failure of TGF-β1 directed phenotypic activation demonstrated in the previous chapter, I sought to examine the effects of *in-vitro* aging on Smad2 and Smad3 signalling by Western blot analysis of TGF-β1 dependent phosphorylation. Work in ION has previously shown that young dermal fibroblasts strongly phosphorylate Smad 2 and Smad3 in response to TGF-β1 [160]. In these experiments, Smad2 and Smad3 activation by TGF-β1 and the effect of *in-vitro* aging were assessed. Smad2 was rapidly phosphorylated (within 15 minutes) after addition of TGF-β1 to quiescent cells and peak activation was observed after 1hr. This kinetic profile did not change across the range of *in-vitro* ages investigated, extending from young (PDL 15), through to near-senescent cells (PDL 39) (Figure 4.5A). Peak Smad2 phosphorylation

(1hr with TGF-β1) was directly compared across the range of *in-vitro* ages demonstrating that the extent of phosphorylation also did not vary with aging (Figure 4.5B).

Smad3 was also phosphorylated in response to TGF-β1 stimulation (Figure 4.6A). The phosphorylation pattern observed was not as consistent across the range of *in-vitro* ages investigated as for Smad2 but despite this, peak activation (3h with TGF-β1) was chosen for a direct comparison of phosphorylation events. As with Smad2, Smad3 phosphorylation did not change with increasing PDL's (Figure 4.6B). These results collectively suggest that age dependent loss of TGF-β1 dependent phenotypic activation was not the result of altered Smad2/3 signalling.

4.2.5 The effect of inhibition of HA synthesis on fibroblast phenotypic conversion

The results from the previous chapter demonstrate that age-related resistance to TGF- β 1-mediated phenotypic activation was associated with age-related attenuation in HA generation, down-regulation in HAS2 expression and inability to assemble HA pericellular coats. In light of these results, 4-methylumbelliferone (4MU) was used to inhibit HA synthesis, to investigate what consequence this has on phenotypic activation. 4MU depletes the UDP-glucuronic acid pool that is essential for HA chain elongation [306], leading to inhibition of HA synthesis and HAS enzyme function. A concentration of 0.5mM 4MU was previously determined as the optimal concentration to yield effective inhibition of HA synthesis with minimal cytotoxicity in dermal fibroblasts [285]. Expression of α -SMA was assessed to investigate the role of HA in myofibroblastic differentiation following incubation with 4MU. Q-PCR assessment revealed that induction of α -SMA by TGF- β 1 was significantly down-regulated in the presence of 4MU (Figure 4.7A). Further analysis by Q-PCR demonstrated 4MU significantly attenuated induction of both HAS2 (Figure 4.7B) and TSG-6 (Figure 4.7C) expression by TGF β 1.

4.2.6 The relationship between HAS2 and fibroblast phenotype

In the previous chapter it was demonstrated that reduced HA generation is associated with a blunted HAS2 response. The importance of the HAS2 isoform of HA synthase was further examined by gene silencing of HAS2 in young cells. Validation of several new HAS2 *Silencer Select* siRNA's (Invitrogen) were investigated (Figure 4.8) and subsequently HAS2 siRNA#2 (ID s6458) at a concentration of 10nM, was chosen to be used for further investigation. HAS2 siRNA transfection resulted in significant inhibition of HAS2 mRNA expression (Figure 4.9A), and abrogation of TGF- β 1 dependent induction of α -SMA (Figure 4.9B).

Furthermore, the ability of a young fibroblast to assemble a HA pericellular coat was lost following HAS2 suppression. Particle exclusion clearly illustrates that cells transfected with a scrambled control exhibit notable HA coats after TGF- β 1 stimulation (Figure 4.9E) compared to unstimulated cells (Figure 4.9C). In contrast, cells transfected with HAS2 siRNA do not assemble notable coats under basal (Figure 4.9D) or TGF- β 1 stimulated (Figure 4.9F) conditions. Measurements of the coat thickness were taken at the widest point of 30 randomly chosen cells from three separate experiments (three different patients). The mean thickness for the scramble –TGF- β 1 (Figure 4.9C) was 3.13 ± 0.42 μ m and 7.50 ± 0.31 μ m in scramble + TGF- β 1 (Figure 4.9E) (P <0.01, paired t-test). In contrast cells that had received the HAS2 siRNA failed to assemble a HA pericellular coat after stimulation with TGF- β 1. The mean thickness for the HAS2 siRNA - TGF- β 1 (Figure 4.9D) was 4.63 ± 0.41 μ m and 4.44 ± 0.32 μ m in HAS2 siRNA + TGF- β 1 (Figure 4.9F) (P = 0.63, paired t-test).

As age-dependent loss of TGF- $\beta1$ induced pericellular coat assembly and myofibroblast phenotype was associated with reduced HAS2 expression, I sought to examine the effect of over-expression of HAS2 on the phenotype of aged fibroblasts. Although over-expression of HAS2 in the aged fibroblast led to the expected increase in HA concentration in the culture supernatant as assessed by ELISA (Figure 4.10A), there was no significant change in α -SMA expression as assessed by Q-PCR (Figure 4.10B)

and immunohistochemistry (Figure 4.10 C&D). Further analysis by particle exclusion revealed no distinguishable change in pericellular HA accumulation following restoration of HAS2 in resting aged fibroblasts (Figure 4.10 E&F). Taking measurements of the coat thickness at the widest point of 30 randomly chosen cells, gave a mean thickness for the aged mock transfected fibroblast coat of $4.82 \pm 0.31 \mu m$ (Figure 4.10E) and $4.41 \pm 0.42 \mu m$ in the aged fibroblast transfected to over-express HAS2 (Figure 4.10F) (P = 0.42, paired t-test).

4.2.7 The role of TSG-6 in myofibroblastic differentiation

The hyaladherin TSG-6 has been demonstrated to be an important mediator of HA pericellular coat assembly [193, 289, 307]. In the previous chapter, age-dependent resistance to phenotypic activation was associated with an age-dependent decrease in TSG-6 expression both at baseline and following TGF- β 1 stimulation. The functional importance of age-dependent reduction in TSG-6 expression was subsequently examined by TSG-6 gene silencing using siRNA. Following transfection with TSG-6 siRNA there was a marked inhibition in the effect of TGF- β 1 on TSG-6 mRNA expression, as assessed by Q-PCR (Figure 4.11A). Abrogation of TGF- β 1 dependent induction of TSG-6 mRNA expression was also associated with a failure of TGF- β 1 to increase α -SMA in the young fibroblast (Figure 4.11B). In light of these results it was hypothesised that assembly of the pericellular coat was dependent on both stimulation of HA *via* HAS2 and also the induction of TSG-6.

4.2.8 The effect of HAS2 restoration and TGF- β_1 stimulation on phenotype in aged fibroblasts

In order to explore this, aged fibroblasts were transfected with HAS2 and subsequently stimulated with TGF- $\beta1$. In these experiments the combination of HAS2 over-expression and TGF- $\beta1$ stimulation, restored the ability of aged fibroblasts to form a pericellular HA coat, as assessed by the exclusion of formalized erythrocytes (Figure 4.12A-C). Taking measurements of the coat thickness at the widest point of 30 randomly chosen cells of each phenotype, gave a mean thickness for the aged mock transfected fibroblast coat of $3.19 \pm 0.27~\mu m$ and $6.59 \pm 0.41~\mu m$ in the aged fibroblast

transfected to over-express HAS2, following TGF- β 1 stimulation (P < 0.001, paired t-test). Transfection with HAS2 did not, however, restore TGF- β 1 responsiveness in terms of the induction of α -SMA, as assessed by immunocytochemistry (Figure 4.12D-F), and QPCR (Figure 4.13A). This suggested a dissociation of pericellular coat formation and regulation of phenotype. In contrast, and consistent with the formation of the pericellular coat, over-expression of HAS2 and increased HA generation, was associated with partial restoration of the induction of TSG-6 following stimulation with TGF- β 1 in the aged fibroblasts (Figure 4.13B).

4.2.9 The effect of IL-1\beta on phenotype of young and aged fibroblasts

Age dependent regulation of HAS2 was further examined by stimulation with IL-1\(\beta\). In contrast to TGF-\beta1 responsiveness, which diminished with age, stimulation of aged cells with IL-1\beta led to a significant induction of HAS2 gene expression (Figure 4.14A) and was also associated with an increase in HA, as assessed by ELISA (Figure 4.14B). TSG-6 induction was also significant following addition of IL-1β, compared to the blunted effect of TGF-\beta1 in aged cells (Figure 4.14C). In contrast stimulation with IL-1β, despite the alterations in HA associated gene regulation, did not lead to any change in expression of α-SMA (Figure 4.14D). The increase in HAS2, associated with induction of the hyaladherin TSG-6, would suggest that IL-1\beta stimulation may induce the formation of a pericellular HA coat and this was confirmed by visualisation of the pericellular HA coat in young and aged cells (Figure 4.15). Taking measurements of the coat thickness at the widest point of 30 randomly chosen cells of each phenotype and "age" gave a mean, thickness for the young fibroblast coat of $3.04 \pm 0.19 \mu m$ at baseline and $8.25 \pm 0.18 \, \mu m$ following IL-1 β stimulation (P < 0.001, paired test). For aged fibroblasts the mean coat thickness at baseline was $3.15 \pm 0.35 \,\mu m$ and following IL-1 β stimulation was $7.95 \pm 0.42 \, \mu m$ (P = 0.001, paired t-test). These data suggests that following IL-1\beta stimulation there is a dissociation of pericellular HA coat assembly and regulation of phenotype.

4.2.10 The relationship between hyaluronan-dependent pericellular coat assembly and myofibroblastic differentiation

Data presented above suggest that TSG-6 dependent regulation of the HA pericellular coat is required for TGF- β 1 phenotypic conversion. However, TGF- β 1 stimulation of HAS2 overexpressing cells and IL-1 β stimulation in the aged phenotype, suggest that the formation of the pericellular coat in itself does not lead to acquisition of a myofibroblastic phenotype. The role of the pericellular coat in TGF- β 1 dependent regulation of phenotype was further examined following its digestion with Hyal (confirmed by particle exclusion) (Figure 4.16A&C). There was no effect on TGF- β 1 dependent induction of HAS2 (Figure 4.17A). In contrast Hyal digestion led to inhibition of TGF- β 1 dependent phenotypic activation as determined by expression of α -SMA by Q-PCR (Figure 4.17B) and immunohistochemistry (Figure 4.16B&D). Furthermore, treatment with Hyal demonstrated significant knock-down of TSG-6 induction by TGF β 1 (Figure 4.17C).

Collectively these data suggests that the pericellular HA coat is therefore necessary but not sufficient to drive fibroblast to myofibroblast activation.

4.2.11 The effects of Smad siRNA on hyaluronan-dependent pericellular coat accumulation

As TGF-β1 signalling through the Smad-dependent pathway is required for myofibroblastic differentiation, the effect of 4MU and Hyal on phosphorylation of Smad2 was analysed by Western blot. To analyse Smad2 phosphorylation, young fibroblasts were incubated for 0, 30 and 60 min with either 4MU (0.5mM), Hyal (200µg/ml) or serum-free medium (control treatment) in the presence or absence of TGF-β1 and protein extracts collected. Consistent with previous results, phosphorylation of Smad2 followed TGF-β1 stimulation and peaked at 30min and 1h for all conditions (Figure 4.18A). Direct comparison of the extent of pSmad2 for all treatments at these time points, demonstrated incubation with 4MU or Hyal had no significant effect on the activation of Smad2 (Figure 4.18B), suggesting a dissociation

of HA regulation (in particular its assembly into a pericellular coat) and Smad signalling.

4.2.12 The effect of HA coat removal on Smad signalling

To support this, young fibroblasts were transfected with siRNA for Smad2 and Smad3 prior to incubation with or without TGF-\beta1 and their ability to assemble a HA pericellular coat assessed by particle exclusion (Figure 4.19). Cells were transfected with a scrambled oligonucleotide (scrambled) as a control. Measurements of the coat thickness were taken at the widest point of 30 randomly chosen cells from three separate experiments (two different patients) for each treatment: The mean thickness for the scramble -TGF- β 1 was 4.02 \pm 0.28 μ m and 8.02 \pm 0.46 μ m in scramble + TGF- β 1 (P <0.01, paired t-test). Cells that had received the Smad2 siRNA generated significant HA coats following TGF-\beta1 stimulation. The mean thickness for the Smad2 siRNA -TGF- β 1 was $4.82 \pm 0.40 \mu m$ and $7.55 \pm 0.39 \mu m$ in Smad2 siRNA + TGF- β 1 (P < 0.01, paired t-test). Cells that had received the Smad3 siRNA generated significant HA coats following TGF-β1 stimulation. The mean thickness for the Smad2 siRNA – TGF-β1 was $3.98 \pm 0.46 \mu m$ and $7.24 \pm 0.56 \mu m$ in Smad2 siRNA + TGF- β 1 (P = <0.01, paired ttest). Collectively these results demonstrated, that for all treatments, stimulation with TGF-\beta1 resulted in formation of a HA pericellular coat, indicating that TGF\beta1dependent HA pericellular coat synthesis was not dependent on Smad signalling.

Effect of ALK-5 inhibition on fibroblast phenotype

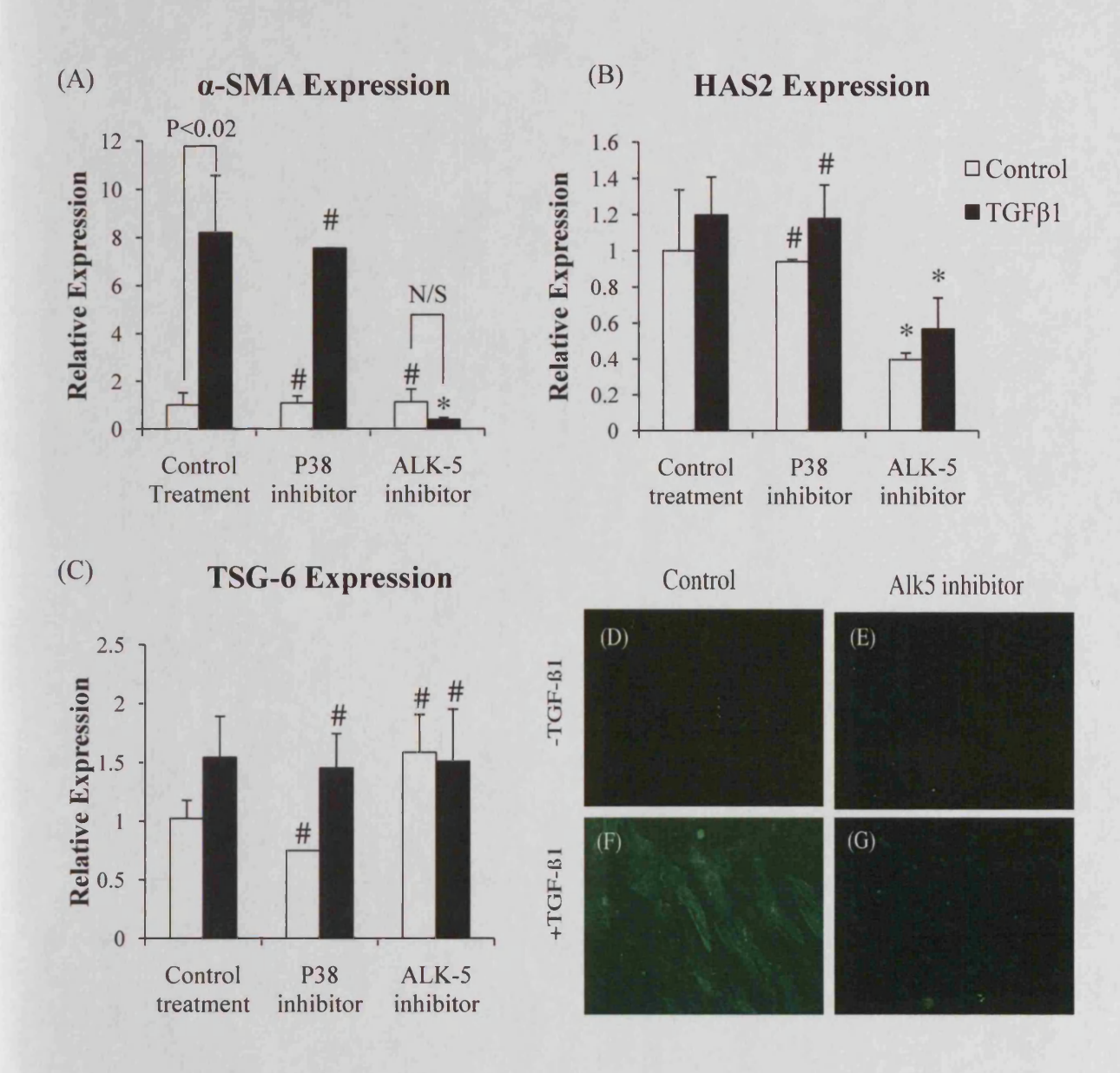


Figure 4.1 Effect of ALK 5 inhibition on a-SMA, HAS2 and TSG-6 expression Confluent monolayers of young dermal fibroblasts were growth-arrested in serum-free medium for 48 hours, prior to addition of either serum-free medium alone (clear bars) or serum-free medium containing 10ng/ml TGFβ1 (black bars) in the absence (control treatment) or presence of the ALK-4/5/7 inhibitor SB431542 or p38 inhibitor SB203580 for 72 hours. Total mRNA was extracted and α-SMA (A) HAS2 (B) and TSG-6 (C) expression was assessed by RT-QPCR. Ribosomal RNA expression was used as an endogenous control and gene expression was assessed relative to control-control cells. The comparative C_T method was used for relative quantification of gene expression and the results are represented as the mean± S.E. of nine individual experiments using cells isolated from three different donors. Statistical analysis was performed by the Student's t test. *, Not significant, *, p <0.05, as compared to control treatment. N/S, not significant. In parallel experiments monolayers of young dermal fibroblasts were growth-arrested in serum-free medium for 48 h. The medium was then replaced with either serum-free medium alone (D,E) or serum-free medium containing 10ng/ml TGF-β₁ (F,G) then fixed and stained for α-SMA, as describe under section 2.4. The cells were then mounted in Vectashield fluorescent mountant, and viewed under UV light. All results shown are representative of dermal fibroblasts from three patient donors. Original magnification x 100.

Autocrine TGF-β1 signalling

TGF-β1 mRNA Expression

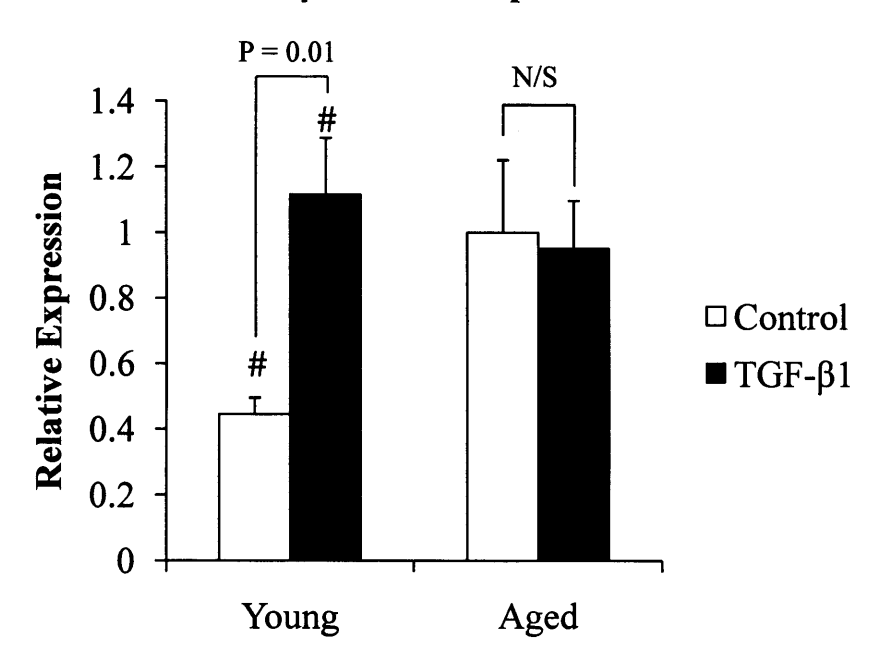


Figure 4.2 Effect of in-vitro aging on endogenous generation of TGF- β 1. Confluent monolayers of patient matched young and aged dermal fibroblasts were growth-arrested in serum-free medium for 48 hours, prior to addition of either serum-free medium alone (clear bars) or serum-free medium containing 10ng/ml TGF- β 1 (black bars) for 72 hours. Total mRNA was extracted and TGF- β 1 expression was assessed by RT-QPCR. Ribosomal RNA expression was used as an endogenous control and gene expression was assessed relative to control-control cells. The comparative C_T method was used for relative quantification of gene expression and the results are represented as the mean± S.E. of six individual experiments using cells isolated from two different donors. Statistical analysis was performed by the Student's t test. t, Not significant, as compared to aged cells. N/S, not significant.

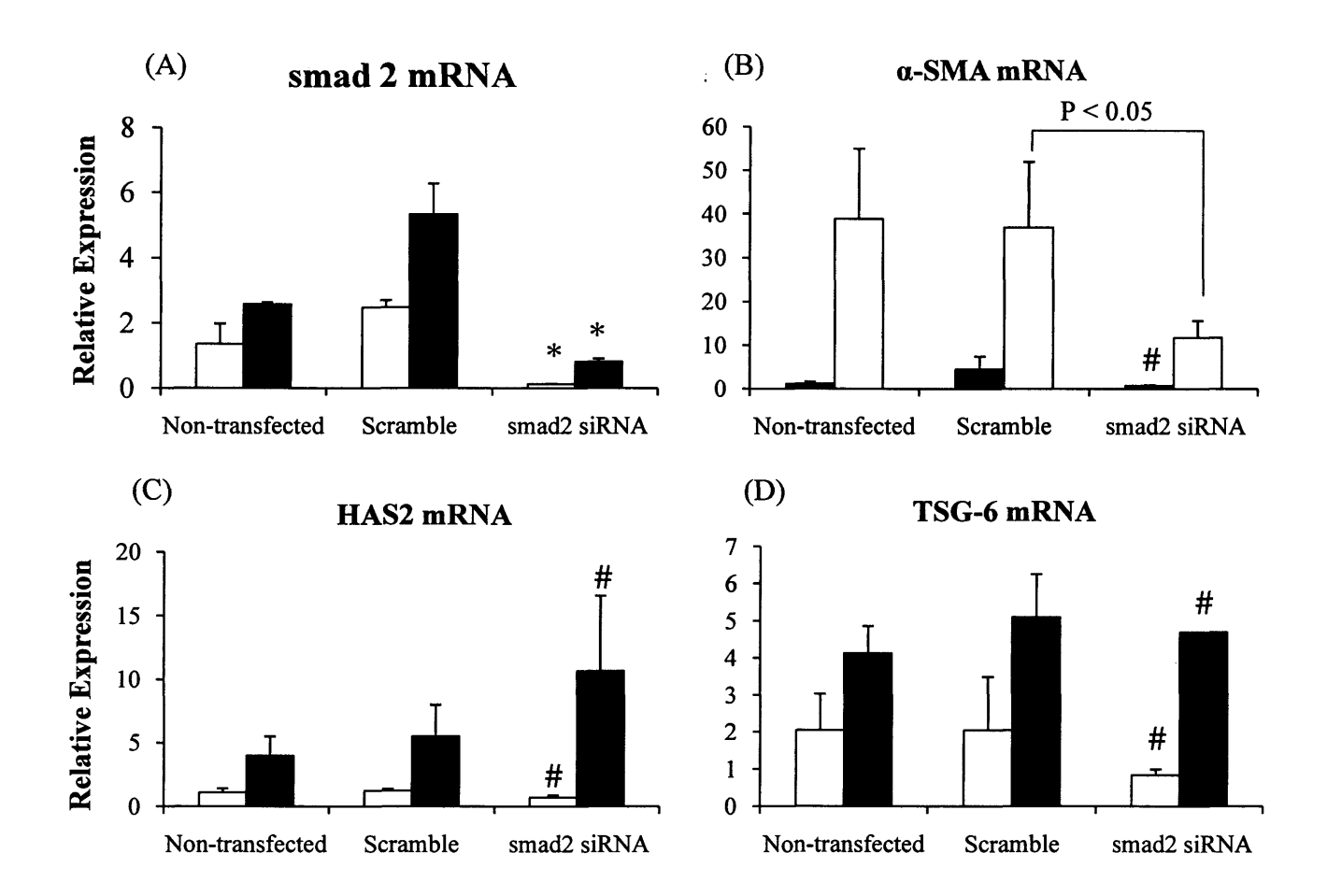


Figure 4.3 Effect of Smad2 siRNA on α-SMA, HAS2 and TSG-6 expression. Confluent monolayers of young dermal fibroblasts were transfected with Smad2 siRNA, a scrambled oligonecleotide (scramble) or serum free medium (non-transfected) as describe under section 2.10 and incubated in medium supplemented with 10% FCS for 24 hours. The medium was then replaced with serum-free medium for 24 hours. The cells were then incubated in either serum-free medium alone (clear bars) or serum-free medium containing 10ng/ml TGF-β1 (black bars) for a further 72 hours and smad2 (A), α-SMA (B), HAS2 (C) and TSG-6 (D) expression assessed by RT-QPCR. Ribosomal RNA expression was used as an endogenous control and gene expression was assessed relative to control scramble cells. The comparative C_T method was used for relative quantification of gene expression and the results are represented as the mean± S.E. of nine individual experiments using cells isolated from three different donors. Statistical analysis was performed by the Student's t test. t, Not significant, t, t, t0.05, as compared to scramble.

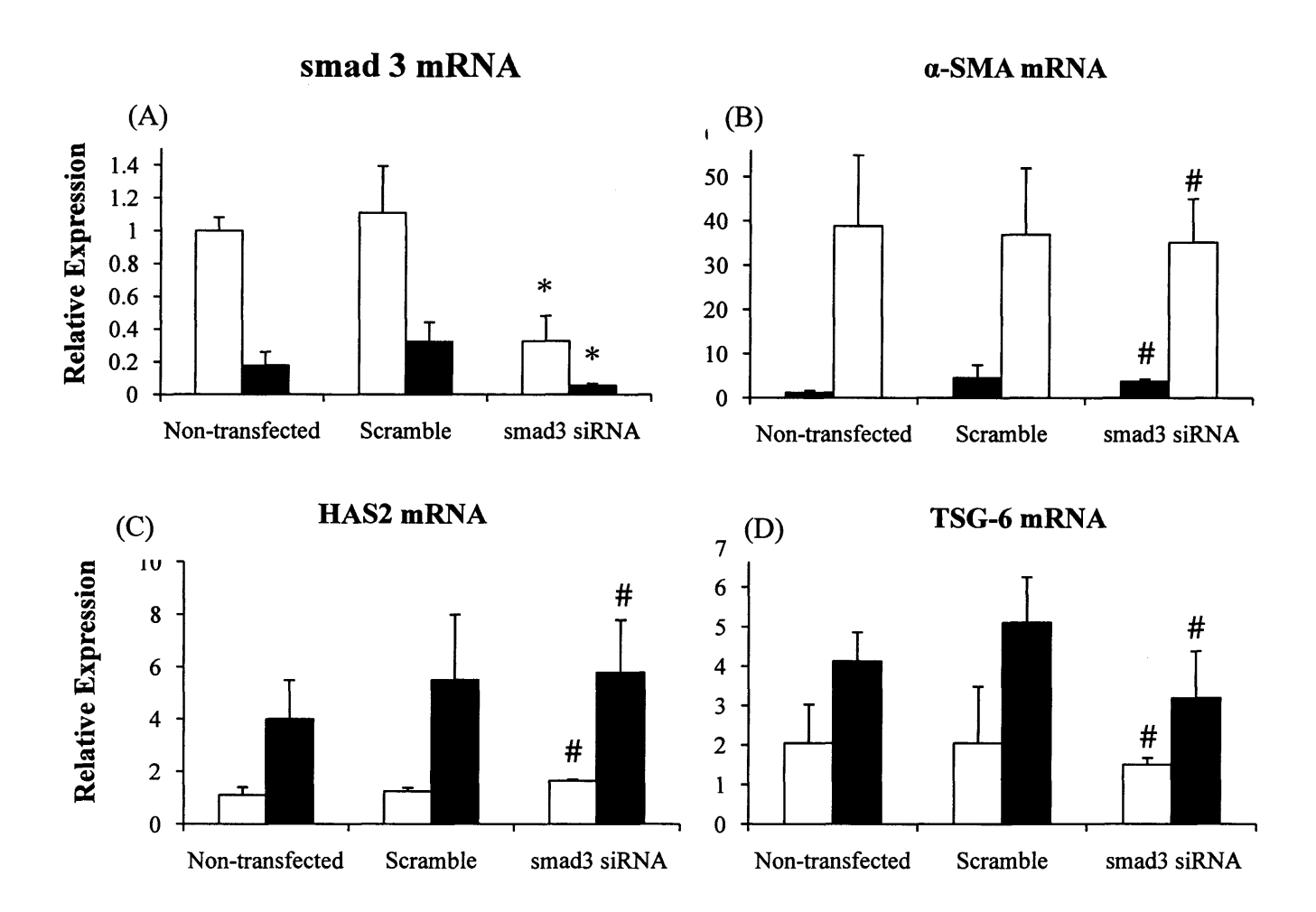


Figure 4.4 Effect of Smad3 siRNA on α-SMA, HAS2 and TSG-6 expression. Confluent monolayers of young dermal fibroblasts were transfected with Smad3 siRNA, a scrambled oligonecleotide (scramble) or serum free medium (non-transfected) as describe under section 2.10 and incubated in medium supplemented with 10% FCS for 24 hours. The medium was then replaced with serum-free medium for 24 hours. The cells were then incubated in either serum-free medium alone (clear bars) or serum-free medium containing 10ng/ml TGF-β1 (black bars) for a further 72 hours and Smad2 (A), α-SMA (B), HAS2 (C) and TSG-6 (D) expression assessed by RT-QPCR. Ribosomal RNA expression was used as an endogenous control and gene expression was assessed relative to control scramble cells. The comparative C_T method was used for relative quantification of gene expression and the results are represented as the mean± S.E. of nine individual experiments using cells isolated from three different donors. Statistical analysis was performed by the Student's t test. t, Not significant, t, t, t0.05, as compared to scramble.

Smad2 Signalling

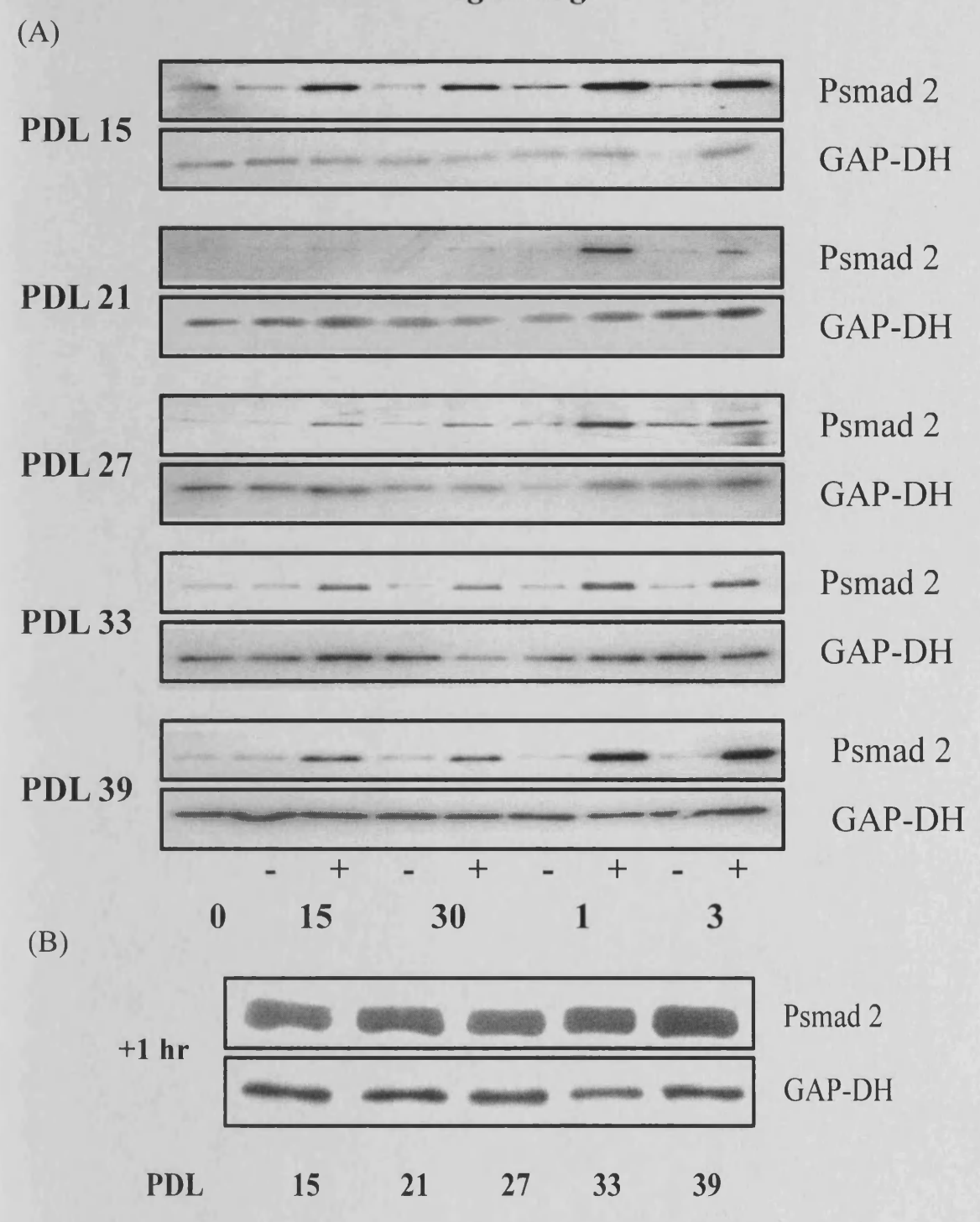


Figure 4.5 Effect of in-vitro ageing on Smad2 signalling. A, confluent monolayers of dermal fibroblasts at the indicated PDL's were growth arrested in serum-free medium for 48 hours. The medium was replaced with either serum-free medium alone or serum-free medium containing 10 ng/ml TGF- $\beta 1$ for the indicated times. B, direct comparison of TGF- $\beta 1$ stimulated cells at 1hr across indicated PDL's. Cell lysates were subsequently subjected to Western blot analysis utilising antibodies against the phosphorylation form of Smad2. Expression of GAP-DH was analysed as a control to ensure equal loading. The results shown are representative of five independent experiments from the same patient donor.

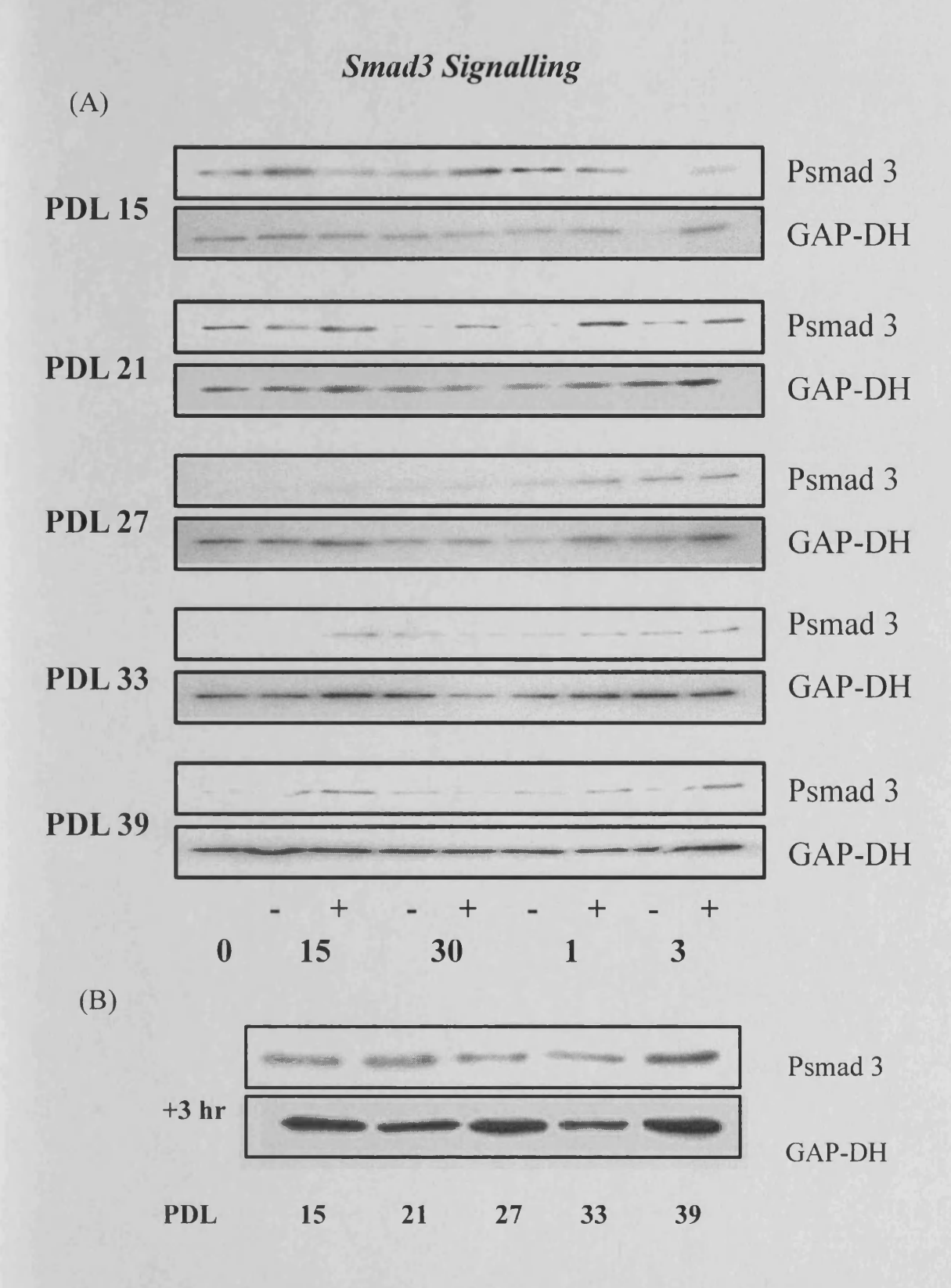


Figure 4.6 Effect of in-vitro ageing on Smad3 signalling. A, confluent monolayers of dermal fibroblasts at the indicated PDL's were growth arrested in serum-free medium for 48 hours. The medium was replaced with either serum-free medium alone or serum-free medium containing 10ng/ml TGF-β1 for the indicated times. B, direct comparison of TGF-β1 stimulated cells at 3 hr across indicated PDL's. Cell lysates were subsequently subjected to Western blot analysis utilising antibodies against the phosphorylation form of Smad3. Expression of GAP-DH was analysed as a control to ensure equal loading. The results shown are representative of five independent experiments from the same patient donor

Effect of inhibition of HA synthesis on fibroblast phenotype

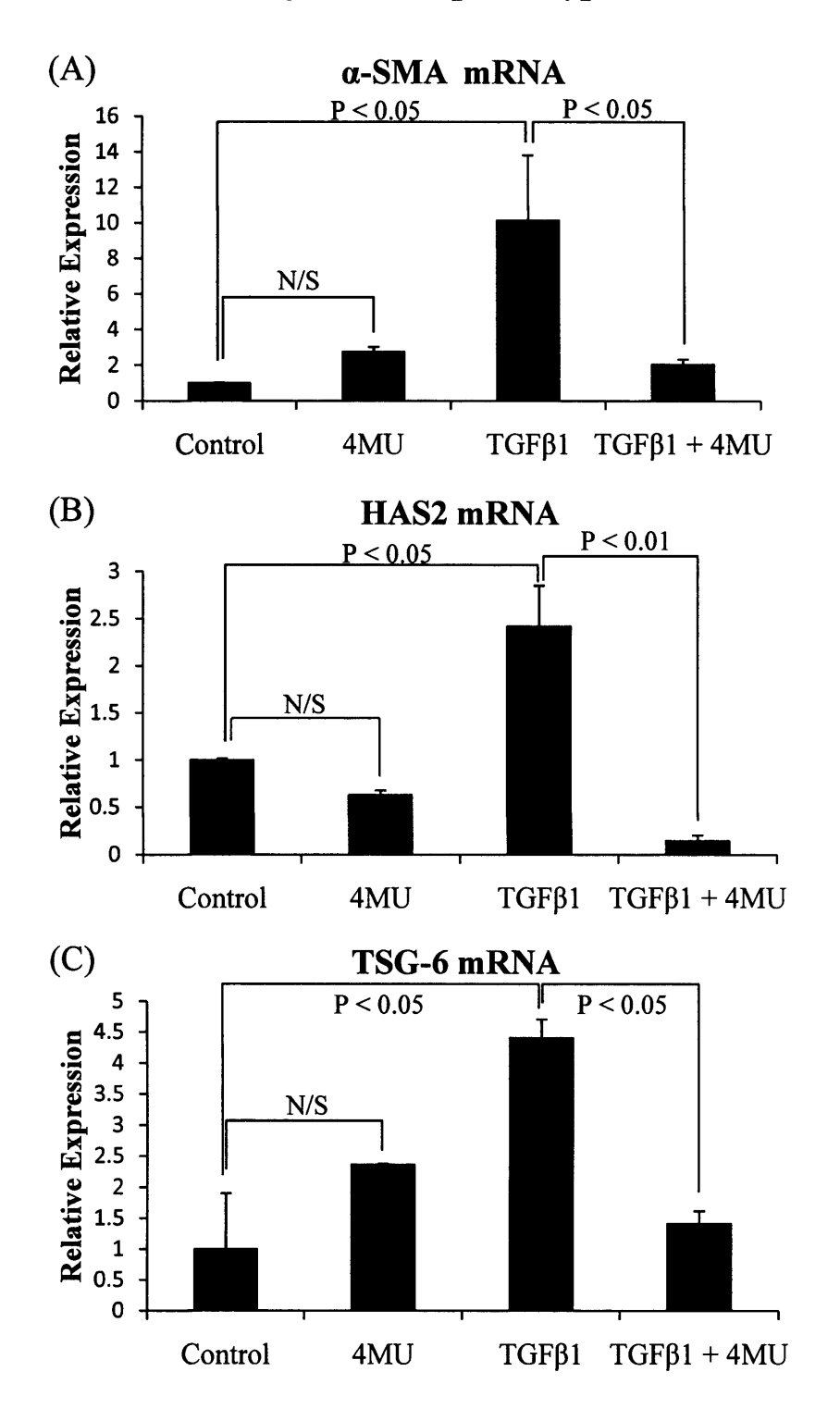


Figure 4.7 α-SMA, HAS2 and TSG-6 mRNA expression following inhibition of HA chain elongation. Confluent monolayers of young dermal fibroblasts were growth arrested in serum-free medium for 48 hours. The medium was then replaced with either serum-free medium alone (Control), serum-free medium containing 0.5 mM 4MU, serum-free medium containing 10ng/ml TGF- $β_1$ or serum-free medium containing both 0.5 mM 4MU and 10ng/ml TGF- $β_1$ for 72 h. mRNA was extracted as describe under section 2.6 and α-SMA (A) HAS2 (B) and TSG-6 expression was assessed by RT-QPCR. Ribosomal RNA expression was used as an endogenous control and gene expression was assessed relative to control cells. The comparative C_T method was used for relative quantification of gene expression and the results are represented as the mean± S.E. of six individual experiments using cells isolated from two different donors. Statistical analysis was performed by Student's t test and statistical significance was taken as p < 0.05. N/S, not Significant.

Optimisation of HAS2 Silencer Select siRNA

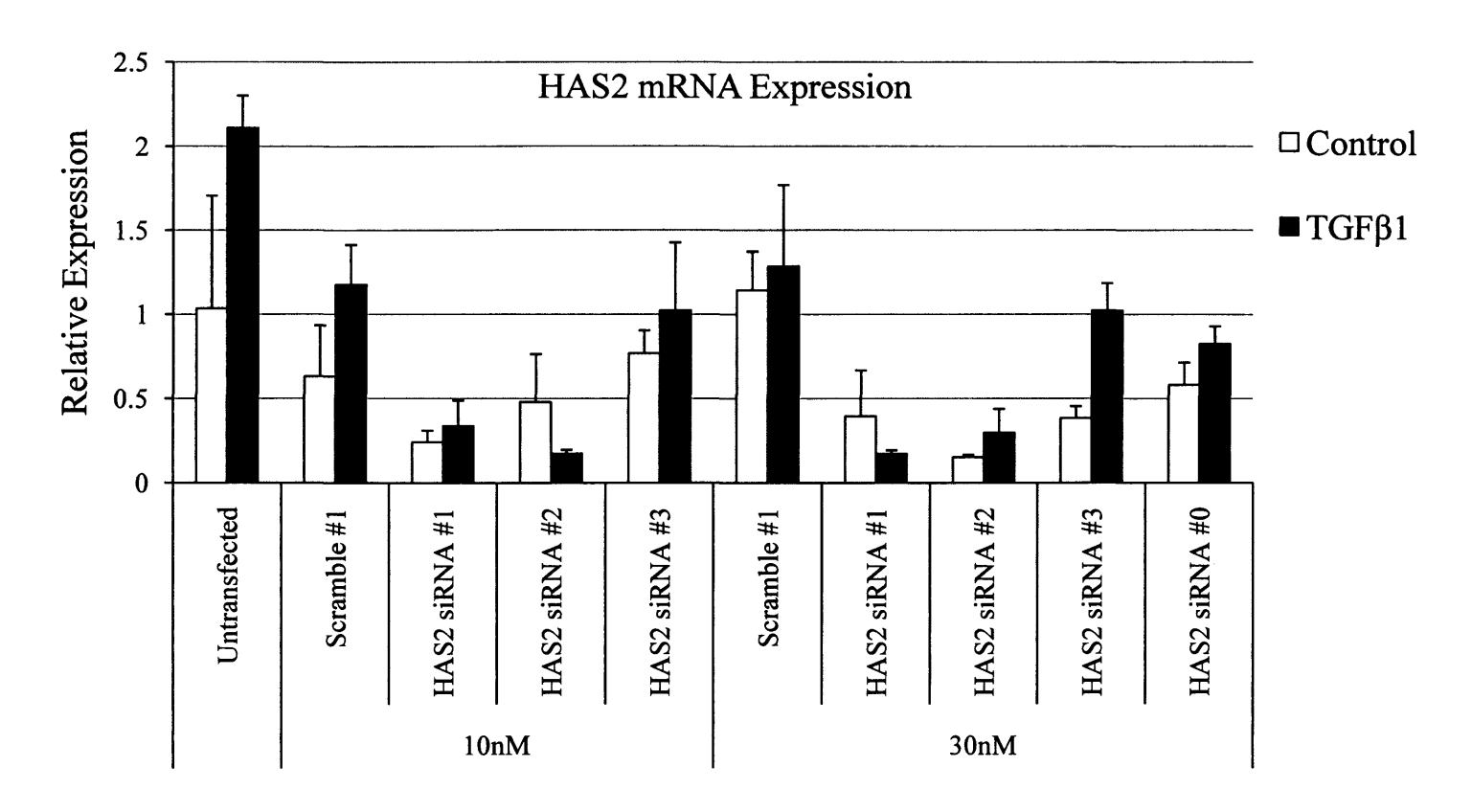


Figure 4.8 Validation of HAS2 Silencer Select siRNA. Young dermal fibroblasts were transfected with three different HAS2 silencer select siRNA's (from Ambion: ID s645(7)(8)(9) donated HAS2 siRNA #(1)(2)(3)) or silencer select scrambled oligoneucleotide control (#1) (scramble) at either 10nM or 30nM. HAS2 siRNA #0 denotes previously used HAS2 siRNA (non-silencer select, 16704). Following transfection cells were incubated in medium supplemented with 10% FBS for 24 h. The medium was then replaced with serum-free medium for a further 24 h, prior to addition of serum-free medium alone (clear bars) or serum-free medium containing 10ng/ml TGF-β₁ (black bars) for 72 h. Total mRNA was extracted and HAS2 expression was assessed by RT-QPCR. Ribosomal RNA expression was used as an endogenous control and gene expression was assessed relative to untransfected samples. The comparative C_T method was used for relative quantification of gene expression and the results are represented as the mean± S.E. of six individual experiments using cells isolated from two different donors.

Effect of HAS2 siRNA on fibroblast phenotype

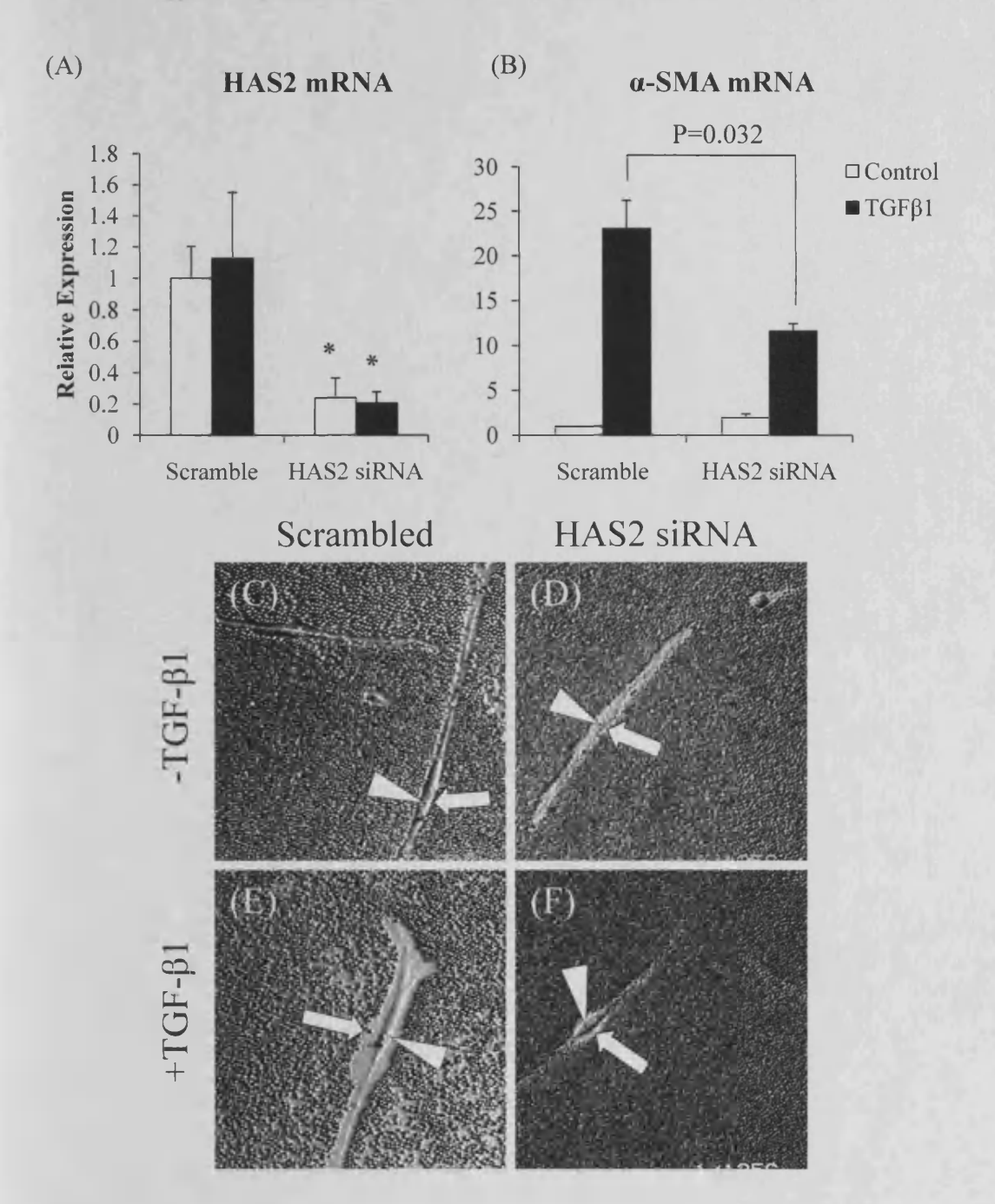


Figure 4.9 Effect of HAS2 siRNA on α-SMA expression and HA pericellular coat formation. Young dermal fibroblasts were transfected with HAS2 siRNA or a scrambled oligoneucleotide control (scramble) as describe under section 2.14 and incubated in medium supplemented with 10% FBS for 24 h. The medium was then replaced with serum-free medium for a further 24 h, prior to addition of serum-free medium alone (clear bars) (C&D) or serum-free medium containing 10ng/ml TGF- $β_1$ (black bars) (E&F) for 72 h before analysis by either Q-PCR or particle exclusion. A-B, total mRNA was extracted and HAS2 (A) and α-SMA (B) expression was assessed by RT-QPCR. Ribosomal RNA expression was used as an endogenous control and gene expression was assessed relative to control-scramble samples. The comparative C_T method was used for relative quantification of gene expression and the results are represented as the mean± S.E. of nine individual experiments using cells isolated from three different donors. Statistical analysis was performed by the Student's t test. *, t <0.05, as compared to scramble. Visualisation of the pericellular HA coat (C-F) was performed by addition of formalised horse erythrocytes as describe under section 2.11. Arrowheads indicate the cell body; Arrows show the extent of the pericellular matrix. Representative of dermal fibroblasts from three patient donors. Original magnification x 200.

HAS2 restoration in aged fibroblasts

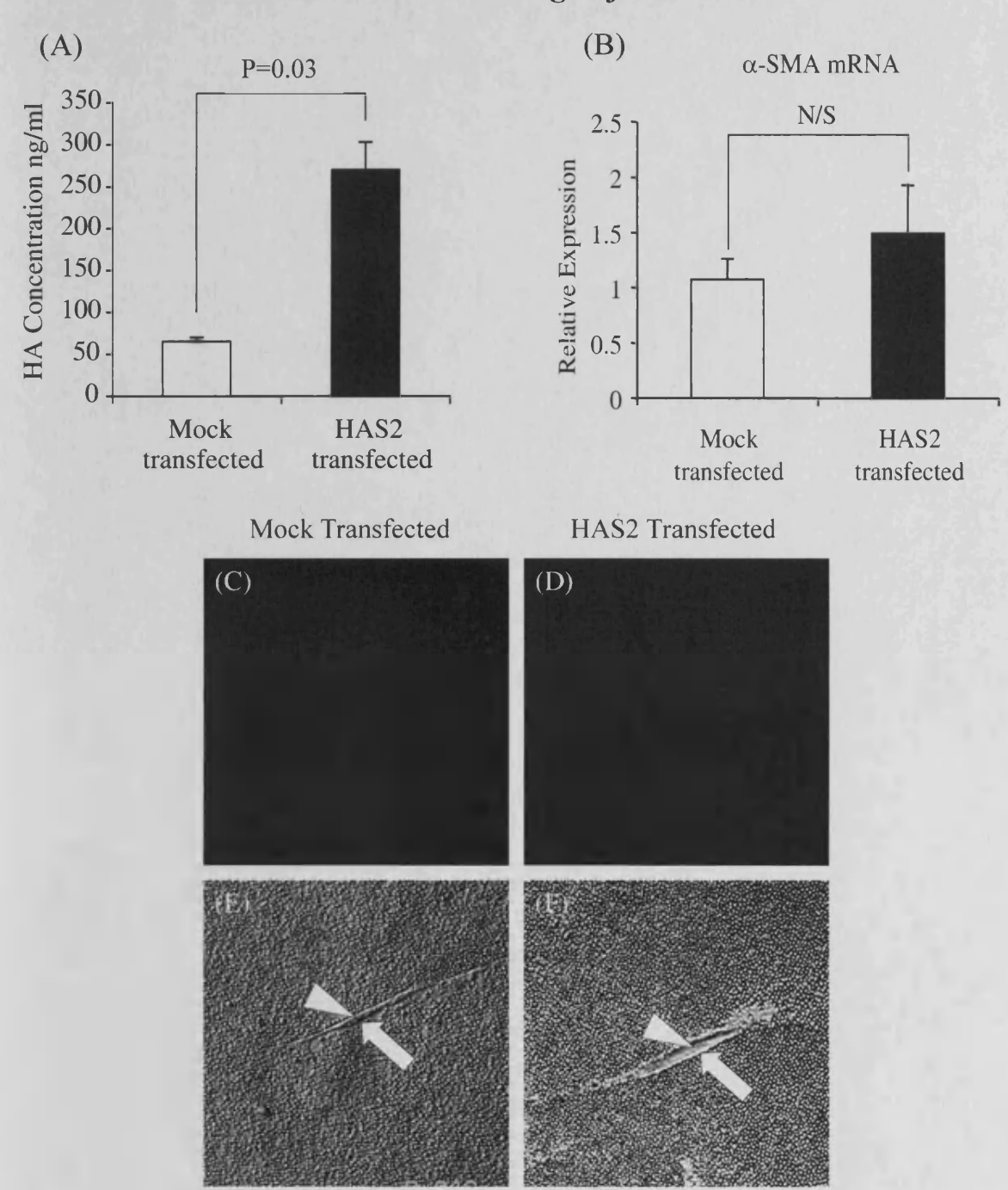


Figure 4.10 Over-expression of HAS2 in aged dermal fibroblasts. Aged dermal fibroblasts were transfected with either HAS2-pCR3.1 (HAS2 transfected) or pCR3.1 (Mock transfected). HA secreted into the culture medium 48 h after transfection was quantified by ELISA (A). Following removal of the culture medium, total mRNA was extracted. α-SMA expression was subsequently assessed by RT-QPCR (B). Ribosomal RNA expression was used as an endogenous control and gene expression was assessed relative to mock transfected. The comparative C_T method was used for relative quantification of gene expression and the results are represented as the mean± S.E. of dermal fibroblasts from nine separate experiments using cells isolated from three patient donors. Statistical analysis was performed by the Student's t test. N/S, not significant. Immunohistochemical analysis was performed to examine α-SMA protein expression on mock transfected (C) and HAS2-overexpressing (D) aged dermal fibroblasts 48 h after transfection. The cells were then fixed and stained for α-SMA, mounted in Vectashield fluorescent mountant, and viewed under UV light. Original magnification x 100. In parallel experiments, the HA pericellular coat was visualised. 48 h after transfection formalised horse erythrocytes were added to mock-transfected (E) or HAS2-overexpressing (F) aged dermal fibroblasts as described under section 2.11 to visualise the HA pericellular coat. Arrows indicate the cell body; arrowheads show the extent of the pericellular matrix. Representative of dermal fibroblasts from two patient donors. Original magnification was x 200.

Effect of TSG-6 siRNA on fibroblast phenotype

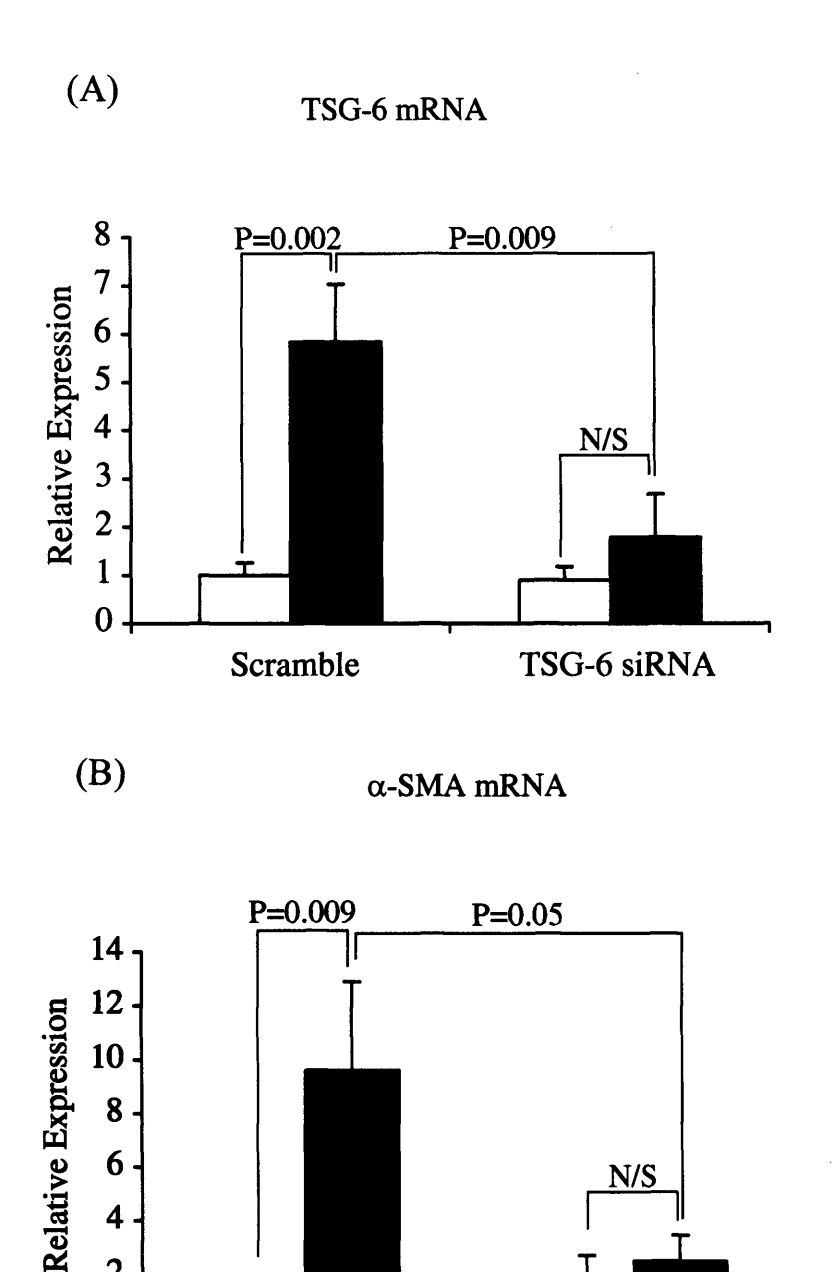


Figure 4.11 Effect of TSG-6 siRNA on a-SMA expression. To further examine the role of TSG-6, young dermal fibroblasts were transfected with TSG-6 siRNA or scrambled oligoneucleotide control (scramble) as describe under section 2.14 and incubated in medium supplemented with 10% FBS for 24 h. The medium was then replaced with serum-free medium for a further 24 h, prior to addition of serum-free medium alone (clear bars) or serum-free medium containing 10ng/ml TGF-β₁ (black bars) for 72 h. Total mRNA was extracted and TSG-6 (B) and α-SMA (C) expression was assessed by RT-QPCR. Ribosomal RNA expression was used as an endogenous control and gene expression was assessed relative to controlscramble samples. The comparative C_T method was used for relative quantification of gene expression and the results are represented as the mean± S.E. of nine individual experiments using cells isolated from three different donors. Statistical analysis was performed by the Student's t test and statistical significance was taken as p < 0.05. N/S (Not Significant)

TSG-6 siRNA

Scramble

2

0

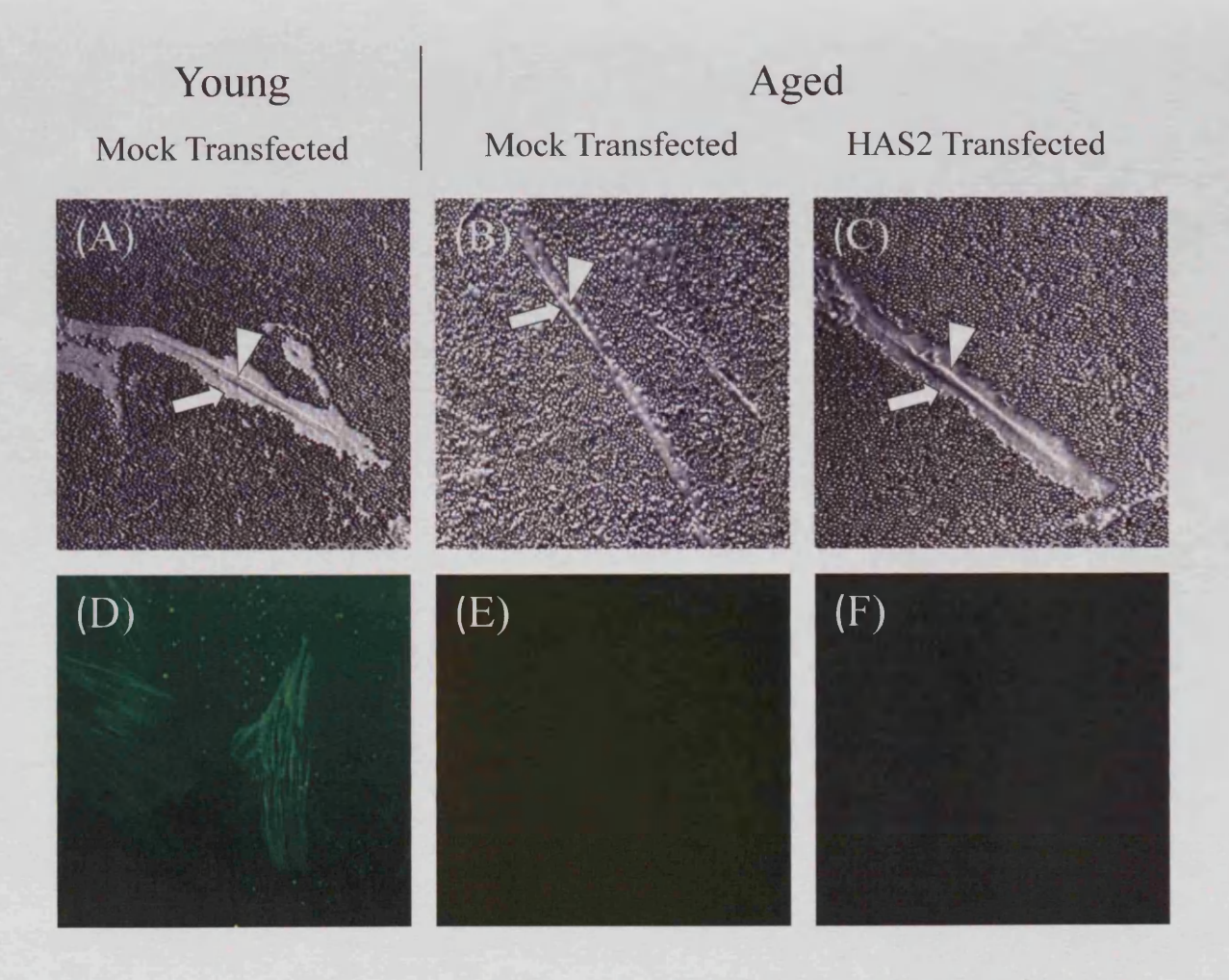
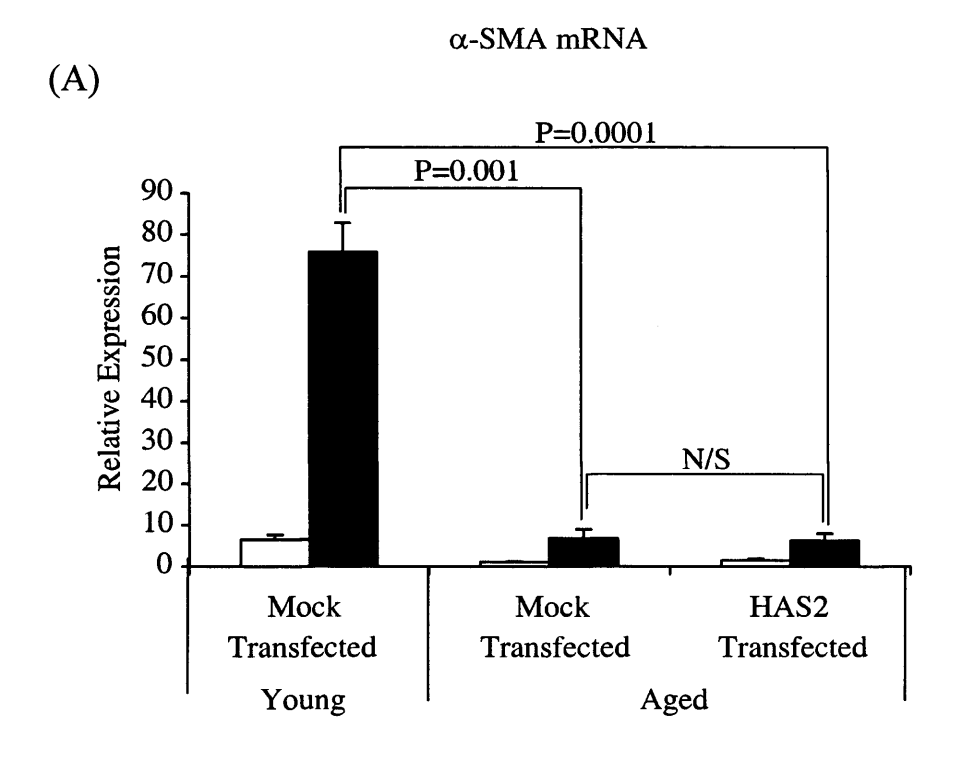


Figure 4.12 Effect of HAS2 restoration on pericellular HA coat assembly and α-SMA expression following TGF- β_1 in aged dermal fibroblasts. Patient matched young (A & D) and aged (B,C,E & F) dermal fibroblasts were transfected either with pCR3.1 alone (mock) (A,B,D & E) or HAS2-pCR3.1 (HAS2) (C & F). 48 h after transfection, cells were incubated in serum-free medium containing 10ng/ml TGF- β_1 for 72 h. Visualisation of pericellular HA coat (A-C) was performed by addition of formalised horse erythrocytes as describe under section 2.12. *Arrows* indicate the cell body; *arrowheads* show the extent of the pericellular matrix. Images are representative of dermal fibroblasts from three patient donors. Original magnification was x 200. D-F, following stimulation cells were fixed and α-SMA visualised by immunohistochemistry as describe under section 2.4. Slides were mounted in Vectashield fluorescent mountant, and viewed under UV light. Original magnification x 100.

HAS2 restoration in aged fibroblasts



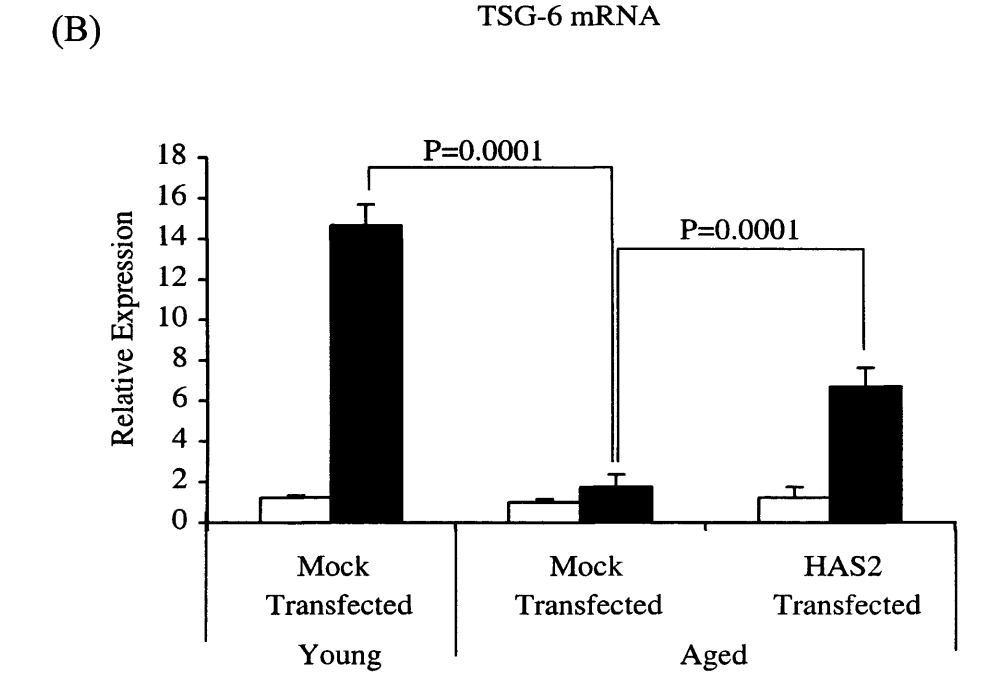


Figure 4.13 Effect of HAS2 over-expression on TGF- β_1 dependent responses in aged dermal fibroblasts. Aged dermal fibroblasts were transfected either with HAS2-pCR3.1 or pCR3.1 alone (mock transfected). Parallel mock transfections were performed on patient matched young dermal fibroblasts. 48 h after transfection, cells were incubated in either serum-free medium alone (clear bars) or serum-free medium containing 10ng/ml TGF- β_1 (black bars) for 72 h. α -SMA (A) and TSG-6 (B) mRNA expression was assessed by RT-QPCR. Ribosomal RNA expression was used as an endogenous control and gene expression was assessed relative to control mock-transfected aged cells. The comparative C_T method was used for relative quantification of gene expression and the results are represented as the mean \pm S.E. of nine individual experiments using cells isolated from three different donors. Statistical analysis was performed by the Student's t test and statistical significance was taken as p < 0.05. N/S, not Significant.

Effect of age on IL-1\beta responsiveness

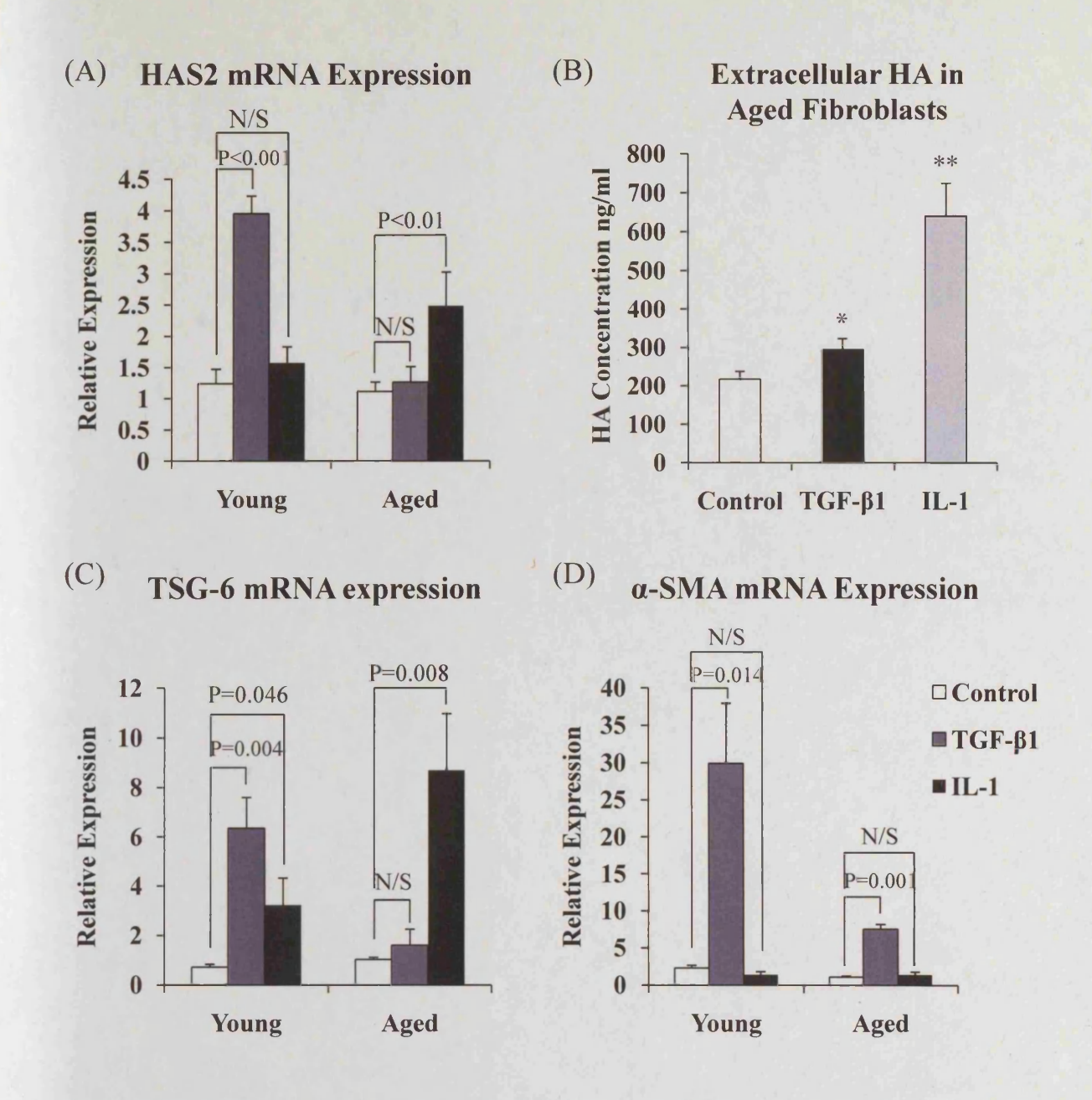


Figure 4.14 HAS2 responsiveness is retained in aged cells following addition of IL-1β. Confluent monolayers of patient matched young and aged dermal fibroblasts were growth arrested in serum-free medium for 48 hours. The medium was then replaced with either serum-free medium alone (clear bars), serum-free medium containing 10ng/ml TGF-β₁ (grey bars) or serum-free medium containing 1ng/ml IL-1β (black bars) for a further 72 h. mRNA was extracted and cDNA prepared as describe under section 2.6. HAS2 (A), TSG-6 (C) and α-SMA (D) expression was assessed by RT-QPCR. Ribosomal RNA expression was used as an endogenous control and gene expression was assessed relative to control aged cells. The comparative C_T method was used for relative quantification of gene expression and the results are represented as the mean± S.E. of six individual experiments using cells isolated from two different donors. Statistical analysis was performed by Student's t test and statistical significance was taken as p < 0.05. N/S, not Significant. HA secreted into the culture medium of aged cells was quantified by ELISA (B). The data are the mean ± S.E. six individual experiments using cells isolated from two different donors. Statistical analysis was performed by Student's t test: *, p < 0.05, ***, p < 0.01 as compared to control cells.

Accumulation of HA dependent pericellular coats by IL-1β

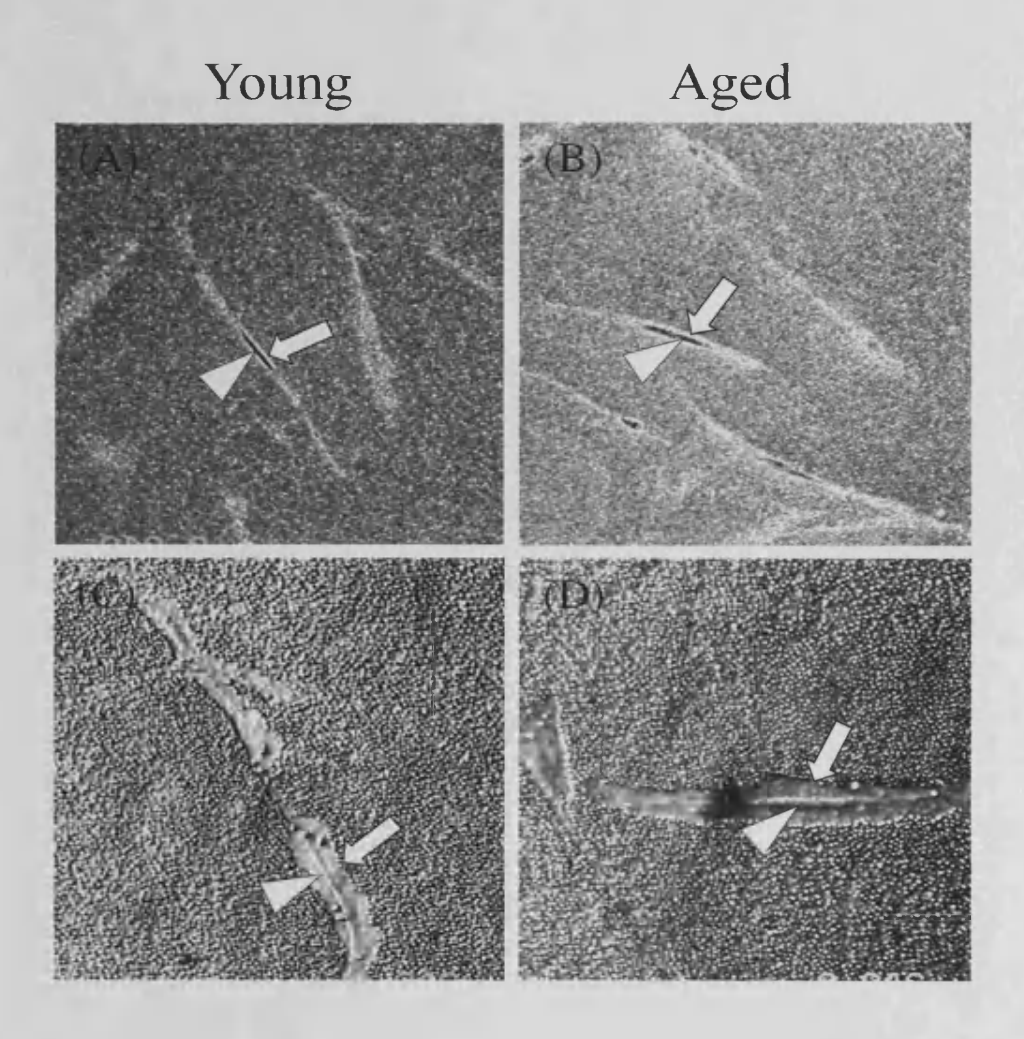


Figure 4.15 Effect of IL-1 β on HA pericellular coat assembly. Subconfluent layers of patient matched young (A & C) and aged (B & D) dermal fibroblasts were growth-arrested in serum-free medium for 48 h. The medium was then replaced with either serum-free medium alone (A & B) or lng/ml IL-1ll (C & D) for 72 h. Formalised horse erythrocytes were then added as describe under section 2.11 to visualise the HA pericellular coat. Zones of exclusion were visualized using Zeiss Axiovert 135 inverted microscope. arrowheads indicate the cell body; Arrows show the extent of the pericellular matrix. Representative of dermal fibroblasts from two patient donors. Original magnification was x 200.

Relationship between HA pericellular coat and phenotypic activation

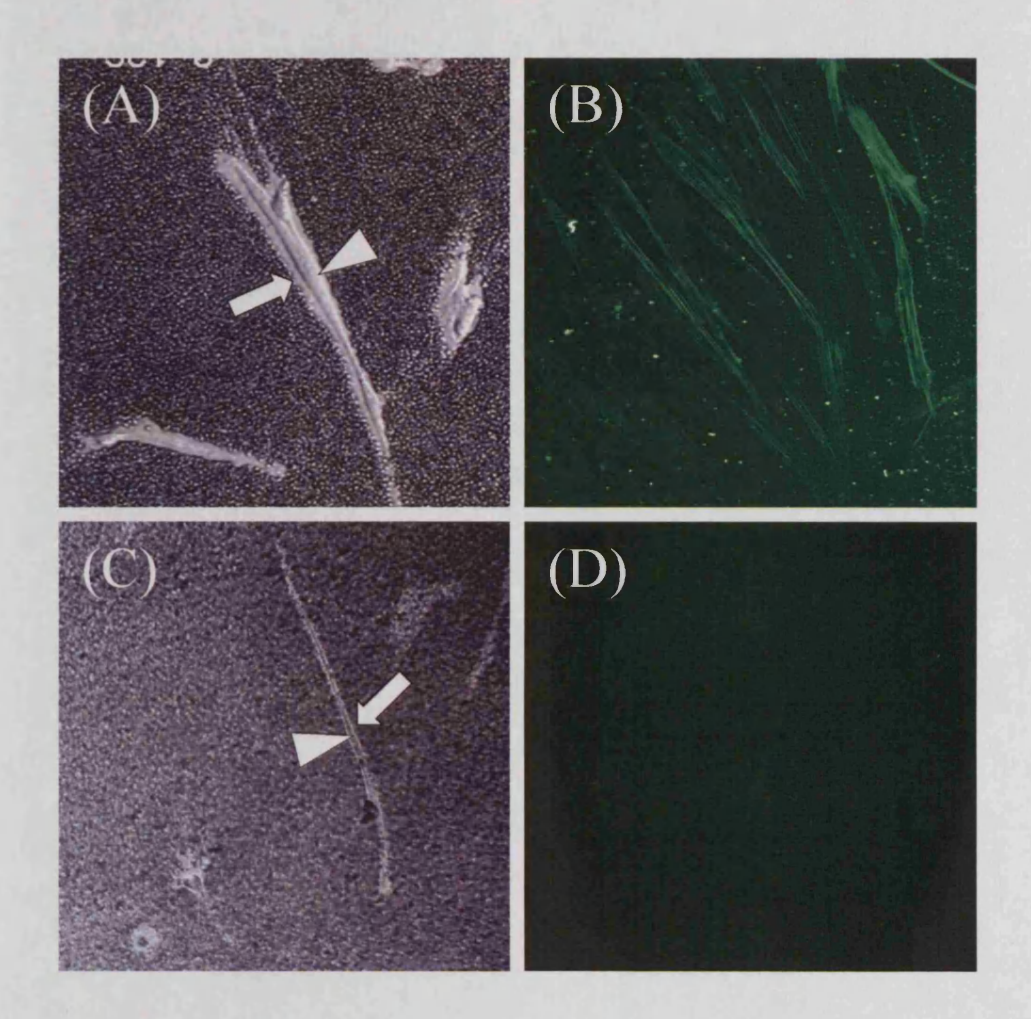


Figure 4.16 Effect of hyaluronidase on HA pericellular coat formation and α-SMA expression. Serum free medium alone (A) or bovine testicular hyaluronidase (200 μg/ml) (C) were added to growth arrested cells for 1h prior to the addition of 10 ng/ml TGF- β_1 and the incubations continued for 72 h. Formalised horse erythrocytes were then added to visualise the HA pericellular coat as describe under section 2.11. Zones of exclusion were visualized using Zeiss Axiovert 135 inverted microscope. Arrows indicate the cell body; arrowheads show the extent of the pericellular matrix. Representative of dermal fibroblasts from two patient donors. Original magnification was x 200. Immunohistochemical analysis was also performed to assess dermal fibroblast phenotype following treatment with hyaluronidase. Serum free medium alone (B) or bovine testicular hyaluronidase (200 μg/ml) (D) were added to growth arrested cells for 1h prior to the addition of 10 ng/ml TGF- β_1 and the incubations continued for 72 h. The cells were fixed and stained for α-SMA, as describe under section 2.4, mounted in Vectashield fluorescent mountant, and viewed under UV light. Original magnification x 100.

Effect of HA coat removal on fibroblast phenotype

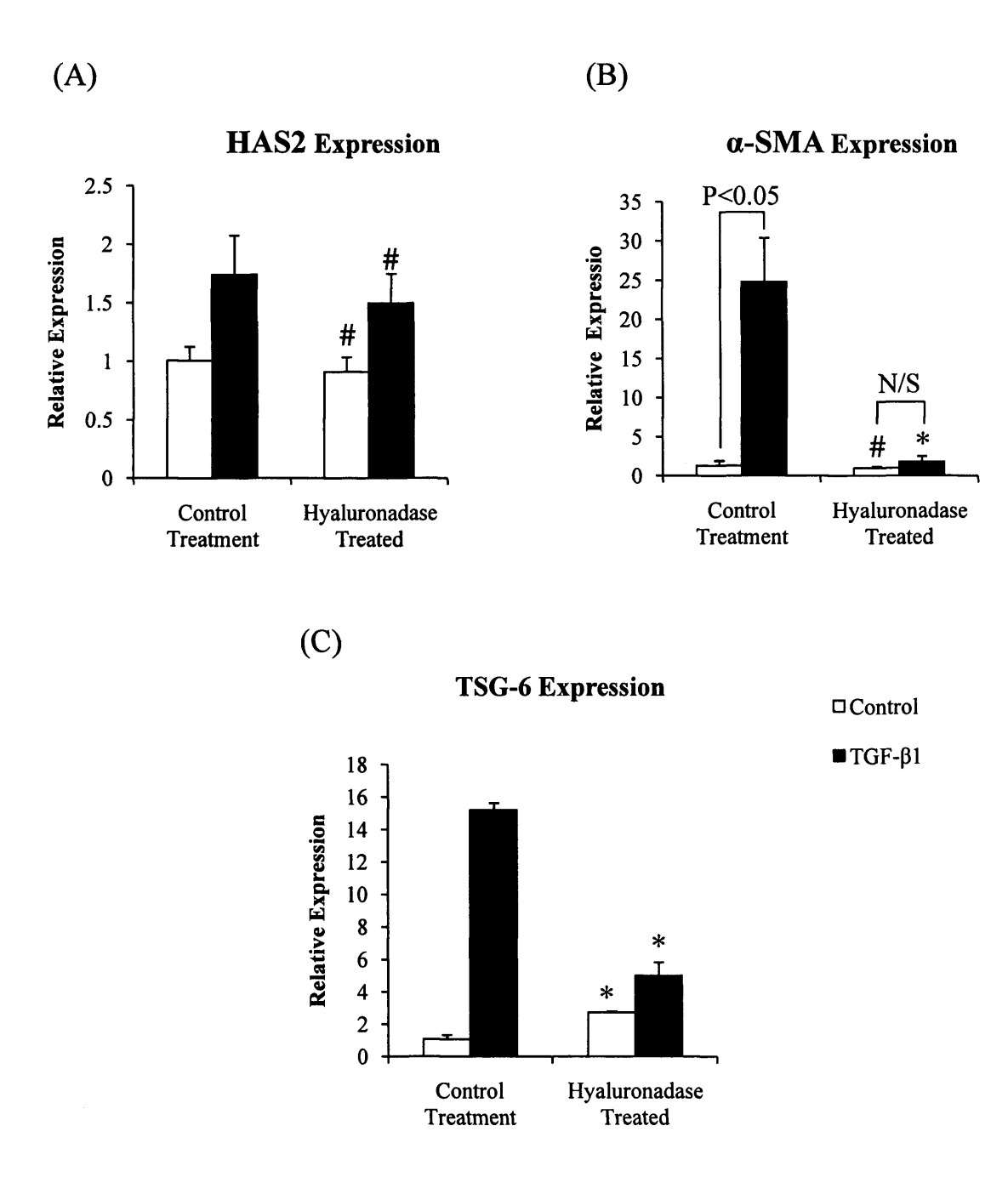


Figure 4.17 Consequence of inhibiting HA coat assembly on TGF- β_1 dependent phenotypic activation of fibroblasts. Confluent monolayers of young dermal fibroblasts were growth-arrested in serum-free medium for 48 h. Bovine testicular hyaluronidase (200 µg/ml) was then added in serum free medium at 37 °C for 1 h, prior to the addition (to the hylauronidase) of either serum free medium alone (clear bars) or 10ng/ml TGF- β_1 (black bars) for a further 72h. In control experiments hyaluronidase treatment was replaced by adding serum free medium alone. HAS2 (A), α -SMA (B) and TSG-6 (C) mRNA expression was assessed by RT-QPCR. Ribosomal RNA expression was used as an endogenous control and gene expression was assessed relative to the control treatment in non-stimulated cells. The comparative C_T method was used for relative quantification of gene expression and the results are represented as the mean± S.E. six individual experiments using cells isolated from two different donors. Statistical analysis was performed by the Student's t test: t, Not Significant, t, p<0.05 as compared to control treatment. N/S, not Significant.

Effect of HA coat removal on Smad2 signalling

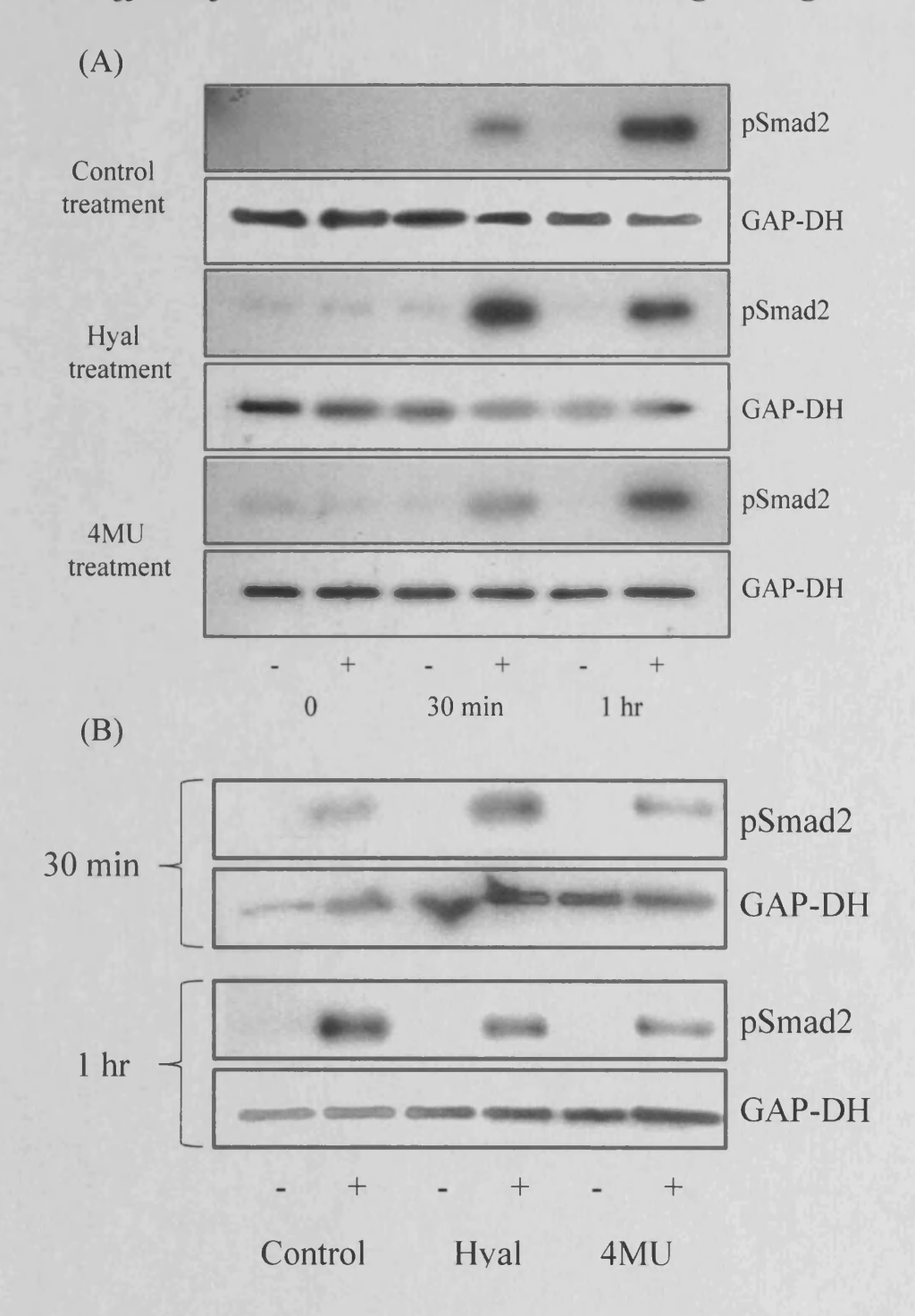


Figure 4.18 Effect of HA disruption on Smad2 signalling. A, confluent monolayers of young dermal fibroblasts were growth arrested in serum-free medium for 48 hours. The medium was replaced with either serum-free medium alone or serum-free medium containing 10 ng/ml TGF- $\beta 1$ in the absence of (control treatment) or presence of either Hyal ($200 \mu \text{g/ml}$) or 4MU (0.05 mM) for the indicated times. B, direct comparison of cell lysates at 30min and 1hr for all treatments. Cell lysates were subsequently subjected to Western blot analysis as describe under section 2.14 utilising antibodies against the phosphorylation form of Smad2. Expression of GAP-DH was analysed as a control to ensure equal loading. The results shown are representative of five independent experiments from the same patient donor.

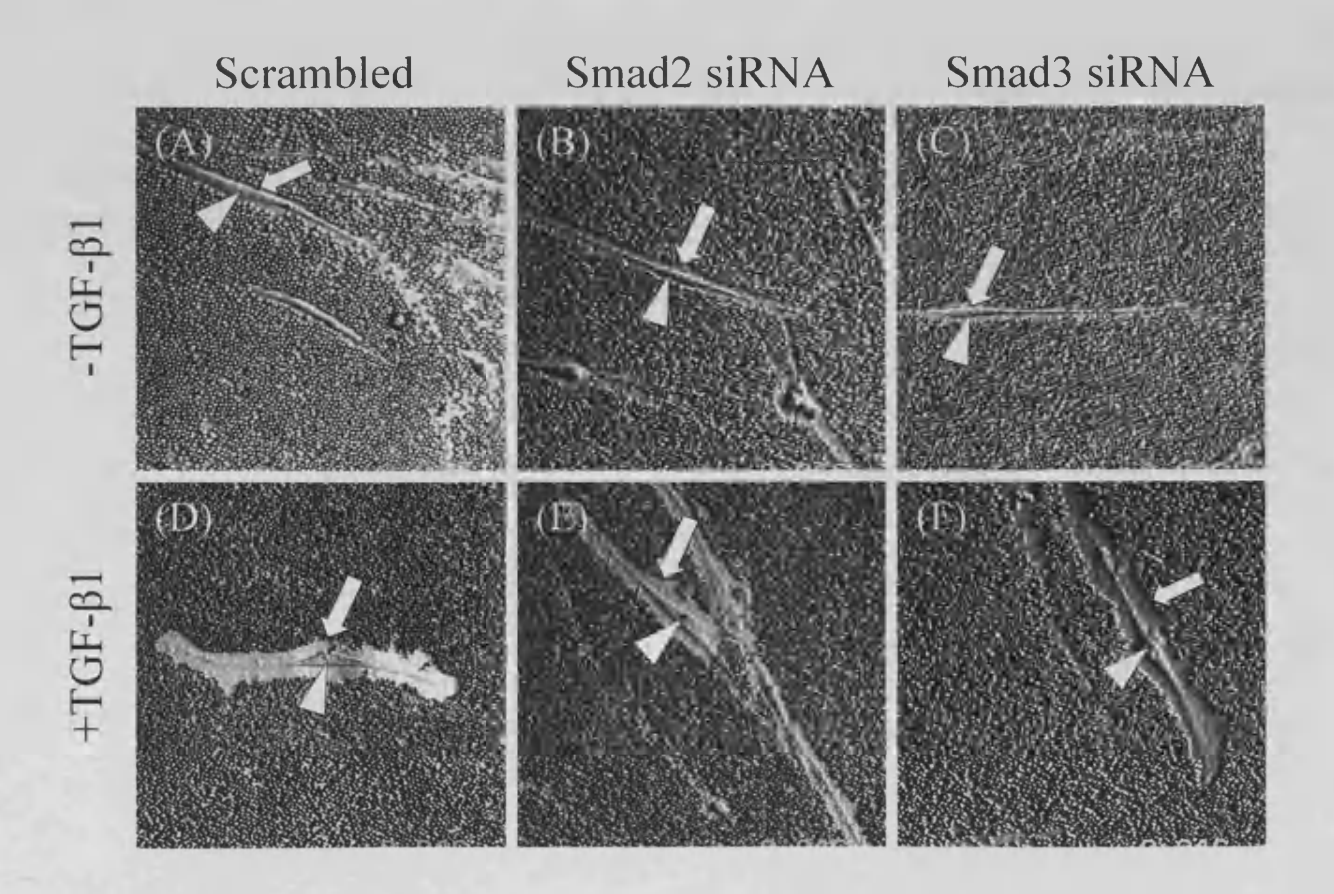


Figure 4.19 Effect of Smad2/3 siRNA on HA pericellular coat formation. Confluent monolayers of young dermal fibroblasts were transfected with either a scrambled oligonecleotide control (A&D), Smad2 siRNA (B&E) or Smad3 siRNA (C&F) as describe under section 2.14, for 48 hours. The medium was then replaced with either serum-free medium alone (A-C) or with serum-free medium containing $10 \text{ng/ml TGF-}\beta_1$ (D-F) for 72 h. Formalised horse erythrocytes were then added as describe under section 2.11 to visualise the HA pericellular coat. Arrowheads indicate the cell body; Arrows show the extent of the pericellular matrix. Representative of dermal fibroblasts from three patient donors. Original magnification x 200

4.3 Discussion

The aim of this chapter was to increase my understanding of the mechanisms which drive the phenotypic and functional changes associated with the differentiation process, particularly those associated with TGF- β 1 signalling and HA regulation. The work from this chapter then addresses how age-related alterations by these two components may explain the differentiation impairment observed with *in-vitro* aging.

Selective ALK5 inhibition in young fibroblasts antagonised induction of α -SMA mRNA and protein expression confirming the involvement of classical TGF- β 1 receptor activation during phenotypic conversion. Interestingly, whilst HAS2 induction was inhibited by the ALK5 inhibitor, TSG-6 induction was not, suggesting that they may be regulated by different signalling pathways. TGF- β 1-mobolizes both Smad-dependent and non-Smad dependent signalling [140]. p38 MAPK has been implicated in the participation of non-Smad TGF- β 1 signalling [129] but showed no involvement in any of the responses to TGF- β 1 examined in this study.

Given the age-dependent failure of TGF-β1-directed phenotypic activation that was demonstrated in the previous chapter, I sought to examine the effects of aging on Smad signalling. In response to TGF-β1 stimulation, Smad2 and Smad3 appear to be phosphorylated synchronously, indicating a functional Smad-dependent TGF-β1 signalling pathway. Furthermore, the extent of phosphorylation did not change across the range of *in-vitro* ages tested, extending from young through to near-senescent cells. This indicates that the differential responses to TGF-β1 of aged cells was not due to an inability of these cells to respond to TGF-β1 stimulation. Consistent with this, young and aged cells generated almost identical levels of TGF-β1 mRNA through autoinduction. Thus, the original hypothesis that aging may be associated with differences in TGF-β receptor expression and functionality appear to be invalid. Despite recent reports that over-expression of Smads were used for treatment of chronic cutaneous wounds that become unresponsive to TGF-β1 [308], restoration of TGF-β1 responsiveness and myofibroblastic conversion in my aged cells by this approach would

presumably prove ineffective. In support of my data, Colwell et al demonstrated that Smad signalling does not change in fetal and adult mouse fibroblasts despite their differential healing responses [309].

Smad 2 and Smad3 are known to activate unique transcriptional targets, based in part on their differential DNA binding activity. Thus, Smad3 binds cognitive GTCT motifs directly, while an insertion in the N-terminal MH1 domain of Smad2 precludes its direct DNA binding, permitting only indirect regulation of gene transcription via binding of transcription factors [310]. The different roles of Smad2 and Smad3 are further highlighted in this chapter by their differential requirement for phenotypic activation as assessed by their knockdown. Consistent with previous observations [285], Smad2 but not Smad3 activation was demonstrated to be essential for TGF- β 1-mediated cellular activation. This data is also supported by others; Evans et al demonstrated that transfection with Smad2 but not Smad3 resulted in TGF- β 1-independent alteration in fibroblast cell phenotype, upregulation of α -SMA and reorganisation of the actin cytoskeleton [112]. Furthermore, Petridou et al demonstrated nuclear translocation of Smad2 is directly responsible for myofibroblast differentiation [294], a phenomenon which was reported for fetal and adult human fibroblasts in response to TGF- β 1 stimulation [311].

Collectively, these data demonstrate that Smad2 signalling (over Smad3) mediates TGF-\(\beta\)1 driven phenotypic conversion. Defective TGF-\(\beta\)1 signalling however cannot explain why *in-vitro* aged cells resist fibroblast-myofibroblast conversion.

It was also interesting to discover that in young cells, whilst TGF-β1 mediated myofibroblastic differentiation was associated with an upregulation of Smad2 expression, Smad3 expression actually declined following TGF-β1 stimulation, despite demonstrating a similar degree of phosphorylation as Smad2. Tissue formation during regeneration after injury demands highly coordinated cell migration and proliferation, followed by cellular differentiation and matrix synthesis and assembly and all of these are biological responses to TGF-β1. In their study, Grotendorst et al [312] present evidence that fibroblast proliferation and differentiation represent two distinct biological

response pathways that are mutually exclusive for cells that have been activated by TGF-β1, that is, cells which are proliferating cannot differentiate and vice versa. It is, therefore, interesting to speculate that reduction in Smad3 in the myofibroblast serves to suppress other TGF-β1-mediated cellular processes such as proliferation. Consistent with this concept, Meran et al showed that whilst Smad3 does not appear to be involved in fibroblast myofibroblast transition, it plays a key role in the regulation of TGF-β1-dependent fibroblast proliferation [160]. In conclusion, from this chapter and the work of others [160, 285] Smad2 and Smad3 are implicated in dermal fibroblast differentiation and proliferation respectively. This would also help explain reports that loss of Smad3 results in a more rapid closure of wounds [136, 137] due to preference over a contractile phenotype.

In the previous chapter, resistance to TGF-\(\beta\)1 directed myofibroblastic differentiation by in-vitro aged fibroblasts was shown to be associated with attenuation in HA generation. It has been speculated that regulating HA pericellular coat assembly, rather than HA synthase isoform activity, is critical for phenotypic conversion [159], whilst others have described the acquisition of a HA coat to be a product rather than a cause of differentiation [266]. To investigate the importance of HA synthesis, the effect of 4MU on TGF-β1 mediated myofibroblastic differentiation of young dermal fibroblasts was studied. Depletion of the UDP-glucuronic acid pool by 4MU has been shown to inhibit HA synthesis and pericellular HA coat formation in a number of cell types including fibroblasts [159, 161, 162, 306, 313]. In one study, 4MU was found to inhibit HA synthesis in cultured human skin fibroblasts but to have no effect on synthesis of any other GAGs [314]. The results from this chapter demonstrate that in the presence of 4MU, induction of α-SMA mRNA was significantly reduced. This was associated with suppression of HAS2 and TSG-6 induction. The resulting response to TGF-β1 stimulation was essentially comparable to the response seen in aged fibroblasts. Collectively this suggests that increased synthesis of HA associated with the young phenotype facilitates fibroblast-myofibroblast transition conferring a role for HA in wound closure.

In the previous chapter in-vitro aging and resistance to phenotypic conversion were accompanied by a failure of induction of HAS2 after addition of TGF-\(\beta\)1. Resistance of oral mucosal fibroblasts to TGF-\$1-mediated myofibroblastic change has also been associated with failure of induction of HAS2 [159]. In light of these findings, the hypothesis that HAS2 isoform activity is critical in driving myofibroblast differentiation was subsequently tested in young cells. Silencing HAS2 gene expression using siRNA led to a significant inhibition of TGF- β_1 dependent induction of α -SMA. These observations led me to determine if isoform specific over-expression of HAS2 was sufficient to restore TGF-\(\beta_1\) responsiveness and phenotypic alteration by in-vitro aged fibroblasts. Although over-expression of HAS2 was associated with increased HA generation, there was no alteration in α -SMA expression, suggesting that restoration of the age dependent decrease in HAS2 expression was not the sole factor leading to the loss of $TGF-\beta_1$ dependent phenotypic sensitivity. This is consistent with the observation that the aged cells retained the ability to induce HAS2 in response to IL-1β suggesting that aging specifically affects TGF-β₁ responses rather than causing a global defect in HAS2 regulation.

Previous studies have demonstrated that the ability of the fibroblast to transform under the influence of TGF- β 1 to myofibroblasts may be related to the capacity of the cell to incorporate HA into a pericellular coat [159] but this has only been speculation. In support of this, in the previous chapter phenotypic conversion and coat formation were intrinsically linked, in that young cells capable of differentiation exhibited HA coats whereas aged cells unable to differentiate failed to exhibit coats. Consistent with this, attenuation of α -SMA induction following HAS2 silencing was associated with impaired HA pericellular coat assembly.

Webber et al showed that inhibition of autocrine TGF-β1 signalling and loss of the myofibroblast phenotype was associated with suppression of the expression of the hyaladherin TSG-6 [162]. In the previous chapter I demonstrated an age-dependent decrease in TSG-6 expression both in unstimulated and in response to TGF-β1. In this chapter I confirm a role for TSG-6 in facilitating fibroblast-myofibroblast differentiation by demonstrating that silencing of TSG-6 gene expression using siRNA led to an

inhibition of TGF- β 1-dependent induction of α -SMA. These results suggests that coordinated induction of HAS2 and TSG-6 facilitation of HA pericellular coat assembly are necessary to allow TGF- β 1-dependent phenotypic activation of fibroblasts, and both components of this response are impaired with *in-vitro* aging.

The importance of the pericellular HA coat in regulating the fibroblast – myofibroblast activation process is further highlighted by the data demonstrating that inhibition of coat formation by Hyal, also prevented TGF- β_1 mediated phenotypic conversion. This result confirmed that the formation of a pericellular HA coat was necessary to drive myofibroblastic differentiation in dermal fibroblasts. This was consistent with recent reports that extracellular HA matrices are an essential mediator in the persistence of the myofibroblast phenotype in lung fibroblasts [162].

This chapter has confirmed that a HA coat is a pre-requisite for fibroblast-myofibroblast differentiation but the functional significance of the pericellular matrix in facilitating this process remains unclear. Recent data from Kultti et al [313] has demonstrated that in several cell types, the HA coat can induce and maintain prominent microvilli in cell plasma membranes that rest on filamentous actin, these microvilli were degraded when the pericellular coat was destroyed and were dependent on an intact cytoskeleton. It is interesting to speculate that the pericellular coat may influence cellular differentiation processes through direct interaction with the actin cytoskeleton.

Formation of a pericellular coat following stimulation with IL-1 β did not facilitate phenotypic activation. Similarly, stimulation of HAS2 over-expressing cells although restoring the cell's ability to form a pericellular coat, was not associated with phenotypic activation. Restoration of high basal level of HA synthesis in the aged dermal fibroblast, however, as a result of HAS2 over-expression, did result in restoration of TGF- β_1 dependent induction of TSG-6, further emphasising its role in mediating HA coat formation. These data therefore suggest that although formation of the pericellular coat is necessary for TGF- β_1 dependent phenotypic activation, the formation of the coat in itself is not the sole driving force and is not sufficient to drive

the myofibroblastic phenotype. Dissociation of coat formation and phenotypic activation points to the involvement of other mechanisms.

This chapter has demonstrated that TGF-\$1 signalling through Smad2-dependent pathway is required for myofibroblastic differentiation. Webber et al demonstrated that assembly of the HA coat in lung myofibroblasts facilitates Smad-dependent responses that maintain the myofibroblast phenotype in lung fibroblasts [162]. In this chapter I addressed the hypothesis that the HA coat may be involved in regulation of Smad signalling. Having shown the HA coat to be a prerequisite for TGF-\beta1-mediated phenotypic conversion it was surprising to discover that disruption of HA synthesis and pericellular coat formation using either 4MU or Hyal did not influence TGF-\$1mediated phosphorylation of Smad2. Likewise, transfection of young cells with Smad2 or Smad3 siRNA's did not impair assembly of HA pericellular coats. Collectively these results demonstrate that TGF-\beta1 mediated dependent HA pericellular coat synthesis does not utilise Smad-dependent signalling pathways. Furthermore, induction of TSG-6 and HAS2 by TGF-\$1 was not suppressed by Smad2 or Smad3 silencing further supporting their involvement in pericellular coat assembly in a manner independent from Smad signalling. Taken together, the data suggest that whilst cytoskeletal remodelling and HA pericellular matrix assembly are both induced by TGF-\$1 they are mediated by independent pathways.

Cross-talk between Smad and non-Smad signalling pathways may enhance TGF-β1-dependent responses in other cell systems [315, 316]. For example, cooperative action of MAP kinase and Smad pathways have been implicated in mediating effects of TGF-β1 on gene targets [124]. Co-localisation of CD44 and TGF-β receptors have been shown to facilitate modulation of both Smad and non-Smad-dependent TGF-β1-mediated events by HA [210]. The data from this chapter suggests that HA may facilitate TGF-β1 dependent differentiation through recruitment of alternative signalling pathways to the classical Smad pathway. Another plausible explanation is that HA influences targets at either the level of the TGF-β receptor or by a separate mechanism downstream of Smad2 signalling.

The salient findings of this chapter are summarised in figure 4.19. In summary the data suggests that resistance to myofibroblastic conversion by aged cells cannot be explained by a global deficit in TGF-β1 signalling. Rather, the data presented demonstrates that coordinated induction of HAS2 and TSG-6 facilitation of HA pericellular coat assembly is necessary for TGF-β1-dependent activation of fibroblasts, and both components of this response are impaired with *in-vitro* aging. This chapter presents further evidence that highlights the intimate involvement of HA in the modulation of fibroblast-myofibroblast differentiation. In conclusion, whilst the synthesis and organisation of HA into a pericellular coat is integral for differentiation to occur, it is not sufficient to correct for the age-dependent defect in phenotypic conversion. It would appear therefore and perhaps not surprisingly, that in addition to pericellular HA coat assembly other mechanisms must become disrupted during *in-vitro* aging leading to impaired cellular differentiation. Ascertaining these other mechanisms forms the drive of the next chapter.

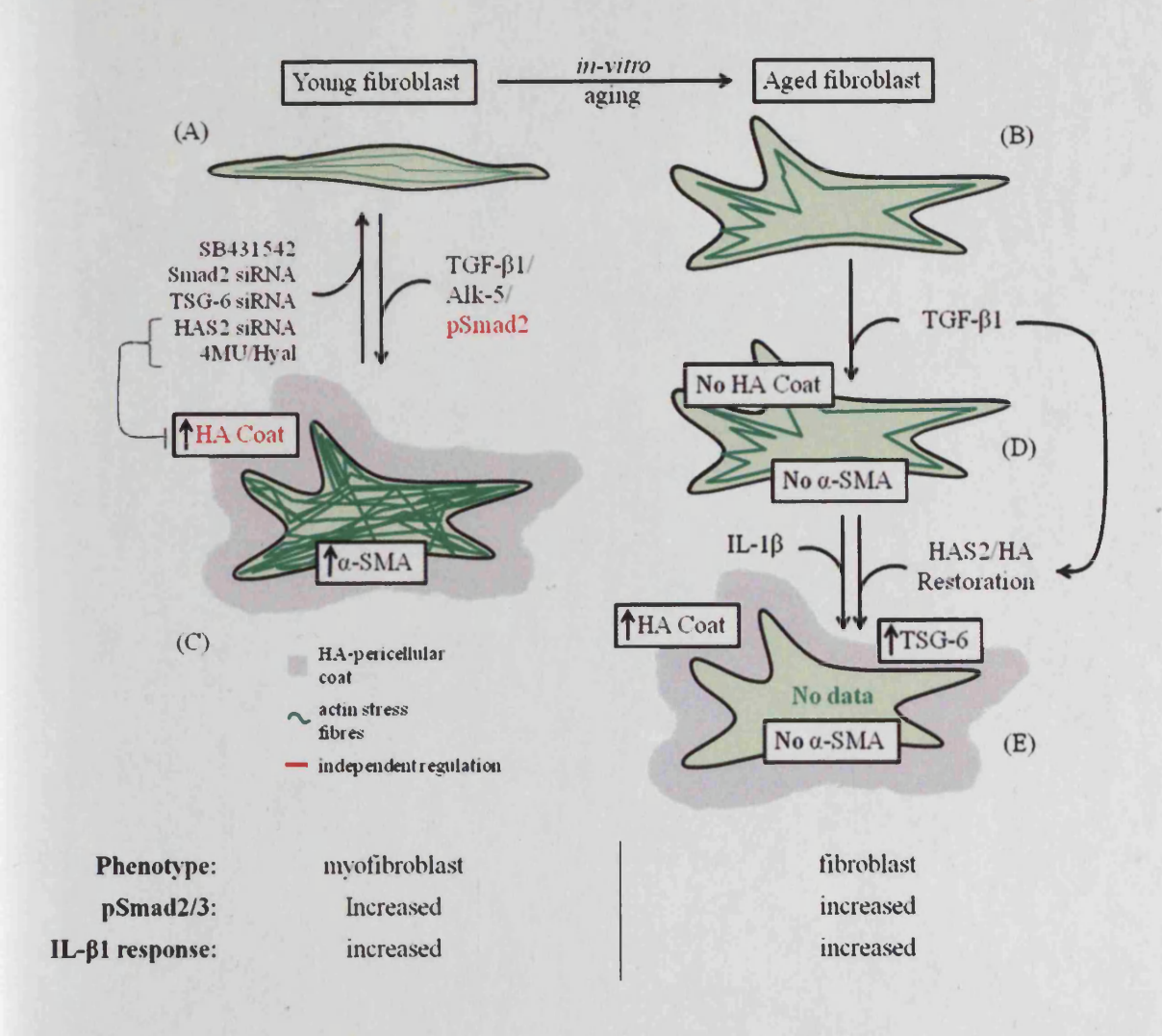


Figure 4.19 Comparison of young and in-vitro aged fibroblast phenotpye. A comparison of cell morphology, HA generation and phenotype of patient matched young (A&C) and aged (B&D&E) based on the analysis compacted from this results chapter. In response to TGF-β1 young fibroblasts (A) readily differentiate into myofibroblastic cells (C) which incorporate prominent stress fibres and α-SMA. This is mediated via activation of Alk-5 and Smad2. Accordingly, phenotypic differentiation is attenuated by the Alk-5 inihibitor SB431542, and Smad2 siRNA. In addition, myofibroblastic differentiation is dependent on HAS2 induction of HA and its assembly into a pericellular coat. Disruption of the coat and HA synthesis with either TSG-6 siRNA, HAS2siRNA, 4MU of Hyal inhibits phenotypic activation. In aged fibroblasts TGF-\(\beta\)1 stimulation alone failed to mediate myofibroblastic differentiation associated with inability to form a HA coat and upregulate α-SMA (D). Restoration of HA levels by HAS2 over-expression in aged cells restored TGF-β1-mediated coat formation and TSG-6 induction but did not lead to acquisition of a myofibroblast phenotype (E). IL-1β failed to promote α-SMA expressing myofibroblasts but did mediate coat assembly through induction of HAS2-dependent HA synthesis and TSG-6. Furthermore the IL-1β response was independent of invitro aging unlike the age-dependent attenuation in TGF\$1 responsiveness observed. Finally Smad signalling did not change between the young and aged phenotype. Dysregulation of Smad signalling did not impair HA coat formation and vice versa indicating these events are independent from each other (red).

Chapter 5 The Role of Hyaluronan-Dependent CD44/EGF Receptor Signalling

5.1 Introduction

Failure of TGF- β_1 -induced differentiation to the myofibroblast phenotype as a consequence of aging is associated with the inability to induce HAS2, a decrease in HA synthesis and a lack of pericellular coat formation. HA synthesis and coat assembly could be restored by forced overexpression of HAS2 followed by TGF- β_1 stimulation. This did not, however, restore the myofibroblast phenotype. Furthermore, despite demonstrating that *in-vitro* aging is associated with attenuation of numerous TGF- β_1 dependent responses, the previous chapter revealed that intrinsic differences in young and aged cells could not be accounted for by variation in their TGF- β signalling machinery. Collectively, this suggests that other factors (in addition to TGF- β_1 and HAS2) must be operative in young cells but have been lost during the aging process.

TGF- β signalling involves a diverse group of cellular elements in addition to the Smad family of proteins. TGF- β -stimulated activation of ERK, p38MAPK and c-Jun NH2-terminal kinase (JNK) has been demonstrated previously in different cell types [317] and furthermore there is evidence for cooperativity of Smad and non-Smad pathways [316]. In the previous chapter the organisation of HA into a pericellular coat by TGF- β 1 was shown to be Smad-independent. Since this process is integral for myofibroblastic conversion it was deduced that Smad-independent TGF- β 1 signalling plays an important role in myofibroblastic differentiation. A further layer of complexity can be added to the understanding of TGF- β signalling by the realisation that it may influence or be influenced by physical and functional interactions with other receptors (cytokine and matrix). For example, in metastatic breast tumour cells [203] and renal proximal tubular epithelial cells [210], CD44 has been shown to be physically linked to the TGF- β 1 receptor I allowing for modulation of both Smad and non-Smad-TGF- β 1 mediated events by HA.

Key stimuli for human dermal fibroblasts are ligands for the epidermal growth factor receptor (EGF-R) [1]. Epidermal growth factor (EGF) is a member of the EGF superfamily of cytokines [318, 319]. They function as pleiotropic effector molecules during

foetal development and pathological processes, such as wound healing and cancer progression [318, 319]. Synergistic effects between TGF-\(\beta\)1 and EGF have been demonstrated to regulate cell phenotype and function in several systems [320-326]. He et al demonstrated that EGF contributes to the differentiation and migration of myofibroblasts induced by TGF-\(\beta\)1 through transactivation of EGF-R [327]. Earlier studies have shown that TGF-\beta1 induces the expression of high-affinity EGF-R in stromal fibroblasts [328] and in the A431 epidermal cell line, TGF-\(\beta\)1 caused increased tyrosine phosphorylation of the EGF-R that was not dependent on protein synthesis [329]. Other studies have shown that TGF-B amplifies the content of EGF-R in granulose cells from rat ovaries and increases EGF-R transcription in kidney fibroblasts [330, 331]. The involvement of EGF-R transactivation in TGF-\(\beta\)-induced fibronectin mRNA expression in mesangial cells was recently reported [317]. Interestingly, in their study the authors showed that TGF-\beta-mediated Smad2 phosphorylation was independent of TGF-β-mediated EGF-R signalling. Equally, in the previous chapter I demonstrated that the TGF-\$1/Smad2 signalling cascade and regulation of HA pericellular matrix assembly represented crucial yet independent events for TGF-\$1mediated myofibroblastic differentiation. This could be conceivably explained with the addition of an EGF-R component.

Furthermore, studies have revealed that fibroblasts aged *in-vitro* demonstrate a reduction in their ability to respond to the mitogenic effects of EGF as compared to cells at an earlier population doubling level [35, 256]. It was determined that the decreased responsiveness of aged cells to EGF was due to preferential loss in EGF-R levels. In fact EGF-R expression decreases by about half in near senescent fibroblasts [35]. Decreased numbers of high and low affinity EGF-R during serial cultivation *in-vitro* have been reported in human endothelial cells [332], and the diminished responsiveness to EGF to chondrocytes derived from aged animals also seems to be due to a reduction in the number of EGF receptors [333]. I therefore postulate that a TGF-β1-dependent and an EGF-R-dependent pathway are both necessary for full myofibroblastic differentiation.

HA is known to influence the differentiation of other cells in a manner dependent on EGF-R and ErbB receptor signalling [295, 326]. Rapid HA accumulation after epidermal wounding occurs through a mechanism requiring cleavage of HB-EGF and activation of EGF-R signalling [222]. Pienimaki et al showed that EGF increased HA synthesis and induced a coat of HA in epidermal keratinocytes through activation of HAS2 mRNA but not HAS1 or HAS3 [318]. In view of my data demonstrating the importance of HAS2 mediated coat formation in phenotypic activation and maintenance [162], I also postulate that HA is a key factor in regulating the coordinated action of the TGF-β1 and EGF signalling pathways, required for acquisition of myofibroblast phenotype, such that defects in both HA synthesis *and* EGF signalling both contribute to age dependent impaired wound healing.

I have demonstrated in the previous chapters an age-related defect in myofibroblast differentiation, associated with impaired synthesis of HAS2 mediated pericellular coat but have failed to prescribe its role in a mechanistic sense. It has previously been demonstrated that maintenance of the chondrocyte phenotype, as well as initial cartilage differentiation, may depend on the close association of the cell with its matrix as well as on cell shape as modulated by the actin cytoskeleton [334]. CD44 is the main receptor associated with the formation of the HA pericellular matrix [219], internalisation of HA [335] and mediation of HA-induced signals. Several studies indicate that the intracellular domain of CD44 selectively interacts with the intracellular actin cytoskeleton [211] via cytoskeletal proteins such as ankyrin [203], filamin [206] and cortactin [336]. It is interesting to speculate that interaction between the HA pericellular matrix and CD44 provides a direct link to the cytoskeleton allowing changes in HA synthesis, organisation and assembly, to modulate cellular phenotype and orchestrate cell function. Furthermore, there is evidence suggesting a relationship between HA production and CD44 expression [337], which led me to hypothesise that age related attenuation in HA synthesis is associated with reduced CD44 expression. Therefore agerelated disruption in HA-CD44 and its interaction with the cytoskeleton may provide an explanation for resistance to phenotypic conversion observed in aged cells.

Although it is well established that fibroblasts bind HA to their surface via the expression of CD44, the cellular responses following ligand-receptor interaction still remain to be clearly established. The capacity of CD44 to form stable complexes with the EGF-R has been previously reported in numerous studies [206, 326, 338]. This chapter further aims to investigate whether CD44/EGF-R interaction plays a role in mediating dermal fibroblast-myofibroblast differentiation.

The aim of this chapter is:

- i To characterise EGF-R signalling in dermal fibroblasts, specifically:
 - -the significance of EGF-R signalling in phenotypic activation
 - -the significance of age-related alterations in EGF-R signalling
- ii To characterise the relationship between EGF-R signalling and HA regulation
- iii To examine whether modulating EGF-R levels can influence the aged phenotype
- iv To characterise the role of CD44, specifically
 - -the significance of CD44 signalling in phenotypic activation
 - -the significance of age-related alterations in CD44 signalling
- v To investigate the relationship between CD44, EGF-R and HA

The results from this chapter will help address the hypothesis that synergy between TGF-β1-dependent pathways and a competent EGF signalling pathway are required for myofibroblastic differentiation and that central to this process is the induction of HAS2 and synthesis of HA. Furthermore I differentiate what contribution that these pathways (Smad and non-Smad) make towards age related impairment in phenotypic activation.

5.2 Results

5.2.1 The role of the EGF-R in TGF-\$1-mediated myofibroblastic differentiation

The relative contribution of TGF- $\beta1$ receptor and EGF receptor signalling in TGF- $\beta1$ dependent fibroblast to myofibroblast phenotypic activation was examined by addition of TGF- $\beta1$ to growth arrested young fibroblasts for 72 hours in the presence of either AG1478, an inhibitor of EGF-R signalling or, the TGF- β -R/Alk5 inhibitor SB431542. Addition of either inhibitor attenuated TGF- $\beta1$ induced expression of α -SMA (Figure 5.1), suggesting that in the absence of exogenous EGF, that TGF- $\beta1$ utilises both its own and the EGF-R to facilitate phenotypic activation. These data also highlighted that EGF is not sufficient to induce myofibroblastic differentiation. As previously demonstrated, TGF- $\beta1$ induces significant upregulation of α -SMA mRNA, however combined addition of TGF- $\beta1$ and EGF demonstrated marginally increased expression than with TGF- $\beta1$ alone. The results using chemical inhibition showed that synergism between TGF- $\beta1$ and EGF involves the activation of EGF-R and ALK-5 signalling.

5.2.2 Effect of aging on EGF-R expression.

Given the age dependent failure of TGF-β1 directed phenotypic activation that was previously demonstrated in chapter 3 and 4, I sought to examine the effects of aging on EGF-R expression. Cell protein was extracted from growth arrested patient matched fibroblasts over a range of different *in-vitro* ages ranging from young (PDL 15) through to near-senescence (PDL 39). Western blot analysis of EGF-R demonstrated that *in-vitro* aging was associated with an age dependent decrease in EGF-R protein expression, with barely detectable levels in near-senescent cells (PDL 33-39) (Figure 5.2A). This was confirmed by densitometry analysis (Figure 5.2B). These results demonstrated that with *in-vitro* aging fibroblasts displayed attenuated levels of endogenous EGF-R. Consistent with these results, Q-PCR analysis revealed an age-dependent attenuation in EGF-R transcription (Figure 5.2C). Young fibroblasts had

significantly higher (~3 fold) EGF-R mRNA expression compared to patient matched aged fibroblasts.

Collectively these results suggest that age dependent loss of TGF- β_1 dependent phenotypic activation is associated with loss of EGF-R.

5.2.3 The effect of EGF-R restoration on TGF-\beta1-mediated myofibroblastic differentiation in aged fibroblasts

I hypothesised that loss of EGF-R may be responsible for loss of TGF-β1 responsiveness in aged fibroblast. Previous studies have demonstrated restoration of age dependent EGF responsiveness by forced over-expression of EGF-R cDNA [35]. To examine the role of age dependent decrease in EGF-R expression in TGF-\(\beta\)1 responsiveness, aged fibroblasts were transfected with cDNA encoding either EGF-R or GFP (as a control). Confirmation of EGF-R over-expression was demonstrated by O-PCR (Figure 5.3A). TGF-β1 responsiveness of EGF-R over-expressing cells was examined by stimulation with TGF-\beta1 for 72hours after transfection. There was no difference in α-SMA expression between EGF-R over-expressing cells and GFP transfected cells following additions of TGF-\beta1 (Figure 5.3B), suggesting that restoration of EGF-R expression in aged cells did not restore TGF-β1 responsiveness. The functional nature of the transfected EGF-R was explored by examining the EGF dependent proliferative response of EGF-R over-expressing aged fibroblasts. These experiments demonstrated significantly increased proliferation, as assessed by [3H]thymidine incorporation, following addition of exogenous EGF to EGF-R overexpressing cells compared to control GFP transfected cells, thus confirming the functionality of the transfected receptor (Figure 5.3C).

5.2.4 The role of EGF in TGF-\$1-mediated myofibroblastic differentiation

Synergy between TGF- β 1 and EGF in regulating cell phenotype is well recognised, in other cell systems [339, 340]. The effect of *in-vitro* aging on the expression of EGF was examined under basal conditions and following stimulation with TGF- β 1 (Figure 5.4A).

Fibroblasts were grown to confluence and serum deprived for 48 hours prior to addition of either recombinant TGF-β1 or serum free medium alone (control treatment) for a further 72 hours. Q-PCR analysis revealed that under basal conditions aged cells exhibited a small but significant attenuation in EGF mRNA. Moreover, following addition of TGF-β1, whilst young cells responded with a significant induction (~7 fold) in EGF mRNA, in contrast aged cells demonstrated no change in EGF mRNA expression. These data demonstrate that in addition to the loss of expression of EGF-R, in-vitro aging is associated with a loss of TGF-\beta1 dependent induction of EGF. This raises the possibility, that loss of autocrine EGF activity may also be involved in age dependent loss of TGF-\beta1 phenotypic activation. To examine this, aged fibroblasts over-expressing EGF-R were co-stimulated with exogenous EGF and TGF-β1. In contrast to stimulation with TGF-\beta1 in isolation, co-stimulation led to augmented phenotypic activation as assessed by expression of α-SMA (Figure 5.4B). It was implicated in the previous chapter that both HAS2 dependent HA synthesis and its assembly into a pericellular matrix by TSG-6 were required for TGF-\(\beta\)1 dependent phenotypic activation of fibroblasts. In addition to α-SMA, co-stimulation led to a restoration of induction of HAS2 (Figure 5.4C) and the hyaladherin TSG-6 (Figure 5.4D), which did not occur following addition of TGF-β1 in isolation.

TGF- β_1 activation of EGF-R has been reported in several studies to be through direct synthesis of EGF [341]. To investigate the participation of EGF in TGF- β_1 -dependent phenotypic activation young cells were treated with TGF- β_1 in the presence of either an anti-EGF antibody or the EGF-R inhibitor AG1478 and the expression of α -SMA assayed by Q-PCR (Figure 5.5). Addition of neutralising anti-EGF antibody inhibited TGF- β_1 -mediated α -SMA accumulation by \sim 50% whilst complete inhibition was achieved using the chemical inhibitor AG1478, as expected from Figure 5.1.

5.2.5 The relationship between the EGF-R and HAS2

The induction of HAS2 in aged cells following restoration of EGF signalling together with the reported up-regulation of HAS2 and HA synthesis mediated by EGF-R signalling in epidermal keratinocytes [342] and human ovarian tumour cells [343] led

me to investigate the role of EGF signalling in regulation of HAS2 in my cell system. TGF-β1 mediated induction of HAS2 in young fibroblasts was significantly attenuated by treatment with the EGF-R inhibitor AG1478 (Figure 5.6A). These data suggested that TGF-β1 induced HAS2 dependent HA synthesis is mediated through EGF-R signalling pathways and further validated EGF as an intermediate signalling molecule.

Previous work has demonstrated that HA through CD44 may directly activate EGF-R in the context of oncogenic signalling [338, 344]. To examine the potential of endogenous HA to activate EGF-R in the absence of exogenous EGF, aged fibroblasts over-expressing both EGF-R and HAS2 were stimulated with TGF-β1 and cell phenotype monitored by quantitation of α-SMA. Under these experimental conditions, TGF-β1 dependent phenotypic activation was restored in the absence of exogenous EGF (Figure 5.7C). This suggests that in aged cells, forced over-expression of HAS2-dependent HA synthesis, removes the need for exogenous EGF in phenotypic activation of EGF-R overexpressing cells. Collectively these data indicate HAS2 participates in phenotypic activation and is downstream of TGF-β1-mediated EGF synthesis

5.2.6 TGF-\$1 activates ERK through EGF-R signalling

EGF-R is required for TGF- β_1 -initiated fibroblast-myofibroblast conversion. Activation of the EGF-R following addition of EGF and TGF- β_1 , in young cells was investigated by western analysis of EGF-R phosphorylation. Phosphorylation of EGF-R was observed 30 min after exposure to EGF (Figure 5.8A), and such activation was inhibited by pre-treatment with the EGF-R inhibitor AG1478 but not the ALK-5 inhibitor. (Figure 5.8B). TGF- β_1 did not alter p-EGF-R levels at 30min in isolation or in combination with EGF (Figure 5.8B). TGF- β_1 -induced EGF-R activation compared to EGF stimulation was both modest and relatively delayed; a significant increase in the phosphorylation of the EGF-R was not evident until 3 hours after addition of TGF- β_1 (Figure 5.8C). These data confirm that TGF- β_1 stimulation leads to phosphorylation of the EGF-R.

Several effector pathways for the EGF-R have been described [345] among them, the MAP Kinase cascades are important as well as being been reported as one of the downstream cascades of TGF- β_1 [345]. In particular, a role for EGF-R-mediated activation of ERK and p38MAPK has been reported [317]. I examined whether these MAPKs are involved in myofibroblastic differentiation by TGF- β_1 . ERK inactivation by the inhibitor PD98059 but not the p38MAPK inhibitor SB203580 significantly inhibited TGF- β_1 mediated α -SMA induction in young dermal fibroblast suggesting involvement of ERK but not p38MAPK signalling during phenotypic activation (Figure 5.9A).

Western analysis was used to investigate the kinetic profile of ERK activation upon stimulation by TGF- $\beta1$ using phospho-specific ERK1/2 antibody. Young cells exhibited significant basal ERK1/2 phosphorylation and although both ERK1 and ERK2 were phosphorylated preferential phosphorylation of ERK2 was observed. My studies have shown that ERK1/2 is activated rapidly (10 mins) following administration of TGF- $\beta1$ in young cells and rapidly returned to below basal levels after 30 mins (Figure 5.9B). Significantly TGF- $\beta1$ mediated ERK activation was markedly attenuated in aged cells (Figure 5.9C), consistent with the age dependent reduction in EGF-R expression, however, basal ERK phosphorylation remained unchanged.

It was hypothesised that EGF-R signalling converge at the ERK signalling pathway to mediate cellular responses. In support of this, activated ERK levels coincided with EGF-R phosphorylation (Figure 5.10A). Furthermore, TGF-β1 mediated activation of ERK was abolished by the EGF-R inhibitor, AG1487, suggesting that kinase activity of EGF-R is thus required for further downstream signalling of p42/p44 MAP kinases (ERK1/2). Age-related resistance to ERK1/2 activation was thus consistent with the age-related deficit in EGF-R levels.

Furthermore, a combinational effect of EGF and TGF-β1 on ERK activation was demonstrated to be greater than administration of either in isolation (Figure 5.10A). Inhibition of EGF-R pathway using AG1478 abolished the synergistic action of EGF on TGF-β1 induced ERK signalling whilst the ALK-5 inhibitor had no effect. This data

shows that EGF contributes to ERK activation induced by TGF-β1 through EGF-R activation.

There was a major discrepancy with this data. It was unclear how TGF-β1 induced ERK1/2 could be activated within 10 minutes and still be downstream of EGF-R phosphorylation, which was not evident until 3 hours after TGF-β1 stimulation. In an effort to explain this, a longer time course for TGF-β1 mediated ERK1/2 phosphorylation was carried out. Interestingly, the results demonstrated a biphasic activation profile. ERK activation was induced at 10 minutes (consistent with the previous data) and in accordance with the proposed model at 3 hours (Figure 5.10B). An explanation for rapid ERK1/2 by TGF-β1 is discussed later.

5.2.7 The differential requirement of EGF and HA signalling in TGF-\(\beta\)1 mediated activation of ERK and Smad2

The relationship between Smad2 and ERK signalling was investigated. As expected from chapter 4, Smad2 phosphorylation was rapidly induced following TGF-β1 stimulation at 10 min. Pre-treatment with the EGF-R inhibitor, AG1487 and anti-EGF antibody significantly suppressed ERK phosphorylation providing further evidence that EGF contributes to ERK activation induced by TGF-β1 through EGF-R activation. In contrast, Smad2 phosphorylation was unaffected (Figure 5.11), suggesting a dissociation of Smad and EGF signalling events by TGF-β1. Furthermore this corroborated with the earlier observation that whilst the former was not altered with *invitro* aging, the latter was.

Activation of EGF-R by HA associated with cytoskeletal reorganisation in head and neck squamous cell carcinoma cells, has been associated with downstream activation of MAP kinase (in particular ERK1 and ERK2) [206] and data presented above suggests that HA is intrinsically linked to EGF-R signalling. The role of HA in TGF-β1 mediated ERK activation was examined by either inhibition of HA synthesis by the depletion of the UDP-glucuronic acid pool using 4MU, or digestion of HA using Hyal. Both inhibition of HA synthesis and degradation of HA inhibited TGF-β1 mediated

activation of ERK1 and ERK2 (Figure 5.11). The requirement of HA for TGF-β1 directed Smad2 phosphorylation was also investigated in the same way. As expected from chapter 4 neither inhibition of HA synthesis nor degradation of HA had an effect on Smad2 activation providing further evidence that the TGF-β-specific Smad pathway is HA independent (Figure 5.9C).

Collectively these data demonstrate that TGF- β 1-mediated Smad signalling is independent from TGF- β -mediated EGF-EGF-R-ERK signalling. Whilst both pathways were required to mediate TGF- β 1-directed cellular differentiation, significantly, agerelated resistance to phenotypic activation was associated with age-related impaired ERK1/2 signalling, a consequence of defective EGF-R and HA signalling.

5.2.8 The expression of CD44 in young and aged fibroblasts and its role in myofibroblastic differentiation through ERK signalling

Acharya et al reported decreased levels of α -SMA in CD44KO fibroblasts compared with CD44WT fibroblasts [201] and the use of CD44 siRNA's have demonstrated inhibition of HA-mediated keratinocyte differentiation [284].

Having demonstrated the importance of HA in phenotypic activation by TGF- β 1 dependent phosphorylation of ERK1/2, I sought to examine the role of the principal receptor for HA, CD44 in phenotypic activation, and its relationship to age associated resistance to the effects of TGF- β 1.

Young fibroblasts were transfected with a specific siRNA for CD44 to determine its functional requirement for myofibroblast conversion. Efficacy of this approach was confirmed by QPCR assessment of CD44 mRNA suppression (Figure 5.12A). Suppression of CD44 expression was associated with abrogation of TGF- β 1 dependent induction of α -SMA as assessed by QPCR (Figure 5.12B) and immunohistochemistry (Figure 5.13F).

In contrast, suppression of CD44 expression did not affect TGF-β1 mediated upregulation of HAS2 (Figure 5.12C). In addition suppression of CD44 had a disruptive effect on the accumulation of pericellular HA. Whilst accumulation of HA outside the cell could be visualised it was assembled in an irregular coat, compared to untransfected and scrambled cells which demonstrate an organised HA coat linearly localised around the cell in a linear fashion (5.12G-I)

It was recently reported by Toole et al that 'clusterization' of CD44 is required for effective functionality [214]. Expression and localisation of CD44 and its relationship to phenotypic activation as assessed by expression of α-SMA, was examined by immunohistochemistry (Figure 5.14). In young cells, as expected, TGF-β1 increased expression of α-SMA (Figure 5.14F), when compared to unstimulated conditions. (Figure 5.13E). This was also associated with a re-localisation of CD44; under basal conditions CD44 was seen predominantly in a linear distribution around the cell periphery (Figure 5.14I). In contrast following TGF-β1 dependent phenotypic activation, CD44 appeared in a diffuse pattern throughout the cell (Figure 5.14J). Aged cells are resistant to TGF-\(\beta\)1 dependent phenotypic activation (Figure 5.14G-H), and this was associated with failure of CD44 re-localisation which remains predominantly in a linear distribution at the cell periphery (Figure 5.14K-L). Although these data demonstrate a defect in CD44 re-localisation associated with age, there was no alteration in CD44 mRNA expression when comparing young and in-vitro aged cells (Figure 5.15). Notably, in both cell types re-localisation of CD44 was associated with a TGF-β1 dependent decrease in CD44 mRNA.

5.2.9 The interaction of CD44 and the EGF-R in phenotypic activation of young and aged fibroblasts.

It was recently reported that CD44 can co-immunoprecipitate with EGF-R in head and neck squamous carcinoma cells [338] and glioblastoma cells [326] and that this functional coupling may mediate cellular responses. Given the dependence of CD44 and EGF-R in TGF-β1 induced phenotypic activation I sought to examine their potential for interaction. Anti-CD44 immunoprecipitation followed by anti EGF-R immunoblot analysis in young cells indicated that a low level of EGF-R is present in the anti-CD44

immunoprecipitated materials (Figure 5.16). TGF- β 1 dependent phenotypic activation in young cells was associated with recruitment of a significant amount of EGF-R to the CD44-EGF-R complex. Inhibition of HA synthesis using 4MU, or digestion of HA using Hyal resulted in a reduction of EGF-R accumulation in the CD44 immunoprecipitant. These results demonstrate that in young cells TGF- β 1 facilitates a physical association of CD44 and EGF-R through a HA-dependent manner.

To determine whether this physical linkage changes with age the distribution of CD44 and EGF-R was subsequently assessed in patient matched young and aged fibroblasts by immunohistochemistry (Figure 5.17-5.21) and confocal microscopy (Figure 5.22-5.26). The results clearly demonstrate co-localisation of CD44 and EGF-R following TGF-β1 dependent phenotypic activation of young cells (Figure 5.18, 5.23 & 5.24) when compared to non-stimulated cells (Figure 5.17 & 5.22). In contrast aged co-localisation of CD44 and EGF-R was not apparent following TGF-β1 stimulation (Figure 5.20 & 5.25) and consistent with earlier data, both unstimulated aged (Figure 5.19 & 5.25) and stimulated aged (Figure 5.20 & 5.25) cell populations, stained poorly for EGF-R as assessed by confocal analysis. An overview of immunohistochemistry (5.21) and confocal (5.26) results are presented. These results suggested that age-dependent defect in TGF-β1-mediated phenotypic activation is associated with an age-dependent loss of EGF-R and subsequent CD44-EGF-R co-localisation.

The importance of HAS2 dependent HA in loss of phenotypic activation and CD44 relocalisation, was examined by TGF- β 1 stimulation of cells transiently transfected with HAS2 (Figure 5.27B) or EGF-R (Figure 5.27C) over-expression vectors either alone, or in combination (Figure 5.27D). Transfection with GFP was used as a mock control (Figure 5.27A). In these experiments the combination of EGF-R and HAS2 over-expression (but not independently) restored co-localisation of CD44 and EGF-R in aged cells.

Collectively these results suggest that TGF- β_1 promotes CD44 and EGF-R association whilst failure to do so in aged cells derives from age-related loss of EGF-R expression and HAS2 induction. A recent report indicates ERK1/2 phosphorylation is triggered by

CD44 interactions [284]. Previous data from this chapter has demonstrated that ERK signalling is EGF-R-dependent (Figure 5.10-11). To identify whether CD44-EGF-R interaction plays a role in signalling to ERK, young cells were treated with an anti-CD44 blocking antibody and ERK1/2 phosphorylation assessed (Figure 5.27E). Basal and TGF-β1 mediated ERK1/2 activation was inhibited by the anti-CD44 blocking antibody, this together with earlier data implies that ERK1/2 activation is downstream of HA dependent CD44- EGF-R association.

5.2.10 Involvement of calcium calmodulin-dependent kinase II

CD44 is known to be linked to various transmembrane and intracytoplasmic signalling pathways in addition to EGF-R [338]. Involvement of Calcium calmodulin-dependent kinase II (CaMKII), a serine/threonine protein kinase that phosphorylates diverse substrates including the cytoskeletal protein filamin, has been demonstrated to be a downstream target of HA-CD44 mediated signalling in head and neck carcinoma cells [206]. In order to examine a potential signalling function for HA-CD44 interactions in my cell system, fibroblasts were treated with or without TGF-\beta1 in the presence of either KN-93, a CaMKII inhibitor, KN-92 a suitable control or no treatment (control treatment). Immunofluorescence analysis of FITC-phalloidin-labelled demonstrated TGF-\$1 phenotypic activation by an increase in stress fibres (Figure 5.28B) and associated with this was up-regulation of a-SMA (Figure 5.28F). KN-93 prevented phenotypic activation, cells were smaller and retained their spindle cell appearance, had less stress fibres (Figure 5.28D), and did not up-regulated a-SMA (Figure 5.28H). KN-92 in contrast had no effect on phenotypic activation, stress fibre formation and a-SMA expression (Figure 5.8C &G).

5.2.11 Effect of disrupting the cytoskeleton on pericellular HA organisation

Having shown that interruption of the pathways that modulate cytoskeletal reorganisation abrogate phenotypic activation, I determined the direct role of the actin cytoskeleton in CD44-mediated pericellular HA assembly. Young dermal fibroblasts were treated with cytochalasin B prior to TGF-β1stimulation. Cytochalasin binds to the

(+) of actin filaments causing destabilization and depolymerisation of the actin network [334]. Although disruption of the cytoskeleton did not significantly alter surface CD44 expression (Figure 5.29B), it did significantly attenuate TGF-β1 mediated α-SMA induction (Figure 5.29A). Cells were processed for histology and HA pericellular matrix assembly (Figure 5.30). Analysis of TRITC-phalloidin-labelled cells demonstrated increased disruption of f-actin organisation associated with increasing concentrations of cytochalasin B (Figure 5.30 E-H). Destabilization of the actin network resulted in cell rounding, consistent with previous findings [334] and changes in pericellular HA formation. In control cells the HA coat was uniformly organised around the cell (Figure 5.30A). Ever increasing concentrations of cytochalasin B did not reduce the amount of pericellular HA as observed for 4MU and Hyal treatments in chapter 4, but rather, the retention of the HA was reduced and instead of a 'coat' a disorganised 'puddle' of HA was observed (Figure 5.30 B-D), similar to the effect of CD44 siRNA. These data indicate that regulation of fibroblast phenotype may depend on the close association of CD44 with the cytoskeleton. Disruption of the f-actin components of the cytoskeleton reduce the anchorage of pericellular HA indicating that cytoskeletal elements regulate CD44-HA binding. These data demonstrate that direct interaction of fibroblasts with their HA matrix is vital for maintenance of phenotype.

TGF-\(\beta\)1 is acting through EGF-R to induce myofibroblastic differentiation

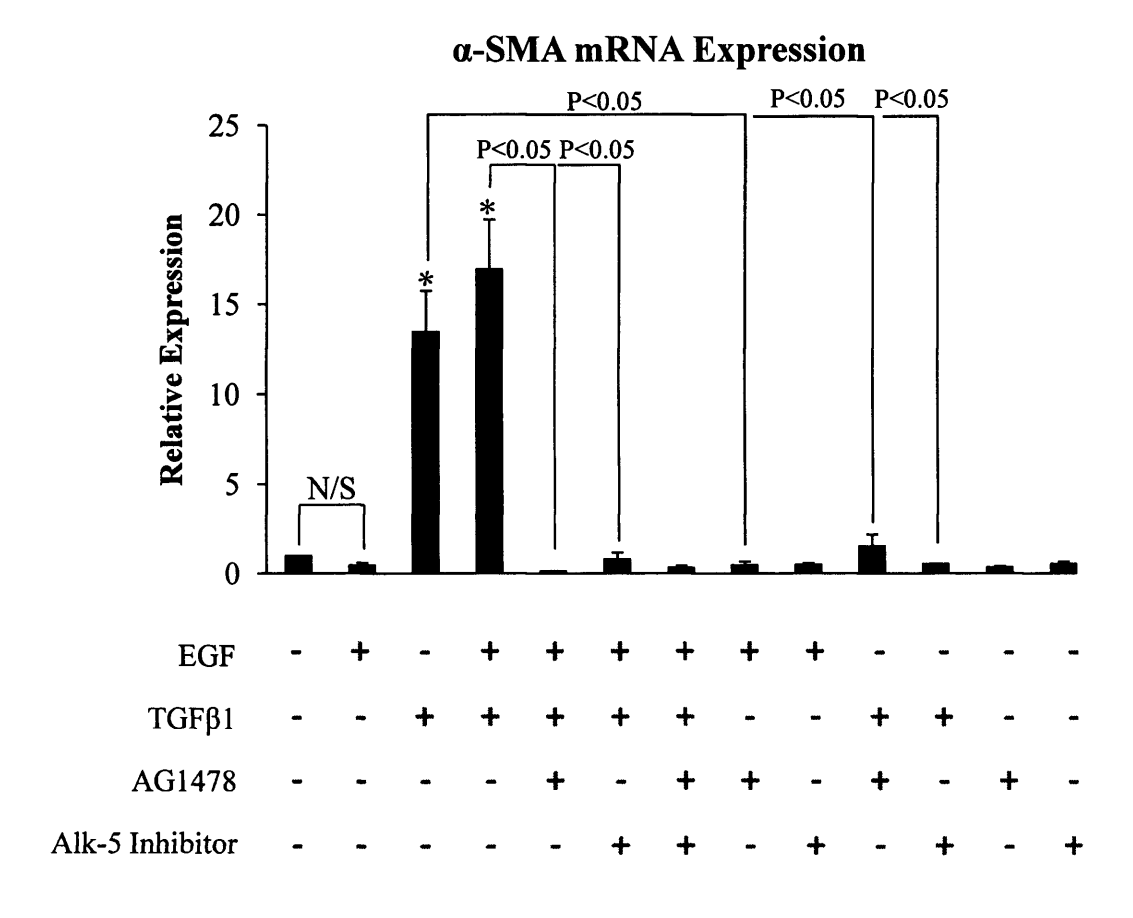


Figure 5.1 Involvement of EGF-R and ALK-5 in phenotypic conversion. Confluent monolayers of young dermal fibroblasts were growth arrested in serum-free medium for 48 hours. Cultures were then incubated in the presence of serum-free medium alone, serum-free medium containing 10ng/ml TGF- β 1, serum-free medium containing 10ng/ml EGF, or both, in combination with either the EGF-R inhibitor AG1478 (10 μ M) and/or the ALK5-specific inhibitor SB431542 (10 μ M) for a further 72 hours. Total mRNA was extracted and α -SMA expression assessed by RT-QPCR. Ribosomal RNA expression was used as an endogenous control and gene expression was assessed relative to cells that had received only serum-free medium alone. The comparative C_T method was used for relative quantification of gene expression and the results are represented as the mean± S.E. of six individual experiments using cells isolated from two different donors. Statistical analysis was performed by the Student's t test: *, p <0.05 as compared to no treatment (lane 1). N/S, not significant.

Aging dermal fibroblasts exhibit reduced EGF-R

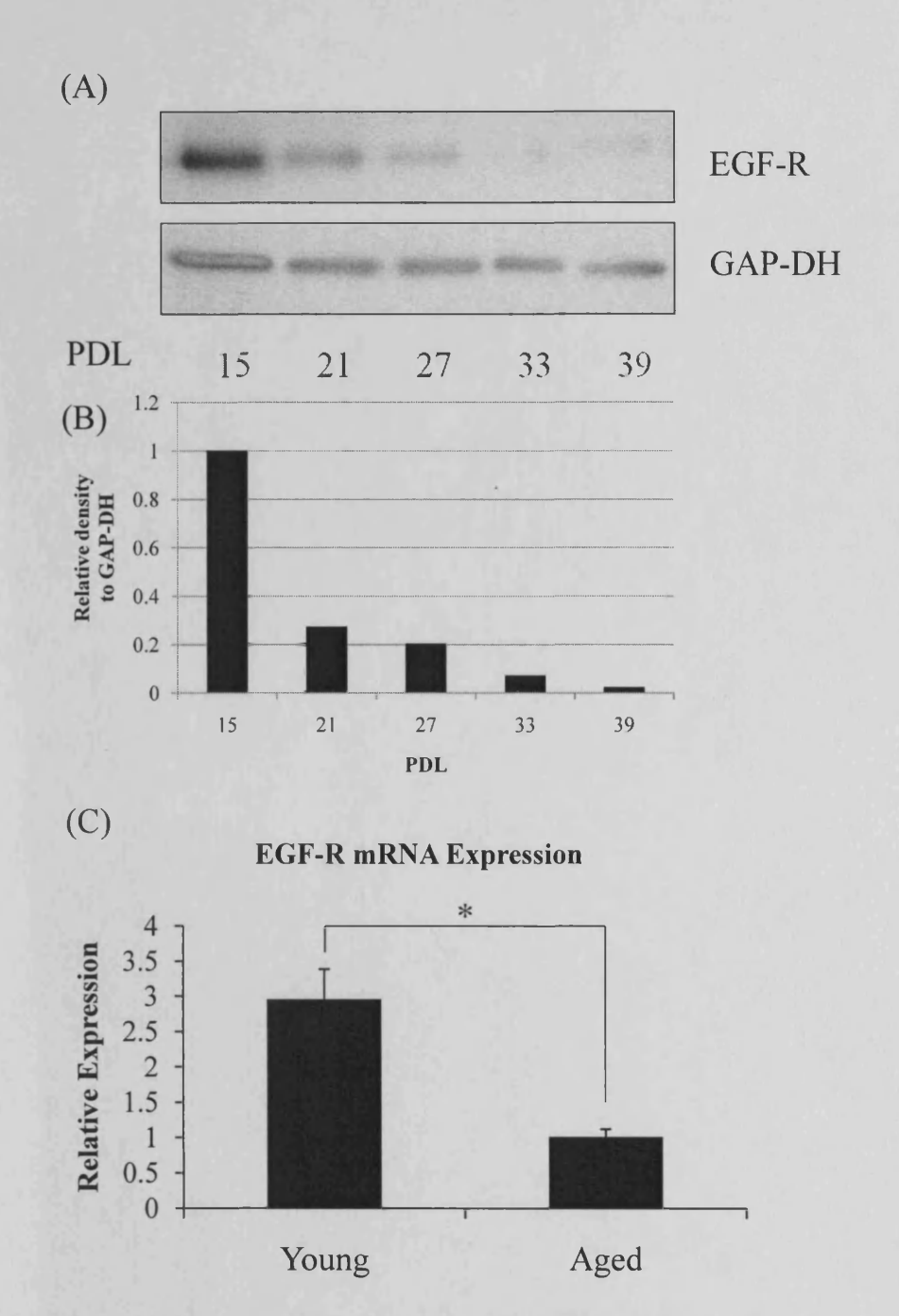
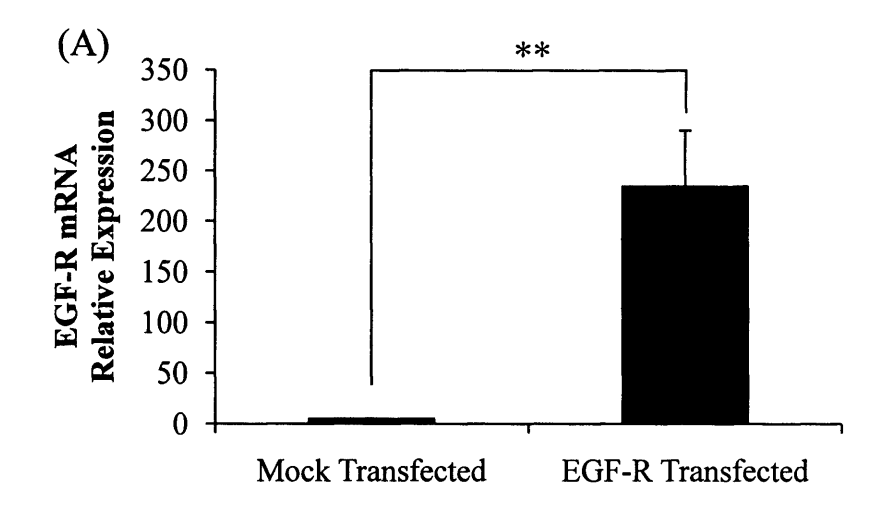
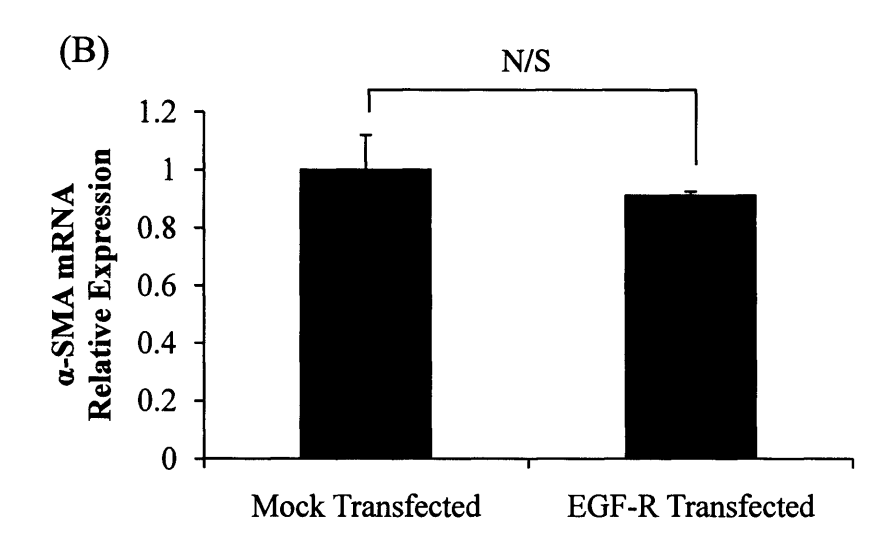


Figure 5.2 Effect of in-vitro aging on EGF-R. A, confluent monolayers of dermal fibroblasts at the indicated PDL's were growth arrested in serum-free medium for 48 hours. Cell protein was extracted, and cell lysates were subjected to Western blot analysis using antibodies against EGF-R as described in section 2.14. Expression of GAP-DH was analysed as a control to ensure equal loading. The results shown are representative of five independent experiments from the same patient donor. B, following scanning densitometry, alterations in EGF-R expression were corrected for the expression of GAP-DH. C, confluent monolayers of patient matched young, and invitro aged dermal fibroblasts were growth arrested in serum-free medium for 48 hours. Total mRNA was extracted and EGF-R mRNA expression was assessed by RT-QPCR. Ribosomal RNA expression was used as an endogenous control and gene expression was assessed relative to control aged cells. The comparative C_T method was used for relative quantification of gene expression and the results are represented as the mean± S.E. of six individual experiments using cells isolated from two different donors. Statistical analysis was performed by the Student's t test: *, p <0.05.

Over-expression of EGF-R





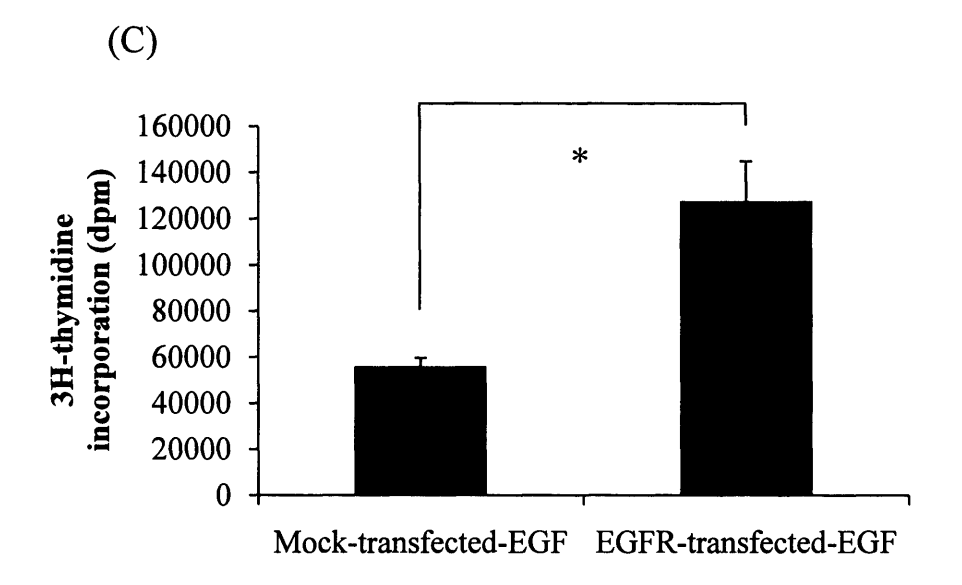


Figure 5.3 Over-expression of EGF-R in aged dermal fibroblasts. Aged dermal fibroblasts were transfected with either EGF-R-pCR3.1 (EGF-R transfected) or GFP (Mock transfected) using nucleofector technology as described in section 2.9. 48 h after transfection, cells were incubated in serum-free medium containing 10 ng/ml TGF- $\beta 1$ for 72 hours. Total mRNA was extracted and EGF-R (A) and α -SMA (B) mRNA expression was assessed by RT-QPCR. Ribosomal RNA expression was used as an endogenous control and gene expression was assessed relative to mock transfected. The comparative C_T method was used for relative quantification of gene expression and the results are represented as the mean± S.E. of nine individual experiments using cells isolated from three different donors. Statistical analysis was performed by the Student's t test: **p<0.01, N/S Not significant. C, EGF induced proliferation was determined by incorporation of $[^3H]$ Thymidine. Expression plasmids for EGF-R or GFP (mock) were introduced into aged fibroblasts using nucleofector technology prior to metabolic labelling, performed by incubation with $1\mu\text{Ci/ml}$ D- $[^3H]$ Thymidine following addition of serum-free medium containing 10 ng/ml EGF for 24 hours. Data are the mean ± S.E. from six individual experiments, using cells isolated from two different donors. Statistical analysis was performed by the Student's t test: *, p<0.05.

EGF expression and combinatory effects of EGF and TGF-\$\beta\$1 in EGF-R transfected aged cells

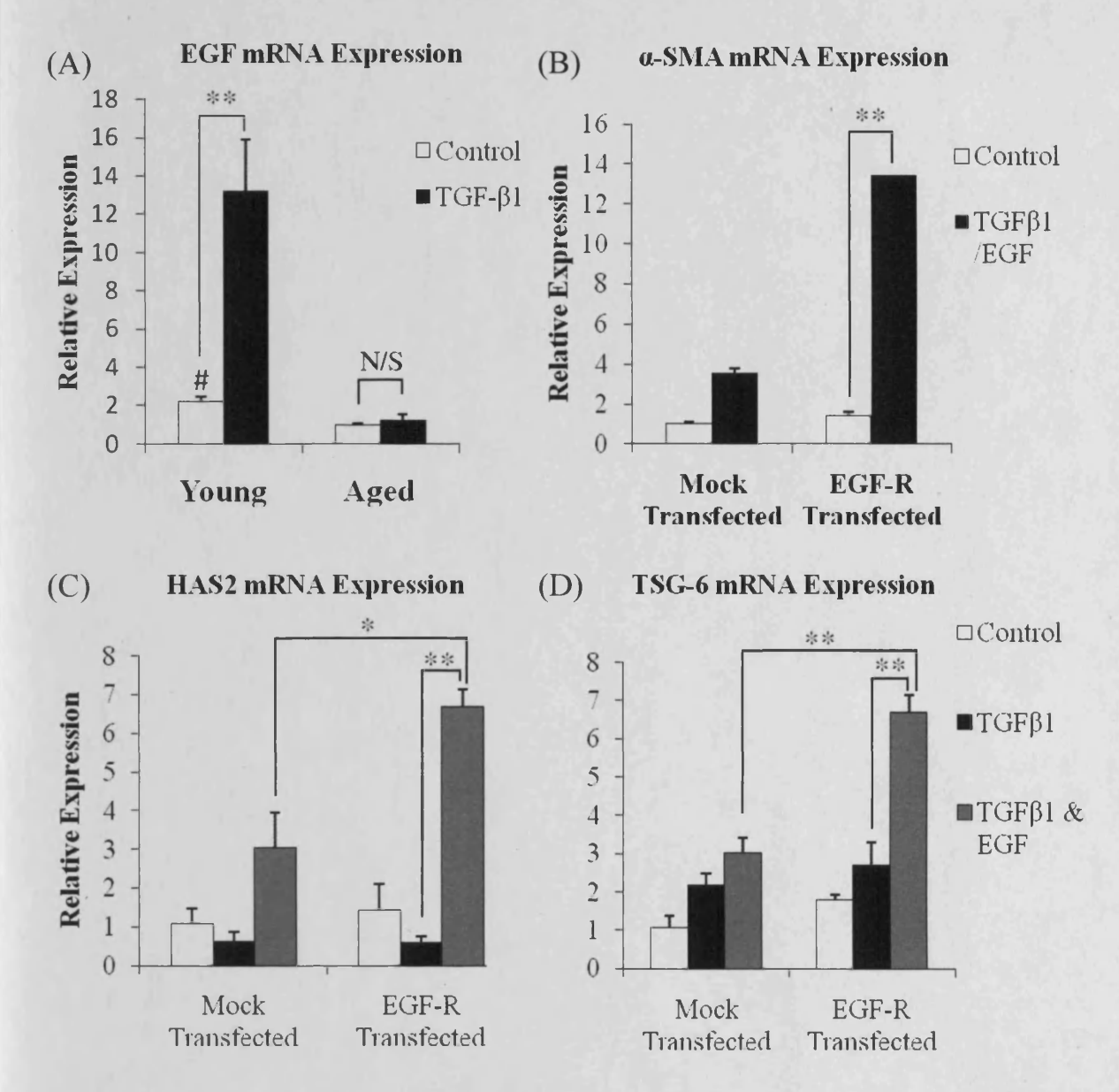


Figure 5.4 Effect of in-vitro aging on EGF expression (A), synergistic effects of TGF-Bl and EGF in EGF-R over-expressed aged cells (B-D) A, confluent monolayers of patient matched young and aged dermal fibroblasts were growth-arrested in serum-free medium for 48 hours, prior to addition of either serum-free medium alone (clear bars) or serum-free medium containing 10ng/ml TGF-β1 (black bars) for 72 hours. Total mRNA was extracted and EGF expression assessed by RT-QPCR. B, aged dermal fibroblasts were transfected either with EGF-R-pCR3.1 (EGF-R transfected) or GFP (mock transfected) using nucleofector technology as described in section 2.9. 48 h after transfection, cells were incubated in either serum-free medium alone (clear bars) or serum-free medium containing 10ng/ml TGF-β1 in combination with 10ng/ml EGF (black bars) for 72 hours and α-SMA expression assessed by RT-QPCR. C-D, aged dermal fibroblasts were transfected either with EGF-R-pCR3.1 (EGF-R transfected) or GFP (mock transfected) using nucleofector technology. 48 hours after transfection, cells were incubated in either serum-free medium alone (clear bars), serum-free medium containing 10ng/ml TGF-\(\beta\)1(black bars) or serum-free medium containing TGF-\(\beta\)1(10ng/ml) in combination with EGF (10ng/ml) (grey bars) for 72 hours. TSG-6 (C) and HAS2 (D) mRNA expression was assessed by RT-QPCR. In all experiments ribosomal RNA expression was used as an endogenous control and gene expression was assessed relative to aged control (A) or mock transfected control (B,C,D). comparative C_T method was used for relative quantification of gene expression and the results are represented as the mean± S.E. of nine individual experiments using cells isolated from three different donors. Statistical analysis was performed by the Student's t test: #p<0.05, as compared to aged cells, *p<0.05, **p<0.01, N/S, not significant.

Neutralisation of EGF diminishes TGF-\$1-induced phenotypic activation

α-SMA mRNA Expression

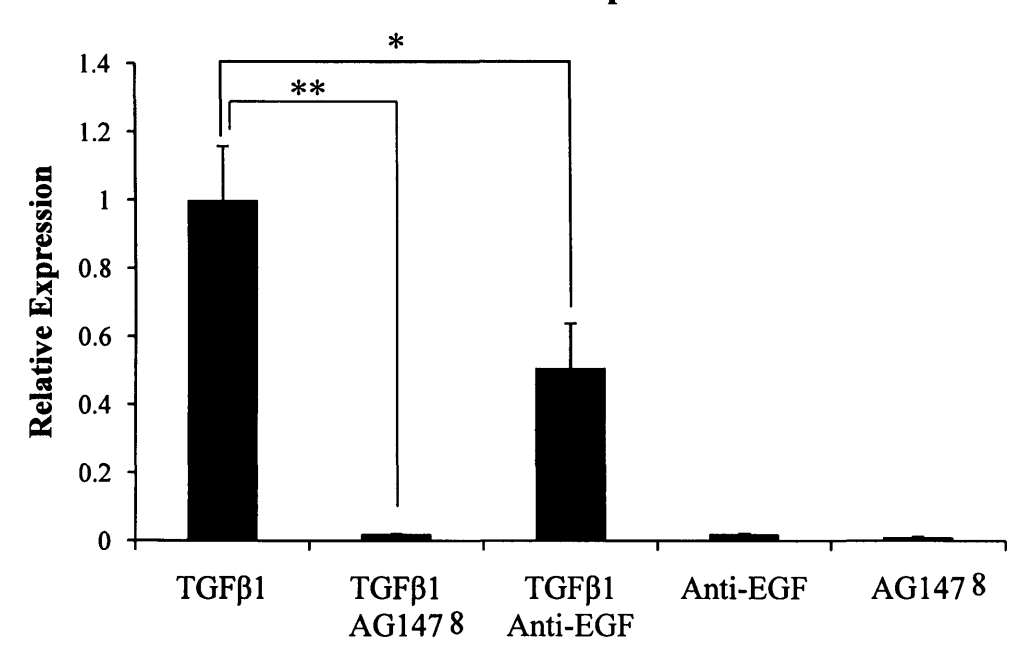


Figure 5.5 Effect of EGF inhibition on phenotypic activation. Confluent monolayers of young dermal fibroblasts were growth arrested in serum-free medium for 48 hours. The medium was replaced with serum-free medium containing TGF-β1(10ng/ml) alone or in combination with either the EGF-R inhibitor AG1478 (10μM) or anti-EGF antibody (10μg/ml) for 72 hours and α-SMA expression assessed by RT-QPCR. Ribosomal RNA expression was used as an endogenous control and gene expression was assessed relative to TGF-β1alone stimulated cells. The comparative C_T method was used for relative quantification of gene expression and the results are represented as the mean± S.E. of six individual experiments using cells isolated from two different donors. Statistical analysis was performed by the Student's t test: *, p <0.05, **, p<0.01.

TGF-\(\beta\)1-mediates HAS2 induction through EGF-R

HAS2 mRNA Expression

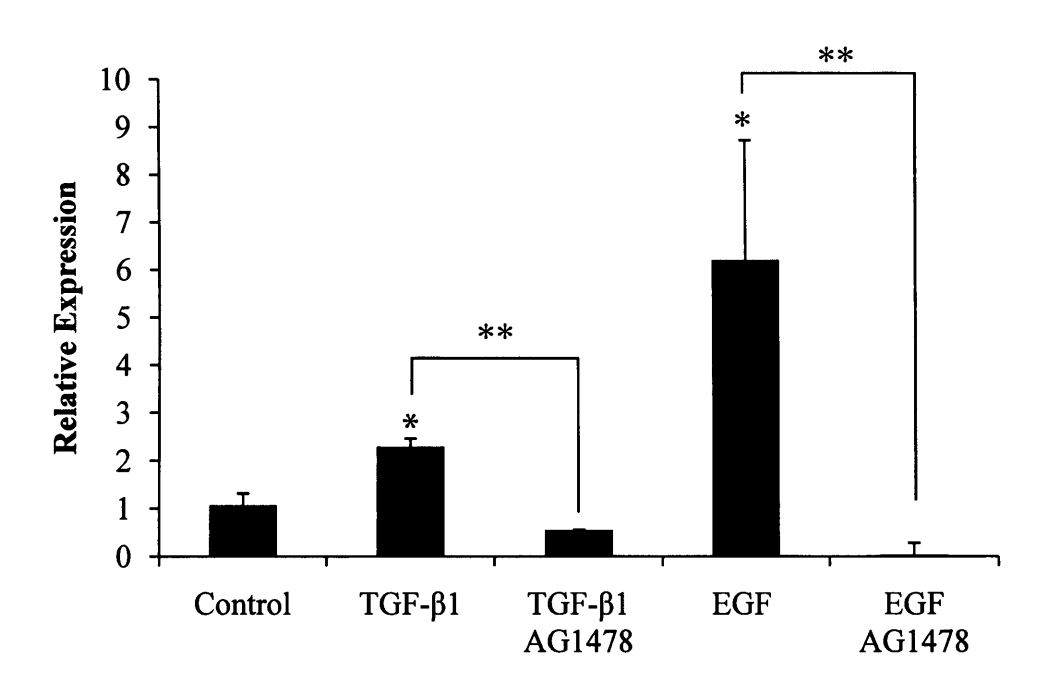
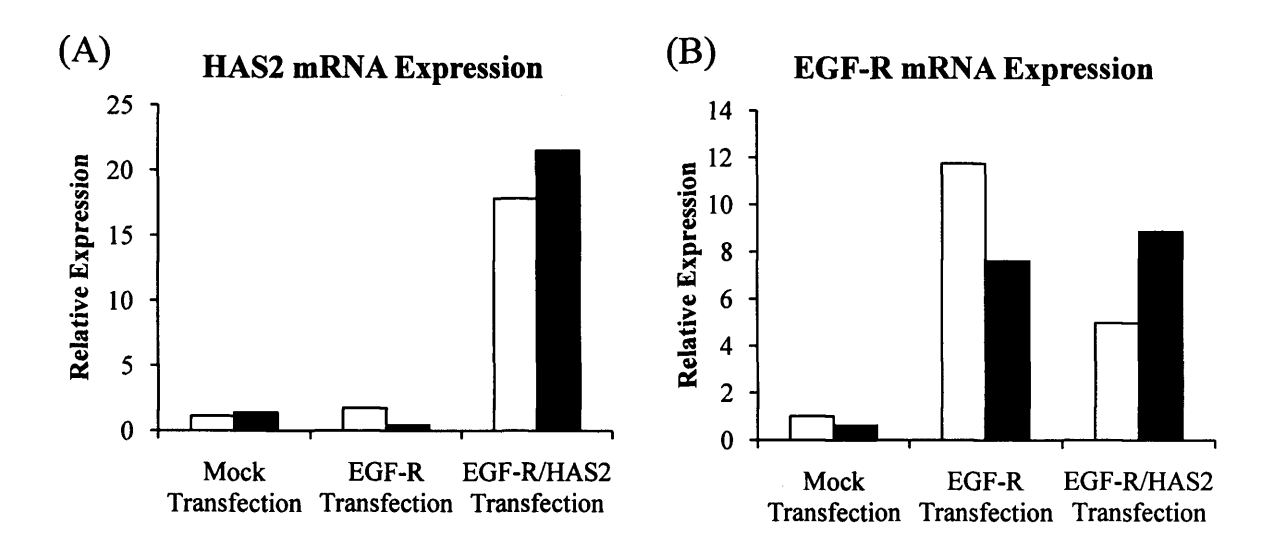


Figure 5.6 Involvement of EGF-R in TGF- β_1 dependent HAS2 induction. Confluent monolayers of young dermal fibroblasts were growth-arrested in serum-free medium for 48 hours, prior to addition of either serum-free medium alone (control), or serum-free medium containing either TGF- $\beta_1(10ng/ml)$ or EGF (10ng/ml) in isolation or in combination with the EGF-R inhibitor AG1478 (10 μ M) for 72 hours. Total mRNA was extracted and HAS2 expression assessed by RT-QPCR. Ribosomal RNA expression was used as an endogenous control and gene expression was assessed relative to TGF- β_1 alone stimulated cells. The comparative C_T method was used for relative quantification of gene expression and the results are represented as the mean± S.E. of six individual experiments using cells isolated from two different donors. Statistical analysis was performed by the Student's t test: *, p<0.05, as compared to control. **, p<0.01.

EGF-R and HAS2 over-expression in aged cells



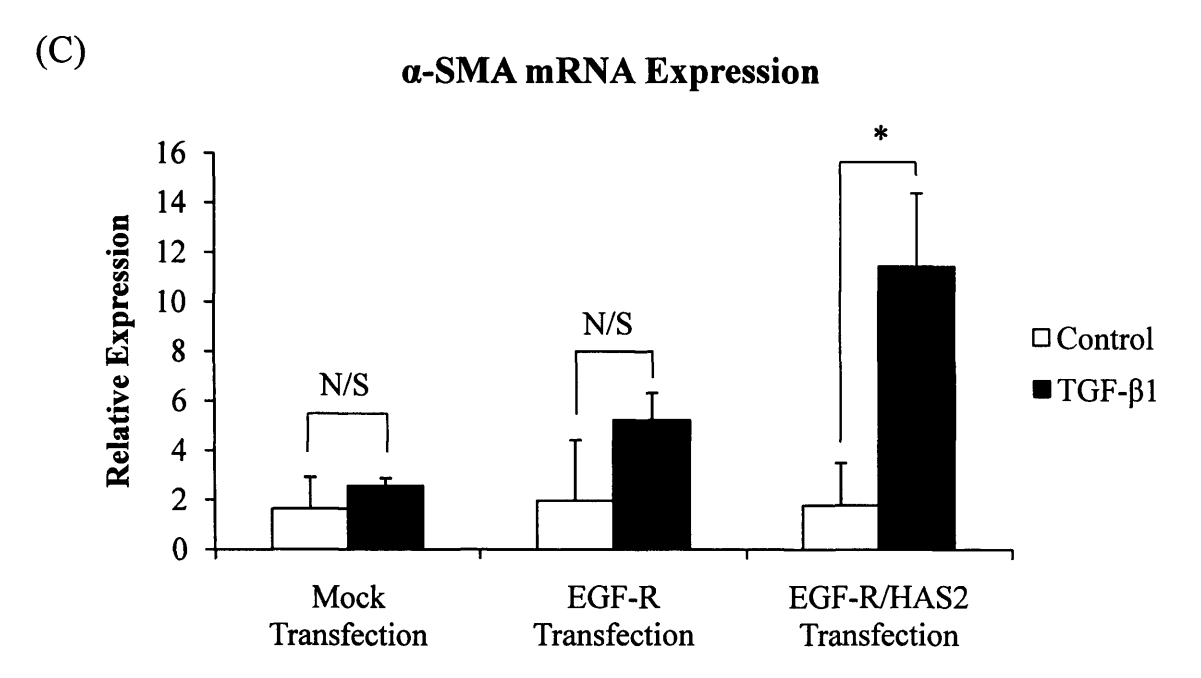
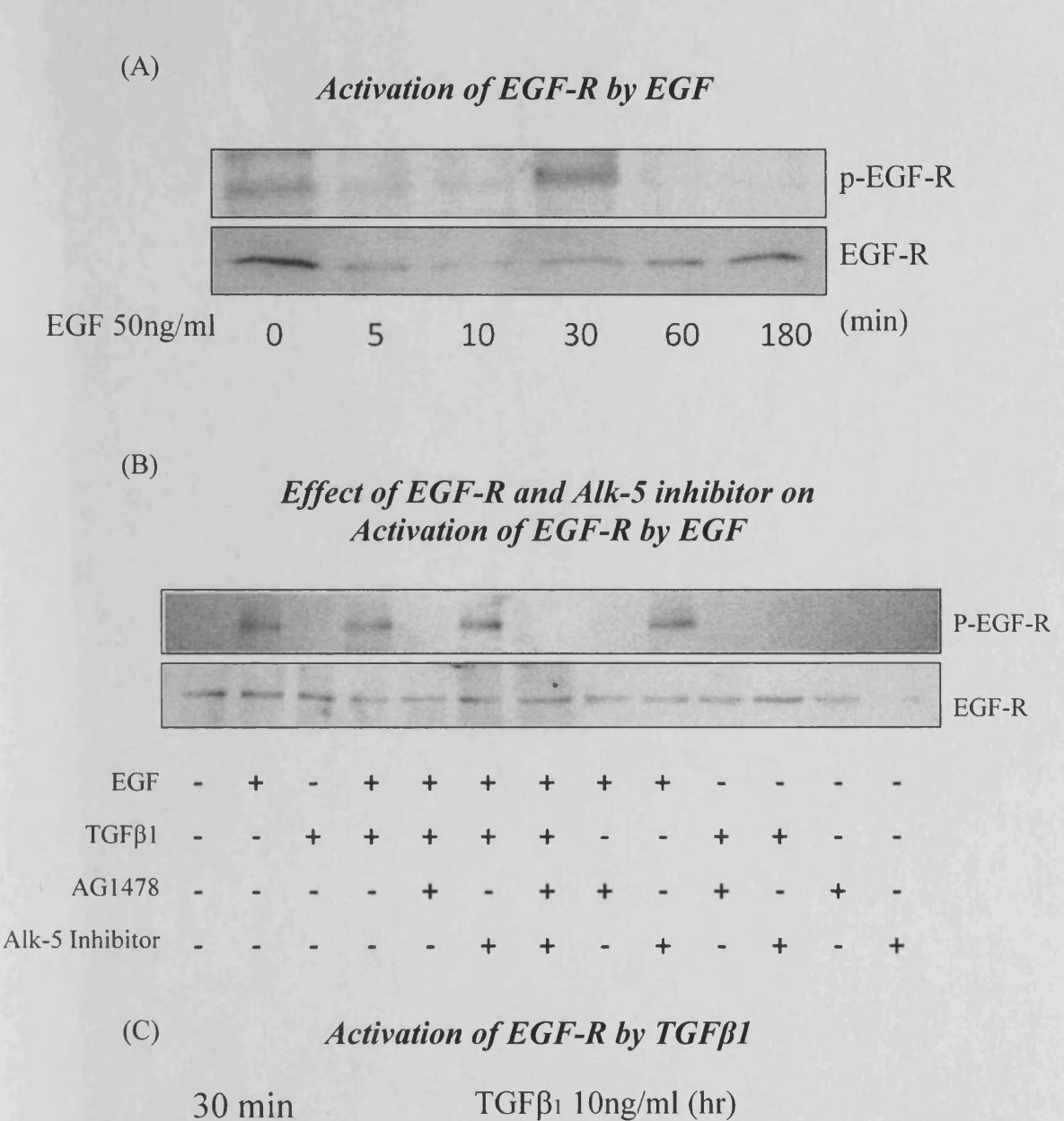


Figure 5.7 Combinatory effects of EGF-R and HAS2 over-expression in aged cells. Aged dermal fibroblasts were transfected either with EGF-R-pCR3.1 alone (EGF-R transfected) or in combination with HAS2-pCR3.1 (EGF-R/HAS2 transfected) or GFP (mock transfected) using nucleofector technology as described in section 2.9. 48 hours after transfection, cells were incubated in either serum-free medium alone (clear bars), or serum-free medium containing 10ng/ml TGF-β1 (black bars) for 72 hours and HAS2 (A), EGF-R (B) and α-SMA (C) mRNA expression assessed by RT-QPCR. Ribosomal RNA expression was used as an endogenous control and gene expression was assessed relative to control mock transfected cells. The comparative C_T method was used for relative quantification of gene expression and the results are represented as the mean± S.E. of six individual experiments using cells isolated from two different donors. Statistical analysis was performed by the Student's t test: *, p <0.05. N/S, not significant.



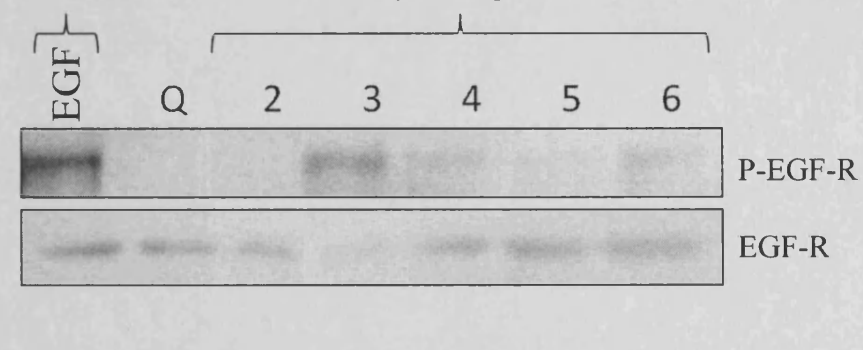
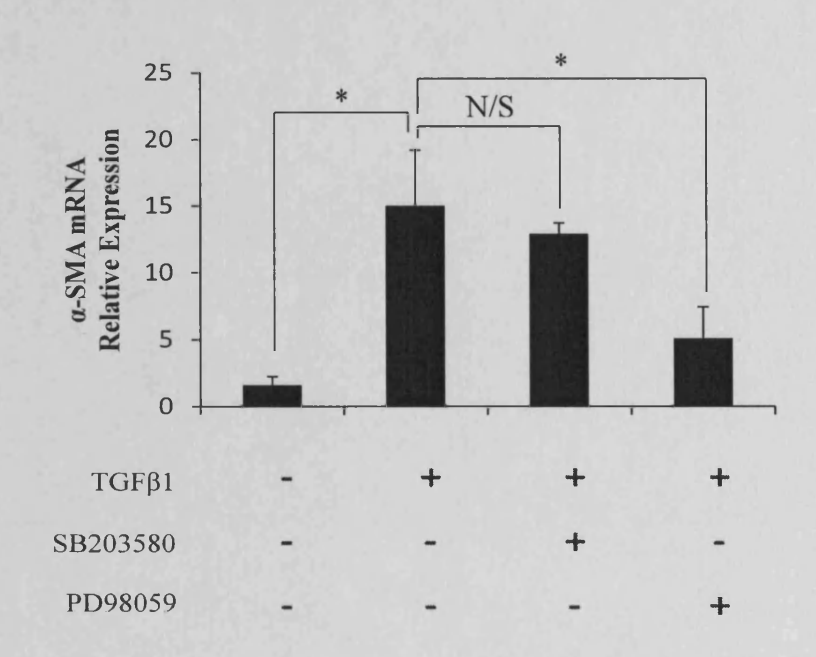
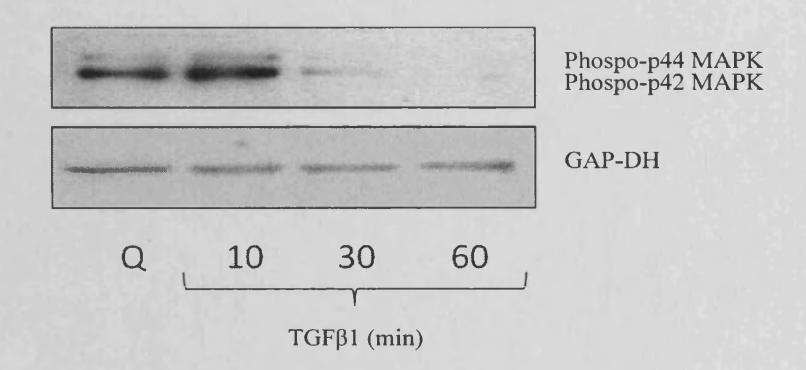


Figure 5.8 EGF-R activation. A, growth arrested confluent monolayers of young dermal fibroblasts were stimulated with EGF (10ng/ml) for the indicated times and were analysed by western blot with antibodies for the phosphorylated form of EGF-R. B, growth arrested confluent monolayers of young dermal fibroblasts were stimulated with either serum free medium alone or containing EGF (10ng/ml) and TGF- β 1 (10ng/ml) in isolation or in combination with or without either the EGF-R inhibitor AG1478 (10 μ M) or the ALK-5 inhibitor SB431542 (10 μ M). Stimulations lasted 30 minutes after which cell lysates were analysed by western blot with antibodies for the phosphorylated form of EGF-R as describe under section 2.14. TGF- β 1 did not alter pEGF-R levels at 30 minutes (B) but did increase EGF-R activation at a later time point (3-4 h) (C). All blots were normalised to antibodies for total EGF-R.

(A) ERK signalling is involved in phenotypic activation



(B) ERK1/2 activation by TGF-β1



(C) Phosphorylation of Erk1/2 by TGFβ1 Diminishes With Age

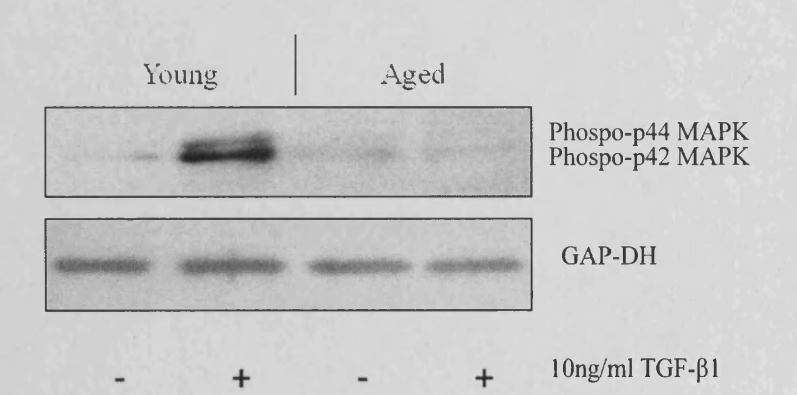


Figure 5.9 The role of ERK in phenotypic conversion (A), $TGF-\beta_1$ dependent activation of ERK signalling (B) and the effects of in-vitro ageing (C). A, confluent monolayers of young dermal fibroblasts were growth-arrested in serum-free medium for 48 hours, prior to addition of either serum-free medium alone or serum-free medium containing 10ng/ml TGF-β1in isolation or in combination with the p38 inhibitor SB203580 (10μM) or the ERK inhibitor PD98059 (10 μ M) for 72 hours. Total mRNA was extracted and α -SMA mRNA expression assessed by RT-QPCR. Ribosomal RNA expression was used as an endogenous control and gene expression was assessed relative to untreated cells. The comparative C_T method was used for relative quantification of gene expression and the results are represented as the mean± S.E. of six individual experiments using cells isolated from two different donors. Statistical analysis was performed by the Student's t test: *, p <0.05, N/S not significant. B, growth arrested confluent monolayers of young dermal fibroblasts (Q) were incubated with 10ng/ml TGF-\beta1 for up to 60 minutes and phosphorylation of ERK1/2 proteins assessed by western analysis at the time points indicated as describe under section 2.14. C, 10ng/ml TGF-β1in serum free medium, was added to confluent growth arrested confluent monolayers of patient matched young, and in-vitro aged dermal fibroblasts for 10 minutes. Cell lysates were prepared for western blot with antibodies for the phosphorylated form of ERK1/2. All blots were normalised to antibodies for GAP-DH.

Synergistic Efffect of EGF and TGFβ₁ on ERK activation is abolished by EGF-R blocker AG1478



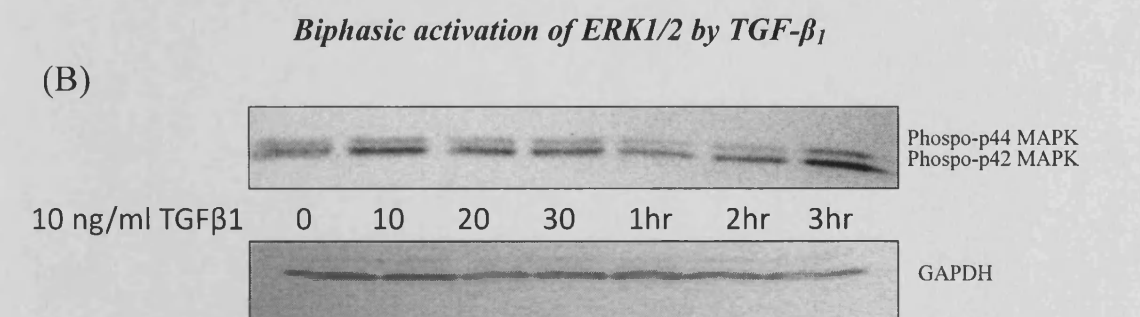


Figure 5.10 Phosphorylation of ERK1/2 coincides with phosphorylation of EGF-R (A), and displays a an early and late response to TGF- β_1 (B). A, growth arrested confluent monolayers of young dermal fibroblasts were stimulated with either serum free medium alone or containing EGF (10ng/ml) and TGF β 1 (10ng/ml) in isolation or in combination with or without either the EGF-R inhibitor AG1478 (10 μ M) or ALK-5 inhibitor SB431542 (10 μ M). Lysates were analysed by western blot with antibodies for the phosphorylated form of EGF-R and the phosphorylated form of ERK1/2 as describe under section 2.14. Stimulations lasted 30 minutes for p-EGF-R and 10 minutes for p-ERK1/2. B, growth arrested confluent monolayers of young dermal fibroblasts were incubated with 10ng/ml TGF- β 1 for up to 3hrs and phosphorylation of ERK1/2 proteins assessed by western analysis at the time points indicated as describe under section 2.14. Blots were normalised to antibodies for total EGF-R (A) and GAP-DH (B).

ERK1/2 phosphorylation is mediated by HA and EGF signalling

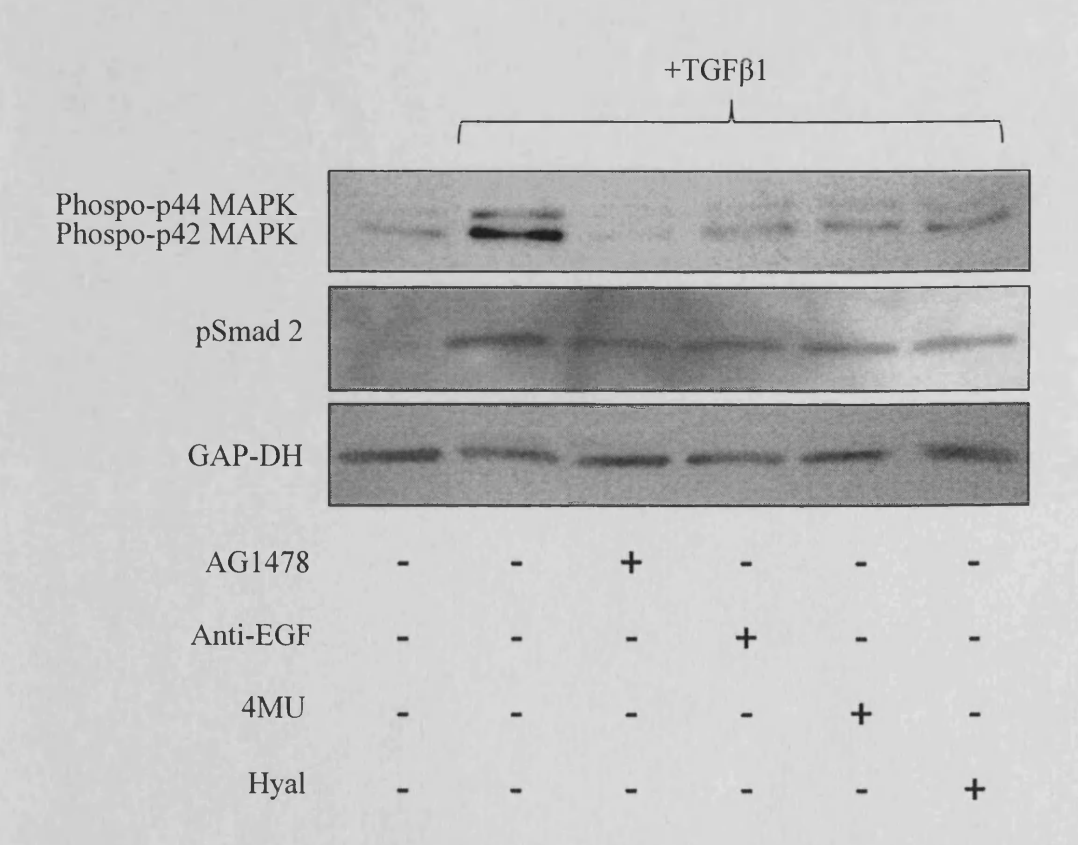


Figure 5.11 The involvement of HA and EGF signalling during ERK activation. The involvement of EGF and HA in activation of ERK1/2 phosphorylation and Smad 2 phosphorylation was analysed by Western blot as describe under section 2.14. Confluent monolayers of growth arrested young dermal fibroblasts were pre-treated with either 10μ M EGF-R inhibitor AG1478 (lane3), 10μ g anti-EGF antibody (lane 4), 0.5mM 4MU (lane5) or 200μ g/ml hyaluronidase (Hyal) (lane6) for 30 minutes prior to a further 10 min incubation with 10ng/ml TGF- β 1. Control cells received serum-free medium alone (lane1). Blots were normalised to antibodies for GAP-DH.

CD44 is required for TGF-\beta1-mediated phenotypic activation

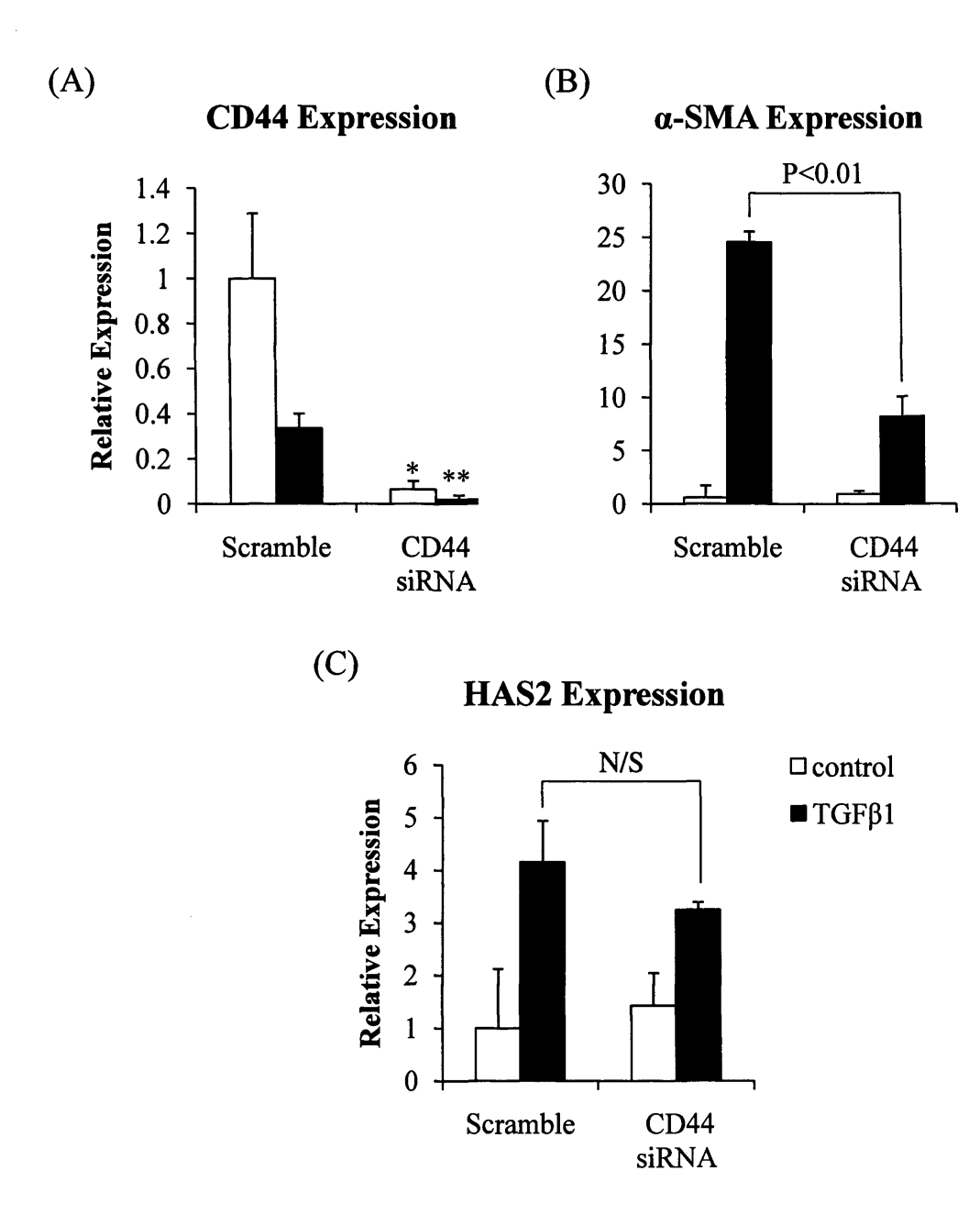


Figure 5.12 Effect of CD44 gene silencing on TGF- β_1 dependent phenotypic activation. Confluent monolayers of young dermal fibroblasts were transfected with CD44 siRNA or scramble oligonecleotide control (scramble) for 48 hours prior to addition of serum-free medium alone (clear bars) or serum-free medium containing 10 ng/ml TGF- β_1 (black bars) for a further 72 hours, and CD44 (A), α -SMA (B) or HAS2 (C) expression assessed by RT-QPCR. Ribosomal RNA expression was used as an endogenous control and gene expression was assessed relative to scramble control-scrambled samples. The comparative C_T method was used for relative quantification of gene expression and the results are represented as the mean± S.E. of six individual experiments using cells isolated from two different donors. Statistical analysis was performed by the Student's t test: *, p <0.05, **, p<0.01as compared to scramble. N/S, not significant.

Effect of CD44 siRNA on α-SMA expression and HA pericellular coat formation

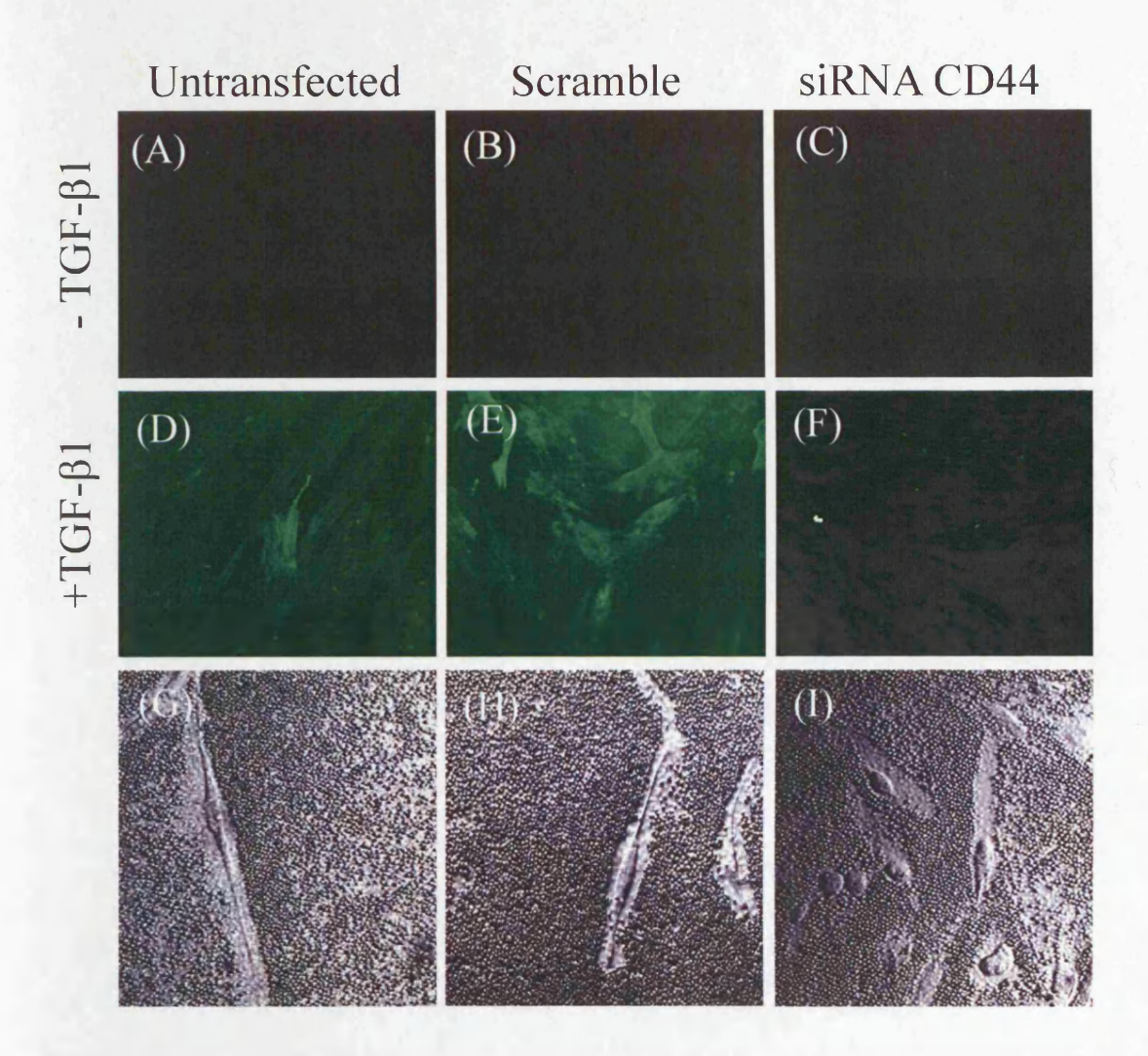


Figure 5.13 Effect of CD44 silencing on α -SMA incorporation and assembly of pericellular HA. Immunohistochemical analysis was performed to assess dermal fibroblast phenotype in un-transfected cells (A,D,G) or cells transfected with either scramble oligonecleotide control (scramble) (B,E,H) or CD44 siRNA (C.F,I) prior to addition of serumfree medium alone (A-C) or in combination with 10ng/ml TGF- β 1(D-I) for a further 72 hours. A-F, cells were fixed and stained for α -SMA, mounted in Vectashield fluorescent mountant, and viewed under UV light as describe under section 2.14. Original magnification was x 100. G-I, Formalised horse erythrocytes were added as described under section 2.11 to visualise the HA pericellular coat. Arrowheads indicate the cell body; Arrows show the extent of the pericellular matrix. Representative of dermal fibroblasts from three patient donors. Original magnification x 200.

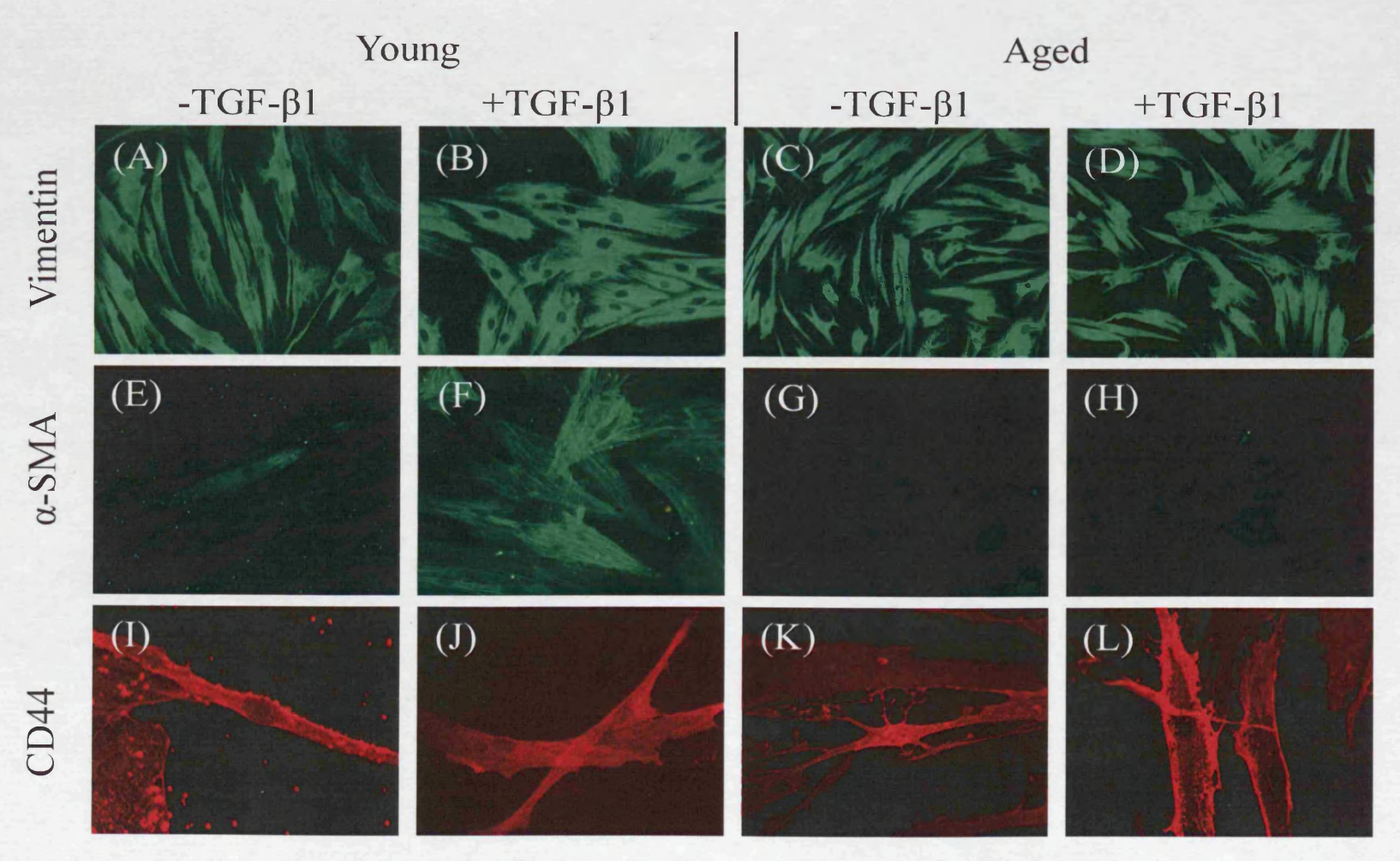


Figure 5.14 Overview of relationship between CD44 expression and phenotypic activation. 70% confluent monolayers of patient matched young (A,B,E,F,I,J) and aged (C,D,G,H,K,L) dermal fibroblasts were growth-arrested in serum-free medium for 48 hours, prior to addition of either serum-free medium alone (A,C,E,G,I,K) or serum-free medium containing 10ng/ml TGF-β1(B,D,F,H,J,L). The cells were fixed and stained for vimentin (A-D), α-SMA (E-H) or CD44 (I-L) as describe under section 2.4. Cells were mounted in Vectashield fluorescent mountant, and viewed under UV light. Representative images of 3 individual experiments using cells isolated from three different donors are shown. Original magnification was x 100.

CD44 expression does not change with age

CD44 mRNA Expression

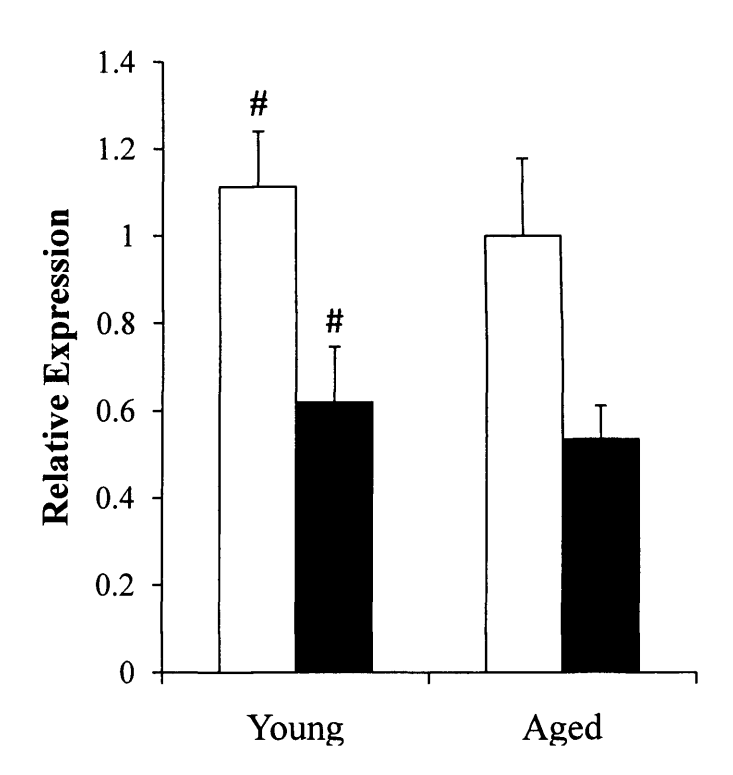


Figure 5.15 Effect of age on CD44 mRNA expression. Monolayers of patient matched young and in-vitro aged dermal fibroblasts were growth-arrested in serum-free medium for 48 hours, prior to addition of either serum-free medium alone (clear bars) or serum-free medium containing 10 ng/ml TGF- β (black bars). Total mRNA was extracted and CD44 expression assessed by RT-QPCR. Ribosomal RNA expression was used as an endogenous control and gene expression was assessed relative to aged control cells. The comparative C_T method was used for relative quantification of gene expression and the results are represented as the mean \pm S.E. of nine individual experiments using cells isolated from three different donors. Statistical analysis was performed by the Student's t test: # not significant as compared to aged cells.

Co-localisation of CD44/EGF-R is dependent on HA

IP: Anti-CD44

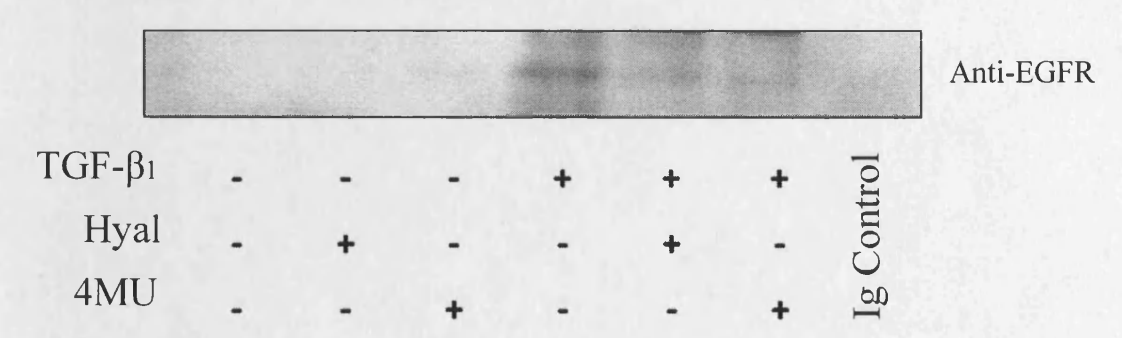


Figure 5.16 Co-localization of CD44 and EGF-R and impact of HA disruption. Western blot analysis of the association of CD44 and EFGR receptors. Cell protein was extracted from confluent monolayers of serum deprived young dermal fibroblasts exposed to either serum-free medium alone (lane1) serum-free medium containing 10 ng/ml TGF-β1 in isolation (lane 4) or in combination with hyaluronidase (Hyal) (200 μg/ml) (lane5) or 4MU (0.5mM) (lane 6) for 3 hr. Subsequently samples were immunoprecipitated (IP) with anti-CD44 antibody, followed by immunoblotting with anti-EGF-R antibody as describe under section 2.15. Specificity of immunoprecipitation was confirmed by negative control reactions performed with IgG control (lane 5) and lane 2 and lane 3 received Hyal and 4MU alone, respectively.

CD44/EGF-R co-localisation in young resting fibroblasts

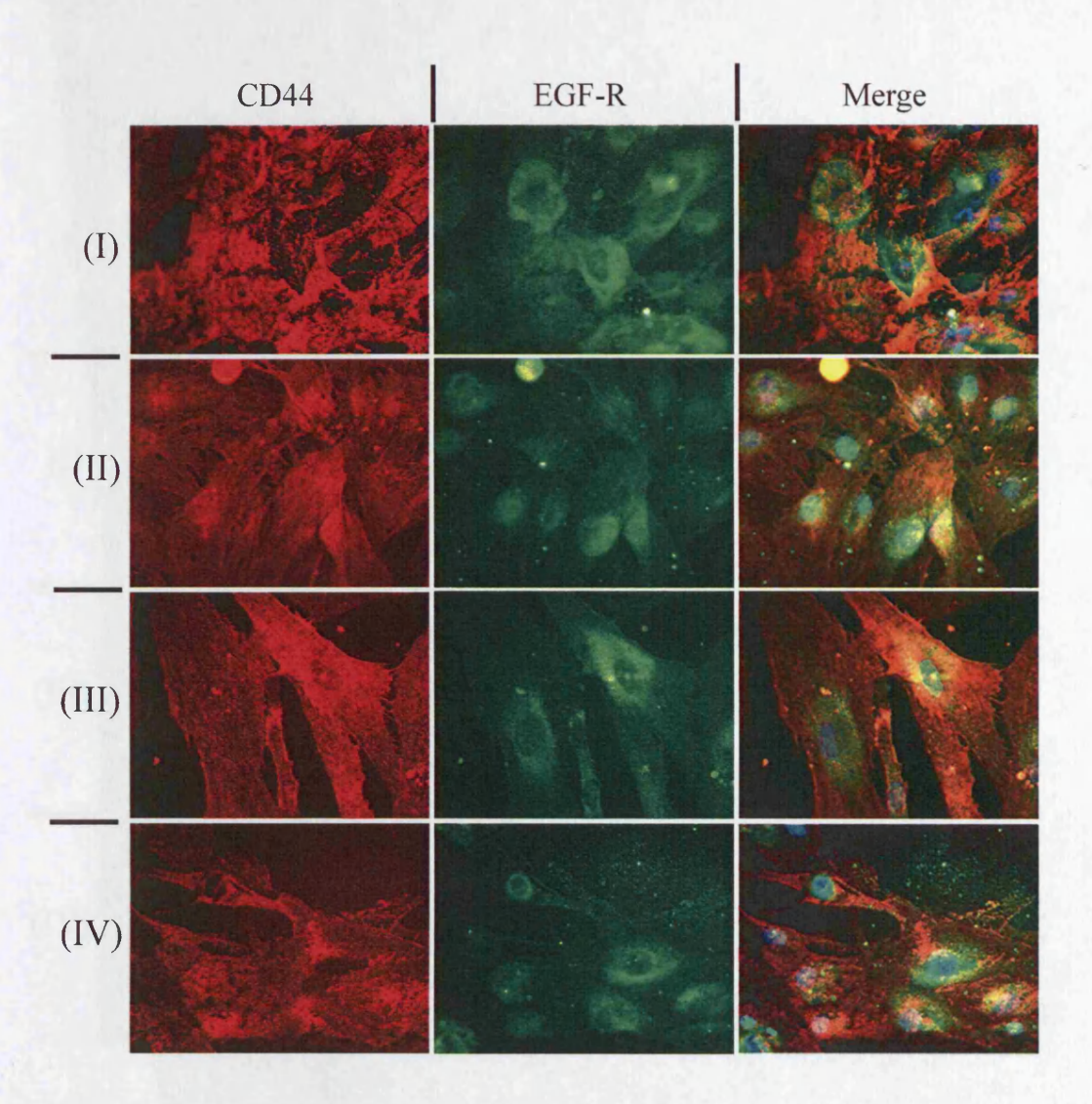


Figure 5.17 Immunocytochemical localisation of CD44 and EGF-R in young resting fibroblasts. 70% confluent monolayers of young dermal fibroblasts were growth-arrested in serum-free medium for 48 hours, prior to addition of serum-free medium for 24h. Cells were fixed and the expression of CD44 (red) and EGF-R (green) were examined by immunocytochemistry and their association examined by merging of individual images (yellow). In merged images DAPI was used to visualise the nuclei (blue). Representative images of 12 individual experiments using cells isolated from four different donors (I-IV) are shown. Original magnification was x 100.

CD44/EGF-R co-localisation in young fibroblasts after TGF-\(\beta\)1 stimulation

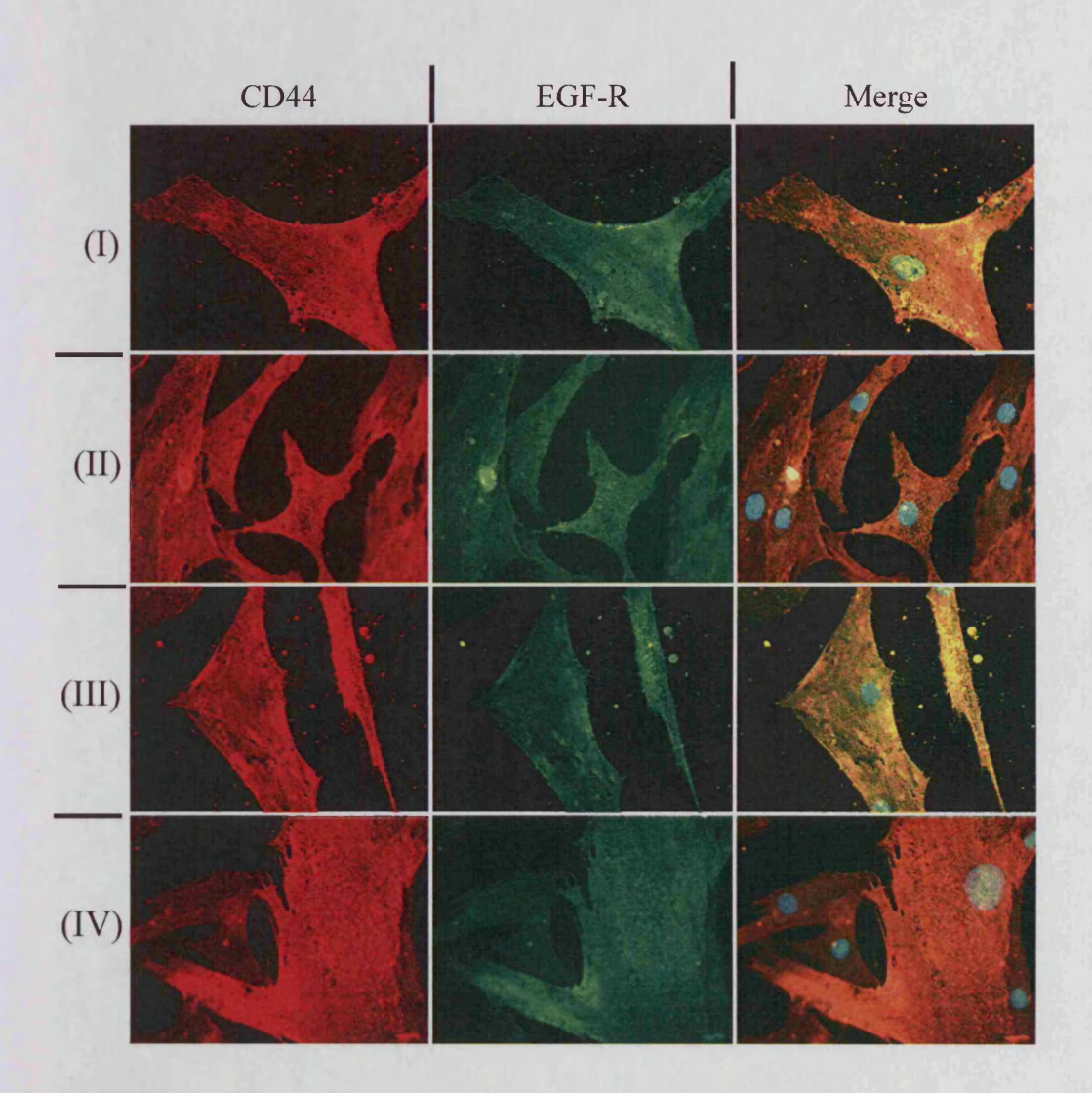


Figure 5.18 Immunocytochemical localisation of CD44 and EGF-R in young fibroblasts stimulated with TGF- β 1. 70% confluent monolayers of young dermal fibroblasts were growth-arrested in serum-free medium for 48 hours, prior to addition of serum-free medium containing 10ng/ml TGF- β 1 for 24h. Cells were fixed and the expression of CD44 (red) and EGF-R (green) were examined by immunocytochemistry and their association examined by merging of individual images (vellow). In merged images DAPI was used to visualise the nuclei (blue). Representative images of 12 individual experiments using cells isolated from four different donors (I-IV) are shown. Original magnification was x 100.

CD44/EGF-R co-localisation in aged resting fibroblasts

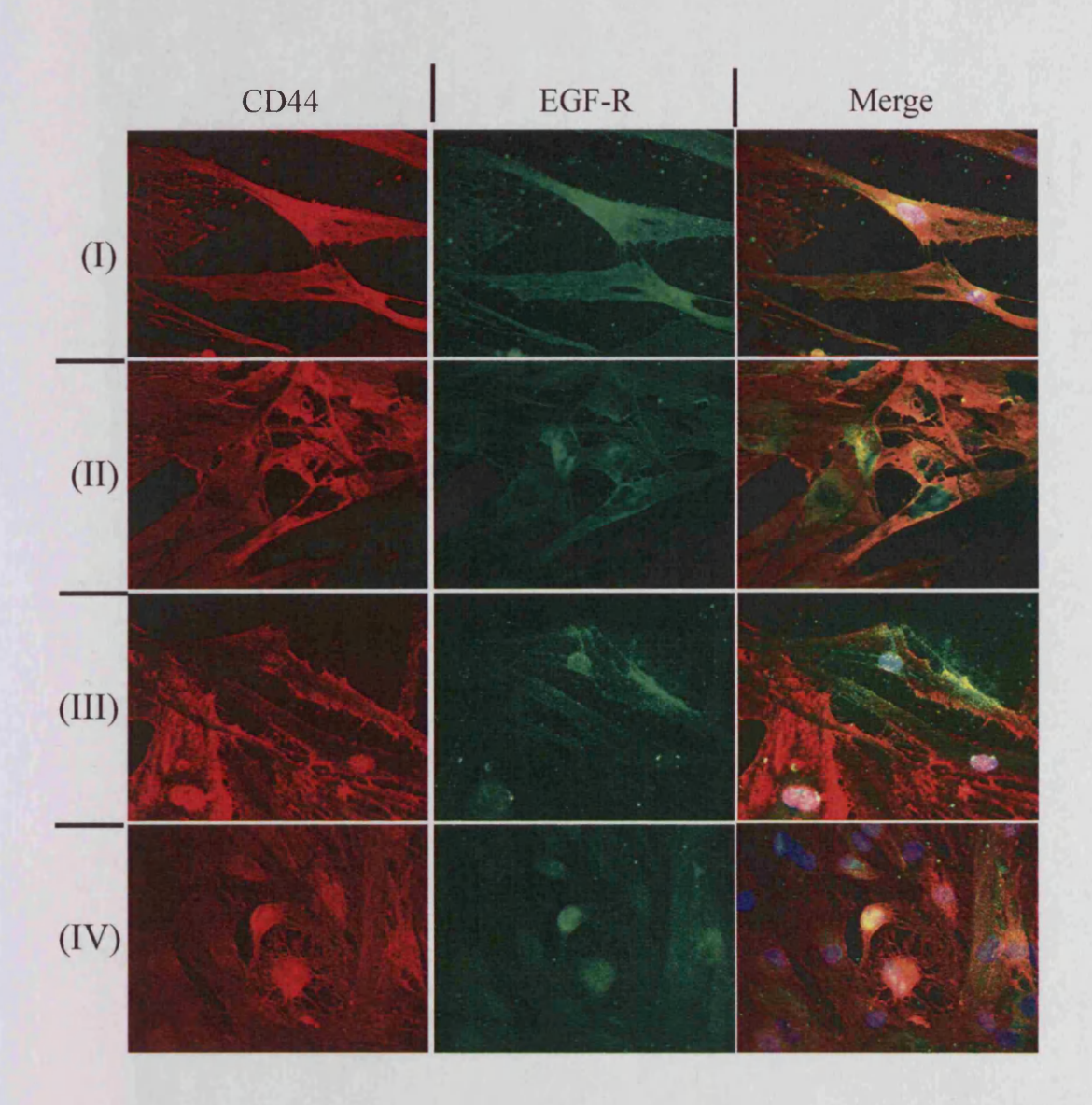


Figure 5.19 Immunocytochemical localisation of CD44 and EGF-R in aged resting fibroblasts. 70% confluent monolayers of aged dermal fibroblasts were growth-arrested in serum-free medium for 48 hours, prior to addition of serum-free medium for 24h. Cells were fixed and the expression of CD44 (red) and EGF-R (green) were examined by immunocytochemistry and their association examined by merging of individual images (yellow). In merged images DAPI was used to visualise the nuclei (blue). Representative images of 12 individual experiments using cells isolated from four different donors (I-IV) are shown. Original magnification was x 100.

CD44/EGF-R co-localisation in aged fibroblasts after TGF\(\beta\)1 stimulation

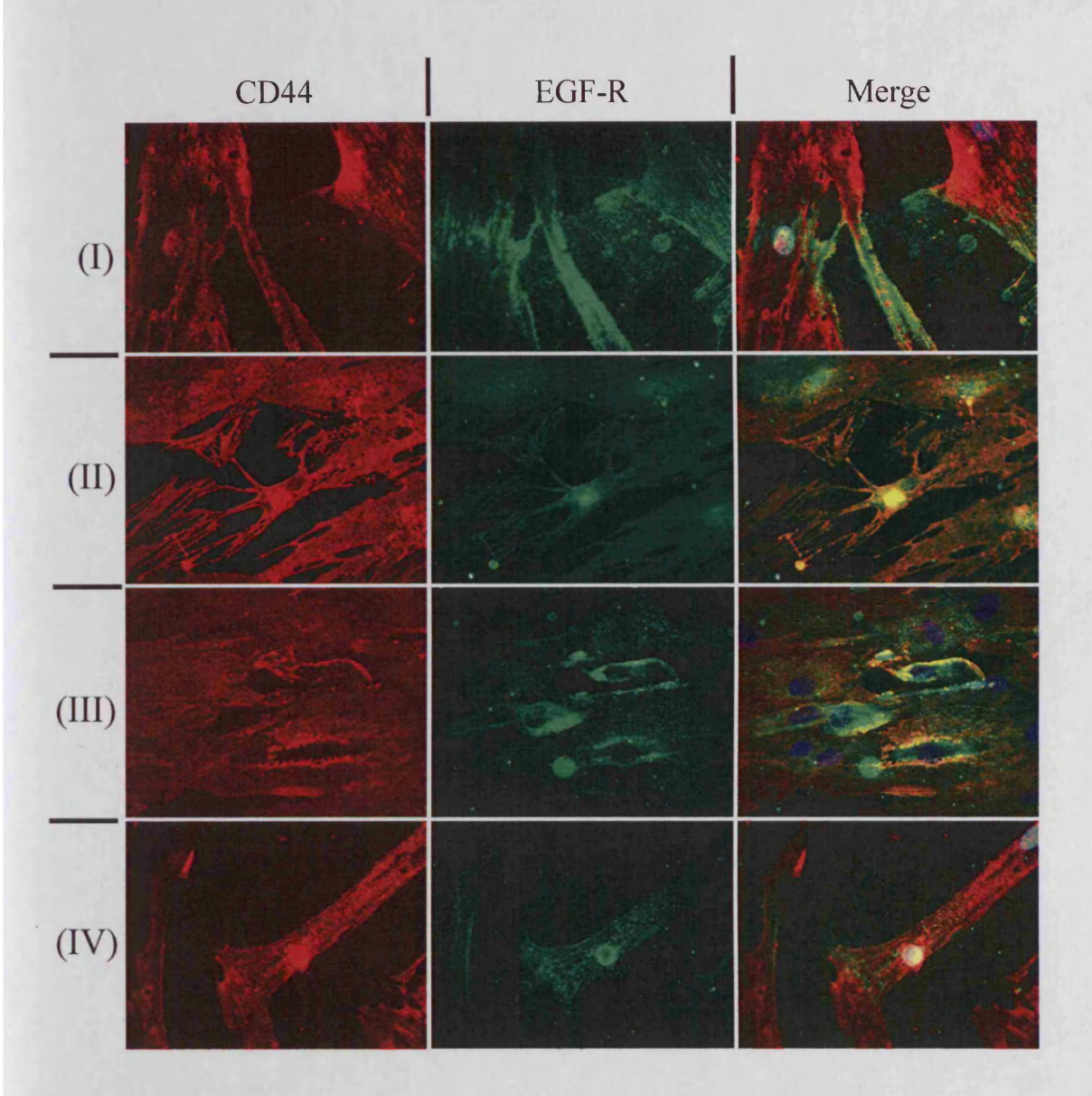


Figure 5.20 Immunocytochemical localisation of CD44 and EGF-R in aged fibroblasts stimulated with TGF-β1. 70% confluent monolayers of aged dermal fibroblasts were growth-arrested in serum-free medium for 48 hours, prior to addition of serum-free medium containing 10ng/ml TGF-β1for 24h. Cells were fixed and the expression of CD44 (red) and EGF-R (green) were examined by immunocytochemistry and their association examined by merging of individual images (yellow). In merged images DAPI was used to visualise the nuclei (blue). Representative images of 12 individual experiments using cells isolated from four different donors (I-IV) are shown. Original magnification was x 100.

Overview of effect of in-vitro aging on CD44/EGF-R co-localisation

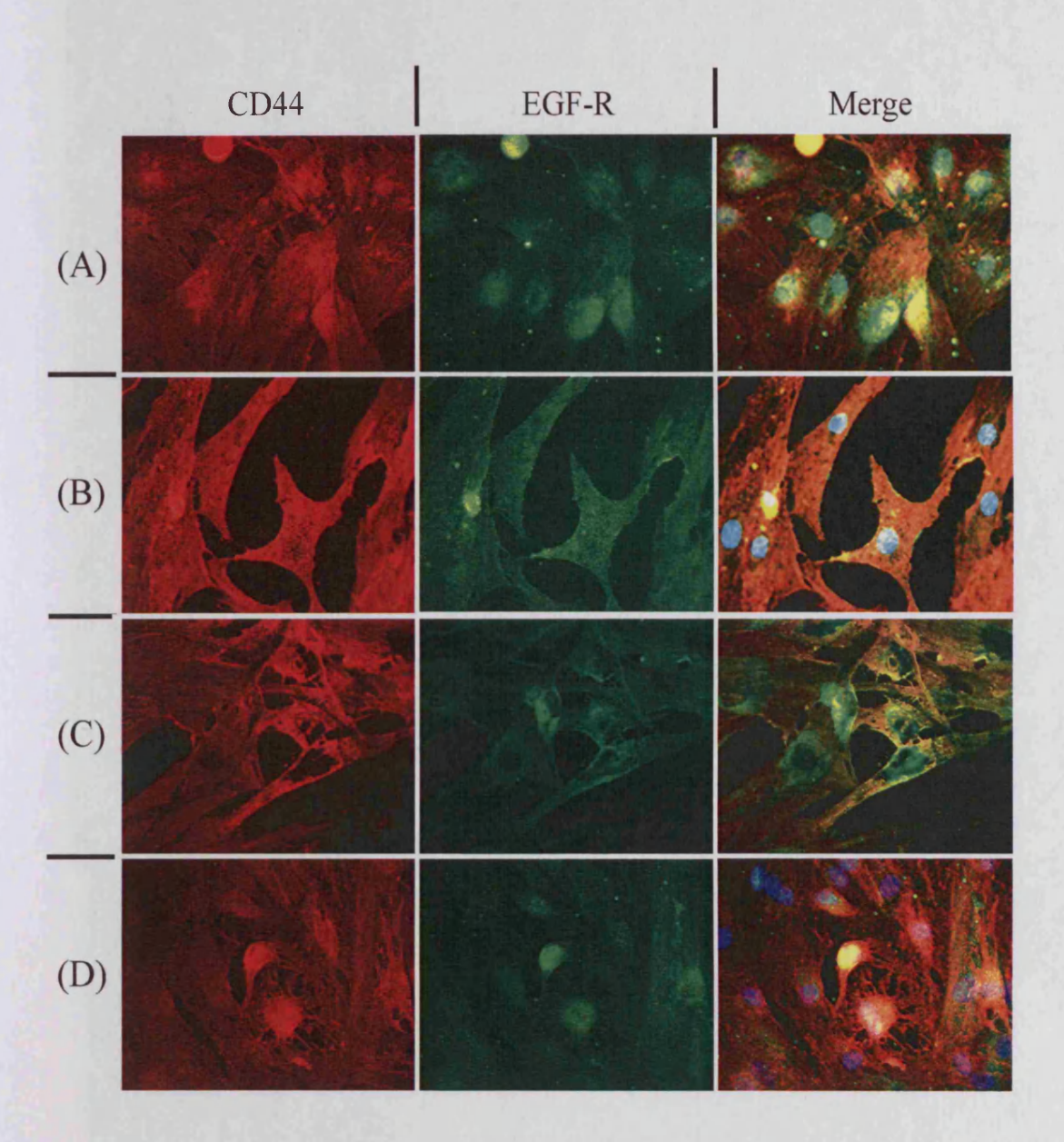


Figure 5.21 Effect of in-vitro aging on co-localization of CD44 and EGF-R. 70% confluent monolayers of patient matched young (A&B) and aged (C&D) dermal fibroblasts were growth-arrested in serum-free medium for 48 hours, prior to addition of either serum-free medium alone (A&C) or serum-free medium containing 10ng/ml TGF-β1(B&D). Cells were fixed and the expression of CD44 (red) and EGF-R (green) were examined by immunocytochemistry and their association examined by merging of individual images (yellow). In merged images DAPI was used to visualise the nuclei (blue). Original magnification was x 100.

CD44/EGF-R co-localisation in young resting fibroblasts

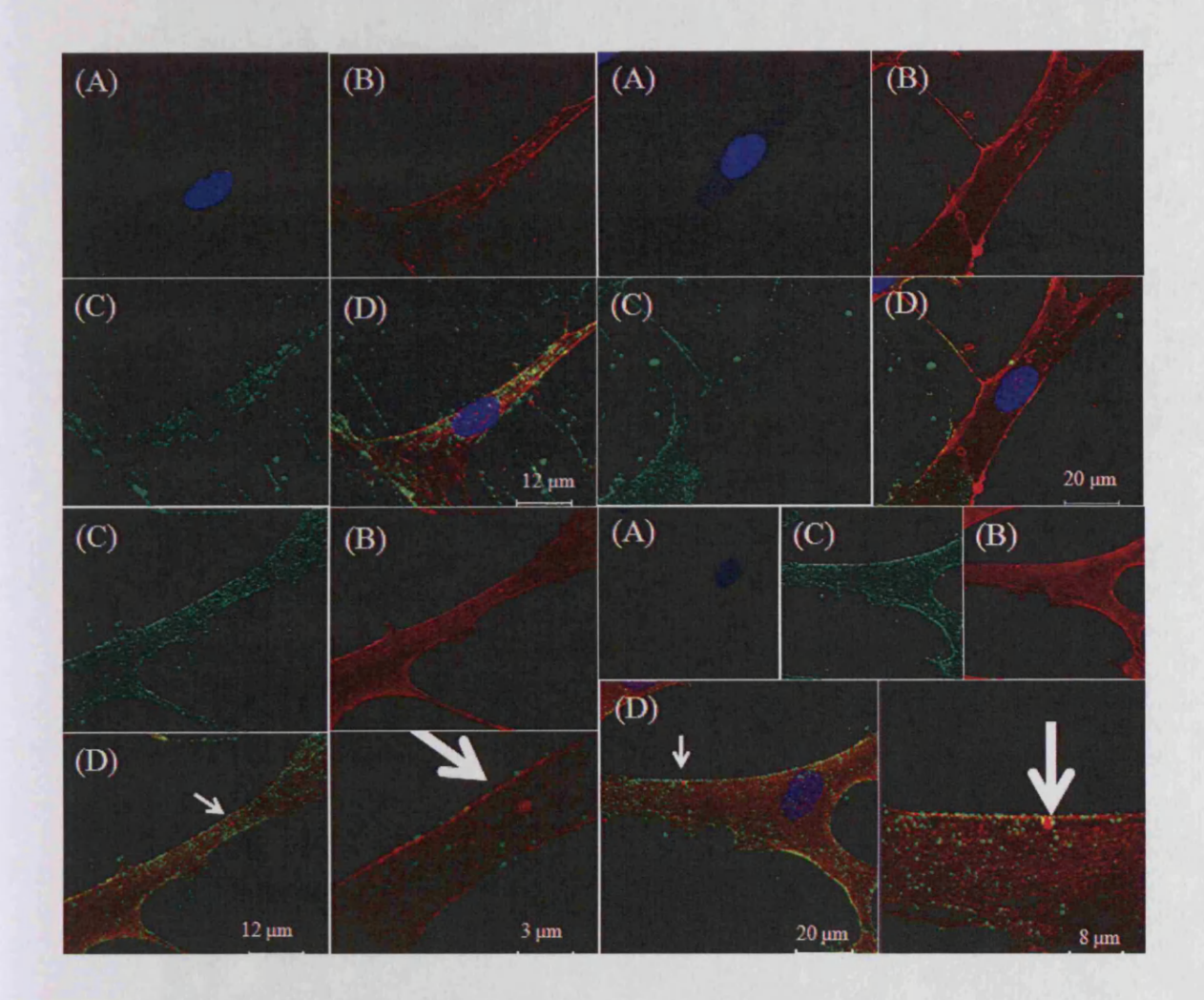


Figure 5.22 Immunocytochemical localisation of CD44 and EGF-R in young resting fibroblasts. 70% confluent monolayers of young dermal fibroblasts were growth-arrested in serum-free medium for 48 hours, prior to addition of serum-free medium for 24h. Cells were fixed and the expression of CD44 (B) and EGF-R (C) was examined by confocal section using the Leica TCS SP2 AOBS confocal microscope, and their association was examined by merging of individual images (D). CD44 label is red, EGF-R label is green, nuclei are counterstained blue with DAPI (A), and co-localisation is represented by yellow. Arrows indicate co-localisation at different magnification Representative images of 6 individual experiments using cells isolated from two different donors are shown.

CD44/EGF-R co-localisation in young fibroblasts after TGF-\(\beta\)1 stimulation

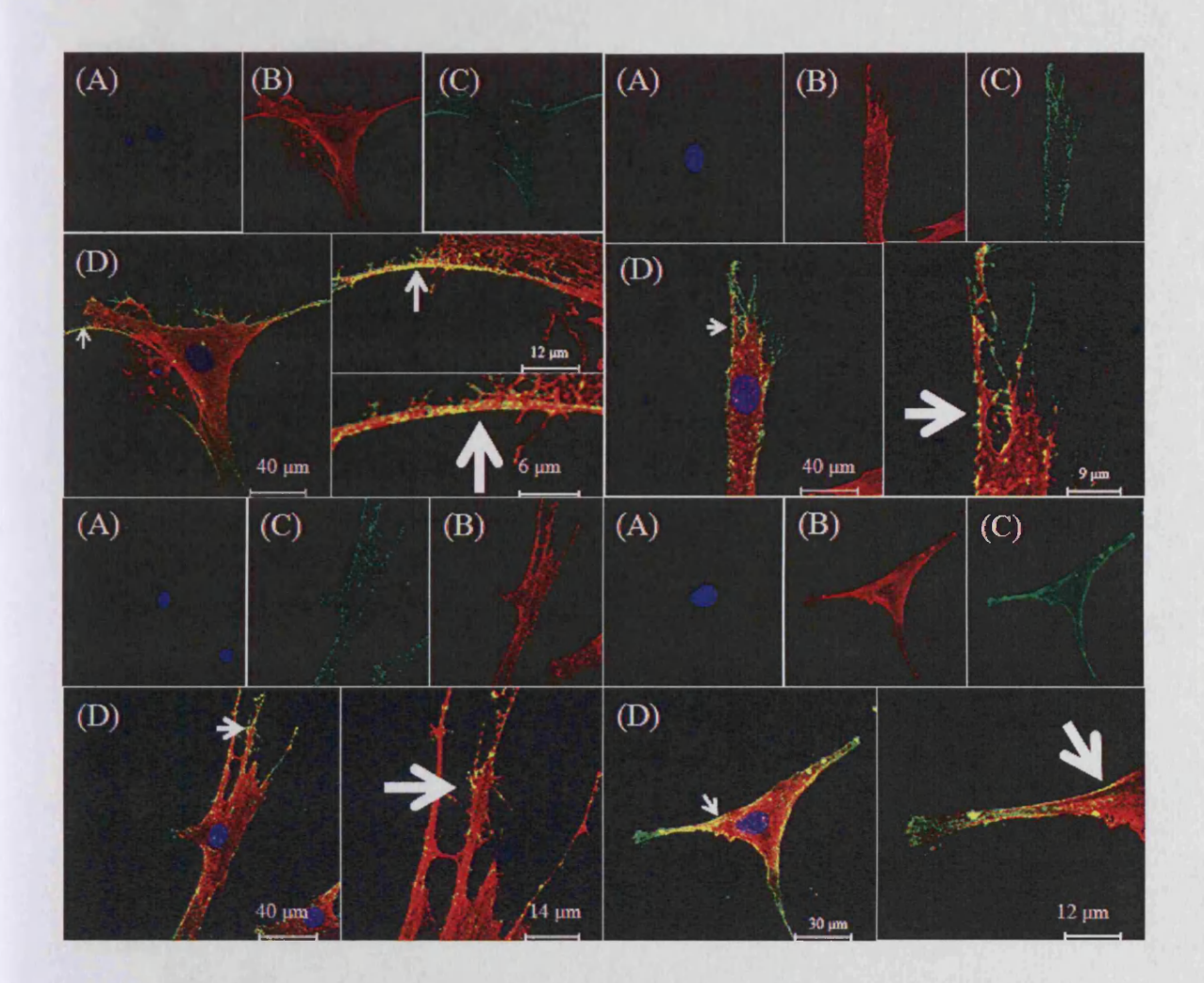


Figure 5.23 Immunocytochemical localisation of CD44 and EGF-R in young fibroblasts stimulated with TGF-β1. 70% confluent monolayers of young dermal fibroblasts were growth-arrested in serum-free medium for 48 hours, prior to addition of serum-free medium containing 10ng/ml TGF-β1for 24h. Cells were fixed and the expression of CD44 (B) and EGF-R (C) was examined by confocal section using the Leica TCS SP2 AOBS confocal microscope, and their association was examined by merging of individual images (D). CD44 label is red, EGF-R label is green, nuclei are counterstained blue with DAPI (A), and colocalisation is represented by yellow. Arrows indicate co-localisation at different magnification Representative images of 6 individual experiments using cells isolated from two different donors are shown.

CD44/EGF-R co-localisation in young fibroblasts after TGF-β1 stimulation

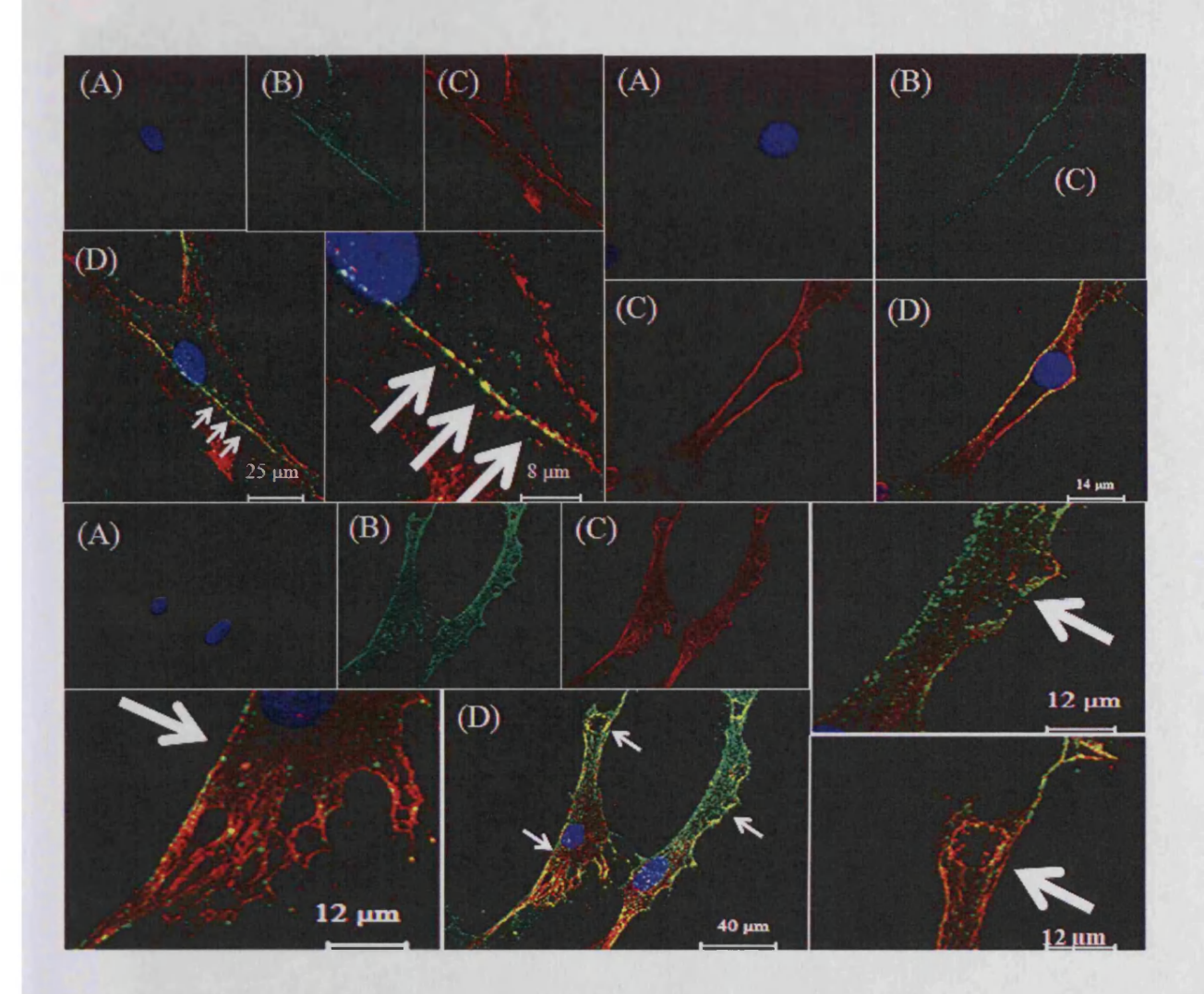


Figure 5.24 Immunocytochemical localisation of CD44 and EGF-R in young fibroblasts stimulated with TGF-β1. 70% confluent monolayers of young dermal fibroblasts were growth-arrested in serum-free medium for 48 hours, prior to addition of serum-free medium containing 10ng/ml TGF-β1 for 24h. Cells were fixed and the expression of CD44 (B) and EGF-R (C) was examined by confocal section using the Leica TCS SP2 AOBS confocal microscope, and their association was examined by merging of individual images (D). CD44 label is red, EGF-R label is green, nuclei are counterstained blue with DAPI (A), and colocalisation is represented by yellow. Arrows indicate co-localisation at different magnification Representative images of 6 individual experiments using cells isolated from two different donors are shown.

CD44/EGF-R co-localisation in aged fibroblasts at rest and after TGF-β1 stimulation

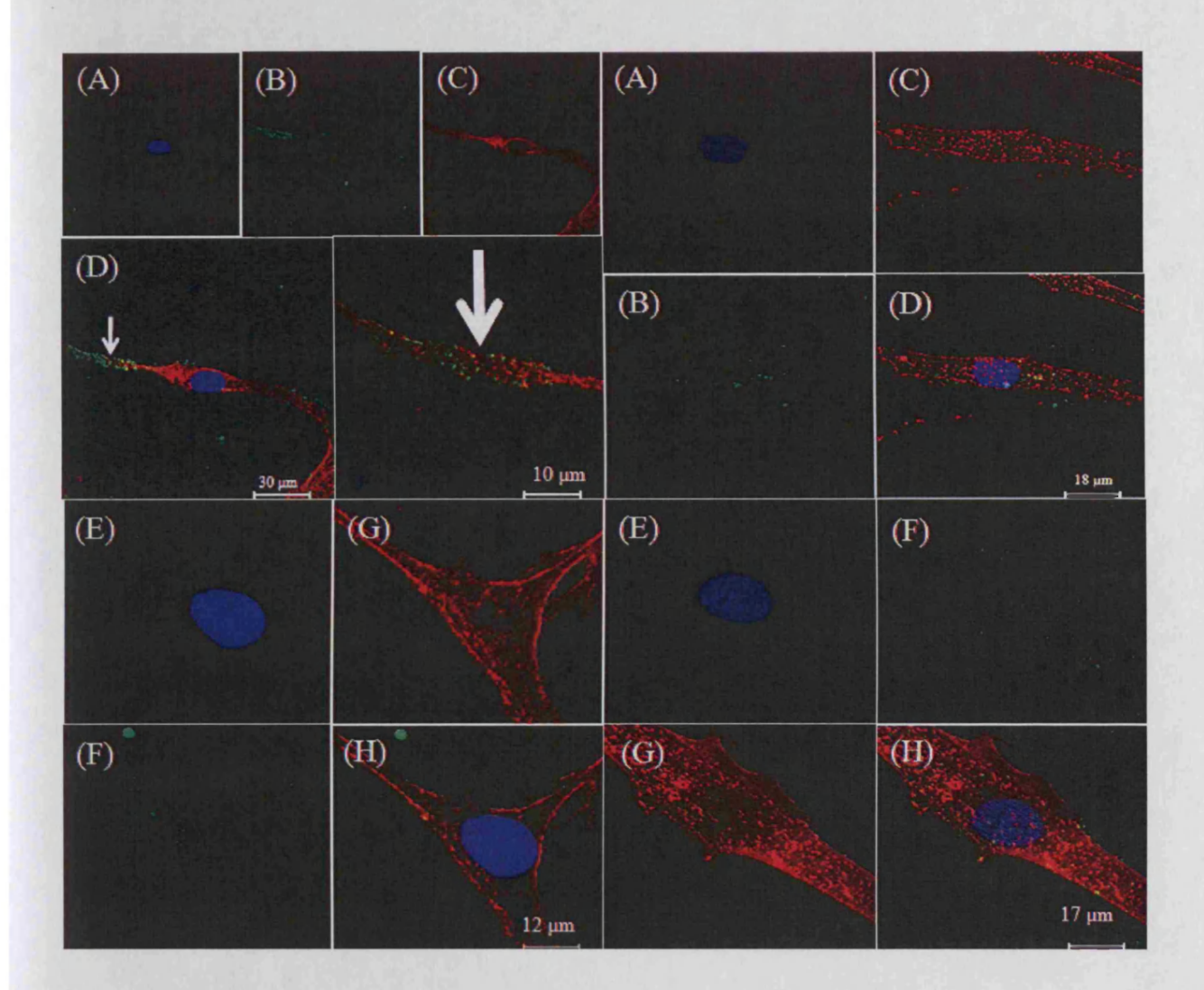


Figure 5.25 Immunocytochemical localisation of CD44 and EGF-R in aged fibroblasts under resting (A-D) and TGF-β1 stimulated (E-H) conditions. 70% confluent monolayers of aged dermal fibroblasts were growth-arrested in serum-free medium for 48 hours, prior to addition of serum-free medium containing alone (A-D) or serum-free medium containing 10ng/ml TGF-β1(E-H) for 24h. Cells were fixed and the expression of EGF-R (B&F) and CD44 (C&G) was examined by confocal section using the Leica TCS SP2 AOBS confocal microscope, and their association was examined by merging of individual images (D&H). CD44 label is red, EGF-R label is green, nuclei are counterstained blue with DAPI (A&E), and co-localisation is represented by yellow. Arrows indicate co-localisation at different magnification Representative images of 6 individual experiments using cells isolated from two different donors are shown.

Overview of effect of in-vitro aging on CD44/EGF-R co-localisation

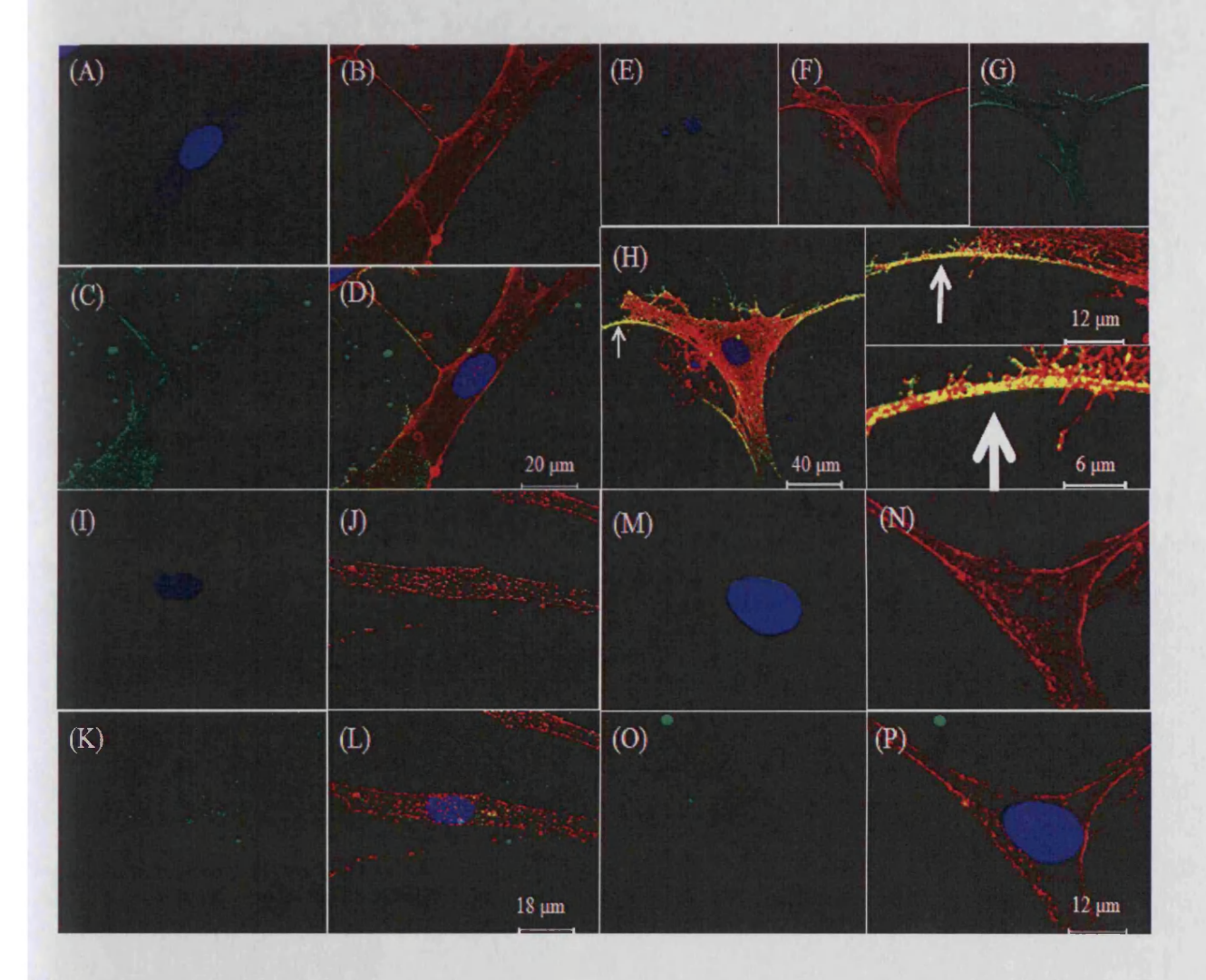


Figure 5.26 Effect of in-vitro aging on co-localization of CD44 and EGF-R. 70% confluent monolayers of patient matched young (A-H) and aged (I-P) dermal fibroblasts were growth-arrested in serum-free medium for 48 hours, prior to addition of either serum-free medium alone (A-D,I-L) or serum-free medium containing 10ng/ml TGF-β1(E-H,M-P). Cells were fixed and the expression of CD44 (B,F,J and N) and EGF-R (C,G,K and O) was examined by confocal section using the Leica TCS SP2 AOBS confocal microscope, and their association was examined by merging of individual images (D,H,L and P). CD44 label is red, EGF-R label is green, nuclei are counterstained blue with DAPI (A,E,I and M), and co-localisation is represented by yellow. Arrows indicate co-localisation at different magnification

HAS2-EGF-R overexpression in aged fibroblasts restores CD44/EGF-R co-localisation

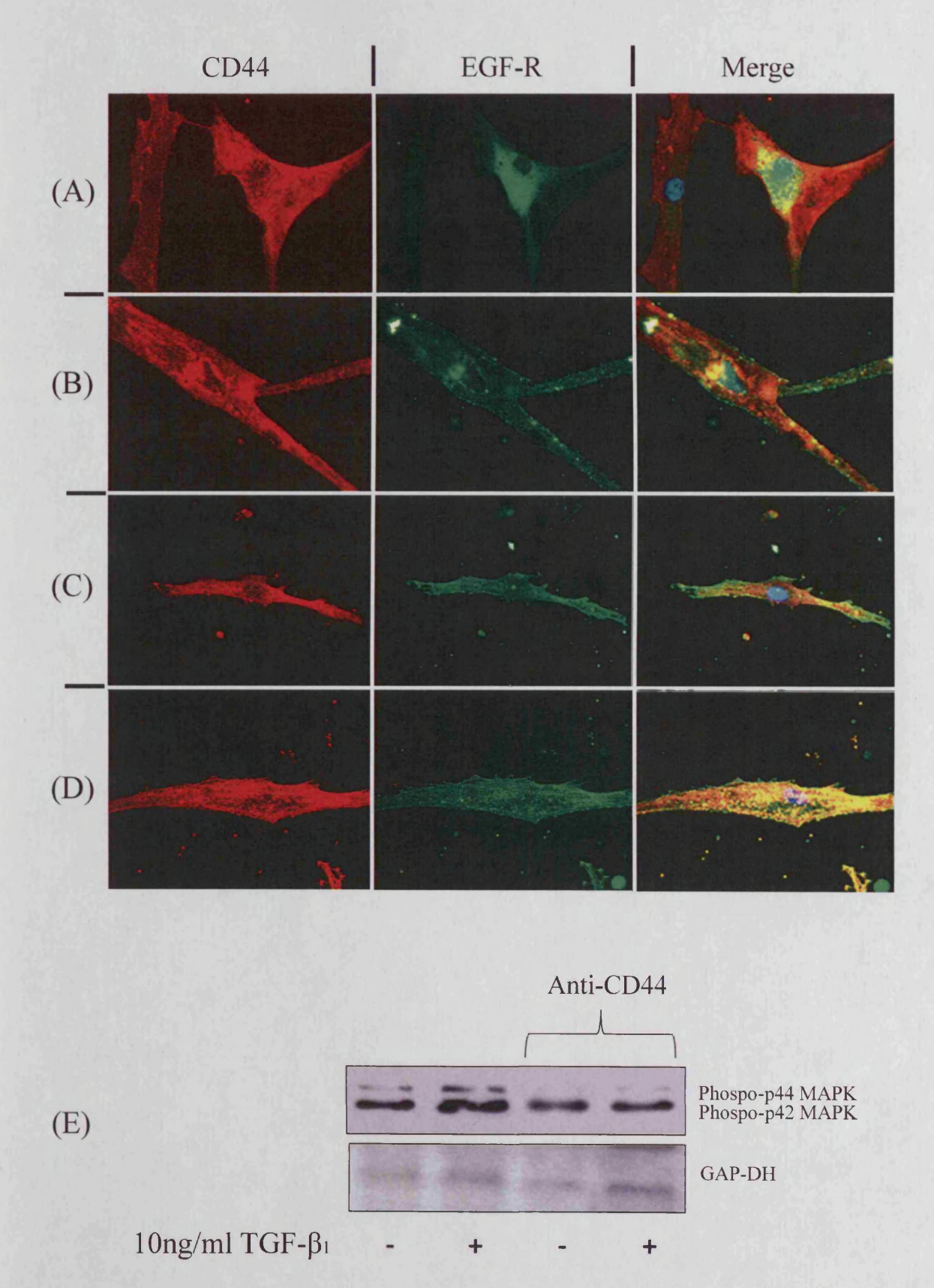


Figure 5.27 Effect of HAS2 and EGF-R over-expression in aged cells on co-Aged dermal fibroblasts were transfected either with localization of CD44 and EGF-R. GFP (mock transfected) (A), HAS2-pCR3.1 (HAS2 transfected) (B) EGF-R-pCR3.1 (EGF-R transfected) (C) .or the combination of HAS2-pCR3.1 and EGF-R-pCR3.1 (D) using nucleofector technology as described in section 2.9. Cells were growth-arrested in serum-free medium for 48 hours, prior to addition of serum-free medium containing 10ng/ml TGF-β1for a further 72 hours. The cells were fixed and the expression of CD44 (red) and EGF-R (green) were examined by immunocytochemistry and their association examined by merging of individual images (yellow). In merged images DAPI was used to visualise the nuclei (blue). Original magnification was x 100. E, confluent monolayers of young dermal fibroblasts were growth-arrested in serum-free medium for 48 hours, prior to addition of either serum-free medium alone, or serum-free medium containing 10ng/ml TGF-β1as indicated for 10 min, in the presence or absence of a blocking antibody to CD44 (final concentration 5µg/ml). Cell lysates were prepared and subjected to western blot analysis for the phosphorylated form of ERK1/2. Blots were normalised to antibodies for GAP-DH.

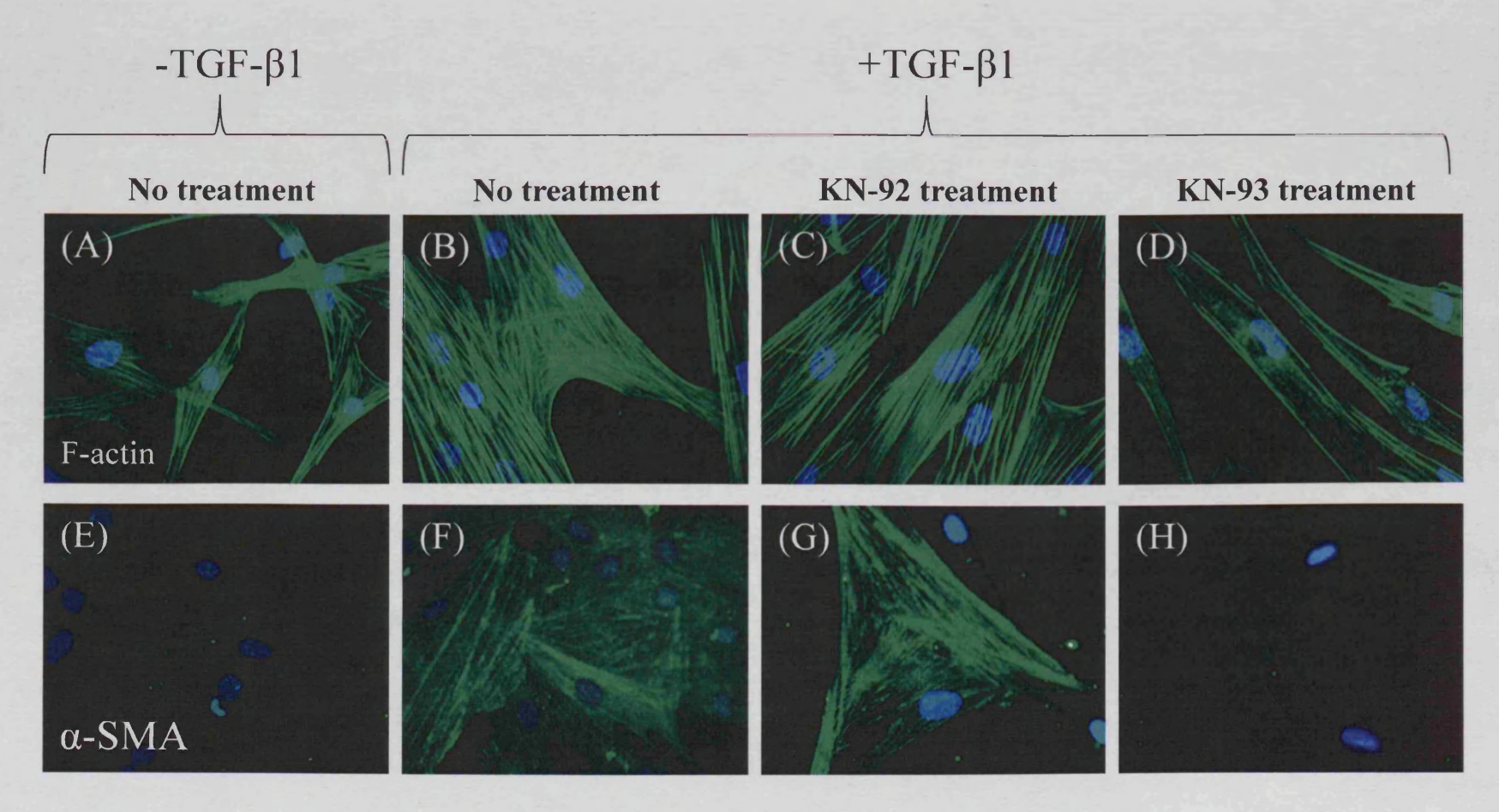
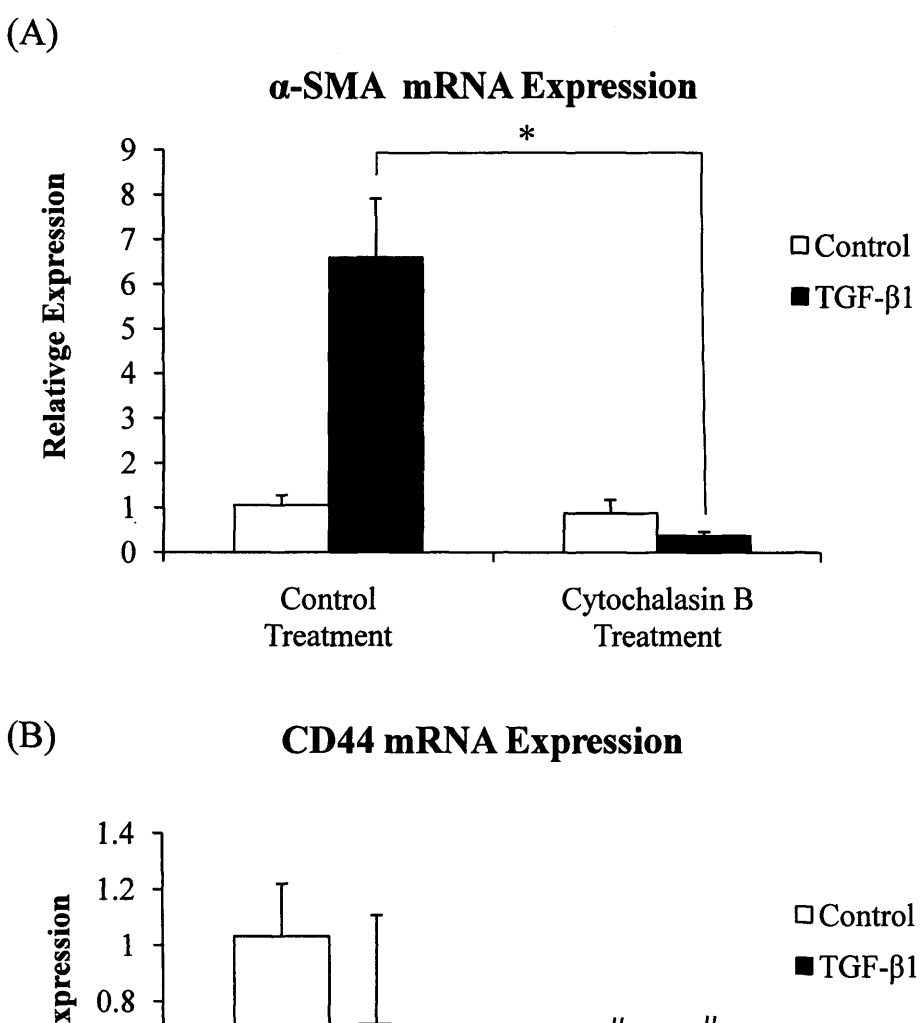


Figure 5.28. Immunohistochemical analysis of F-actin and α-SMA expression in young fibroblasts following KN-93 treatment. 50% confluent monolayers of young dermal fibroblasts were growth-arrested in serum-free medium for 48 hours, prior to addition of serum-free medium alone (A&E) or containing 10ng/ml TGF-β1(B,C,D,F,G,H) in the absence (A,B,E,F) or presence of KN-92(5μM) (C&G) or KN-93(5 μM) (D&H) for 72h. Cells were fixed and filamentous actin was visualised with fluorescein-conjugated phalloidin (A-D) or antibodies for the detection of α-SMA were added as described under section 2.4. The cells were then mounted in Vectashield fluorescent mountant, and viewed under UV light. DAPI was used to visualise the nuclei (blue). Representative images of 6 individual experiments using cells isolated from two different donors are shown. Original magnification x 100.

Cytoskeletal disruption inhibits phenotypic conversion



TGF-β1

Control

Control

Control

Treatment

Cytochalasin B

Treatment

Treatment

Figure 5.29 Consequence of disrupting the cytoskeleton on α -SMA (A) and CD44 (B) expression. Confluent monolayers of young dermal fibroblasts were growth-arrested in serum-free medium for 48 h. Cytochalasin B (10μ M) was then added in serum free medium at 37 °C for 1 h, prior to the addition of either serum free medium alone (clear bars) or 10 ng/ml TGF- β_1 (black bars) for a further 72h. In control treatments cytochalasin B was replaced by adding serum free medium alone. α -SMA (A) and CD44 (B) mRNA expression was assessed by RT-QPCR. Ribosomal RNA expression was used as an endogenous control and gene expression was assessed relative to the control treatment in non-stimulated cells. The comparative C_T method was used for relative quantification of gene expression and the results are represented as the mean \pm S.E. six individual experiments using cells isolated from two different donors. Statistical analysis was performed by the Student's t test: t, not Significant, as compared to control treatment. *,P<0.01.

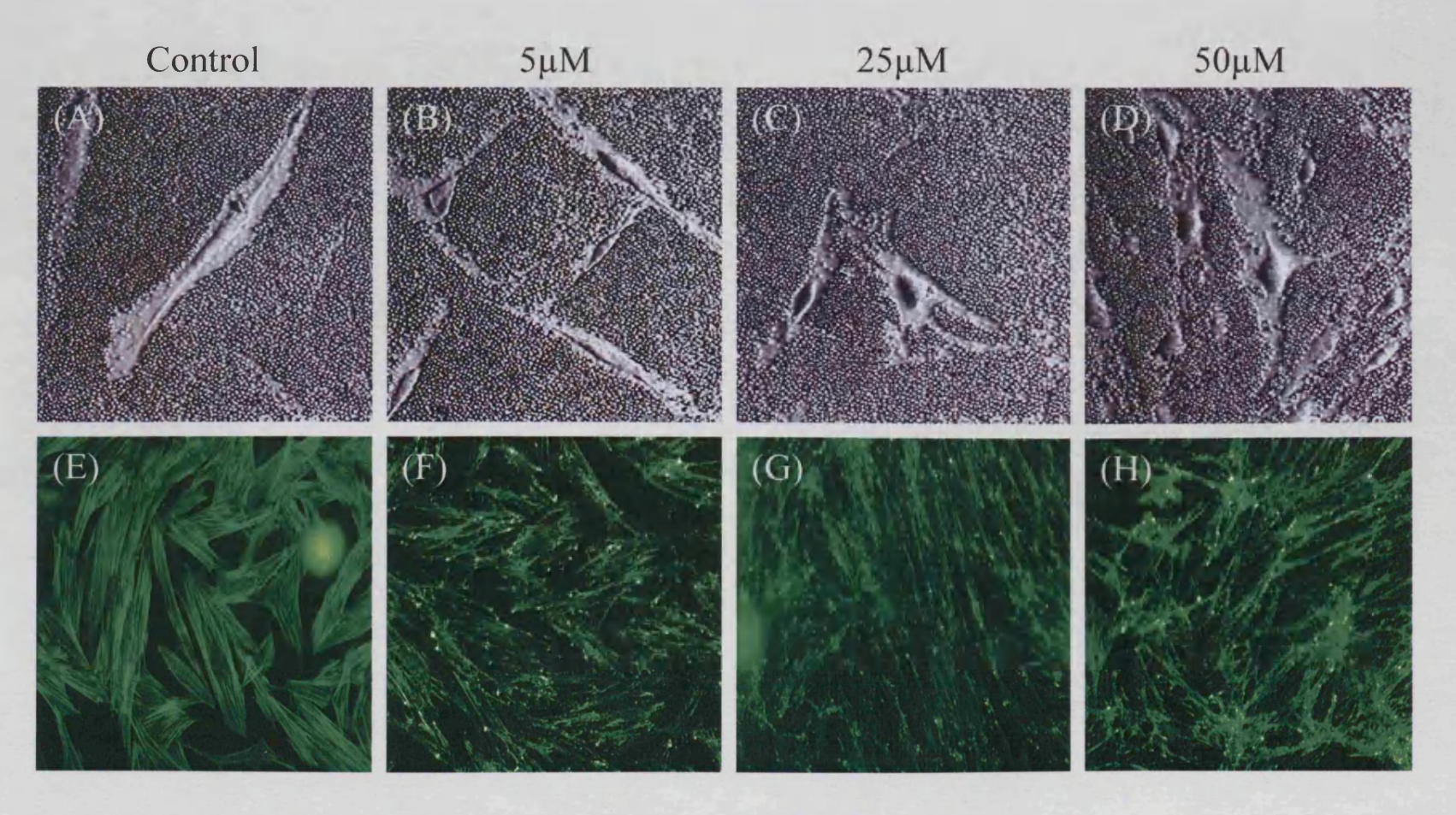


Figure 5.30 Effect of cytochalasin B on HA pericellular coat assembly and organisation of actin cytoskeleton. Serum free medium alone (A&E) or increasing concentrations of cytochlasin B (B-D,F-H) were added to growth arrested cells for 1h prior to the addition of 10ng/ml TGF- β_1 and the incubations continued for 72 h. A-D, formalised horse erythrocytes were then added to visualise the HA pericellular coat as described in section 2.11. Zones of exclusion were visualized using Zeiss Axiovert 135 inverted microscope. Original magnification was x 200. E-H, cells were fixed and filamentous actin was visualised with fluorescein-conjugated phalloidin as describe under section 2.4. The cells were then mounted in Vectashield fluorescent mountant, and viewed under UV light. Original magnification was x 100. All images are representative of six individual experiments using cells isolated from two different donors.

5.3 Discussion

This chapter demonstrates that as well as HAS2, functional EGF-R is required for TGFβ1 stimulated phenotypic activation of fibroblasts, and both are lost with *in-vitro* aging. Furthermore the results demonstrate the need for a synergistic activation of both TGF-B receptor associated signalling with the indirect activation of the EGF-R by TGF-\$1. This synergy is supported by suppression of TGF-B1 driven phenotypic activation by either inhibition of Smad signalling, or inhibition of the activity of the EGF-R using AG1478. These data therefore further emphasize the importance of age dependent decrease in the expression of EGF-R in age dependent alterations in fibroblast functions such as proliferation, as well as regulation of phenotypic activation, two aspects of dermal fibroblast behaviour which are fundamentally important to wound healing. The data also suggest that activation of the EGF-R is related to TGF-\(\beta\)1 dependent stimulation of EGF. EGF administration was insufficient to induce α-SMA, however, the combinatory effect of EGF and TGF-β1 was greater than that of TGF-β1 alone. This synergistic effect was inhibited by EGF-R blockade, suggesting that EGF contributes to the differentiation of myofibroblasts induced by TGF-\$1 through EGF-R activation. Age associated decreased activation of the EGF-R is related to both decreased expression of EGF-R, as previously demonstrated [276] and also abrogation of TGF-β1 stimulated EGF synthesis. In support of this, it was possible to partially restore age dependent TGF-\(\beta\)1 phenotypic activation by over-expression of the EGF-R, and costimulation with TGF-β1 and EGF.

My data with the neutralising EGF antibody affirmed a role for EGF as an intermediate signalling molecule for TGF- β 1 dependent fibroblast differentiation. However, the modest inhibition elicited by neutralising EGF antibody compared to the complete inhibition by EGF-R inhibitor AG1478, suggests EGF may not be the only signalling molecule involved in TGF- β 1 induced EGF-R activation. In addition to EGF, five other ligands are known to bind to EGF-R namely, amphiregulin, epiregulin, betacellulin, TGF α and Heparin-binding EGF-like growth factor (HB-EGF). In particular the liberation of HB-EGF has been widely implicated as an intermediate signalling

molecule for EGF-R activation [222, 346], whilst several studies have demonstrated direct transactivation of EGF-R by TGF-β1 can occur in a manner independent of EGF-R ligands. [327, 342].

With regards to the role of HAS2 dependent HA regulation in the control of fibroblast phenotypic activation, the data presented in this chapter builds upon the previous chapters demonstrating loss of HAS2 induction by TGF-\$\beta\$1 in aged cells. Blockade of the EGF-R signalling pathway was shown to prevent myofibroblastic differentiation of young fibroblasts, a process I demonstrated in the previous chapters to be influenced by HA. I now report that HAS2-dependent HA synthesis, is regulated by EGF-R signalling as pharmacological blockade by AG1478 attenuates its TGF-\beta1-dependent upregulation. It has previously been reported that EGF can upregulate HA synthesis by adult dermal fibroblasts and oral fibroblasts [347] and that this is required for the manifestation of their respective motogenic activities [244]. EGF also induces HAS2dependent HA biosynthesis in rat epidermal keratinocytes [318]. Data presented in this chapter confirm the stimulatory effect of EGF on HA synthesis, from this we can extrapolate that EGF represents an intermediate signalling molecule for TGF-\(\beta\)1 dependent induction of HAS2. Perhaps in hindsight, confirmation of reduced HAS2 expression or HA accumulation should have been assessed following addition of the neutralising EGF antibody. The involvement of EGF-R pathway has been implicated in mediating HA synthesis previously in epidermal keratinocytes [348]. This is consistent with a recent publication that demonstrates wounding induced synthesis of HA in organotypic epidermal cultures is downstream of EGF-R signalling [222]. Here I demonstrate that age associated EGF-R loss may directly disrupt HAS2-dependent HA accumulation.

The data presented also suggests that HA itself facilitates subsequent EGF-R signalling which may occur in a ligand/EGF independent way. The potential involvement of HA, and its principle receptor CD44, in modulation of EGF-dependent responses is well recognised in tumour cells. For example, in the absence of exogenous EGF, EGF-R can be directly activated by HA through EGF-R interactions with CD44 [349]. In the context of wound healing, EGF dependent motogenic responses of dermal fibroblasts

requires functionality of the HA receptor, CD44 [150]. The relationship between EGF signalling and HAS2 dependent HA synthesis however has not been previously explored in the context of age associated defects in wound healing and fibroblast function. The demonstration that the need for exogenous EGF could be overcome by over-expression of HAS2 in this study also suggests that the EGF-R could be activated by HA, although whether this activation is the result of direct receptor activation, or through HA dependent activation of its own receptor remains to be determined. Furthermore, restoration of phenotypic activation in the aged cells by over-expression of EGF-R together with co-stimulation by TGF-β1 and EGF is associated with restoration of HAS2 induction. Collectively, this implies EGF synthesis is upstream of HAS2-dependent HA accumulation.

CD44 is the main hyaluronan binding receptor and with HA it participates in many vital functions such as migration, adhesion proliferation and differentiation. Using a CD44specific siRNAs strategy, I showed that down-regulation of CD44 inhibits HA-mediated phenotypic activation of young cells. Considering the variation in HA biosynthesis, it was surprising to find that relative expression of CD44 did not alter between young and aged fibroblasts. But rather with age, there is a failure of CD44 re-localisation, which in the young cells, is associated with TGF-\beta1 stimulation and phenotypic activation. How CD44 re-distribution from a discrete punctate to diffuse pattern facilitates differentiation in a mechanistic sense in unknown. A further vexing result revealed expression of CD44 mRNA was downregulated by TGF-\(\beta\)1 stimulation, a phenomena previously reported in keratinocytes [279]. One possible explanation for this downregulation is that enhanced cytoskeletal linkage through CD44 re-localisation may lead to stabilization of CD44 at the cell surface, thus retarding its internalisation [334]. Previous studies have shown that cytokine induced regulation of HA binding by CD44 may in addition to CD44 transcription be dependent on alternate splice variant expression or post translational modifications such as glycosylation or sulphation [337] events which could, in theory, be effected by in-vitro aging.

HA binding to chondrocytes has been shown to upregulate the phosphorylation of CD44 [334], which can influence its interaction with cytoskeletal components [350].

Conversely in this chapter it was demonstrated that cytoskeletal elements may regulate CD44-HA binding since cytoskeletal disruption using cytochalasin B proved detrimental to the anchorage and structure of pericellular HA around the cell. CD44 expression itself did not change so it is likely that the capacity for HA to bind to CD44 was affected. The spatial organization of CD44 at the cell surface, for example, has been reportedly controlled via cytoskeletal interactions [334] so it would be easy to imagine how the structure of the pericellular HA matrix could be disrupted in this manner. In addition to artificial cytoskeletal-disrupting agents such as cytochalasin B, natural agents include nitrogen Oxide (NO). It is interesting to consider that NO is known to be elevated in degenerative disorders [351].

In the young cells, CD44 re-localisation is associated with co-localisation of CD44 with EGF-R as demonstrated by immunoprecipitation and immunohistochemistry studies. Consistent with this, Ellis et al demonstrated that fibroblast activation by EGF requires the cooperative interaction of EGF-R and the matrix receptor CD44. They present a model whereby receptor cooperativity may involve a physical association between activated EGF-R and CD44 within membrane "platforms" leading to transactivation [150]. They also propose that endogenously produced HA is only required for manifestation of EGF motogenicity. In contrast, the data from this chapter demonstrates that inhibition of HA synthesis, prevents co-localisation of CD44 and EGF-R suggesting that HA binding to CD44 directly regulates this functional coupling. It is also interesting to speculate that HA may be involved in regulating its own synthesis through feedback interactions between CD44 and EGF-R. Taken together these data demonstrate that HA may drive an increase in the association of CD44 and the EGF-R, which subsequently facilitates EGF-R signalling. Disruption of this mechanism due to a deficit in HAS2 and EGF-R contributes to age related impairment of fibroblast to myofibroblast activation since over-expression of both components in aged cells restores phenotypic activation with associated restoration of CD44-EGF-R colocalisation.

Previous studies into the pathogenesis of head and neck squamous cell carcinomas, have demonstrated direct activation of EGF-R tyrosine kinase activity by the addition of exogenous HA, which in turn stimulates downstream MAPK (in particular ERK1 and ERK2) pathways and carcinoma cell growth [349]. Furthermore, TGF-β1-mediated EGF-R transactivation was shown to activate the ERK pathway in mesangial cells [317] whilst Tsatas et al [326] demonstrate that the kinase activity of EGF-R is required for further downstream signalling of ERK1 and ERK2 by HA in a glioma cell line.

In this chapter I have demonstrated using the ERK inhibitor PD98059 that TGF-β1 mediated- fibroblast differentiation signals through the MAPK/ERK pathway. The data suggests that ERK1/2 activation signals downstream of EGF mediated EGF-R activation and its HA-dependent association with CD44, since AG1478, anti-EGF antibody, HA disruption, or CD44 inhibition all suppressed ERK1/2 phosphorylation. One caveat from this study is that ERK activation was observed with biphasic phosphorylation at 10 minutes and 3 hours after TGF-β1 stimulation. The delayed activation corresponded with EGF-R phosphorylation (both occurring at 3 hours) however, the initial phase (10 minutes) after TGF-β1 stimulation was too rapid to result from EGF-R phosphorylation and cannot be explained by the present data alone.

Studies in rat hepatocytes have demonstrated an age-related decline in EGF stimulated MAPK activation, and in particular ERK2 associated with age-related decline in proliferative capacity [352]. Vigetti et al [284] show convincing evidence that during aging, HA can modulate cell migration involving CD44-mediated signalling through ERK1/2. I have demonstrated that consistent with age-dependent decrease in EGF-R expression and its association with CD44, there was an age-dependent decrease in TGF-β1 dependent activation of ERK1 and 2. This signalling pathway is however distinct from EGF/ligand activation of EGF-R, since CD44 blockade whilst inhibiting ERK1/2 phosphorylation did not influence HAS2 expression which is also EGF-R dependent. Collectively, the current data suggests HA dependent CD44-EGF-R co-localisation is a pre-requisite for phosphorylation of ERK and subsequent phenotypic activation by TGF-β1. I have demonstrated that with *in-vitro* aging, impaired CD44-EGF-R signalling results in impaired ERK1/2 signalling, leading to resistance to phenotypic conversion.

Clearly a basal state of ERK signalling was evident in quiescent cells and this did not alter with aging. This may point to the existence of other mechanisms that utilises EGF-R-independent ERK1 and ERK2 or could just indicate that the effects of aging are restricted to upstream events i.e. age-related EGF-R deficit. The results using chemical inhibition showed that TGF-β1 mediated phenotypic activation involves the activation of EGF-R and ERK1/2 since EGF-R blockade with AG1478 or ERK inactivation by the inhibitor PD98059 resulted in a significant decrease in α-SMA expression in young fibroblasts. The effects of ERK inhibition were less impressive indicating that other pathways may converge from EGF-R/CD44 activation that are involved in cell differentiation, CD44 for example is known to be linked to various transmembrane and intracytoplasmic signalling pathways in addition to EGF-R, including those involving phospholipase C (PLC)-gamma-1, P13 kinase, and others [338]. One paper by Bourgignon et al propose a model for HA/CD44 interaction with EGF-R in human head and neck squamous carcinoma cells [206]. Two pathways are described that converge from EGF-R/CD44, one culminating with ERK1/2 activation and the other with cytoskeletal reorganisation via phosphorylation of the cytoskeletal protein filamin. CaMKII is responsible for activating filamin and similarly in this chapter I demonstrated that it is required for myofibroblastic differentiation. It is interesting to speculate that such a mechanism described by Bourguignon et al could provide a signalling function for my own model. That is, HA-CD44-EGF-R interacts with cytoskeletal proteins and regulates cytoskeletal reorganisation required for cellular differentiation. Whether this is an event downstream of, or as Bourguignon et al propose is separate to ERK1/2 activation remains unknown and further investigation is required.

In the previous chapter, and consistent with previous observations [264], Smad2 but not Smad3 activation was demonstrated to be essential for TGF- β 1-mediatedcellular activation. As mentioned earlier, TGF- β 1 mobilizes both Smad-dependent and Smadindependent signalling [140]. In the current study I have demonstrated that activation of Smad2 and EGF-R/ERK1/2 pathways work in a complimentary way to coordinate TGF- β 1 mediated α -SMA induction. Phosphorylation of Smad2 was not affected by anti-EGF antibody, AG1478, or HA disruption by Hyal and 4MU, signifying that TGF- β 1-directed Smad2 signalling is independent of EGF-R signalling and its modulation by

HA. Consistent with this, Smad2 was efficiently phosphorylated in young (EGF-R present) and aged (EGF-R not present) dermal fibroblasts. These pathways also display differential responses to *in-vitro* aging; TGF- β 1 dependent activation of Smad is unaffected by cellular aging whilst TGF- β 1 dependent EGF-R/HAS2 signalling is suppressed with aging.

My data demonstrates that the loss of TGF-β1 responsiveness in aged cells is not due to global but to specific deficits (i.e. EGF-R and HAS2). Signalling from some surface receptors is decreased in aging [353], and this decrease is likely controlled separately from global cell dysfunction. To support this, I found that the receptor CD44 levels were relatively unchanged in aged cells. Furthermore, Smad phosphorylation did not change with age proving that at least some signalling pathways were intact in aged cells.

The salient findings of this chapter are summarised in figure 5.27. In addition to HAS2 there was loss of EGF-R in aged cells and both are required for normal fibroblast functionality. Analysis of molecular events revealed that in young cells, TGF- β 1 dependent phenotypic activation utilises two distinct but cooperating pathways that involve TGF-R β /Smad2 activation and EGF mediated EGF-R/ERK1/2 signalling and the latter is compromised with *in-vitro* aging. I present evidence that the HA receptor, CD44 co-localises with the EGF-R following activation by TGF- β 1. This interaction is HA-dependent as disruption of HA synthesis abrogates this association and inhibits subsequent downstream signalling of ERK1/2. In aged fibroblasts this association is lost with resultant suppression of ERK1/2 activation. Forced over-expression of EGF-R and HAS2 in aged cells restored TGF- β 1-mediated HA-CD44/EGF-R association and α -SMA induction.

In summary, the data suggests that HA serves as a signal integrator and facilitates the capacity for CD44 to physically associate with EFG-R. This complex is necessary for propagating TGF-β1 intracellular signals via EGF-R-dependent transduction pathways necessary for myofibroblastic differentiation. It would appear that as important as HA is in orchestrating fibroblast behaviour, a functional relationship between CD44 and EGF-R is vital to transduce the HA signal. This explains why recovery of HAS2-induced HA

levels in aged cells is insufficient to restore TGF- $\beta1$ responsiveness in the aged phenotype without combined restoration of EGF-R apparatus.

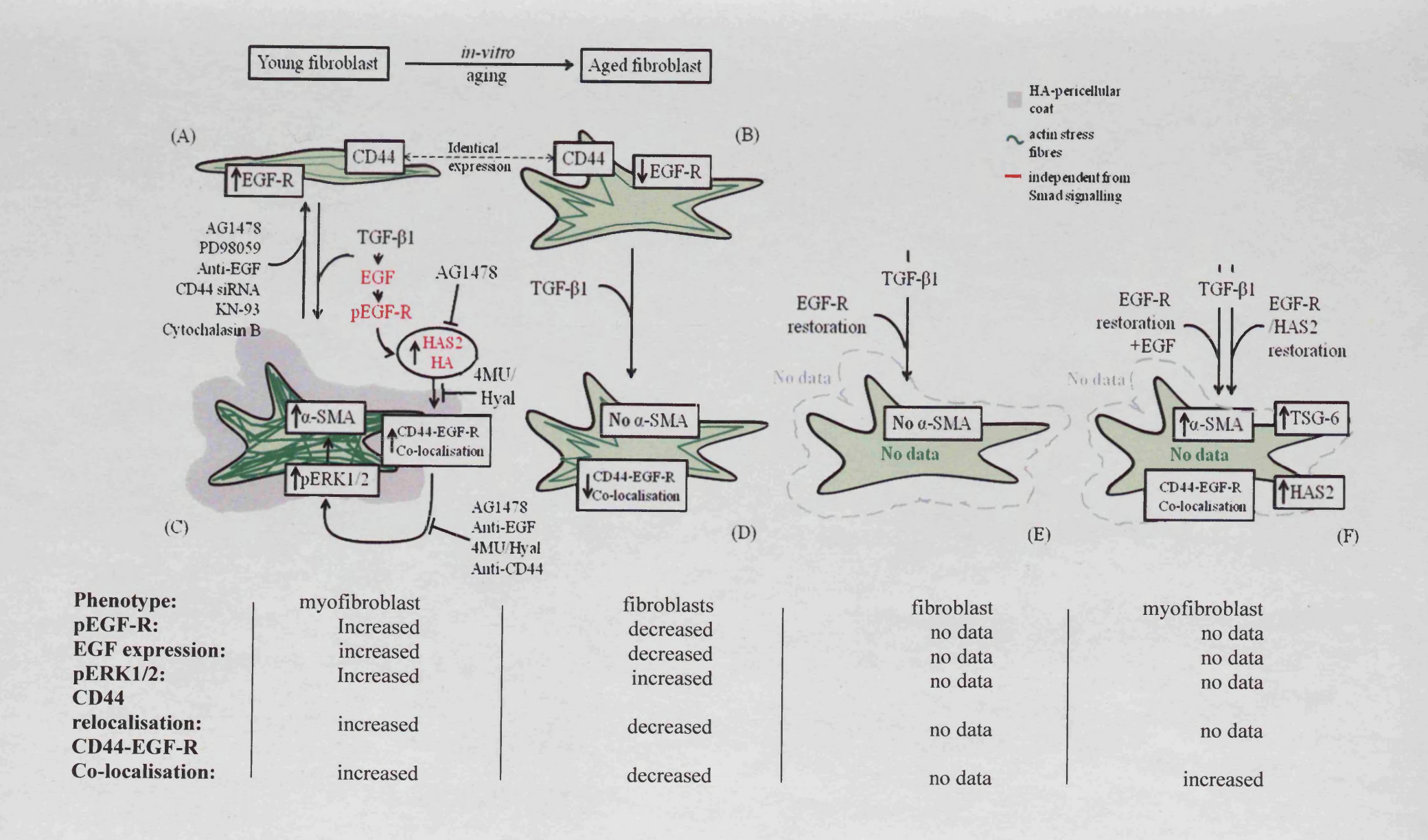


Figure 5.27 Comparison of young and in-vitro aged fibroblast phenotype. A comparison of cell morphology, HA generation and phenotype of patient matched young (A&C) and aged (B&D&E&F) dermal fibroblasts based on the analysis compacted from this results chapter. In response to TGF-\$1 young fibroblasts (A) readily differentiate into myofibroblastic cells (C), which incorporate prominent stress fibres and α-SMA and is mediated via activation of EGF-R by EGF. Accordingly phenotypic activation is impaired by the EGF-R inhibitor AG1478 and anti-EGF antibody. HAS2-dependent HA synthesis is regulated by EGF-R signalling since AG1478 prevents HAS2 induction by TGF-β1. Stimulation with TGF-B1 drives CD44-EGF-R co-localisation and inhibition with either 4MU or Hyal confers this association is HA dependent. In addition, TGF-\$1 mediated myofibroblastic differentiation is dependent on activation of ERK1/2 and accordingly is attenuated by ERK1/2 inhibitor PD98059. Furthermore, TGF-\$\beta\$1-mediated ERK activation was dependent on EGF-R signalling and CD44-HA modulation since AG1478, anti-EGF antibody, 4MU, Hyal and anti-CD44 antibody all hindered ERK activation. Smad2 phosphorylation was unaltered using the same pharmacological inhibition suggesting a dissociation in intracellular signalling events (red text). In-vitro aged fibroblasts (B) demonstrate reduced EGF-R levels and fail to reach phenotypic maturity in response to TGFβ1 associated with reduced induction of EGF and a failure of CD44-EGF-R co-localisation (D). CD44 expression is identical in young and aged phenotype but in response to TGF-β1 young cells demonstrate CD44 re-location whereas aged cells do not. Restoration of EGF-R levels in aged cells failed to restore the potential for phenotypic activation by TGF-\(\beta\)1 (E). Restoration of EGF-R levels and co-stimulation with TGF-β1 and EGF in aged fibroblasts led to augmented phenotypic activation characterised by up-regulated α -SMA and induction of HAS2 and TSG-6. (F) Restoration of both EGF-R and HAS2 allowed for TGF\$1 mediated myofibroblastic differentiation without the need for exogenous EGF (F). This was also associated with restoration of CD44-EGF-R co-localisation.

Chapter 6 General Discussion

The data presented herein provide a mechanism to explain age dependent resistance of dermal fibroblasts to phenotypic activation. Figure 6.1 illustrates my current proposed model. Synergy between TGF-β1-dependent pathways and competent EGF-R-signalling pathways are required for TGF-\$\beta_1\$-dependent fibroblast-myofibroblast differentiation. This contains at least two distinct but cooperating pathways that involve TGF-β1-Smad2 activation (step 1) and HA dependent EGF-R-ERK1/2 signalling (steps 2-8) and the latter is compromised during in-vitro aging. In a young cell TGF-β1-mediated synthesis of EGF (step 2) phosphorylates the EGF-R (step 3). Activation of the EGF-R signalling pathway is required for elevated transcription of HAS2 induced HA accumulation (step 4) and its assembly into a pericellular coat (step 5). The HA-binding protein TSG-6 has been shown to be critical in facilitating this step. I propose that binding of HA to its receptor CD44 orchestrates its association with EGF-R, (step 6) while signalling downstream of this complex triggers phosphorylation of the p42/p44 MAP kinases, ERK1 and ERK2 (step 7) and cytoskeletal activation via calmodulindependent kinase II (step 8). Activation of these pathways together with Smad dependent transcriptional regulation of α-SMA is then responsible for reorganisation of the actin cytoskeleton required for phenotypic activation (step 9).

With *in-vitro* aging, numerous aspects of this signalling cascade (highlighted in *red*) are impaired, including decreased expression of EGF-R, suppression of TGF-β1 dependent EGF synthesis and the resultant failure of induction of HAS2 dependent HA and its assembly into a pericellular coat. The result of this is loss of CD44-EGF-R colocalisation leading to selective impairment of the ERK1/2 signalling pathway and resistance to phenotypic maturation. This model has the potential to be a major advancement in the field of wound healing and to change the way TGF-β1 promoted myofibroblast differentiation is viewed; however there remain a number of uncertainties relating to the proposed mechanism which are now discussed for each step.

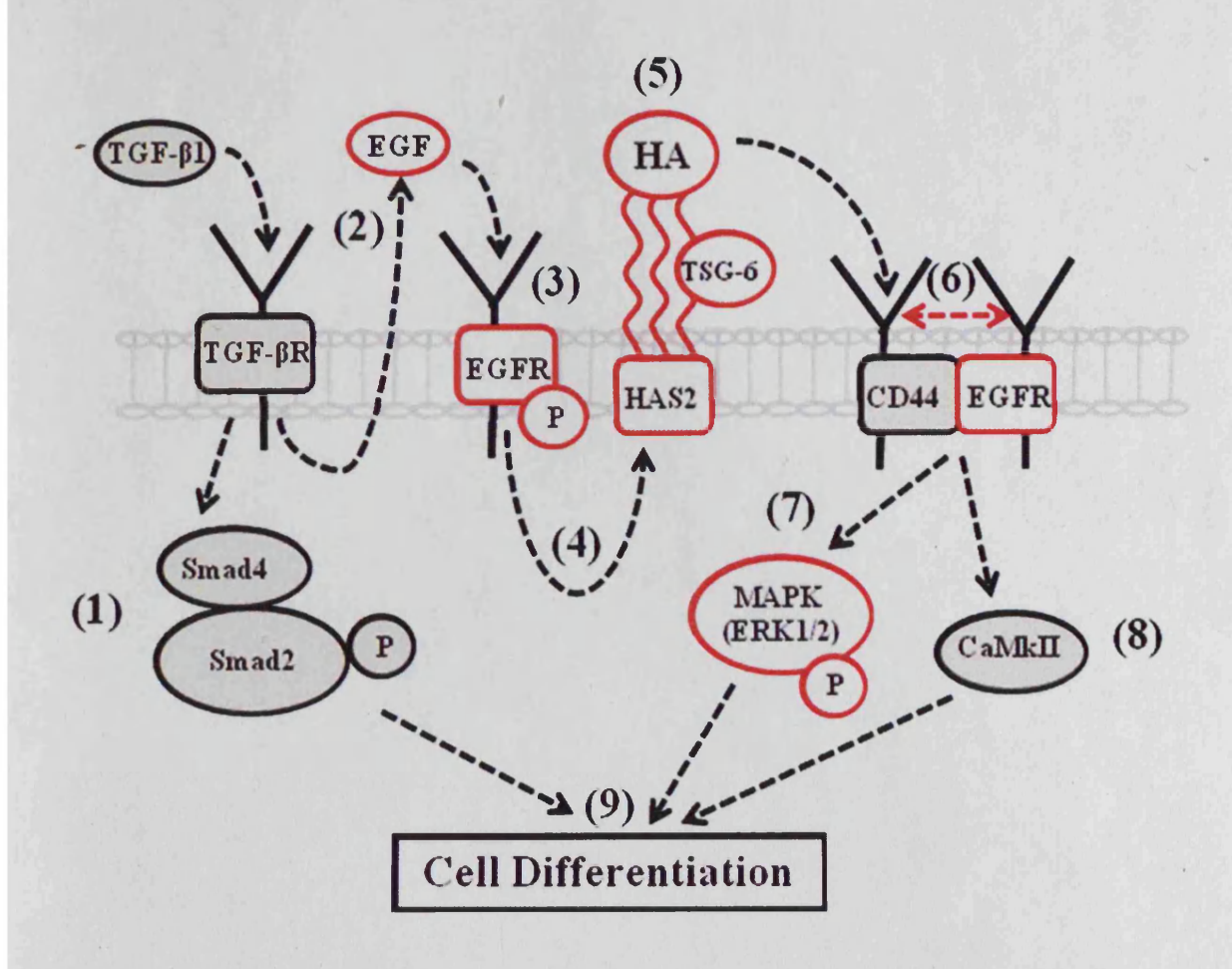


Figure 6.1 Proposed model for the signal transduction pathways involved in TGF-β1-mediated fibroblast-myofibroblast differentiation. The age-related defects in this pathway (highlighted red) confer resistance to myofibroblastic differentiation.

(1) Smad phosphorylation causes dissociation from the receptor and stimulation of assembly of heteromeric complexes between the phosphorylated R-Smad and the Co-Smad, Smad4. This results in nuclear accumulation of this complex and subsequent transcriptional activation of target genes. In turn, this cascade activates the transcription of an inhibitory Smad (Smad 7), which can interact with the TGF-β receptor to block Smad activation. Whilst the data suggests that TGF signalling machinery is intact following in-vitro aging we cannot exclude potential age-related differences downstream of Smad phosphorylation. It would be interesting to further investigate Smad4 and Smad7 expression in young and aged cells.

Furthermore, autocrine generation of TGF-β1 levels remained constant in young and aged fibroblasts. Collectively these results suggested that deficits in TGF-β1 responsiveness by aged cells could not be attributed to a global deficit in TGF-β1 signalling. It could be argued, however, that the interpretation that young and aged cells share identical autocrine TGF-β1 signalling would have been more convincing had examination of TGF-β1 at the level of transcription been combined with measurement of protein synthesis by ELISA. Furthermore, TGF-β1 is generated in a biologically inactive form, requiring activation before subsequent signalling can occur [354, 355]. Therefore, since the activity of any generated TGF-β was not assessed by bioassay it is also worth considering that the *activity* of TGF-β1 generated by young and aged cells could have varied despite apparent similar generation.

- **(2)** The data suggests that activation of EGF-R by TGF-β1 was mediated through synthesis of EGF. The mechanism regulating induction of EGF by TGF-\(\beta\)1 was not investigated. Transcriptional control of human EGF is poorly understood. It has been shown that 5.5 kb of the 5'- 6 flanking region of the mouse EGF gene is sufficient to direct reporter gene expression [356, 357]. In addition, studies of the mouse EGF 5' UTR have shown an element located between 51 and 35 bases upstream of the EGF transcription start site is required for basal activity of the EGF promoter [358]. Three proteins bind to this region, one of which is either Sp1 or a closely related protein [359]. In a recent study using 2085 bp of the human EGF promoter in pull-down assays of extracts from human keratinocytes, the CREB, Sp-1, NFkB and AP-1 transcription factors were all implicated in EGF transcriptional control [360]. The elements involved with the TGF-β1-dependent induction of EGF, however, were not examined. It would be interesting to analyse the human EGF promoter in more detail and investigate the intracellular signalling initiated by TGF-\beta1 to define the mechanisms of EGF induction by TGF-β1.
- (3) Consistent with previous studies [35]. I demonstrated a decrease in EGF-R expression as cells age. Matrisian et al [256] argue that decreased responsiveness to EGF associated with aging is dependent solely on loss of receptor, however this is not

always reported. Tran et al [1] observed that as fibroblasts near senescence not only is there less receptors for EGF, the remaining receptors face upregulated signal attenuation as the dephosphorylating protein tyrosine phosphatase activity is increased. Furthermore age-associated delay in the rate of receptor phosphorylation after EGF stimulation and impairment in receptor/ligand trafficking has been reported [361]. Specifically Reenstra et al add there is an age-associated decrease and delay in the number of occupied receptors that are transported intracellularly and in their rate of clearance from the plasma membrane [361]. Whilst I have demonstrated aging-related downregulation of EGF-R levels, combined upregulation of protein phosphatases, and/or deficits in EGF-R-processing mechanisms cannot be dismissed and could contribute to tipping the kinase/phosphatase balance in favour of de-phosphorylated EGF-R. It would be interesting therefore to investigate whether specific tyrosine phophatases and altered receptor activation and trafficking attenuates EGF-R signalling in an aging manner. In retrospect, the number of binding sites should have been assessed [35] to ensure a decrease in EGF binding sites correlated with aging, this would rule out that fewer EGF-R were differentially presented.

An important question is what mechanisms could be responsible for age-dependent reduction in EGF-R transcription? Basal EGF-R expression is reported to be tightly regulated by microRNA-7 [362]. MicroRNAs (miRs) are small, endogenous, noncoding RNAs that bind to target mRNA inducing translational repression of the target gene, or degradation of the target mRNA. A single miR can regulate many targets and miR-7 over-expression in cancer cells down-regulates both EGF-R expression and the expression of EGF-R signalling pathway intermediates [362]. My pilot data, using QPCR for the mature miR-7, have demonstrated that reduced expression of EGF-R in aged fibroblasts is associated with an increased expression of miR-7. To date, however, the relationship between mi-R-7 expression and dysregulation of EGF-R has not been examined in dermal fibroblasts. It would be interesting to use miR-7 over-expression [362] in young cells and miR-7 antagomirs in aged cells to determine whether miR-7 is the key regulator of EGF-R expression.

The EGF-R is a transmembrane glycoprotein that constitutes one of four closely related members of the erbB family of tyrosine kinase receptors: EGF-R (ErbB-1), HER2/c-neu (ErbB-2), Her 3 (ErbB-3) and Her 4 (ErbB-4) [363]. Whilst this study has focused on EGF-R (ErbB-1) its potential for interaction with other members of the erbB superfamily has been demonstrated [319]. There is growing evidence that in glioma cell lines for example there is dual interaction with CD44 by both EGF-R and ErbB2 that is comparable to the mechanism proposed in this communication [326]. Furthermore ErbB2-ERK signalling and HAS regulation are functionally coupled in human ovarian tumour cells [205]. HA may play an important role in activating CD44-associated p185^{HER2} kinase activity required for the onset of human ovarian tumour cell growth [364]. It would therefore be interesting to extend the present data to investigate the regulation of fibroblast phenotype by HER2/ErbB-2.

(4) HAS2 expression and induction are essential to the differentiation process. An important question is how do EGF-R and TGFβR1 synergise to control HAS2 expression. Work in ION has identified the transcription start site of the HAS2 gene [365], and subsequent *in silico* analysis of the 3 kb of genomic DNA upstream of HAS2 identified a number of putative transcription factor binding sites (TFBSs) of potential functional significance in EGF and TGF-β1-signalling. These include multiple recognition motifs for the binding of activator protein 1 (AP1), extracellular signal-regulated kinases (ERKs), signal transducers and activator of transcription (STAT)1 and 3, and the Smad family of transcription factors. It has also been shown that specificity protein (Sp)1 and Sp3 are required for HAS2 mRNA synthesis in renal proximal tubular epithelial cells (PTC) [365, 366]. In addition, recent preliminary data demonstrated that siRNA knockdown of Sp1 and Sp3 inhibits HAS2 up-regulation stimulated by IL-1β in these cells. It would be interesting therefore to investigate the involvement of Sp1/Sp3 in the HAS2 transcriptional responses to TGF-β1-driven differentiation.

The posttranscriptional regulation of HAS2 mRNA by its natural antisense RNA, HAS2AS, has recently been described in osteosarcoma cells [367]. Preliminary work in ION has demonstrated that stimulation with TGF-β1 in PTC induced coordinated temporal profiles of HAS2AS and HAS2 transcription, and it was postulated that

transcription of the antisense RNA stabilises or augments HAS2 mRNA expression in these cells. It is interesting to speculate therefore that a modification in HASAS expression in aged dermal fibroblasts could contribute to diminished HAS2 induction by TGF-β1 associated with the aged phenotype.

(5) One of the principle differences between young and aged dermal fibroblast was the inability of the latter to form pericellular HA coats which was demonstrated to be necessary for driving the myofibroblastic phenotype. Resistance to myofibroblastic conversion coupled with failure to synthesis HA coats was also reported for oral fibroblasts [159]. Despite its obvious involvement, the functional role of the HA coat in phenotypic conversion has however remained elusive. Myofibroblasts are controlled by the mechanical microenvironment, in particular, by the organisation and stiffness of the ECM [368]. Whilst increasing the matrix ridgity has been shown to increase α-SMA expression [369] stress release leads to reduced α-SMA [370]. Even though TGF-β1 is always present following wounding the mechanical characteristics of the environment appear to modulate its action to induce either migration or contraction [68]. The role of the pericellular matrix in mechanotransduction and cell response to strain has been described in several studies. It has been postulated that structured HA may form the basis of a dynamic and changing network through which cells may communicate and respond to external forces. Several studies provide evidence that in response to mechanical strain, cells can respond by synthesising a matrix that allows the cells to adapt to the new mechanical environment. For example an increase in pericellular HA has been described in human cervical fibroblasts [371], smooth muscle cells [372] and lung fibroblasts [373] in response to cyclic stretch. It is therefore interesting to speculate that the pericellular HA coat can acts as a mechano-sensor in response to cellular injury, triggering and maintaining the contractile phenotype through mechanical cues from the surrounding tissue. By this rational one can see why the failure of aged fibroblasts to synthesis a HA coat could be detrimental to the progression of wound closure and scar formation.

Interestingly one study demonstrated that exogenous HA can act as a scavenger of reactive oxygen species (ROS) and confer protection from oxidative damage in

fibroblasts [374] during which it undergoes degradation [375]. Injury by ROS has been shown to play a critical role in the degenerative changes that are characterised by a decline in cell numbers and viability which occurs with aging. Cells may undergo premature senescence in response to a variety of external stimuli, for example oxidative stress and the accumulation of senescent fibroblasts within age-related chronic wounds have been explained by oxidative stress [94]. It is therefore interesting to speculate that the HA coat plays a protective role and as cells age excess ROS could induce shedding of pericellular HA. This could theoretically explain loss of pericellular HA with aging. An increase in low-molecular-weight HA due to depolymerisation of HA might be expected but this was clearly not the case in my in-vitro aging model.

Versican expression hampers HA pericellular coat formation [193]. In a recent paper, Suwan et al [248] generated mice whose versican demonstrated decreased HA binding affinity, thereby exhibiting fibroblasts with a disorganised HA matrix. They make the convincing argument that disruption of the HA network structure caused constitutive ERK1/2 phosphorylation via CD44 and led to premature senescence. It is interesting to speculate that modifications in HA (i.e. loss of coat), could be the catalyst for initiating cells to undergo cellular aging and senescence as opposed to my model where diminished HA levels are a consequence of cellular aging. It would be interesting to test these hypothesises further; fibroblast populations could be cultured through to senescence in varying HA concentrations to establish if a reduced HA environment confers protection against premature senescence i.e. can we prolong the proliferative lifespan of fibroblasts and hence extend senescence?

There is a current focus on the role of hyaladherins, such as IαI, TSG-6 and versican, in regulating HA pericellular coat formation. Recent published data suggests that the balance between theses hyaladherins maintains an equilibrium that regulars the assembly of the pericellular coat [193, 194, 248]. Mechanisms which regulate HA binding proteins like TSG-6 may present alternative therapeutic targets for the control of HA coat formation and regulation of TGF-β1-dependent wound healing responses.

(6) The data indicate that the affect of TGF-β1 on myofibroblast differentiation and HA generation is mediated through EGF-R signalling. Our data suggest that EGF-R activation can occur through either of two mechanisms. The first involves direct interaction with EGF leading to HAS2 induction. The second involves interaction with CD44 and is mediated by HA. Previous workers from this laboratory have shown that the accumulation of HA that occurs alongside fibroblast to myofibroblast differentiation was associated with re-localisation of CD44, from a punctuate distribution to a more diffuse staining pattern [266]. The functional consequences of these observations were not determined. Here I have shown that in addition to re-localisation, CD44 physically associates with EGF-R. Redistribution of cell surface CD44 may well facilitate this process. Accordingly age-dependent failure of CD44-EGF-R interaction was associated with age-dependent failure of CD44 localisation. Webber et al. demonstrated in lung fibroblasts that CD44 re-localisation coincided with a redistribution of ALK5 (TGFRI) from lipid rafts [161]. In HeLa, A431 and Hep2 cells, EGF-R localises to lipid-rafts on the cell-surface and this sequesters a fraction of the receptors in a state inaccessible to ligand binding [376]. Furthermore, cholesterol depletion of the plasma membrane of HaCaT cells releases EGF-R to discrete areas on the membrane where they become activated [377]. Which (if any) of these mechanisms are operative in primary dermal fibroblasts and myofibroblasts, is not known. It would be interesting to investigate the cellular localisation (lipid-raft, non-raft or cytoskeletal-associated) of CD44 and EGF-R associated with the young and aged phenotypes to test the theory that CD44 relocalisation coincides with increased trafficking to lipid raft-associated pools where it associates with EGF-R [209].

Mature human EGF-R is a 170-kDa transmembrane glycoprotein composed of a single polypeptide chain of 1186 amino acid residues [378]. Alteration in EGF-R expression is frequently associated with malignant transformation of epithelial tissues, including oral mucosa. It was revealed that there is a truncated EGF-R mRNA (~1.5-kb) in oral squamous cell carcinoma cell lines and in all keratinocyte cell lines [378]. The potential biological relevance of the truncated receptor are currently being explored. One potential mechanism is that the truncated EGF-R may be able to form inactive heterodimers with the cell surface EGF-R and interfere with signal transduction. In

A431 cells, soluble truncated EGF-R has been shown to inhibit tyrosine kinase activity of the transmembrane receptor [379]. If this hypothesis is true, then it is interesting to speculate that the full-length EGF-R/truncated EGF-R ratio would be critical in EGF-R activation. This truncated EGF-R has been reported to span 53 kDa - 100 kDa [378]. I have demonstrated in dermal fibroblasts that anti-CD44-mediated young immunoprecipitation followed by anti-EGF-R immunoblotting revealed a single band at ~160kDa with no additional lower molecular weight bands so it is safe to presume this corresponded with the full length EGF-R. Whilst immunoprecipitation of CD44 and EGF-R was not performed in aged cells, it is interesting to predict detection of a lower molecular weight band corresponding to truncated EGF-R. An age-dependent increase in truncated EGF-R could provide an additional mechanism for diminished EGF-R activity.

(7) When phosphorylated, ERK can either phosphorylate a number of cytoplasmic targets or may translocate to the nucleus and activate transcription factors such as c-fos, Elk-1 [343] and STAT3. STAT3 activation by ERK has been reported to facilitate expression of HAS2, hyaluronan synthesis, and CD44 expression in epidermal keratinocytes [343, 380]. It is interesting to speculate that transcription of factors such as STAT3 downstream from ERK activation may be partly responsible for EGF-R dependent HAS2 induction (stage 4). This could provide an explanation for the rapid activation of ERK that was observed in chapter 5.

Preliminary work in this laboratory has demonstrated that in a HA-rich environment early and late ERK1/2 activation results in a proliferative response to TGF- β 1, whilst in a non-HA rich environment only early ERK1/2 activation occurs resulting in an anti-proliferative response to TGF- β 1. Further investigation is needed therefore to decipher the biphasic nature of ERK1/2 activation in my system. It is interesting to speculate that early activation of ERK1/2 is involved in HAS2 induction leading to a HA-rich environment which facilitates further activation of ERK1/2 (late) required for TGF- β 1 mediated responses.

- **(8)** Several studies indicate that the intracellular domain of CD44 selectively interacts with the intracellular actin cytoskeleton [207] which provides a direct transmembrane linkage between HA and the cytoskeleton. Much of the interest in HA has arisen from its association with pathological processes, particularly cancer [214]. HA-mediated transmembrane interactions between CD44 isoforms and cytoskeletal proteins such as ankyrin [203], filamin [205, 206] and cortactin [336] have been reported to play a pivotal role in regulating tumour cell behaviour. The work from this thesis has described that phenotypic activation is dependent on at least one signalling pathway downstream of HA-CD44 targets (i.e. CaMKII) which can regulate cytoskeletal organisation. Whilst still inconclusive, the current data does supports a functional role of the HA coat in regulating the actin cytoskeletal activities in my model. In Chapters 3 & 4 I demonstrated that changes in HA modulate fibroblast phenotype and in Chapter 5 I show that an intact cytoskeleton is important for maintenance of the HA pericellular coat. Collectively these data enables us to speculate that both inside-out and outside-in communication patterns are likely to be occurring such that there is a constant flow of information to and from the cell and its surrounding HA matrix. Admittedly, further clarification is needed to elucidate what other signalling pathways are involved in HA-CD44-EGF-R modulation of the cytoskeleton and how these may be altered with in-vitro aging.
- Work by ION, and others have demonstrated that cross-talk between ERK MAP kinase and Smad signalling pathways may enhance TGF- β 1 dependent responses in other cell systems [315, 381]. The mitogen-activated protein kinases, ERK are involved in TGF- β 1 signalling via cross-talking with the Smad pathway required for fibroblast differentiation [382] and migration [383]. To my knowledge this is the first time that the synergistic involvement of these signalling pathways has been implicated in the impaired regulation of dermal fibroblast-myofibroblast activation in the context of cellular aging. This raises the question how ERK1/2 signalling and Smad signalling finally converge on the gene level to up-regulate α -SMA and phenotypic activation? Proteins from the MAP Kinase pathway have been shown to modify the outcome of Smad signalling through several means. They are capable of altering phosphorylation of the Smads [384]. However, this is unlikely to occur in my system as I have previously

shown that Smad phosphorylation is similar in young and aged fibroblast phenotypes. They may serve to regulate the capacity of Smad proteins to translocate to the nucleus [385]. They are also capable of physically interacting with transcription factors, thus regulating transcription of Smad target proteins in the nucleus [386, 387]. Further investigation is therefore required to elucidate potential interaction between the MAPK/Smad pathways, and to determine signalling events downstream of Smad2 and ERK1/2 phosphorylation to delineate the kinetics involved in the regulation of fibroblast differentiation by TGF-β1.

This data indicates that decreased functioning in aged cells is not due to a global deficit but to specific deficits and the results highlight EGF-R and HAS2 expression as markers of age-related alterations in the fibroblast cell proteome. This begs the question as to why cellular activities and proteome makeup are altered such that EGF-R levels for example are diminished in the face of *in-vitro* aging whilst Smad proteins for example remain constant. If it was a senescent-associated mechanism, i.e. to prevent replication, it would be more advantageous to alter cyclin activation at a key point of convergence further downstream. Thus, it seems there is a need to suppress immediate postreceptor signalling at the EGF-R and limit both genetic and epigenetic responses. Although a general mechanism for the limited responsiveness of aged cells has yet to be established, this body of work ascribes to the 'gate theory' of aging [388], which states that the membrane might play the role as the 'gate' to modulate the signals for the aging phenotype. Hence in my model, EGF-R and HAS2 can be thought of as 'gatekeeper' molecules in this respect because they represent potential targets for modulating the aging process. Accordingly, the results clearly demonstrate the possibility of reversing the aged phenotype, to the functionally active young phenotype, by restoration of membrane signalling apparatus i.e. EGF-R and HAS2.

What are the actual ramifications of these findings for age related wound healing? During aging dermal fibroblasts lose both proliferative and basal migrative capacity [67] and to this we can now add capacity for myofibroblastic differentiation. The end result is delayed or incomplete wound healing in aged adults. To compensate, in the past, growth factors have been used in clinical trials as adjuvants in non-healing

wounds, but as I alluded to in my opening paragraph, with limited success [35]. Such findings are not surprising having demonstrated in this body of work that age-related resistance to myofibroblastic conversion can be explained not by impaired growth factor availability but by intrinsic cellular defects. These data demonstrate that reduced responsiveness to TGF-β1 results from deficits in the apparatus required for cell surface receptor-mediated signal transduction (EGF-R) and matrix remodelling (HAS2). Hence one can imagine that in a wound environment as fibroblasts rapidly approach senescence upon mitogenesis the addition of growth factors like TGF-\$1 would not compensate for inherent impaired cellular activities. One must be careful in applying the results of the findings from in-vitro experiments to in vivo clinical problems however the implications of this study are that interventions to improve healing in aged skin need to be targeted toward improving cell responsiveness by enhancing cell signalling and augmenting the cell response. My data thus support the use of EGF-R and HAS2 gene transfer to non-healing wounds in the elderly as a more rationale therapy than application of growth factors, since the rate limiting step is receptor/synthase signalling and not factor availability (although EGF was shown to be reduced in aged cells).

Because the duration of aging in humans makes it almost impossible to perform *in-vivo* studies, for now fibroblast cultures remain a powerful model for aging-related studies [35, 55, 284]. However, perhaps alternative methodologies to cellular senescence are necessary to study the essence of cellular changes with age, for example an association appears to exist between cellular stress resistance and organismal aging (reviewed in [54]. Probably the biggest difference between *in-vivo* and *in-vitro* conditions is that cells in culture are deprived of interactions with other cell types and the release of growth factors and hormones. For instance differences in cell behaviour have been reported between 2-D and 3-D culture systems, showing how the microenvironment is essential to cell behaviour and function [389]. The next logical step would be to apply this *in-vitro* model into a 3-D culture system. The use of fibroblast-populated collagen lattices and organotypic models for example have proved effective in providing a more *in-vivo* like environment whilst avoiding some of the uncontrollable variables associated with whole animal studies [222, 390]. Loss of capacity for senescence is, of course, a necessary step for immortalization and, ultimately, transformation into a malignant

phenotype [54]. Beyond the context of age-related wound healing this model may also prove useful in studies of the relationship between replicative aging, HA and tumorigenesis.

The work outlined in this thesis has identified a novel functional relationship between CD44 and EGF-R in dermal fibroblasts that is mediated through interactions with the HA dependent pericellular coat. The obvious implication of this system is the capacity for HA to regulate cellular phenotype. The data suggests this may be achieved through interactions with the actin cytoskeleton. The proposed model provides new insights not only into the mode by which HA may facilitate cellular differentiation but also how modifying their matrix environment with aging, dermal fibroblasts can acquire a more susceptible phenotype that promotes defective wound healing. In conclusion, this work demonstrates intrinsic deficits in EGF-R signalling are responsible for the changes in HA synthesis, organisation and assembly observed with *in-vitro* aging and ultimately this confers resistance to TGF-β1 mediated fibroblast-myofibroblast differentiation. The proposed mechanism should not be considered as an endpoint, but rather, one that provides a blueprint for future investigations. Further studies to elucidate details of these pathways should provide new opportunities for modifying the wound healing response and for ameliorating clinical conditions that involve age-related complications.

References

- 1. Tran, K.T., et al., Aging-related attenuation of EGF receptor signaling is mediated in part by increased protein tyrosine phosphatase activity. Experimental Cell Research, 2003. **289**(2): p. 359-367.
- 2. Gosain, A. and L.A. DiPietro, *Aging and wound healing*. World J Surg, 2004. **28**(3): p. 321-6.
- 3. Ashcroft, G.S., S.J. Mills, and J.J. Ashworth, *Ageing and wound healing*. Biogerontology, 2002. **3**(6): p. 337-45.
- 4. McMahon, D.J., C.W. Schwab, and D. Kauder, *Comorbidity and the elderly trauma patient*. World J Surg, 1996. **20**(8): p. 1113-9; discussion 1119-20.
- 5. Pittman, J., Effect of aging on wound healing: current concepts. J Wound Ostomy Continence Nurs, 2007. 34(4): p. 412-5; quiz 416-7.
- 6. Martin, P., Wound healing--aiming for perfect skin regeneration. Science, 1997. **276**(5309): p. 75-81.
- 7. Singer, A.J. and R.A. Clark, *Cutaneous wound healing*. N Engl J Med, 1999. **341**(10): p. 738-46.
- 8. DiPietro, L.A., et al., MIP-1alpha as a critical macrophage chemoattractant in murine wound repair. The Journal of Clinical Investigation, 1998. 101(8): p. 1693-1698.
- 9. Ross, R. and E.P. Benditt, Wound healing and collagen formation. II. Fine structure in experimental scurvy. J Cell Biol, 1962. 12: p. 533-51.
- 10. Hunt, T.K., et al., Studies on inflammation and wound healing: angiogenesis and collagen synthesis stimulated in vivo by resident and activated wound macrophages. Surgery, 1984. 96(1): p. 48-54.
- 11. Yonezawa, Y., H. Kondo, and T.A. Nomaguchi, Age-related changes in serotonin content and its release reaction of rat platelets. Mechanisms of Ageing and Development, 1989. 47(1): p. 65-75.
- 12. Silverman, E.M. and A.G. Silverman, *Granulocyte adherence in the elderly*. Am J Clin Pathol, 1977. **67**(1): p. 49-52.
- 13. Rivard, A., et al., Age-dependent impairment of angiogenesis. Circulation, 1999. **99**(1): p. 111-20.
- 14. Cohen, B.J., R.G. Cutler, and G.S. Roth, Accelerated wound repair in old deer mice (Peromyscus maniculatus) and white-footed mice (Peromyscus leucopus). J Gerontol, 1987. 42(3): p. 302-7.
- 15. Lipschitz, D.A. and K.B. Udupa, *Influence of aging and protein deficiency on neutrophil function*. J Gerontol, 1986. **41**(6): p. 690-4.
- 16. Ashcroft, G.S., M.A. Horan, and M.W. Ferguson, Aging is associated with reduced deposition of specific extracellular matrix components, an upregulation of angiogenesis, and an altered inflammatory response in a murine incisional wound healing model. J Invest Dermatol, 1997. 108(4): p. 430-7.
- 17. Swift, M.E., et al., Age-related alterations in the inflammatory response to dermal injury. J Invest Dermatol, 2001. 117(5): p. 1027-35.

- 18. Danon, D., M.A. Kowatch, and G.S. Roth, *Promotion of wound repair in old mice by local injection of macrophages*. Proc Natl Acad Sci U S A, 1989. **86**(6): p. 2018-20.
- 19. Ashcroft, G.S., et al., Estrogen accelerates cutaneous wound healing associated with an increase in TGF-betal levels. Nat Med, 1997. 3(11): p. 1209-15.
- 20. Swift, M.E., H.K. Kleinman, and L.A. DiPietro, *Impaired wound repair and delayed angiogenesis in aged mice*. Lab Invest, 1999. **79**(12): p. 1479-87.
- 21. Puolakkainen, P.A., et al., The enhancement in wound healing by transforming growth factor-beta 1 (TGF-beta 1) depends on the topical delivery system. J Surg Res, 1995. 58(3): p. 321-9.
- 22. Plisko, A. and B.A. Gilchrest, *Growth factor responsiveness of cultured human fibroblasts declines with age.* J Gerontol, 1983. **38**(5): p. 513-8.
- 23. Reed, M.J., N.S. Ferara, and R.B. Vernon, *Impaired migration, integrin function, and actin cytoskeletal organization in dermal fibroblasts from a subset of aged human donors.* Mech Ageing Dev, 2001. **122**(11): p. 1203-20.
- 24. West, M.D., *The cellular and molecular biology of skin aging*. Arch Dermatol, 1994. **130**(1): p. 87-95.
- 25. Bruce, S.A. and S.F. Deamond, Longitudinal study of in vivo wound repair and in vitro cellular senescence of dermal fibroblasts. Exp Gerontol, 1991. **26**(1): p. 17-27.
- 26. Butcher, E.O. and J. Klingsberg, *Age, gonadectomy, and wound healing in the palatal mucosa of the rat.* Oral Surg Oral Med Oral Pathol, 1963. **16**: p. 484-93.
- 27. Billingham, R.E. and P.S. Russell, Studies on wound healing, with special reference to the phenomenon of contracture in experimental wounds in rabbits' skin. Ann Surg, 1956. 144(6): p. 961-81.
- 28. Billingham, R.E. and P.S. Russell, *Incomplete wound contracture and the phenomenon of hair neogenesis in rabbits' skin.* Nature, 1956. 177(4513): p. 791-2.
- 29. Fatah, M.F. and C.M. Ward, The morbidity of split-skin graft donor sites in the elderly: the case for mesh-grafting the donor site. Br J Plast Surg, 1984. 37(2): p. 184-90.
- 30. Yamaura, H. and T. Matsuzawa, *Decrease in capillary growth during aging*. Exp Gerontol, 1980. **15**(2): p. 145-50.
- 31. Arthur, W.T., et al., Growth factors reverse the impaired sprouting of microvessels from aged mice. Microvasc Res, 1998. 55(3): p. 260-70.
- 32. Kramer, R.H., et al., Synthesis of extracellular matrix glycoproteins by cultured microvascular endothelial cells isolated from the dermis of neonatal and adult skin. J Cell Physiol, 1985. 123(1): p. 1-9.
- 33. Ashcroft, G.S., et al., Human ageing impairs injury-induced in vivo expression of tissue inhibitor of matrix metalloproteinases (TIMP)-1 and -2 proteins and mRNA. J Pathol, 1997. 183(2): p. 169-76.
- 34. Ashcroft, G.S., et al., Age-related differences in the temporal and spatial regulation of matrix metalloproteinases (MMPs) in normal skin and acute cutaneous wounds of healthy humans. Cell Tissue Res, 1997. **290**(3): p. 581-91.
- 35. Shiraha, H., et al., Aging Fibroblasts Present Reduced Epidermal Growth Factor (EGF) Responsiveness Due to Preferential Loss of EGF Receptors. J Biol Chem, 2000. 275(25): p. 19343-19351.

- 36. Ashcroft, G.S., M.A. Horan, and M.W. Ferguson, The effects of ageing on wound healing: immunolocalisation of growth factors and their receptors in a murine incisional model. J Anat, 1997. 190 (Pt 3): p. 351-65.
- 37. Bauer, E.A., et al., Diminished response of Werner's syndrome fibroblasts to growth factors PDGF and FGF. Science, 1986. 234(4781): p. 1240-3.
- 38. Ashcroft, G.S., et al., Age-related changes in the temporal and spatial distributions of fibrillin and elastin mRNAs and proteins in acute cutaneous wounds of healthy humans. J Pathol, 1997. 183(1): p. 80-9.
- 39. Pieraggi, M.T., et al., [The fibroblast]. Ann Pathol, 1985. 5(2): p. 65-76.
- 40. Pienta, K.J. and D.S. Coffey, Characterization of the subtypes of cell motility in ageing human skin fibroblasts. Mech Ageing Dev, 1990. **56**(2): p. 99-105.
- 41. Albini, A., et al., Decline of fibroblast chemotaxis with age of donor and cell passage number. Coll Relat Res, 1988. 8(1): p. 23-37.
- 42. Kondo, H., T.A. Nomaguchi, and Y. Yonezawa, Effects of serum from human subjects of different ages on migration in vitro of human fibroblasts. Mech Ageing Dev, 1989. 47(1): p. 25-37.
- 43. Shevitz, J., C.S. Jenkins, and V.B. Hatcher, *Fibronectin synthesis and degradation in human fibroblasts with aging*. Mech Ageing Dev, 1986. **35**(3): p. 221-32.
- 44. Muggleton-Harris, A.L., P.S. Reisert, and R.L. Burghoff, In vitro characterization of response to stimulus (wounding) with regard to ageing in human skin fibroblasts. Mech Ageing Dev, 1982. 19(1): p. 37-43.
- 45. Gibson, J.M., S.B. Milam, and R.J. Klebe, *Late passage cells display an increase in contractile behavior*. Mech Ageing Dev, 1989. **48**(2): p. 101-10.
- 46. Sussman, M.D., Aging of connective tissue: physical properties of healing wounds in young and old rats. Am J Physiol, 1973. 224(5): p. 1167-71.
- 47. Quirinia, A. and A. Viidik, The influence of age on the healing of normal and ischemic incisional skin wounds. Mech Ageing Dev, 1991. **58**(2-3): p. 221-32.
- 48. Lovell, C.R., et al., Type I and III collagen content and fibre distribution in normal human skin during ageing. Br J Dermatol, 1987. 117(4): p. 419-28.
- 49. Stephens, P., et al., An analysis of replicative senescence in dermal fibroblasts derived from chronic leg wounds predicts that telomerase therapy would fail to reverse their disease-specific cellular and proteolytic phenotype. Experimental Cell Research, 2003. 283(1): p. 22-35.
- 50. Fisher, G.J., et al., *Pathophysiology of premature skin aging induced by ultraviolet light*. N Engl J Med, 1997. **337**(20): p. 1419-28.
- 51. Campisi, J., *The role of cellular senescence in skin aging*. J Investig Dermatol Symp Proc, 1998. **3**(1): p. 1-5.
- 52. Dimri, G.P., et al., A biomarker that identifies senescent human cells in culture and in aging skin in vivo. Proc Natl Acad Sci U S A, 1995. 92(20): p. 9363-7.
- 53. Hayflick, L. and P.S. Moorhead, *The serial cultivation of human diploid cell strains*. Exp Cell Res, 1961. **25**: p. 585-621.
- 54. Pedro de Magalhaes, J., From cells to ageing: a review of models and mechanisms of cellular senescence and their impact on human ageing. Experimental Cell Research, 2004. **300**(1): p. 1-10.
- 55. Cristofalo, V.J., et al., Relationship between donor age and the replicative lifespan of human cells in culture: A reevaluation. Proc Natl Acad Sci U S A, 1998. 95(18): p. 10614-10619.

- 56. Cristofalo, V.J. and R.J. Pignolo, *Molecular markers of senescence in fibroblast-like cultures*. Experimental Gerontology, 1996. **31**(1-2): p. 111-123.
- 57. Itahana, K., J. Campisi, and G.P. Dimri, *Mechanisms of cellular senescence in human and mouse cells*. Biogerontology, 2004. 5(1): p. 1-10.
- 58. Di Leonardo, A., et al., DNA damage triggers a prolonged p53-dependent G1 arrest and long-term induction of Cip1 in normal human fibroblasts. Genes Dev, 1994. 8(21): p. 2540-51.
- 59. Marcotte, R. and E. Wang, Replicative Senescence Revisited. 2002. p. B257-269.
- 60. Kipling, D., *Telomeres, replicative senescence and human ageing.* Maturitas, 2001. **38**(1): p. 25-37; discussion 37-8.
- 61. Mondello, C., et al., Telomere length in fibroblasts and blood cells from healthy centenarians. Exp Cell Res, 1999. **248**(1): p. 234-42.
- 62. Campisi, J., Cellular senescence as a tumor-suppressor mechanism. Trends Cell Biol, 2001. 11(11): p. S27-31.
- 63. Campisi, J., From cells to organisms: can we learn about aging from cells in culture? Exp Gerontol, 2001. 36(4-6): p. 607-18.
- 64. Campisi, J., et al., Cellular senescence, cancer and aging: the telomere connection. Exp Gerontol, 2001. 36(10): p. 1619-37.
- de Magalhaes, J.P., et al., No increase in senescence-associated betagalactosidase activity in Werner syndrome fibroblasts after exposure to H2O2. Ann N Y Acad Sci, 2004. 1019: p. 375-8.
- 66. Tesco, G., et al., Growth Properties and Growth Factor Responsiveness in Skin Fibroblasts from Centenarians. Biochemical and Biophysical Research Communications, 1998. 244(3): p. 912-916.
- 67. Ashcroft, G.S., M.A. Horan, and M.W. Ferguson, *The effects of ageing on cutaneous wound healing in mammals.* J Anat, 1995. **187 (Pt 1)**: p. 1-26.
- 68. Hinz, B., Formation and Function of the Myofibroblast during Tissue Repair. J Invest Dermatol, 2007. 127(3): p. 526-537.
- 69. Ellis, I.R. and S.L. Schor, Differential Effects of TGF-[beta]1 on Hyaluronan Synthesis by Fetal and Adult Skin Fibroblasts: Implications for Cell Migration and Wound Healing. Experimental Cell Research, 1996. 228(2): p. 326-333.
- 70. Hinz, B., et al., *The myofibroblast: one function, multiple origins*. Am J Pathol, 2007. **170**(6): p. 1807-16.
- 71. Rajkumar, V.S., et al., Shared expression of phenotypic markers in systemic sclerosis indicates a convergence of pericytes and fibroblasts to a myofibroblast lineage in fibrosis. Arthritis Res Ther, 2005. 7(5): p. R1113-23.
- 72. Desmouliere, A., C. Chaponnier, and G. Gabbiani, *Tissue repair, contraction, and the myofibroblast.* Wound Repair and Regeneration, 2005. **13**(1): p. 7-12.
- 73. Meyer-ter-Vehn, T., et al., Contractility as a Prerequisite for TGF-{beta}-Induced Myofibroblast Transdifferentiation in Human Tenon Fibroblasts. 2006. p. 4895-4904.
- 74. Tomasek, J.J., et al., Myofibroblasts and mechano-regulation of connective tissue remodelling. Nat Rev Mol Cell Biol, 2002. 3(5): p. 349-63.
- 75. Hinz, B. and G. Gabbiani, *Mechanisms of force generation and transmission by myofibroblasts*. Curr Opin Biotechnol, 2003. **14**(5): p. 538-46.
- 76. Wang, J., R. Zohar, and C.A. McCulloch, *Multiple roles of alpha-smooth muscle actin in mechanotransduction*. Exp Cell Res, 2006. **312**(3): p. 205-14.

- 77. Critchley, D.R., Focal adhesions the cytoskeletal connection. Curr Opin Cell Biol, 2000. **12**(1): p. 133-9.
- 78. Watterson, K.R., et al., Regulation of fibroblast functions by lysophospholipid mediators: Potential roles in wound healing. Wound Repair and Regeneration, 2007. 15(5): p. 607-616.
- 79. Gabbiani, G., *The myofibroblast in wound healing and fibrocontractive diseases*. J Pathol, 2003. **200**(4): p. 500-3.
- 80. Moulin, V., et al., Modulated Response to Cytokines of Human Wound Healing Myofibroblasts Compared to Dermal Fibroblasts. Experimental Cell Research, 1998. 238(1): p. 283-293.
- 81. Eyden, B., Electron microscopy in the study of myofibroblastic lesions. Semin Diagn Pathol, 2003. 20(1): p. 13-24.
- 82. Ronnov-Jessen, L., et al., The origin of the myofibroblasts in breast cancer. Recapitulation of tumor environment in culture unravels diversity and implicates converted fibroblasts and recruited smooth muscle cells. J Clin Invest, 1995. 95(2): p. 859-73.
- 83. Shephard, P., et al., Myofibroblast Differentiation Is Induced in Keratinocyte-Fibroblast Co-Cultures and Is Antagonistically Regulated by Endogenous Transforming Growth Factor-{beta} and Interleukin-1. 2004. p. 2055-2066.
- 84. Chipev, C.C. and M. Simon, Phenotypic differences between dermal fibroblasts from different body sites determine their responses to tension and TGFbeta1. BMC Dermatol, 2002. 2: p. 13.
- 85. Serini, G. and G. Gabbiani, *Mechanisms of myofibroblast activity and phenotypic modulation*. Exp Cell Res, 1999. **250**(2): p. 273-83.
- 86. Stephens, P., et al., Skin and oral fibroblasts exhibit phenotypic differences in extracellular matrix reorganization and matrix metalloproteinase activity. Br J Dermatol, 2001. 144(2): p. 229-237.
- 87. Grinnell, F., Fibroblasts, myofibroblasts, and wound contraction. J Cell Biol, 1994. 124(4): p. 401-4.
- 88. Murphy, G. and A.J. Docherty, *The matrix metalloproteinases and their inhibitors*. Am J Respir Cell Mol Biol, 1992. 7(2): p. 120-5.
- 89. Kondo, S., *The roles of cytokines in photoaging*. J Dermatol Sci, 2000. **23 Suppl** 1: p. S30-6.
- 90. Darby, I., O. Skalli, and G. Gabbiani, Alpha-smooth muscle actin is transiently expressed by myofibroblasts during experimental wound healing. Lab Invest, 1990. 63(1): p. 21-9.
- 91. Maltseva, O., et al., Fibroblast growth factor reversal of the corneal myofibroblast phenotype. Invest Ophthalmol Vis Sci, 2001. 42(11): p. 2490-5.
- 92. Komuro, T., *Re-evaluation of fibroblasts and fibroblast-like cells*. Anat Embryol (Berl), 1990. **182**(2): p. 103-12.
- 93. Koumas, L., et al., Fibroblast Heterogeneity: Existence of Functionally Distinct Thy 1+ and Thy 1- Human Female Reproductive Tract Fibroblasts. Am J Pathol, 2001. **159**(3): p. 925-935.
- 94. Wall, I.B., et al., Fibroblast Dysfunction Is a Key Factor in the Non-Healing of Chronic Venous Leg Ulcers. J Invest Dermatol, 2008.
- 95. Shannon, D.B., et al., Phenotypic differences between oral and skin fibroblasts in wound contraction and growth factor expression. Wound Repair Regen, 2006. 14(2): p. 172-8.

- 96. Megan, E.S., et al., Site-specific production of $TGF-\beta$; in oral mucosal and cutaneous wounds. Wound Repair and Regeneration, 2008. **16**(1): p. 80-86.
- 97. Rolfe, K.J., et al., Differential gene expression in response to transforming growth factor-β1 by fetal and postnatal dermal fibroblasts. Wound Repair and Regeneration, 2007. **15**(6): p. 897-906.
- 98. Lorenz, H.P., et al., *The fetal fibroblast: the effector cell of scarless fetal skin repair.* Plast Reconstr Surg, 1995. **96**(6): p. 1251-9; discussion 1260-1.
- 99. Rolfe, K.J., et al., A role for TGF-beta1-induced cellular responses during wound healing of the non-scarring early human fetus? J Invest Dermatol, 2007. 127(11): p. 2656-67.
- 100. Mogford, J.E., et al., Effect of age and hypoxia on TGFbetal receptor expression and signal transduction in human dermal fibroblasts: impact on cell migration. Journal of Cell Physiology, 2002. 190(2): p. 259-65.
- 101. Chin, D., et al., What is transforming growth factor-beta (TGF-[beta])? British Journal of Plastic Surgery, 2004. 57(3): p. 215-221.
- 102. Schrementi, M.E., et al., Site-specific production of TGF- betal; in oral mucosal and cutaneous wounds. Wound Repair and Regeneration, 2008. 16(1): p. 80-86.
- 103. Jakowlew, S.B., et al., Differential regulation of the expression of transforming growth factor-beta mRNAs by growth factors and retinoic acid in chicken embryo chondrocytes, myocytes, and fibroblasts. J Cell Physiol, 1992. **150**(2): p. 377-85.
- 104. Villiger, P.M. and M. Lotz, Differential expression of TGF beta isoforms by human articular chondrocytes in response to growth factors. J Cell Physiol, 1992. 151(2): p. 318-25.
- 105. Piek, E., C.H. Heldin, and P. Ten Dijke, Specificity, diversity, and regulation in TGF-beta superfamily signaling. Faseb J, 1999. 13(15): p. 2105-24.
- 106. Leask, A. and D.J. Abraham, TGF-{beta} signaling and the fibrotic response. FASEB J, 2004. 18(7): p. 816-827.
- 107. Roberts, A.B., *Molecular and cell biology of TGF-beta*. Miner Electrolyte Metab, 1998. **24**(2-3): p. 111-9.
- 108. Roberts, A.B., et al., Transforming growth factor type beta: rapid induction of fibrosis and angiogenesis in vivo and stimulation of collagen formation in vitro. Proc Natl Acad Sci U S A, 1986. 83(12): p. 4167-71.
- 109. Kagami, S., et al., Coordinated expression of beta 1 integrins and transforming growth factor-beta-induced matrix proteins in glomerulonephritis. Lab Invest, 1993. **69**(1): p. 68-76.
- 110. Desmoulière, A., Factors influencing myofibroblast differentiation during wound healing and fibrosis. Cell Biology International, 1995. 19(5): p. 471-471.
- 111. Desmouliere, A., et al., Transforming growth factor-beta 1 induces alphasmooth muscle actin expression in granulation tissue myofibroblasts and in quiescent and growing cultured fibroblasts. J. Cell Biol., 1993. 122(1): p. 103-111.
- 112. Evans, R.A., et al., TGF-[beta]1-mediated fibroblast-myofibroblast terminal differentiation--the role of smad proteins. Experimental Cell Research, 2003. 282(2): p. 90-100.
- 113. Massague, J., TGF-beta signal transduction. Annu Rev Biochem, 1998. 67: p. 753-91.

- 114. Shull, M.M., et al., Targeted disruption of the mouse transforming growth factor-beta 1 gene results in multifocal inflammatory disease. Nature, 1992. 359(6397): p. 693-9.
- 115. Hogan, B.L., Bone morphogenetic proteins: multifunctional regulators of vertebrate development. Genes Dev, 1996. 10(13): p. 1580-94.
- 116. Kingsley, D.M., The TGF-beta superfamily: new members, new receptors, and new genetic tests of function in different organisms. Genes Dev, 1994. 8(2): p. 133-46.
- 117. Pannu, J., et al., An increased transforming growth factor beta receptor type I:type II ratio contributes to elevated collagen protein synthesis that is resistant to inhibition via a kinase-deficient transforming growth factor beta receptor type II in scleroderma. Arthritis Rheum, 2004. 50(5): p. 1566-77.
- 118. Evans, R.A., et al., TGF-beta1-mediated fibroblast-myofibroblast terminal differentiation-the role of Smad proteins. Exp Cell Res, 2003. 282(2): p. 90-100.
- 119. Desmouliere, A., et al., Transforming growth factor-beta 1 induces alphasmooth muscle actin expression in granulation tissue myofibroblasts and in quiescent and growing cultured fibroblasts. J Cell Biol, 1993. 122(1): p. 103-11.
- 120. Vaughan, M.B., E.W. Howard, and J.J. Tomasek, Transforming growth factor-beta1 promotes the morphological and functional differentiation of the myofibroblast. Exp Cell Res, 2000. 257(1): p. 180-9.
- 121. Border, W.A. and E. Ruoslahti, *Transforming growth factor-beta in disease: the dark side of tissue repair.* J Clin Invest, 1992. **90**(1): p. 1-7.
- 122. Leask, A., *TGFbeta, cardiac fibroblasts, and the fibrotic response*. Cardiovasc Res, 2007. **74**(2): p. 207-12.
- 123. Okuda, S., et al., Elevated expression of transforming growth factor-beta and proteoglycan production in experimental glomerulonephritis. Possible role in expansion of the mesangial extracellular matrix. J Clin Invest, 1990. **86**(2): p. 453-62.
- 124. Fraser, D., L. Wakefield, and A. Phillips, *Independent regulation of transforming growth factor-beta1 transcription and translation by glucose and platelet-derived growth factor*. Am J Pathol, 2002. **161**(3): p. 1039-49.
- 125. Sanderson, N., et al., Hepatic expression of mature transforming growth factor beta 1 in transgenic mice results in multiple tissue lesions. Proc Natl Acad Sci U S A, 1995. 92(7): p. 2572-6.
- 126. Koch, R.M., et al., *Incisional wound healing in transforming growth factor-betal null mice.* Wound Repair Regen, 2000. **8**(3): p. 179-91.
- 127. Derynck, R. and X.H. Feng, *TGF-beta receptor signaling*. Biochim Biophys Acta, 1997. **1333**(2): p. F105-50.
- 128. Ebner, R., et al., Determination of type I receptor specificity by the type II receptors for TGF-beta or activin. Science, 1993. 262(5135): p. 900-2.
- 129. Moustakas, A. and C.H. Heldin, *Non-Smad TGF-beta signals*. J Cell Sci, 2005. **118**(Pt 16): p. 3573-84.
- 130. Moustakas, A., S. Souchelnytskyi, and C.H. Heldin, *Smad regulation in TGF-beta signal transduction*. J Cell Sci, 2001. **114**(Pt 24): p. 4359-69.
- 131. Massague, J. and D. Wotton, Transcriptional control by the TGF-beta/Smad signaling system. Embo J, 2000. 19(8): p. 1745-54.

- 132. Uemura, M., et al., Smad2 and Smad3 play different roles in rat hepatic stellate cell function and alpha-smooth muscle actin organization. Mol Biol Cell, 2005. **16**(9): p. 4214-24.
- 133. Hu, B., Z. Wu, and S.H. Phan, Smad3 mediates transforming growth factor-beta-induced alpha-smooth muscle actin expression. Am J Respir Cell Mol Biol, 2003. 29(3 Pt 1): p. 397-404.
- 134. Liu, C., et al., Smads 2 and 3 are differentially activated by transforming growth factor-beta (TGF-beta) in quiescent and activated hepatic stellate cells. Constitutive nuclear localization of Smads in activated cells is TGF-beta-independent. J Biol Chem, 2003. 278(13): p. 11721-8.
- 135. Ashcroft, G.S., et al., Mice lacking Smad3 show accelerated wound healing and an impaired local inflammatory response. Nat Cell Biol, 1999. 1(5): p. 260-6.
- 136. Sumiyoshi, K., et al., Exogenous Smad3 Accelerates Wound Healing in a Rabbit Dermal Ulcer Model. J Investig Dermatol, 2003. 123(1): p. 229-236.
- 137. Wang, Y., et al., Smad3 null mice display more rapid wound closure and reduced scar formation after a stab wound to the cerebral cortex. Experimental Neurology, 2007. 203(1): p. 168-184.
- 138. Datto, M.B., et al., Targeted disruption of Smad3 reveals an essential role in transforming growth factor beta-mediated signal transduction. Mol Cell Biol, 1999. 19(4): p. 2495-504.
- 139. Chen, Y., et al., Matrix Contraction by Dermal Fibroblasts Requires Transforming Growth Factor-{beta}/Activin-Linked Kinase 5, Heparan Sulfate-Containing Proteoglycans, and MEK/ERK: Insights into Pathological Scarring in Chronic Fibrotic Disease. 2005. p. 1699-1711.
- 140. Derynck, R. and Y.E. Zhang, Smad-dependent and Smad-independent pathways in TGF-beta family signalling. Nature, 2003. 425(6958): p. 577-84.
- 141. Wilkes, M.C., et al., Transforming growth factor-beta activation of phosphatidylinositol 3-kinase is independent of Smad2 and Smad3 and regulates fibroblast responses via p21-activated kinase-2. Cancer Res, 2005. 65(22): p. 10431-40.
- 142. Tomasek, J.J., et al., Regulation of alpha-smooth muscle actin expression in granulation tissue myofibroblasts is dependent on the intronic CArG element and the transforming growth factor-betal control element. Am J Pathol, 2005. 166(5): p. 1343-51.
- 143. Arany, P.R., et al., Absence of Smad3 confers radioprotection through modulation of ERK-MAPK in primary dermal fibroblasts. Journal of Dermatological Science, 2007. 48(1): p. 35-42.
- 144. Lee, Y.S. and C.M. Chuong, Activation of protein kinase A is a pivotal step involved in both BMP-2- and cyclic AMP-induced chondrogenesis. J Cell Physiol, 1997. 170(2): p. 153-65.
- 145. Wu, L., et al., Transforming growth factor-betal fails to stimulate wound healing and impairs its signal transduction in an aged ischemic ulcer model: importance of oxygen and age. Am J Pathol, 1999. **154**(1): p. 301-9.
- 146. Cromack, D.T., et al., Acceleration of tissue repair by transforming growth factor beta 1: identification of in vivo mechanism of action with radiotherapy-induced specific healing deficits. Surgery, 1993. 113(1): p. 36-42.

- 147. Mustoe, T.A., et al., A phase II study to evaluate recombinant platelet-derived growth factor-BB in the treatment of stage 3 and 4 pressure ulcers. Arch Surg, 1994. 129(2): p. 213-9.
- 148. Kurban, R.S. and J. Bhawan, *Histologic changes in skin associated with aging.* J Dermatol Surg Oncol, 1990. **16**(10): p. 908-14.
- 149. Lavker, R.M., P.S. Zheng, and G. Dong, Aged skin: a study by light, transmission electron, and scanning electron microscopy. J Invest Dermatol, 1987. 88(3 Suppl): p. 44s-51s.
- 150. Ellis, I.R., A.M. Schor, and S.L. Schor, EGF AND TGF-[alpha] motogenic activities are mediated by the EGF receptor via distinct matrix-dependent mechanisms. Experimental Cell Research, 2007. 313(4): p. 732-741.
- 151. Stern, R. and H.I. Maibach, *Hyaluronan in skin: aspects of aging and its pharmacologic modulation*. Clinics in Dermatology, 2008. **26**(2): p. 106-122.
- 152. Almond, A., *Hyaluronan*. Cell Mol Life Sci, 2007. **64**(13): p. 1591-6.
- 153. Stern, R., *Hyaluronan catabolism: a new metabolic pathway*. European Journal of Cell Biology, 2004. **83**(7): p. 317-325.
- 154. Weigel, P.H., V.C. Hascall, and M. Tammi, *Hyaluronan synthases*. J Biol Chem, 1997. **272**(22): p. 13997-4000.
- 155. Reed, R.K., K. Lilja, and T.C. Laurent, *Hyaluronan in the rat with special reference to the skin*. Acta Physiol Scand, 1988. 134(3): p. 405-11.
- 156. Chen, W.Y.J. and G. Abatangelo, *Functions of hyaluronan in wound repair*. Wound Repair and Regeneration, 1999. 7(2): p. 79-89.
- 157. Toole, B.P., *Hyaluronan is not just a goo!* The Journal of Clinical Investigation, 2000. **106**(3): p. 335-336.
- 158. Girish, K.S. and K. Kemparaju, *The magic glue hyaluronan and its eraser hyaluronidase: A biological overview.* Life Sciences, 2007. **80**(21): p. 1921-1943.
- 159. Meran, S., et al., *Involvement of hyaluronan in regulation of fibroblast phenotype*. J Biol Chem, 2007. **282**(35): p. 25687-97.
- 160. Meran, S., et al., Hyaluronan Facilitates Transforming Growth Factor-Î²1-mediated Fibroblast Proliferation. Journal of Biological Chemistry, 2008. **283**(10): p. 6530-6545.
- 161. Webber, J., et al., Modulation of TGFbetal-dependent myofibroblast differentiation by hyaluronan. Am J Pathol, 2009. 175(1): p. 148-60.
- Webber, J., et al., Hyaluronan orchestrates transforming growth factor-betal-dependent maintenance of myofibroblast phenotype. J Biol Chem, 2009. **284**(14): p. 9083-92.
- 163. Toole, B.P., *Hyaluronan in morphogenesis*. Semin Cell Dev Biol, 2001. **12**(2): p. 79-87.
- 164. Longaker, M.T., et al., Studies in fetal wound healing. V. A prolonged presence of hyaluronic acid characterizes fetal wound fluid. Ann Surg, 1991. 213(4): p. 292-6.
- 165. Noble, P.W., *Hyaluronan and its catabolic products in tissue injury and repair*. Matrix Biology, 2002. **21**(1): p. 25-29.
- 166. Toole, B.P., *Hyaluronan promotes the malignant phenotype*. Glycobiology, 2002. **12**(3): p. 37R-42R.

- 167. Stern, R., A.A. Asari, and K.N. Sugahara, *Hyaluronan fragments: An information-rich system*. European Journal of Cell Biology, 2006. **85**(8): p. 699-715.
- 168. Itano, N. and K. Kimata, *Mammalian hyaluronan synthases*. IUBMB Life, 2002. **54**(4): p. 195-9.
- 169. Itano, N., et al., Three isoforms of mammalian hyaluronan synthases have distinct enzymatic properties. J Biol Chem, 1999. 274(35): p. 25085-92.
- 170. Fraser, J.R., T.C. Laurent, and U.B. Laurent, *Hyaluronan: its nature, distribution, functions and turnover.* J Intern Med, 1997. **242**(1): p. 27-33.
- 171. McCourt, P.A., How does the hyaluronan scrap-yard operate? Matrix Biol, 1999. 18(5): p. 427-32.
- 172. Stern, R. and M.J. Jedrzejas, *Hyaluronidases: Their Genomics, Structures, and Mechanisms of Action.* 2006. p. 818-839.
- 173. Bourguignon, L.Y., et al., CD44 interaction with Na+-H+ exchanger (NHE1) creates acidic microenvironments leading to hyaluronidase-2 and cathepsin B activation and breast tumor cell invasion. J Biol Chem, 2004. 279(26): p. 26991-7007.
- 174. Lepperdinger, G., B. Strobl, and G. Kreil, *HYAL2*, a human gene expressed in many cells, encodes a lysosomal hyaluronidase with a novel type of specificity. J Biol Chem, 1998. **273**(35): p. 22466-70.
- 175. Laurent, T.C. and J.R. Fraser, *Hyaluronan*. Faseb J, 1992. 6(7): p. 2397-404.
- 176. Feinberg, R.N. and D.C. Beebe, *Hyaluronate in vasculogenesis*. Science, 1983. **220**(4602): p. 1177-9.
- 177. McBride, W.H. and J.B. Bard, *Hyaluronidase-sensitive halos around adherent cells. Their role in blocking lymphocyte-mediated cytolysis.* J Exp Med, 1979. **149**(2): p. 507-15.
- 178. Delmage, J.M., et al., The selective suppression of immunogenicity by hyaluronic acid. Ann Clin Lab Sci, 1986. 16(4): p. 303-10.
- 179. Jiang, D., J. Liang, and P.W. Noble, *Hyaluronan in Tissue Injury and Repair*. Annu Rev Cell Dev Biol, 2007. **23**(1): p. 435-461.
- 180. Taylor, K.R., et al., Hyaluronan fragments stimulate endothelial recognition of injury through TLR4. J Biol Chem, 2004. 279(17): p. 17079-84.
- 181. Termeer, C.C., et al., Oligosaccharides of hyaluronan are potent activators of dendritic cells. J Immunol, 2000. 165(4): p. 1863-70.
- 182. West, D.C., et al., Fibrotic healing of adult and late gestation fetal wounds correlates with increased hyaluronidase activity and removal of hyaluronan. Int J Biochem Cell Biol, 1997. 29(1): p. 201-10.
- 183. Mackool, R.J., G.K. Gittes, and M.T. Longaker, Scarless healing. The fetal wound. Clin Plast Surg, 1998. 25(3): p. 357-65.
- 184. Powell, J.D. and M.R. Horton, *Threat matrix: low-molecular-weight hyaluronan* (HA) as a danger signal. Immunol Res, 2005. 31(3): p. 207-18.
- 185. Xu, H., et al., Effect of hyaluronan oligosaccharides on the expression of heat shock protein 72. J Biol Chem, 2002. 277(19): p. 17308-14.
- 186. Toole, B.P., Hyaluronan and its binding proteins, the hyaladherins. Curr Opin Cell Biol, 1990. 2(5): p. 839-44.
- 187. Zhao, M., et al., Evidence for the covalent binding of SHAP, heavy chains of inter-alpha-trypsin inhibitor, to hyaluronan. J Biol Chem, 1995. 270(44): p. 26657-63.

- 188. Day, A.J. and G.D. Prestwich, *Hyaluronan-binding proteins: tying up the giant.* J Biol Chem, 2002. **277**(7): p. 4585-8.
- 189. Spicer, A.P., A. Joo, and R.A. Bowling, Jr., A hyaluronan binding link protein gene family whose members are physically linked adjacent to chondroitin sulfate proteoglycan core protein genes: the missing links. J Biol Chem, 2003. 278(23): p. 21083-91.
- 190. Lesley, J., et al., TSG-6 Modulates the Interaction between Hyaluronan and Cell Surface CD44. J Biol Chem, 2004. 279(24): p. 25745-25754.
- 191. Blundell, C.D., et al., Determining the Molecular Basis for the pH-dependent Interaction between the Link Module of Human TSG-6 and Hyaluronan. J Biol Chem, 2007. 282(17): p. 12976-12988.
- 192. Blundell, C.D., et al., Determining the Molecular Basis for the pH-dependent Interaction between the Link Module of Human TSG-6 and Hyaluronan. Journal of Biological Chemistry, 2007. **282**(17): p. 12976-12988.
- 193. Selbi, W., et al., Characterization of hyaluronan cable structure and function in renal proximal tubular epithelial cells. Kidney Int, 2006. **70**(7): p. 1287-1295.
- 194. Selbi, W., et al., Overexpression of Hyaluronan Synthase 2 Alters Hyaluronan Distribution and Function in Proximal Tubular Epithelial Cells. J Am Soc Nephrol, 2006. 17(6): p. 1553-1567.
- 195. Milner, C.M. and A.J. Day, TSG-6: a multifunctional protein associated with inflammation. J Cell Sci, 2003. 116(10): p. 1863-1873.
- 196. Turley, E.A., P.W. Noble, and L.Y.W. Bourguignon, Signaling Properties of Hyaluronan Receptors. J Biol Chem, 2002. 277(7): p. 4589-4592.
- 197. Rouschop, K.M.A., et al., CD44 Disruption Prevents Degeneration of the Capillary Network in Obstructive Nephropathy via Reduction of TGF-betal-Induced Apoptosis. J Am Soc Nephrol, 2006. 17(3): p. 746-753.
- 198. Huebener, P., et al., CD44 Is Critically Involved in Infarct Healing by Regulating the Inflammatory and Fibrotic Response. J Immunol, 2008. 180(4): p. 2625-2633.
- 199. DeGrendele, H.C., P. Estess, and M.H. Siegelman, Requirement for CD44 in activated T cell extravasation into an inflammatory site. Science, 1997. 278(5338): p. 672-5.
- 200. Vachon, E., et al., *CD44 is a phagocytic receptor*. Blood, 2006. **107**(10): p. 4149-58.
- 201. Acharya, P.S., et al., Fibroblast migration is mediated by CD44-dependent TGF{beta} activation. J Cell Sci, 2008. 121(9): p. 1393-1402.
- 202. Zhu, D. and L.Y. Bourguignon, Interaction between CD44 and the repeat domain of ankyrin promotes hyaluronic acid-mediated ovarian tumor cell migration. J Cell Physiol, 2000. 183(2): p. 182-95.
- 203. Bourguignon, L.Y.W., et al., Hyaluronan Promotes Signaling Interaction between CD44 and the Transforming Growth Factor beta Receptor I in Metastatic Breast Tumor Cells. J Biol Chem, 2002. 277(42): p. 39703-39712.
- 204. Bourguignon, L.Y.W., P.A. Singleton, and F. Diedrich, Hyaluronan-CD44 Interaction with Rac1-dependent Protein Kinase N-{gamma} Promotes Phospholipase C{gamma}1 Activation, Ca2+ Signaling, and Cortactin-Cytoskeleton Function Leading to Keratinocyte Adhesion and Differentiation. 2004. p. 29654-29669.

- 205. Bourguignon, L.Y.W., E. Gilad, and K. Peyrollier, Heregulin-mediated ErbB2-ERK Signaling Activates Hyaluronan Synthases Leading to CD44-dependent Ovarian Tumor Cell Growth and Migration. Journal of Biological Chemistry, 2007. 282(27): p. 19426-19441.
- 206. Bourguignon, L.Y.W., et al., Hyaluronan-CD44 Interaction with Leukemia-associated RhoGEF and Epidermal Growth Factor Receptor Promotes Rho/Ras Co-activation, Phospholipase Cϵ-Ca2+ Signaling, and Cytoskeleton Modification in Head and Neck Squamous Cell Carcinoma Cells. Journal of Biological Chemistry, 2006. 281(20): p. 14026-14040.
- 207. Bourguignon, L.Y.W., Hyaluronan-mediated CD44 activation of RhoGTPase signaling and cytoskeleton function promotes tumor progression. Seminars in Cancer Biology, 2008. 18(4): p. 251-259.
- 208. Bourguignon, L.Y., P.A. Singleton, and F. Diedrich, Hyaluronan-CD44 interaction with Rac1-dependent protein kinase N-gamma promotes phospholipase Cgammal activation, Ca(2+) signaling, and cortactin-cytoskeleton function leading to keratinocyte adhesion and differentiation. J Biol Chem, 2004. 279(28): p. 29654-69.
- 209. Ito, T., et al., Hyaluronan Regulates Transforming Growth Factor-{beta}1 Receptor Compartmentalization. J Biol Chem, 2004. 279(24): p. 25326-25332.
- 210. Ito, T., et al., Hyaluronan Attenuates Transforming Growth Factor-{beta}1-Mediated Signaling in Renal Proximal Tubular Epithelial Cells. Am J Pathol, 2004. 164(6): p. 1979-1988.
- 211. Turley, E.A. and S. Roth, *Interactions between the carbohydrate chains of hyaluronate and chondroitin sulphate*. Nature, 1980. **283**(5744): p. 268-71.
- 212. Evanko, S.P., J.C. Angello, and T.N. Wight, Formation of Hyaluronan- and Versican-Rich Pericellular Matrix Is Required for Proliferation and Migration of Vascular Smooth Muscle Cells. Arterioscler Thromb Vasc Biol, 1999. 19(4): p. 1004-1013.
- 213. Evanko, S.P., et al., *Hyaluronan-dependent pericellular matrix*. Advanced Drug Delivery Reviews, 2007. **59**(13): p. 1351-1365.
- 214. Toole, B.P., *Hyaluronan: from extracellular glue to pericellular cue.* Nature Reviews Cancer, 2004. **4**(7): p. 528-539.
- 215. Clarris, B.J. and J.R. Fraser, On the pericellular zone of some mammalian cells in vitro. Exp Cell Res, 1968. 49(1): p. 181-93.
- 216. Evanko, S.P., et al., *Hyaluronan-dependent pericellular matrix*. Advanced Drug Delivery Reviews. **In Press, Corrected Proof**.
- 217. Knudson, C.B., *Hyaluronan receptor-directed assembly of chondrocyte pericellular matrix.* J Cell Biol, 1993. **120**(3): p. 825-34.
- 218. LeBaron, R.G., D.R. Zimmermann, and E. Ruoslahti, *Hyaluronate binding properties of versican*. J Biol Chem, 1992. **267**(14): p. 10003-10.
- 219. Knudson, C.B., Hyaluronan and CD44: strategic players for cell-matrix interactions during chondrogenesis and matrix assembly. Birth Defects Res C Embryo Today, 2003. **69**(2): p. 174-96.
- 220. Bentley, J.P., *Rate of chondroitin sulfate formation in wound healing*. Ann Surg, 1967. **165**(2): p. 186-91.
- 221. Knudson, C.B. and W. Knudson, *Hyaluronan-binding proteins in development, tissue homeostasis, and disease.* Faseb J, 1993. 7(13): p. 1233-41.

- 222. Monslow, J., et al., Wounding-Induced Synthesis of Hyaluronic Acid in Organotypic Epidermal Cultures Requires the Release of Heparin-Binding EGF and Activation of the EGFR. J Invest Dermatol, 2009. 129(8): p. 2046-2058.
- 223. Tammi, R., et al., Hyaluronan synthase induction and hyaluronan accumulation in mouse epidermis following skin injury. J Invest Dermatol, 2005. **124**(5): p. 898-905.
- 224. Feusi, E., et al., Enhanced hyaluronan synthesis in the MRL-Fas(lpr) kidney: role of cytokines. Nephron, 1999. **83**(1): p. 66-73.
- 225. Yung, S., G.J. Thomas, and M. Davies, *Induction of hyaluronan metabolism after mechanical injury of human peritoneal mesothelial cells in vitro*. Kidney Int, 2000. **58**(5): p. 1953-62.
- 226. Bronson, R.E., C.N. Bertolami, and E.P. Siebert, *Modulation of fibroblast growth and glycosaminoglycan synthesis by interleukin-1*. Coll Relat Res, 1987. 7(5): p. 323-32.
- 227. Foschi, D., et al., Hyaluronic acid prevents oxygen free-radical damage to granulation tissue: a study in rats. Int J Tissue React, 1990. 12(6): p. 333-9.
- 228. Barrois, B., et al., Efficacy and tolerability of hyaluronan (ialuset) in the treatment of pressure ulcers: a multicentre, non-randomised, pilot study. Drugs R D, 2007. 8(5): p. 267-73.
- 229. Wisniewski, H.G. and J. Vilcek, TSG-6: an IL-1/TNF-inducible protein with anti-inflammatory activity. Cytokine Growth Factor Rev, 1997. 8(2): p. 143-56.
- 230. David-Raoudi, M., et al., Differential effects of hyaluronan and its fragments on fibroblasts: Relation to wound healing. Wound Repair and Regeneration, 2008. 16(2): p. 274-287.
- 231. de la Motte, C.A., et al., Mononuclear leukocytes bind to specific hyaluronan structures on colon mucosal smooth muscle cells treated with polyinosinic acid:polycytidylic acid: inter-alpha-trypsin inhibitor is crucial to structure and function. Am J Pathol, 2003. 163(1): p. 121-33.
- 232. Frost, S.J. and P.H. Weigel, *Binding of hyaluronic acid to mammalian fibrinogens*. Biochim Biophys Acta, 1990. **1034**(1): p. 39-45.
- West, D.C., et al., Angiogenesis induced by degradation products of hyaluronic acid. Science, 1985. **228**(4705): p. 1324-6.
- 234. Rooney, P., et al., Angiogenic oligosaccharides of hyaluronan enhance the production of collagens by endothelial cells. J Cell Sci, 1993. 105 (Pt 1): p. 213-8.
- 235. Jiang, D., et al., Regulation of lung injury and repair by Toll-like receptors and hyaluronan. Nat Med, 2005. 11(11): p. 1173-9.
- 236. King, S.R., W.L. Hickerson, and K.G. Proctor, *Beneficial actions of exogenous hyaluronic acid on wound healing*. Surgery, 1991. **109**(1): p. 76-84.
- 237. Nakamura, M., M. Hikida, and T. Nakano, Concentration and molecular weight dependency of rabbit corneal epithelial wound healing on hyaluronan. Curr Eye Res, 1992. 11(10): p. 981-6.
- 238. Laurent, C., S. Hellstrom, and L.E. Stenfors, *Hyaluronic acid reduces* connective tissue formation in middle ears filled with absorbable gelatin sponge: an experimental study. Am J Otolaryngol, 1986. 7(3): p. 181-6.
- 239. Balazs, E.A. and J.L. Denlinger, *Clinical uses of hyaluronan*. Ciba Found Symp, 1989. **143**: p. 265-75; discussion 275-80, 281-5.

- 240. Croce, M.A., et al., Hyaluronan affects protein and collagen synthesis by in vitro human skin fibroblasts. Tissue and Cell, 2001. 33(4): p. 326-331.
- 241. Meyer, L.J., et al., Reduced hyaluronan in keloid tissue and cultured keloid fibroblasts. J Invest Dermatol, 2000. 114(5): p. 953-9.
- 242. Meran, S., et al., *Involvement of Hyaluronan in Regulation of Fibroblast Phenotype*. J. Biol. Chem., 2007. **282**(35): p. 25687-25697.
- 243. Meran, S., et al., Hyaluronan Facilitates Transforming Growth Factor-{beta}1-mediated Fibroblast Proliferation. J. Biol. Chem., 2008. 283(10): p. 6530-6545.
- 244. Ellis, I., J. Banyard, and S.L. Schor, Differential response of fetal and adult fibroblasts to cytokines: cell migration and hyaluronan synthesis. Development, 1997. 124(8): p. 1593-1600.
- 245. Chen, W.Y., et al., Differences between adult and foetal fibroblasts in the regulation of hyaluronate synthesis: correlation with migratory activity. J Cell Sci, 1989. 94(3): p. 577-584.
- 246. Matuoka, K. and Y. Mitsui, Changes in cell-surface glycosaminoglycans in human diploid fibroblasts during in vitro aging. Mechanisms of Ageing and Development, 1981. 15(2): p. 153-163.
- 247. Matuoka, K., et al., A decrease in hyaluronic acid synthesis by aging human fibroblasts leading to heparan sulfate enrichment and growth reduction. Aging (Milano), 1989. 1(1): p. 47-54.
- 248. Suwan, K., et al., Versican/PG-M Assembles Hyaluronan into Extracellular Matrix and Inhibits CD44-mediated Signaling toward Premature Senescence in Embryonic Fibroblasts. J Biol Chem, 2009. **284**(13): p. 8596-604.
- 249. Ohno, T., S. Hirano, and B. Rousseau, Age-associated changes in the expression and deposition of vocal fold collagen and hyaluronan. Ann Otol Rhinol Laryngol, 2009. 118(10): p. 735-41.
- 250. Butler, J.E., T.H. Hammond, and S.D. Gray, Gender-related differences of hyaluronic acid distribution in the human vocal fold. Laryngoscope, 2001. 111(5): p. 907-11.
- 251. Isnard, N., et al., Modulation of cell-phenotype during in vitro aging. Glycosaminoglycan biosynthesis by skin fibroblasts and corneal keratocytes. Experimental Gerontology, 2002. 37(12): p. 1379-1387.
- 252. Meyer, L.J.M. and R. Stern, *Age-Dependent Changes of Hyaluronan in Human Skin.* J Investig Dermatol, 1994. **102**(3): p. 385-389.
- 253. Cristofalo, V.J., et al., Relationship between donor age and the replicative lifespan of human cells in culture: A reevaluation. Proceedings of the National Academy of Sciences of the United States of America, 1998. 95(18): p. 10614-10619.
- 254. Enoch, S., Phenotypic and genotypic characterisation of oral mucosal and patient matched skin fibroblasts, in Dental School. 2006, Cardiff University: Cardiff.
- 255. Stephens, P., *Aging of the skin*. Aging of organs and systems, ed. Aspinall. 2003, London: Kluwer Academic Publishers. 29-71.
- 256. Matrisian, L.M., D. Davis, and B.E. Magun, *Internalization and processing of epidermal growth factor in aging human fibroblasts in culture*. Experimental Gerontology, 1987. **22**(2): p. 81-89.
- 257. Rattan, S.I. and A. Derventzi, *Altered cellular responsiveness during ageing*. Bioessays, 1991. **13**(11): p. 601-6.

- 258. Carpenter, G., The EGF receptor: a nexus for trafficking and signaling. Bioessays, 2000. 22(8): p. 697-707.
- 259. Gabbiani, G., *The myofibroblast in wound healing and fibrocontractive diseases*. The Journal of Pathology, 2003. **200**(4): p. 500-503.
- 260. Desmouliere, A., I.A. Darby, and G. Gabbiani, Normal and pathologic soft tissue remodeling: role of the myofibroblast, with special emphasis on liver and kidney fibrosis. Lab Invest, 2003. 83(12): p. 1689-707.
- 261. Eddy, A.A., *Progression in chronic kidney disease*. Adv Chronic Kidney Dis, 2005. **12**(4): p. 353-65.
- 262. Schuppan, D., et al., Fibrosis of liver, pancreas and intestine: common mechanisms and clear targets? Acta Gastroenterol Belg, 2000. 63(4): p. 366-70.
- 263. Desmouliere, A., et al., Transforming Growth Factor betal induces alphasmooth muscle actin expression in granulation tissue myofibroblasts and in quuescent and growing cultured fibroblasts. The Journal of Cell Biology, 1993. 122(1): p. 103-111.
- 264. Evans, R.A., et al., TGF-beta1-mediated fibroblast-myofibroblast terminal differentiation-the role of Smad proteins. Experimental Cell Research, 2003. 282(2): p. 90-100.
- 265. Jon E. Mogford, N.T.A.C.D.G.Y.X.T.A.M., Effect of age and hypoxia on TGF.
- 266. Jenkins, R.H., et al., Myofibroblastic Differentiation Leads to Hyaluronan Accumulation through Reduced Hyaluronan Turnover. J Biol Chem, 2004. 279(40): p. 41453-41460.
- 267. Croce, M.A., et al., Hyaluronan affects protein and collagen synthesis by in vitro human skin fibroblasts. Tissue and Cell, 2001. 33(4): p. 326-331.
- 268. Tammi, M.I., A.J. Day, and E.A. Turley, *Hyaluronan and homeostasis: a balancing act.* The Journal of Biological Chemistry, 2002. **277**(7): p. 4581-4.
- 269. Ito, T., et al., Hyaluronan attenuates TGF-β1 mediated signalling in renal proximal tubular epithelial cells. The American Journal of Pathology, 2004. **164**(6): p. 1979-1788.
- 270. Ito, T., et al., *Hyaluronan regulates TGF-β1 receptor compartmentalisation*. The Journal of Biological Chemistry, 2004. **279**(24): p. 25326-25332.
- 271. Gerdin, B. and R. Hallgren, Dynamic role of hyaluronan (HYA) in connective tissue activation and inflammation. 1997. p. 49-55.
- 272. Evanko, S.P., J.C. Angello, and T.N. Wight, Formation of hyaluronan- and versican-rich pericellular matrix is required for proliferation and migration of vascular smooth muscle cells. Arterioscler Thromb Vasc Biol, 1999. 19(4): p. 1004-13.
- 273. Stephens, P., et al., Skin and oral fibroblasts exhibit phenotypic differences in extracellular matrix reorganization and matrix metalloproteinase activity. British Journal of Dermatology, 2001. 144(2): p. 229-37.
- 274. Vigetti, D., et al., Hyaluronan-CD44-ERK1/2 Regulate Human Aortic Smooth Muscle Cell Motility during Aging. J. Biol. Chem., 2008. 283(7): p. 4448-4458.
- 275. Vigetti, D., et al., Matrix metalloproteinase 2 and tissue inhibitors of metalloproteinases regulate human aortic smooth muscle cell migration during in vitro aging. FASEB J., 2006. **20**(8): p. 1118-1130.
- 276. Shiraha, H., et al., Aging Fibroblasts Present Reduced Epidermal Growth Factor (EGF) Responsiveness Due to Preferential Loss of EGF Receptors. J. Biol. Chem., 2000. 275(25): p. 19343-19351.

- 277. Ashcroft, G.S., M.A. Horan, and M.W. Ferguson, *The effects of ageing on cutaneous wound healing in mammals.* J Anat, 1995. **187**: p. 1-26.
- 278. Tammi, R., et al., Hyaluronate accumulation in human epidermis treated with retinoic acid in skin organ culture. J Invest Dermatol, 1989. 92(3): p. 326-32.
- 279. Pasonen-Seppanen, S., et al., EGF Upregulates, Whereas TGF-[beta] Downregulates, the Hyaluronan Synthases Has2 and Has3 in Organotypic Keratinocyte Cultures: Correlations with Epidermal Proliferation and Differentiation. J Invest Dermatol, 2003. 120(6): p. 1038-1044.
- 280. Zoltan-Jones, A., et al., Elevated hyaluronan production induces mesenchymal and transformed properties in epithelial cells. J Biol Chem, 2003. **278**(46): p. 45801-10.
- 281. Rilla, K., et al., Changed lamellipodial extension, adhesion plaques and migration in epidermal keratinocytes containing constitutively expressed sense and antisense hyaluronan synthase 2 (Has2) genes. J Cell Sci, 2002. 115(Pt 18): p. 3633-43.
- 282. Sugiyama, Y., et al., Putative hyaluronan synthase mRNA are expressed in mouse skin and TGF-beta upregulates their expression in cultured human skin cells. J Invest Dermatol, 1998. 110(2): p. 116-21.
- 283. Liu, N., et al., Hyaluronan synthase 3 overexpression promotes the growth of TSU prostate cancer cells. Cancer Res, 2001. 61(13): p. 5207-14.
- 284. Vigetti, D., et al., *Hyaluronan-CD44-ERK1/2 Regulate Human Aortic Smooth Muscle Cell Motility during Aging.* J Biol Chem, 2008. **283**(7): p. 4448-4458.
- 285. Meran, S., The Association between the metabolism of Hyaluronan Facilitates and Fibroblast Phenotype, in ION. 2008, Cardiff University: Cardiff.
- 286. Sussmann, M., et al., Induction of Hyaluronic Acid Synthase 2 (HAS2) in Human Vascular Smooth Muscle Cells by Vasodilatory Prostaglandins. Circ Res, 2004. 94(5): p. 592-600.
- 287. Funderburgh, J.L., M.M. Mann, and M.L. Funderburgh, *Keratocyte phenotype mediates proteoglycan structure: a role for fibroblasts in corneal fibrosis.* J Biol Chem, 2003. **278**(46): p. 45629-37.
- 288. Day, A.J. and C.A. de la Motte, *Hyaluronan cross-linking: a protective mechanism in inflammation?* Trends Immunol, 2005. **26**(12): p. 637-43.
- 289. Fulop, C., et al., Impaired cumulus mucification and female sterility in tumor necrosis factor-induced protein-6 deficient mice. Development, 2003. 130(10): p. 2253-61.
- 290. Selbi, W., et al., Over-expression of hyaluronan synthase 2 alters hyaluronan distribution and function in proximal tubular epithelial cells. The Journal of the American Society of Nephrology, 2006. 17(6): p. 1553-1567.
- 291. Guo, Y., S.C. Jacobs, and N. Kyprianou, Down-regulation of protein and mRNA expression for transforming growth factor-beta (TGF-beta1) type I and type II receptors in human prostate cancer. Int J Cancer, 1997. 71(4): p. 573-9.
- 292. Kim, I.Y., et al., Loss of expression of transforming growth factor beta type I and type II receptors correlates with tumor grade in human prostate cancer tissues. Clin Cancer Research, 1996. 2(8): p. 1255-1261.
- 293. Di Guglielmo, G.M., et al., Distinct endocytic pathways regulate TGF-[beta] receptor signalling and turnover. Nat Cell Biol, 2003. 5(5): p. 410-421.

- 294. Petridou, S., et al., TGF-{beta} Receptor Expression and Smad2 Localization Are Cell Density Dependent in Fibroblasts. Invest. Ophthalmol. Vis. Sci., 2000. 41(1): p. 89-95.
- 295. Camenisch, T.D., et al., Heart-valve mesenchyme formation is dependent on hyaluronan-augmented activation of ErbB2-ErbB3 receptors. Nat Med, 2002. 8(8): p. 850-5.
- 296. Tofuku, K., et al., *HAS3-related hyaluronan enhances biological activities necessary for metastasis of osteosarcoma cells*. Int J Oncol, 2006. **29**(1): p. 175-83.
- 297. Nishida, Y., M. Yoshioka, and J. St-Amand, The top 10 most abundant transcripts are sufficient to characterize the organs functional specificity: evidences from the cortex, hypothalamus and pituitary gland. Gene, 2005. 344: p. 133-41.
- 298. Wilkinson, T.S., et al., Overexpression of hyaluronan synthases alters vascular smooth muscle cell phenotype and promotes monocyte adhesion. J Cell Physiol, 2006. 206(2): p. 378-85.
- 299. Mogford, J.E., et al., Effect of age and hypoxia on TGFbeta1 receptor expression and signal transduction in human dermal fibroblasts: impact on cell migration. J Cell Physiol, 2002. 190(2): p. 259-65.
- 300. Shi, Y. and J. Massague, Mechanisms of TGF-beta signaling from cell membrane to the nucleus. Cell, 2003. 113(6): p. 685-700.
- 301. Miyazawa, K., et al., Two major Smad pathways in TGF-beta superfamily signalling. Genes Cells, 2002. 7(12): p. 1191-204.
- 302. Brown, K.A., J.A. Pietenpol, and H.L. Moses, A tale of two proteins: differential roles and regulation of Smad2 and Smad3 in TGF-beta signaling. J Cell Biochem, 2007. 101(1): p. 9-33.
- 303. Piek, E., et al., Functional characterization of transforming growth factor beta signaling in Smad2- and Smad3-deficient fibroblasts. J Biol Chem, 2001. 276(23): p. 19945-53.
- 304. Bourguignon, L.Y., et al., Hyaluronan Promotes Signaling Interaction between CD44 and the Transforming Growth Factor beta Receptor I in Metastatic Breast Tumor Cells. The Journal of Biological Chemistry, 2002. 277(42): p. 39703-12.
- 305. Ito, T., et al., Hyaluronan attenuates TGF-β1 mediated signalling in renal proximal tubular epithelial cells. The American Journal of Pathology, 2004. **164**(6): p. 1979-1988.
- 306. Kakizaki, I., et al., A novel mechanism for the inhibition of hyaluronan biosynthesis by 4-methylumbelliferone. J Biol Chem, 2004. **279**(32): p. 33281-9.
- 307. Rugg, M.S., et al., Characterization of Complexes Formed between TSG-6 and Inter-{alpha}-inhibitor That Act as Intermediates in the Covalent Transfer of Heavy Chains onto Hyaluronan. 2005. p. 25674-25686.
- 308. Kim, B.C., et al., Fibroblasts from chronic wounds show altered TGF-beta-signaling and decreased TGF-beta Type II receptor expression. J Cell Physiol, 2003. 195(3): p. 331-6.
- 309. Colwell, A.S., et al., Fetal and adult fibroblasts have similar TGF-betamediated, Smad-dependent signaling pathways. Plast Reconstr Surg, 2006. 117(7): p. 2277-83.

- 310. Felici, A., et al., TLP, a novel modulator of TGF-beta signaling, has opposite effects on Smad2- and Smad3-dependent signaling. Embo J, 2003. **22**(17): p. 4465-77.
- 311. Pratsinis, H., et al., Differential proliferative response of fetal and adult human skin fibroblasts to transforming growth factor-beta. Wound Repair Regen, 2004. 12(3): p. 374-83.
- 312. Grotendorst, G.R., H. Rahmanie, and M.R. Duncan, Combinatorial signaling pathways determine fibroblast proliferation and myofibroblast differentiation. FASEB J, 2004. 18(3): p. 469-479.
- 313. Kultti, A., et al., Hyaluronan synthesis induces microvillus-like cell surface protrusions. J Biol Chem, 2006. 281(23): p. 15821-8.
- 314. Nakamura, T., et al., Hyaluronic-acid-deficient extracellular matrix induced by addition of 4-methylumbelliferone to the medium of cultured human skin fibroblasts. Biochem Biophys Res Commun, 1995. 208(2): p. 470-5.
- 315. Hayashida, T., M. Decaestecker, and H.W. Schnaper, Cross-talk between ERK MAP kinase and Smad signaling pathways enhances TGF-beta-dependent responses in human mesangial cells. Faseb J, 2003. 17(11): p. 1576-8.
- 316. Zhang, M., D. Fraser, and A. Phillips, ERK, p38, and Smad signaling pathways differentially regulate transforming growth factor-betal autoinduction in proximal tubular epithelial cells. Am J Pathol, 2006. 169(4): p. 1282-93.
- 317. Uchiyama-Tanaka, Y., et al., Involvement of HB-EGF and EGF receptor transactivation in TGF-[beta1]-mediated fibronectin expression in mesangial cells. Kidney Int, 2002. **62**(3): p. 799-808.
- 318. Pienimaki, J.P., et al., Epidermal growth factor activates hyaluronan synthase 2 in epidermal keratinocytes and increases pericellular and intracellular hyaluronan. J Biol Chem, 2001. 276(23): p. 20428-35.
- 319. Wells, A., *EGF receptor*. The International Journal of Biochemistry & Cell Biology, 1999. **31**(6): p. 637-643.
- 320. Grande, M., et al., Transforming growth factor-beta and epidermal growth factor synergistically stimulate epithelial to mesenchymal transition (EMT) through a MEK-dependent mechanism in primary cultured pig thyrocytes. Journal of Cell Science, 2002. 115(Pt 22): p. 4227-36.
- 321. Song, K., T.L. Krebs, and D. Danielpour, Novel permissive role of EGF in TGF-beta signaling and growth suppression: Mediation by stabilization of TGF-beta receptor type II. The Journal of Bioliogical Chemistry, 2006.
- 322. Docherty, N.G., et al., TGF-beta1-induced EMT can occur independently of its proapoptotic effects and is aided by EGF receptor activation. Am J Physiol Renal Physiol, 2006. 290(5): p. F1202-1212.
- 323. Tian, Y.-C., et al., Epidermal growth factor and transforming growth factor-[beta]1 enhance HK-2 cell migration through a synergistic increase of matrix metalloproteinase and sustained activation of ERK signaling pathway. Experimental Cell Research, 2007. 313(11): p. 2367-2377.
- 324. Uttamsingh, S., et al., Synergistic effect between EGF and TFG-β1 in inducing oncogenic properties of intestinal epithelial cells. Oncogene, 2008. 27: p. 2626-1634.
- 325. He, J. and H.E.P. Bazan, Epidermal Growth Factor Synergism with TGF-{beta}1 via PI-3 Kinase Activity in Corneal Keratocyte Differentiation. Invest. Ophthalmol. Vis. Sci., 2008. 49(7): p. 2936-2945.

- 326. Tsatas, D., et al., EGF receptor modifies cellular responses to hyaluronan in glioblastoma cell lines. Journal of Clinical Neuroscience, 2002. 9(3): p. 282-288.
- 327. He, J. and H.E. Bazan, Epidermal growth factor synergism with TGF-beta1 via PI-3 kinase activity in corneal keratocyte differentiation. Invest Ophthalmol Vis Sci, 2008. 49(7): p. 2936-45.
- 328. Hongo, M., et al., Distribution of epidermal growth factor (EGF) receptors in rabbit corneal epithelial cells, keratocytes and endothelial cells, and the changes induced by transforming growth factor-beta 1. Exp Eye Res, 1992. 54(1): p. 9-16.
- 329. Goldkorn, T. and J. Mendelsohn, Transforming growth factor beta modulates phosphorylation of the epidermal growth factor receptor and proliferation of A431 cells. Cell Growth Differ, 1992. 3(2): p. 101-9.
- 330. Bendell, J.J. and J.H. Dorrington, *Epidermal growth factor influences growth and differentiation of rat granulosa cells*. Endocrinology, 1990. **127**(2): p. 533-40.
- 331. Thompson, K.L., R. Assoian, and M.R. Rosner, Transforming growth factor-beta increases transcription of the genes encoding the epidermal growth factor receptor and fibronectin in normal rat kidney fibroblasts. J Biol Chem, 1988. 263(36): p. 19519-24.
- 332. Matsuda, T., et al., Decreased response to epidermal growth factor during cellular senescence in cultured human microvascular endothelial cells. J Cell Physiol, 1992. **150**(3): p. 510-6.
- 333. Ribault, D., et al., Age-related decrease in the responsiveness of rat articular chondrocytes to EGF is associated with diminished number and affinity for the ligand of cell surface binding sites. Mech Ageing Dev, 1998. 100(1): p. 25-40.
- 334. Nofal, G.A. and C.B. Knudson, *Latrunculin and Cytochalasin Decrease Chondrocyte Matrix Retention*. Journal of Histochemistry and Cytochemistry, 2002. **50**(10): p. 1313-1324.
- 335. Tammi, R., et al., *Hyaluronan enters keratinocytes by a novel endocytic route for catabolism.* J Biol Chem, 2001. **276**(37): p. 35111-22.
- 336. Bourguignon, L.Y.W., et al., CD44 Interaction with c-Src Kinase Promotes Cortactin-mediated Cytoskeleton Function and Hyaluronic Acid-dependent Ovarian Tumor Cell Migration. J Biol Chem, 2001. 276(10): p. 7327-7336.
- 337. Jones, S.G., T. Ito, and A.O. Phillips, Regulation of proximal tubular epithelial cell CD44-mediated binding and internalisation of hyaluronan. The International Journal of Biochemistry & Cell Biology, 2003. 35(9): p. 1361-1377.
- 338. Wang, S.J. and L.Y.W. Bourguignon, Hyaluronan and the Interaction Between CD44 and Epidermal Growth Factor Receptor in Oncogenic Signaling and Chemotherapy Resistance in Head and Neck Cancer. Arch Otolaryngol Head Neck Surg, 2006. 132(7): p. 771-778.
- 339. Grande, M., et al., Transforming growth factor-beta and epidermal growth factor synergistically stimulate epithelial to mesenchymal transition (EMT) through a MEK-dependent mechanism in primary cultured pig thyrocytes. J Cell Sci, 2002. 115(Pt 22): p. 4227-36.
- 340. Song, K., T.L. Krebs, and D. Danielpour, Novel permissive role of epidermal growth factor in transforming growth factor beta (TGF-beta) signaling and

- growth suppression. Mediation by stabilization of TGF-beta receptor type II. J Biol Chem, 2006. **281**(12): p. 7765-74.
- 341. Kutz, S.M., et al., TGF-[beta]1-induced PAI-1 expression is E box/USF-dependent and requires EGFR signaling. Experimental Cell Research, 2006. 312(7): p. 1093-1105.
- 342. Pasonen-Seppanen, S.M., et al., All-trans Retinoic Acid-Induced Hyaluronan Production and Hyperplasia Are Partly Mediated by EGFR Signaling in Epidermal Keratinocytes. J Invest Dermatol, 2007. 128(4): p. 797-807.
- 343. Bourguignon, L.Y., E. Gilad, and K. Peyrollier, *Heregulin-mediated ErbB2-ERK signaling activates hyaluronan synthases leading to CD44-dependent ovarian tumor cell growth and migration.* J Biol Chem, 2007. **282**(27): p. 19426-41.
- 344. Humes, H.D., et al., Effects of transforming growth factor-beta, transforming growth factor-alpha, and other growth factors on renal proximal tubule cells. Lab Invest, 1991. 64(4): p. 538-45.
- 345. Tian, Y.C., et al., Epidermal growth factor and transforming growth factor-betal enhance HK-2 cell migration through a synergistic increase of matrix metalloproteinase and sustained activation of ERK signaling pathway. Exp Cell Res, 2007. 313(11): p. 2367-77.
- 346. Uttamsingh, S., et al., Synergistic effect between EGF and TGF-beta1 in inducing oncogenic properties of intestinal epithelial cells. Oncogene, 2008. 27(18): p. 2626-34.
- 347. Yamada, Y., et al., Differential Regulation by IL-1[beta] and EGF of Expression of Three Different Hyaluronan Synthases in Oral Mucosal Epithelial Cells and Fibroblasts and Dermal Fibroblasts: Quantitative Analysis Using Real-Time RT-PCR. J Investig Dermatol, 2004. 122(3): p. 631-639.
- 348. Saavalainen, K., et al., The Human Hyaluronan Synthase 2 Gene Is a Primary Retinoic Acid and Epidermal Growth Factor Responding Gene. J. Biol. Chem., 2005. 280(15): p. 14636-14644.
- 349. Bourguignon, L.Y.W., et al., Hyaluronan-CD44 Interaction with Leukemia-associated RhoGEF and Epidermal Growth Factor Receptor Promotes Rho/Ras Co-activation, Phospholipase C{epsilon}-Ca2+ Signaling, and Cytoskeleton Modification in Head and Neck Squamous Cell Carcinoma Cells. J. Biol. Chem., 2006. **281**(20): p. 14026-14040.
- 350. Isacke, C.M., The role of the cytoplasmic domain in regulating CD44 function. J Cell Sci, 1994. 107 (Pt 9): p. 2353-9.
- 351. Stefanovic-Racic, M., J. Stadler, and C.H. Evans, *Nitric oxide and arthritis*. Arthritis Rheum, 1993. **36**(8): p. 1036-44.
- 352. Liu, Y., et al., Age-related Decline in Mitogen-activated Protein Kinase Activity in Epidermal Growth Factor-stimulated Rat Hepatocytes. J. Biol. Chem., 1996. 271(7): p. 3604-3607.
- 353. Aoyagi, M., et al., Kinetics of 125I-PDGF binding and down-regulation of PDGF receptor in human arterial smooth muscle cell strains during cellular senescence in vitro. J Cell Physiol, 1995. 164(2): p. 376-84.
- 354. Munger, J.S., et al., The integrin alpha v beta 6 binds and activates latent TGF beta 1: a mechanism for regulating pulmonary inflammation and fibrosis. Cell, 1999. **96**(3): p. 319-28.

- 355. Yu, Q. and I. Stamenkovic, Cell surface-localized matrix metalloproteinase-9 proteolytically activates TGF-beta and promotes tumor invasion and angiogenesis. Genes Dev, 2000. 14(2): p. 163-76.
- 356. Pascall, J.C. and K.D. Brown, Structural analysis of the 5'-flanking sequence of the mouse epidermal growth factor gene. J Mol Endocrinol, 1988. 1(1): p. 5-11.
- 357. Pascall, J.C., et al., Cloning and characterization of a gene encoding pig epidermal growth factor. J Mol Endocrinol, 1991. 6(1): p. 63-70.
- 358. Fenton, S.E., N.S. Groce, and D.C. Lee, Characterization of the mouse epidermal growth factor promoter and 5'-flanking region. Role for an atypical TATA sequence. J Biol Chem, 1996. 271(48): p. 30870-8.
- 359. Pascall, J.C. and K.D. Brown, *Identification of a minimal promoter element of the mouse epidermal growth factor gene.* Biochem. J., 1997. **324**(3): p. 869-875.
- 360. Sakaguchi, M., et al., S100A11, an dual mediator for growth regulation of human keratinocytes. Mol Biol Cell, 2008. 19(1): p. 78-85.
- 361. Reenstra, W.R., M. Yaar, and B.A. Gilchrest, Aging Affects Epidermal Growth Factor Receptor Phosphorylation and Traffic Kinetics. Experimental Cell Research, 1996. 227(2): p. 252-255.
- Webster, R.J., et al., Regulation of epidermal growth factor receptor signaling in human cancer cells by microRNA-7. J Biol Chem, 2009. **284**(9): p. 5731-41.
- 363. Herbst, R.S., Review of epidermal growth factor receptor biology. International Journal of Radiation Oncology*Biology*Physics, 2004. **59**(2, Supplement 1): p. S21-S26.
- 364. Bourguignon, L.Y.W., et al., Interaction between the Adhesion Receptor, CD44, and the Oncogene Product, p185HER2, Promotes Human Ovarian Tumor Cell Activation. J Biol Chem, 1997. 272(44): p. 27913-27918.
- 365. Monslow, J., et al., *Identification and analysis of the promoter region of the human hyaluronan synthase 2 gene.* J Biol Chem, 2004. **279**(20): p. 20576-81.
- 366. Monslow, J., et al., Sp1 and Sp3 mediate constitutive transcription of the human hyaluronan synthase 2 gene. J Biol Chem, 2006. **281**(26): p. 18043-50.
- 367. Chao, H. and A.P. Spicer, Natural antisense mRNAs to hyaluronan synthase 2 inhibit hyaluronan biosynthesis and cell proliferation. J Biol Chem, 2005. **280**(30): p. 27513-22.
- 368. Hinz, B. and G. Gabbiani, Cell-matrix and cell-cell contacts of myofibroblasts: role in connective tissue remodeling. Thromb Haemost, 2003. **90**(6): p. 993-1002
- 369. Hinz, B., et al., Alpha-smooth muscle actin expression upregulates fibroblast contractile activity. Mol Biol Cell, 2001. 12(9): p. 2730-41.
- 370. Hinz, B., et al., Mechanical tension controls granulation tissue contractile activity and myofibroblast differentiation. Am J Pathol, 2001. **159**(3): p. 1009-20
- 371. Takemura, M., et al., Cyclic mechanical stretch augments hyaluronan production in cultured human uterine cervical fibroblast cells. Mol Hum Reprod, 2005. 11(9): p. 659-65.
- 372. Lee, R.T., et al., Mechanical strain induces specific changes in the synthesis and organization of proteoglycans by vascular smooth muscle cells. J Biol Chem, 2001. 276(17): p. 13847-51.
- 373. Bai, K.J., et al., The role of hyaluronan synthase 3 in ventilator-induced lung injury. Am J Respir Crit Care Med, 2005. 172(1): p. 92-8.

- 374. Campo, G.M., et al., Reduction of DNA fragmentation and hydroxyl radical production by hyaluronic acid and chondroitin-4-sulphate in iron plus ascorbate-induced oxidative stress in fibroblast cultures. Free Radic Res, 2004. 38(6): p. 601-11.
- 375. Soltes, L., et al., *Degradative action of reactive oxygen species on hyaluronan*. Biomacromolecules, 2006. 7(3): p. 659-68.
- 376. Roepstorff, K., et al., Sequestration of epidermal growth factor receptors in non-caveolar lipid rafts inhibits ligand binding. J Biol Chem, 2002. 277(21): p. 18954-60.
- 377. Lambert, S., et al., Ligand-independent activation of the EGFR by lipid raft disruption. J Invest Dermatol, 2006. 126(5): p. 954-62.
- 378. Shintani, S., et al., Intragenic mutation analysis of the human epidermal growth factor receptor (EGFR) gene in malignant human oral keratinocytes. Cancer Res, 1999. **59**(16): p. 4142-7.
- 379. Basu, A., et al., Inhibition of tyrosine kinase activity of the epidermal growth factor (EGF) receptor by a truncated receptor form that binds to EGF: role for interreceptor interaction in kinase regulation. Mol Cell Biol, 1989. 9(2): p. 671-7.
- 380. Pasonen-Seppanen, S.M., et al., All-trans retinoic acid-induced hyaluronan production and hyperplasia are partly mediated by EGFR signaling in epidermal keratinocytes. J Invest Dermatol, 2008. 128(4): p. 797-807.
- 381. Zhang, M., D. Fraser, and A. Phillips, ERK, p38, and Smad Signaling Pathways Differentially Regulate Transforming Growth Factor-{beta}1 Autoinduction in Proximal Tubular Epithelial Cells. Am J Pathol, 2006. 169(4): p. 1282-1293.
- 382. Hashimoto, S., et al., Transforming growth Factor-beta1 induces phenotypic modulation of human lung fibroblasts to myofibroblast through a c-Jun-NH2-terminal kinase-dependent pathway. Am J Respir Crit Care Med, 2001. 163(1): p. 152-7.
- 383. Javelaud, D., et al., Disruption of basal JNK activity differentially affects key fibroblast functions important for wound healing. J Biol Chem, 2003. 278(27): p. 24624-8.
- 384. Funaba, M. and M. Murakami, A sensitive detection of phospho-Smad1/5/8 and Smad2 in Western blot analyses. J Biochem Biophys Methods, 2008. **70**(6): p. 816-9.
- 385. Engel, M.E., et al., Interdependent SMAD and JNK signaling in transforming growth factor-beta-mediated transcription. J Biol Chem, 1999. 274(52): p. 37413-20.
- 386. Zhang, Y., X.H. Feng, and R. Derynck, Smad3 and Smad4 cooperate with c-Jun/c-Fos to mediate TGF-beta-induced transcription. Nature, 1998. 394(6696): p. 909-13.
- 387. Javelaud, D. and A. Mauviel, Crosstalk mechanisms between the mitogenactivated protein kinase pathways and Smad signaling downstream of TGF-beta: implications for carcinogenesis. Oncogene, 2005. 24(37): p. 5742-50.
- 388. Yeo, E.-J. and S.C. Park, Age-dependent agonist-specific dysregulation of membrane-mediated signal transduction: emergence of the gate theory of aging. Mechanisms of Ageing and Development, 2002. 123(12): p. 1563-1578.
- 389. Jacks, T. and R.A. Weinberg, *Taking the study of cancer cell survival to a new dimension*. Cell, 2002. **111**(7): p. 923-5.

390. Dallon, J.C. and H.P. Ehrlich, *A review of fibroblast-populated collagen lattices*. Wound Repair Regen, 2008. **16**(4): p. 472-9.

Appendix 1: Buffers and Reagents

Block Buffer: 5 % (vol/vol) Tween-20, 0.05 % (wt/vol) NaN₃ in

PBS

Guanidine Buffer (4 M): 4 M guanidine, 50 mM sodium acetate, 0.5 %

(vol/vol) triton X-100, 0.05 % (wt/vol) sodium

azide, pH 6

Hyaluronidase Buffer: 20 mM sodium acetate, 0.15 M NaCl, 0.05 %

(wt/vol) sodium azide, pH 6

PAGE Reducing Buffer (3 x): 62.5 mM Tris (pH 6.8), 30 % (vol/vol) glycerol, 6

% (wt/vol) SDS, 0.03 % (vol/vol) bromophenol

blue, 15 % (vol/vol) 2β mercaptoethanol

PAGE Reducing Buffer (5 x): 62.5 mM Tris (pH 6.8), 50 % (vol/vol) glycerol,

10 % (wt/vol) SDS, 0.05 % (vol/vol) bromophenol

blue, 25 % (vol/vol) 2β mercaptoethanol

PCR Loading Buffer: 30 % (vol/vol) glycerol, 0.1 % (wt/vol) Orange G

Phosphate Buffered Saline (PBS): 2.68 mM KCl, 1.47 mM KH₂PO₄, 137 mM NaCl,

8.1 mM Na₂HPO₄

Pronase Buffer: 100 mM Tris, 0.05 % (wt/vol) sodium azide, pH

8.0

Reagent Diluent: 1.4 % (wt/vol) BSA, 0.05 % (vol/vol) Tween-20 in

PBS, pH 7.2-7.4

Running Buffer: 25 mM Tris, 192 mM glycine, 3.5 mM SDS, pH

8.3

Stripping Buffer: 64 mM Tris, 69 mM SDS, 0.7 % (vol/vol) 2\beta

mercaptoethanol

TAE Buffer: 40 mM Tris, 40 mM acetic acid, 10 mM EDTA

Transfer Buffer: 25 mM Tris, 192 mM glycine, 20 % (vol/vol)

methanol

Tris Buffered Saline (TBS): 20 mM Tris, 137 mM NaCl, pH 7.6

Triton Buffer (0.2 %): 25 mM Tris, 0.2 % (vol/vol) Triton X-100, 56 mM

caproic acid, 13 mM EDTA, pH 7.5

Triton Buffer (1 %): 25 mM Tris, 1 % (vol/vol) Triton X-100, 0.4 M

guanidine, 56 mM caproic acid, 13 mM EDTA,

pH 7.5

Urea Buffer (8 M): 8 M urea, 20 mM Bis-Tris buffer, pH 6, 0.2 %

(vol/vol) Triton X-100

Wash Buffer: 0.05 % (vol/vol) Tween-20 in PBS, pH 7.2-7.4